Exploiting the synergies of unmanned aerial vehicles (UAVs) and 5G network

Debashisha Mishra

UNIVERSITÉ DE LORRAINE

École doctorale IAEM Lorraine

Exploiting the synergies of unmanned aerial vehicles (UAVs) and 5G network

THÈSE

présentée et soutenue publiquement le 13 Juin 2023

pour l'obtention du

Doctorat de l'Université de Lorraine

(Docteur en informatique)

par

Debashisha Mishra

Composition of the jury

President :	Dr. Nathalie Mitton	INRIA Lille-Nord Europe, France
Reviewers :	Prof. Fabrice Valois	INSA Lyon, France
	Prof. Kaushik Chowdhury	Northeastern University, Boston, USA
Examiners :	Dr. Nathalie Mitton	INRIA Lille-Nord Europe, France
	Dr. Thouraya Toukabri	Ericsson, Île-de-France, France
	Prof. E. Veronica Belmega	Université Gustave Eiffel (UGE), France
	Prof. Ye-Qiong Song	Université de Lorraine - ENSEM, France
Invites :	Prof. François Charoy	Université de Lorraine - TELECOM Nancy, France
Supervisor :	Prof. Enrico Natalizio	Université de Lorraine, France

Laboratoire Lorrain de Recherche en Informatique et ses Applications — UMR 7503

Acknowledgments

I would like to thank everyone who encouraged and supported me during my PhD program at Université de Lorraine, Nancy, France. First and foremost, I must express my sincere gratitude to my adviser Prof. Enrico NATALIZIO for accepting me as his student. His consistent mentoring, support to pursue my own research interests and engagement through the learning process during the PhD program have helped me to acquire many concepts at early stage; thank him very much for always having an open door for my questions and uncountable hours of discussions and guidance to accomplish research challenges.

My heartfelt gratitude goes to all of the co-authors of the published publications throughout the course of my Doctorate, especially Nicola, Angelo, Emiliano, Boris, Prasanna, Himank, Osama, Anna Maria, Valeria, Prof. Marco Di Felice, Prof. Ian F. Akyildiz, as well as the anonymous reviewers who took the time to read and remark on my work. I would also want to thank my wonderful colleagues at the Autonomous Robotics Research Center, Technology Innovation Institute in the United Arab Emirates for their unwavering support and guidance.

I owe immense gratitude to Prof. Ye-Qiong Song, Prof. Laurent Ciarletta, Prof. Vincent Chevrier and Prof. Sylvain Contassot-Vivier for their continuous effort to help me in deep driving into research scope and helpful advice. I would like to thank all my peer lab members who indirectly or directly helped me towards building a robust research atmosphere at SIMBIOT research team of LORIA lab. I consider to have a great time with my peer members for many technical concepts and social companionship. I did like to thank Jean-Baptiste, Théo, Runbo, Amaury, Diego, Dr. Vishal, Dr. Dimple for encouraging me to go ahead with my interest and helping me to improve my knowledge by constant interactions. The advice, motivation, and support I received from them has helped me tremendously in many aspects of life, not just work. For the most part, however, I just want to express my gratitude for their companionship.

And finally, I would like to use this opportunity to thank all my family members for the unceasing encouragement, support and patience. I will be eternally thankful to them for bringing me into this world and allowing me to pursue my ambition. The entire journey would not have been meaningful without the blessing and grace of almighty God.

Thanks for everything!

Debashisha Mishra

Dedicated to my loving parents and family.
For their endless love, support and encouragement.

Abstract

As an expanding subject of aerial robotics, Unmanned Aerial Vehicles (UAVs) have received substantial research attention within the wireless networking research community. As soon as national legislations enable UAVs to fly autonomously, we will witness swarms of UAV filling the skies of our smart cities to complete diverse missions: package delivery, infrastructure monitoring, event videography, surveillance, tracking, etc. Fifth generation (5G) and beyond cellular networks can improve UAV communications in a variety of ways and thus benefit the UAV ecosystem. There is a wide variety of wireless applications and use cases that can benefit from the capabilities of these smart devices, including the UAV's inherent characteristics of agile mobility in three-dimensional space, autonomous operation, and intelligent placement. The broad goal of this thesis is to provide a comprehensive analysis of the synergies that may be realized when combining 5G and beyond cellular networks with UAV technology.

This thesis presents four types of UAV and cellular ecosystem integration models. "UAV-assisted cellular paradigm" refers to communication scenarios in which UAVs are used as flying (or aerial) base stations or as relays to augment current terrestrial cellular connectivity or to mitigate disaster situations. The "cellular-assisted UAV paradigm" foresees the integration of UAVs into the current cellular network as a new aerial user (flying UE) to serve a wide variety of applications and use cases. The "UAV-to-UAV paradigm" stresses the collective strength of a fleet of UAVs as a swarm and communication amongst UAVs inside the swarm. The "hybrid non-terrestrial paradigm" encompasses satellite and aerial networks, therefore examining the whole spectrum of communication links from the ground to the air to the space in the form of an integrated space-air-ground communication network.

Initially, this thesis focuses on aerial base stations, which have gained great academic attention in order to provide flexible, on-demand communication services to ground users. On this occasion, we build and construct a proof-of-concept prototype platform that delineates the design components required to implement such platforms in the real world, and we then explain the necessity for optimal placement of aerial base stations. To support a heterogeneous class of 5G services from various vertical industries, we propose a slicing-aware aerial base station framework for ground users with differentiated traffic requirements. Second, we describe aerial users who are supported by current cellular infrastructure and examine difficulties such as coexistence of aerial users and ground users, handovers, and communication-aware trajectory optimization. A swarm of UAVs opens up new opportunities for new services and applications since the UAVs may independently coordinate their operations and work together to complete a given task. As part of this thesis, we offer centralized and decentralized network models for UAV-to-UAV (U2U) communication inside swarm and conduct a full investigation of sidelink-assisted U2U communication with performance assessment. Expanding beyond terrestrial networks, the 6G concept includes non-terrestrial networks such as satellite and aerial networks, and so investigates a wide range of disparate communication channels on the way to the ultimate goal of a unified space-air-ground infrastructure. To ensure that the development activities of business, academia, and independent research organizations are in sync, standardization bodies like 3GPP have established study topics and working groups. This dissertation shines a light on several innovative 6G enabling technologies and presents the in-depth research and evaluation of communication technology candidates, socio-economic concerns, and standardization activities being undertaken

to harmonize UAV operations across varied geographical landscapes.

Keywords: UAV, 4G, LTE, 5G, New Radio, Drone, Robotics, Communication

Résumé

En tant que sujet en expansion de la robotique aérienne, les véhicules aériens sans pilote (UAV) ont fait l'objet d'une attention particulière de la part de la communauté de recherche sur les réseaux sans fil. Dès que les législations nationales permettront aux drones de voler de manière autonome, nous verrons des essaims de drones envahir le ciel de nos villes intelligentes pour accomplir diverses missions : livraison de colis, surveillance des infrastructures, vidéographie événementielle, surveillance, suivi, etc. Les réseaux cellulaires de cinquième génération (5G) et au-delà peuvent améliorer les communications des drones de diverses manières et profiter ainsi à l'écosystème des drones. Il existe une grande variété d'applications sans fil et de cas d'utilisation qui peuvent bénéficier des capacités de ces dispositifs intelligents. L'objectif général de cette thèse est de fournir une analyse complète des synergies qui peuvent être réalisées en combinant les réseaux cellulaires 5G et au-delà avec la technologie des drones.

Cette thèse présente quatre types de modèles d'intégration de l'écosystème des drones et des réseaux cellulaires. Le paradigme cellulaire assisté par drone fait référence à des scénarios de communication dans lesquels les drones sont utilisés comme stations de base volantes (ou aériennes) ou comme relais pour augmenter la connectivité cellulaire terrestre actuelle ou pour atténuer les situations de catastrophe. Le paradigme des drones à assistance cellulaire prévoit l'intégration des drones dans le réseau cellulaire actuel en tant que nouvel utilisateur aérien (UE volant) pour servir une grande variété d'applications et de cas d'utilisation. Le paradigme drone à drone met l'accent sur la force collective d'une flotte de drones en tant qu'essaim et sur la communication entre les drones à l'intérieur de l'essaim. Le paradigme hybride non terrestre englobe les réseaux satellitaires et aériens, ce qui permet d'examiner le réseau de communication intégré espace-air-sol.

Dans un premier temps, cette thèse se concentre sur les stations de base aériennes afin de fournir des services de communication flexibles et à la demande aux utilisateurs au sol. À cette occasion, nous construisons une plateforme prototype de validation du concept et expliquons la nécessité d'un placement optimal des stations de base aériennes. Pour prendre en charge une classe hétérogène de services 5G provenant de diverses industries verticales, nous proposons un cadre de station de base aérienne sensible au découpage pour les utilisateurs au sol ayant des exigences de trafic différenciées. Ensuite, nous décrivons les utilisateurs aériens qui sont pris en charge par l'infrastructure cellulaire actuelle et examinons les difficultés telles que la coexistence des utilisateurs aériens et des utilisateurs au sol, les transferts et l'optimisation des trajectoires en fonction des communications. Un essaim de drones ouvre de nouvelles perspectives pour de nouveaux services et applications. Dans le cadre de cette thèse, nous proposons des modèles de réseaux centralisés et décentralisés pour la communication de drone à drone (U2U) au sein de l'essaim et menons une étude complète de la communication U2U assistée par des lignes de fuite avec une évaluation des performances. Au-delà des réseaux terrestres, le concept de la 6G inclut les réseaux non terrestres tels que les réseaux satellitaires et aériens, et étudie ainsi un large éventail de canaux de communication disparates sur la voie de l'objectif ultime d'une infrastructure espace-air-sol unifiée. Cette thèse met en lumière plusieurs technologies 6G innovantes et présente la recherche et l'évaluation approfondies des candidats aux technologies de communication, les préoccupations socio-économiques et les activités de normalisation entreprises pour harmoniser les opérations des drones dans des paysages géographiques variés.

Mots-clés: Drones, 4G, LTE, 5G, New Radio, Robotique, Communication

Contents

List of Figures

List of Tables

List of Publications

1. Mishra, Debashisha, and Enrico Natalizio. "A survey on cellular-connected UAVs: Design challenges, enabling 5G/B5G innovations, and experimental advancements." Computer Networks 182 (2020): 107451.
DOI- https://doi.org/10.1016/j.comnet.2020.107451

2. Mishra, Debashisha, Anna Maria Vegni, Valeria Loscrí, and Enrico Natalizio. "Drone networking in the 6G era: A technology overview." IEEE Communications Standards Magazine 5, no. 4 (2021): 88-95.
DOI- https://doi.org/10.1109/MCOMSTD.0001.2100016

3. Mishra, Debashisha, Nicola Roberto Zema, and Enrico Natalizio. "A high-end IoT devices framework to foster beyond-connectivity capabilities in 5G/B5G architecture." IEEE Communications Magazine 59.1 (2021): 55-61.
DOI- https://doi.org/10.1109/MCOM.001.2000504

4. Mishra, Debashisha, Angelo Trotta, Emiliano Traversi, Marco Di Felice, and Enrico Natalizio. "Cooperative Cellular UAV-to-Everything (C-U2X) communication based on 5G sidelink for UAV swarms." Computer Communications 192 (2022): 173-184.
DOI- https://doi.org/10.1016/j.comcom.2022.06.001

5. Mishra, Debashisha, Angelo Trotta, Marco Di Felice, and Enrico Natalizio. "Performance analysis of multi-hop communication based on 5G sidelink for cooperative UAV swarms." In 2021 IEEE International Mediterranean Conference on Communications and Networking (MeditCom), pp. 395-400. IEEE, 2021.
DOI- https://doi.org/10.1109/MeditCom49071.2021.9647449

6. Bushnaq, Osama M., Debashisha Mishra, Enrico Natalizio, and Ian F. Akyildiz. "Unmanned aerial vehicles (UAVs) for disaster management." In Nanotechnology-Based Smart Remote Sensing Networks for Disaster Prevention, pp. 159-188. Elsevier, 2022.
DOI- https://doi.org/10.1016/B978-0-323-91166-5.00013-6

7. Debashisha Mishra, Emiliano Traversi, Angelo Trotta, Prasanna Raut, Boris Galkin, Marco Di Felice and Enrico Natalizio. "An EASIER way of Slicing Resources in Aerial Base Station (UAV-BS) towards Coexistence of Heterogeneous 5G Services", Submitted to IEEE Access, 2023. **Under Review**.

Chapter 1

Introduction

1.1 Unmanned Aerial Vehicles (UAVs)

Unmanned Aerial Vehicles, abbreviated as UAVs, are aircrafts without any human pilot onboard, mainly controlled and managed remotely or via embedded autonomous computer programs. UAVs are also popularly known as drones. It is a new paradigm emerged from aerial robotics with enormous potential for enabling new applications in diverse areas and business opportunities [1–3]. The global UAV market was valued at US$ 20.68 billion in 2017 and is expected to reach US$ 59.82 billion by 2026, at a compound annual growth rate (CAGR) of 14.20% during a forecast period [4].

Unique features of UAVs pertaining to high mobility in three-dimensional space, autonomous operation, flexible deployment tend to find appealing solutions for wide range of applications including civil, public safety, Industrial IoT platforms (IIoT), security and defence sectors, cyber physical systems, atmospheric and environmental observation etc [5–7]. By leveraging other emerging technologies like Artificial Intelligence(AI), Internet of Things (IoT), Augmented Reality/Virtual Reality(AR/VR), UAVs have been able to showcase substantial value proposition to a wide range of civil and industrial applications across diverse areas. The UAVs are flying platforms and hence, the emerging use cases for each of the mentioned applications demand a secure, reliable wireless communication infrastructure for command and control, as well as an efficient information dissemination towards the ground control station (GCS) [8, 9].

On this advent, there are two main research directions to be investigated. *First, how to integrate a suitable wireless communication platform into UAVs for ubiquitous connectivity and seamless service for the identified use cases. Second, what are the scientific and technological challenges that arise from such integration.* This thesis aims on both the aforementioned directions and highlight several distinctive characteristics, challenges with state-of-the-art solutions from the viewpoint of aerial communication and networking.

UAVs are inherently mobile in nature and hence, require wireless support for communication needs [10, 11]. This wireless communication support can be provided over licensed or unlicensed spectrum. Unlicensed spectrum is shared by multiple parties and are more prone to interference/contention scenarios. On the other hand, licensed spectrum allocates reliable channel resources for UAV communications and also requires regulatory decisions to be adhered to. The licensed spectrum operations for UAV can be realized via several ways, *e.g.,* through satellite network or through separate dedicated licensed spectrum allocated for only UAVs, or by existing cellular frequency bands. Satellite spectrum is well suited for wide area coverage, but often limited by higher costs, higher latency and lower throughput. Laying out a dedicated spectrum

for UAV operations is costly and requires substantial effort to build a system supporting drone operations [12]. The support from the cellular network tends to balance above trade-offs in a cost-effective way by offering practical mission range, higher throughput and lower latency. To this end, the UAV ecosystem can benefit from cellular networks [13, 14] for communication, networking and sensing purpose.

1.2 Control and Data links for UAV Communication

From the communication viewpoint, the requirements of UAV can be classified into two broad categories [15]:

- **Control and Non-Payload Communication (CNPC) -** It refers to the time critical control and safety commands needed for the UAV to accomplish a given mission. CNPC includes the navigation, waypoint updates, telemetry report and air traffic control (ATC) updates to ensure secure and reliable UAV operation. CNPC usually demands highly secure and reliable link with low data rate (few hundred Kb/s) requirements. The reliability requirement for CNPC is less than 10^{-3} packet error rate (PER).
- **Payload Communication -** It refers to all the information dissemination activities carried out by UAV pertaining to a UAV mission. For instance, in a surveillance operation, UAV needs to transmit real time video to the ground station/remote pilot via payload communication. Payload communication demands the underlying transmission medium to be capable of supporting high data rates (often higher in full HD video transmission or wireless backhauling).

Table 1.1 summarizes the rate and latency requirements for above two types of links.

Table 1.1: UAV control and data link requirements [16]

Type	**CNPC Uplink**	**CNPC Downlink**	**Payload**
Rate	∼100 Kbps	∼100 Kbps	∼50 Mbps
Latency	-	∼50 ms	Identical to Ground UE

1.3 Cellular Network

The cellular network or mobile network is a radio network distributed in geographical land in the form of multiple cells *e.g.,* ideal hexagonal cells in simplest form. Each cell covers several ground users and is typically served by a fixed cell tower or base station transceiver having one or more antennas. The base station is connected to other core network components to facilitate downlink and uplink data transmission form remote data networks in the Internet. Depending on the gradual evolution over several decades, from First generation (1G) to Fifth generation (5G), there has been several modifications to above fundamental architecture of the cellular network. In Fig. 1.1, we show key network elements depicting similarities and differences in 4G long term evolution (LTE) and 5G new radio (NR) standalone (5G-SA) cellular network.

Recently, the deployment of 5G cellular network and ambitious requirements of beyond 5G *i.e.,* Sixth Generation (6G) wireless networks envision to cater to a wider variety of goals in terms of higher coverage and extended connectivity, ultra-reliable low latency communication (uRLLC), support for massive number of devices via machine type communication (mMTC),

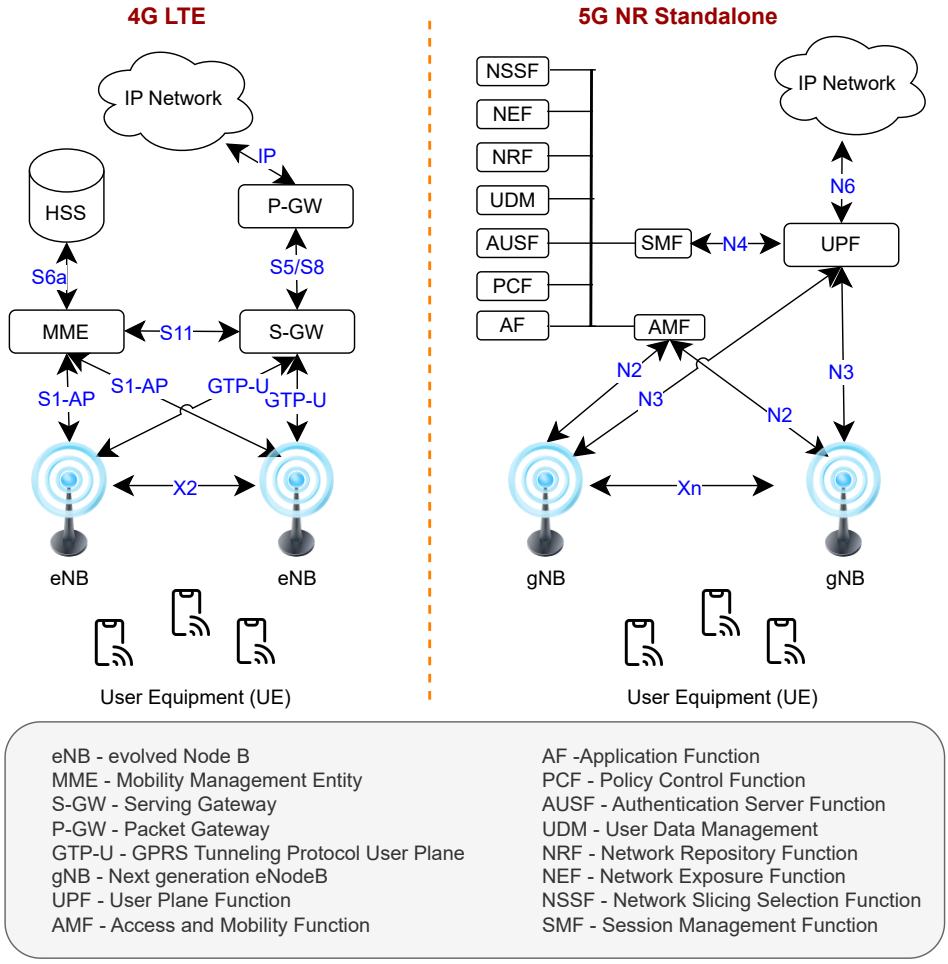

Figure 1.1: Cellular network architecture: (a) 4G LTE, (b) 5G NR Standalone.

greater bandwidth and throughput (enhanced mobile broadband or eMBB) [17, 18]. The new specifications in Third Generation Partnership Project (3GPP) Rel-15 and improvements for 5G NR is designed to offer the above mentioned features [19]. The UAVs are envisioned to be an essential part of 5G and beyond networks with potentials of supporting high data transmission (∼10 Gbits/s), stringent latency (1 ms round trip delay) and enhancements to radio access technologies (RATs). Moreover, the licensed mobile spectrum provides wide accessibility beyond visual line of sight (BVLoS), secure and reliable connectivity enabling cost-effective UAV operation for a multitude of use cases [20–22].

1.4 Integration Synergies of UAVs and Cellular System

Having looked at the brief introduction about UAVs and cellular network, one obvious follow-up question that catch our attention is - "*how do we integrate this two fundamentally different and independently evolving ecosystems (UAV and Cellular) to bring the best from both worlds?*" In this section, we answer this "how" question and describe **four** different paradigms of integrating UAV with cellular network, thus forming the basis of UAV-cellular communication and networking [23, 24], as shown in Fig. 1.2. Each of this paradigm is explained in the following subsections.

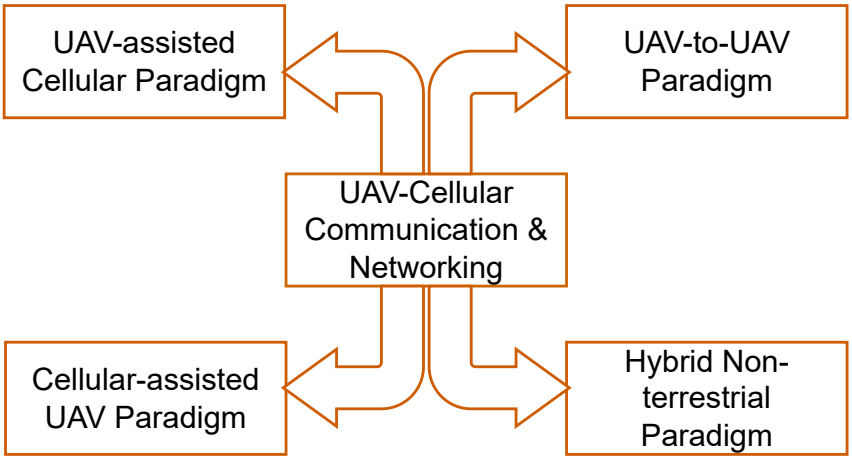

Figure 1.2: Integration opportunities of UAV with Cellular Network

1.4.1 UAV-assisted Cellular Paradigm

In this first paradigm, "UAV-assisted Cellular", the UAV offers help to existing cellular network by acting as a temporary wireless infrastructure in specific situations to provide improved communication services to ground users. Hence, in literature, it is also popularly known as UAV-aided cellular network. Specific examples include aerial base stations, aerial relays, sensory gateway or localization anchors, that can intelligently reposition themselves to assist the existing terrestrial cellular system to improve the user perceivable Quality of Experience (QoE), spectral efficiency and coverage gains [25, 26]. This paradigm is shown in Fig. 1a. With the great ability to dynamically reposition itself, the integration of UAV brings many advantages to existing terrestrial cellular system [10, 27]. The base station mounted on the UAV (*i.e.,* aerial base station or UAV-BS) could be provisioned on demand, which is an absolute appealing solution for disaster management, search and rescue or emergency response. The coverage and data rate of existing cellular networks can be improved by optimal 3D placement and coordination of aerial base stations to cater the user's need in hotspot areas. These benefits definitely cope well with diverse, dynamic and increasing data demands in 5G and beyond cellular systems. Chapter 2 and Chapter 3 present more details on this paradigm.

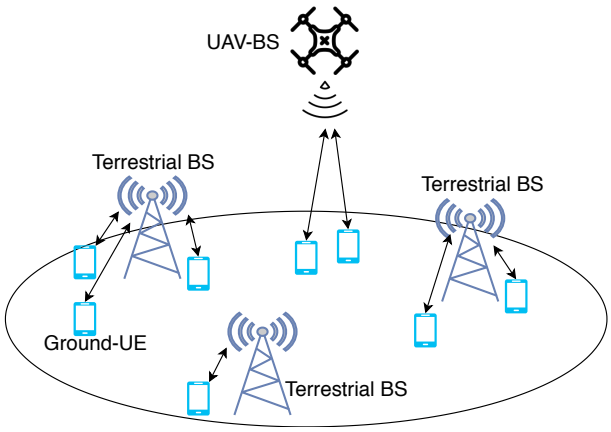

Figure 1.3: UAV-assisted Cellular Paradigm

1.4.2 Cellular-assisted UAV Paradigm

In the second paradigm, "Cellular-assisted UAV", existing cellular network deployment offers help to the UAV ecosystem in performing its mission where the UAV acts as a flying **aerial user** being served by ground cellular base stations. In literature, it is also popularly known as aerial UE or cellular-connected UAV or UAV-UE or drone-UE or 5G-connected drone and so on. This paradigm is shown in Fig. 1b. It has attracted significant research interest in recent times, because of the numerous use cases it can support and several open research challenges in establishing reliable wireless connectivity with ground base stations [28]. Chapter 4 presents more details on this paradigm.

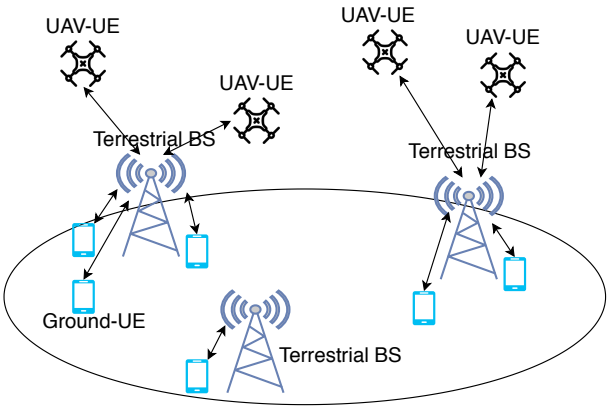

Figure 1.4: Cellular-assisted UAV Paradigm

1.4.3 UAV-to-UAV (U2U) Paradigm

In the third paradigm, "UAV-to-UAV", a swarm of cellular-connected UAVs or UAV-BSs reliably communicate directly with each other sharing the cellular spectrum with ground UEs to facilitate autonomous flight behaviours, cooperation in a UAV fleets, and collision avoidance. Such peer-to-peer connectivity in a multi-UAV mission is shown in Fig. 1c. In [29, 30], the authors investigated reliable and direct UAV-to-UAV (U2U) communications that leverage same frequency spectrum with uplink of ground UEs. Chapter 5 presents more details on this paradigm.

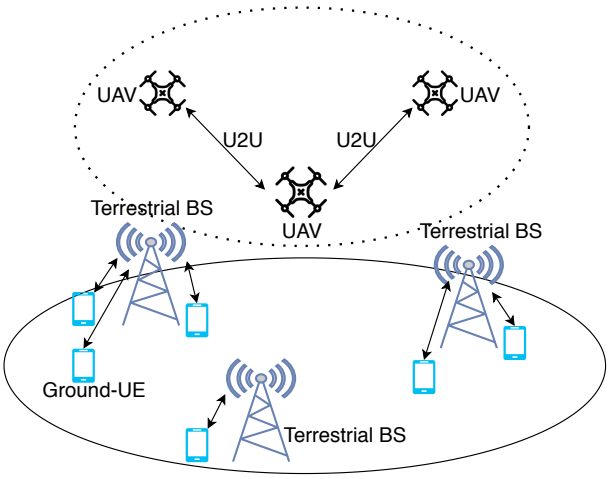

Figure 1.5: UAV-to-UAV Paradigm

1.4.4 Hybrid Non-terrestrial Paradigm

"Hybrid Non-terrestrial paradigm" brings forward the notion of an integrated space-aerial-ground communication network encompassing an intermediary swarm of UAVs establishing linkages between ground and space network. The integration of heterogeneous networks, such as '5G with satellites' or '5G with UAVs', is already a part of the standardization process for 5G by 3GPP. The links that connect the ground network with aerial ones make it possible to communicate through ground-to-aerial (G2A) and aerial-to-ground (A2G) links, which complement the wireless broadband access provided by the ground infrastructure. There are continuing discussions to build and construct network architecture that combines cross-layer, high and low altitude platforms (HAPs and LAPs), and space satellites into conventional cellular networks in order to inject more capacity and improve coverage for underserved regions in a cost-effective way [31]. This form of integrated terrestrial and non-terrestrial network elements is shown in Fig. 1d.

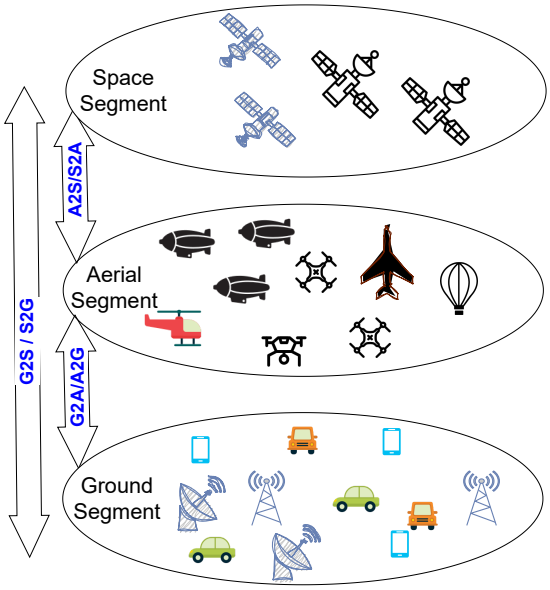

Figure 1.6: Hybrid Non-terrestrial Paradigm

Satellites and other means of long-distance communication fall under the "space" category. Satellite communication backbone (SATCOM) is centered on earth expanding to different orbital depths of the universe. Space-to-aerial (S2A) and aerial-to-space (A2S) transmission lines are an effective cross-layer inter-working method for transferring information from satellites to "aerial" and then to "ground" segment. The aerial segment is a key layer in implementing the multi-dimensional and inter-operational network of 6G vision because to its capacity to efficiently bind the other two levels, which are separated by thousands of kilometers. HAPs work with decreased transmission latency, cheaper cost, simple mobility in emergency scenarios, and broad coverage with high elevation angles, in contrast to SATCOM. Existing works demonstrate the cooperation between SATCOM and HAP for robust beamforming or boosting communication confidentiality. LAPs serve as a connecting connection to ground devices in cases when HAPs are not desired owing to their expensive cost in common civilian applications (e.g., temporary hotspots, sporting events). The LAPs could then bridge the link to HAPs and then to the space segment, enabling end-to-end communication from the ground device to the space network. Chapter 6 presents more details on this paradigm.

1.5 Scope of the thesis

This thesis provides a holistic perspective to UAV-enabled cellular communication and networking encompassing all of the above mentioned integration synergies. Precisely, finding answers to below set of fundamental questions remain the major objective of this thesis.

Q1. What are the emerging use cases in which UAV-cellular integration bring best from both ecosystem?

Q2. What are the special difficulties introduced by the propagation medium when UAVs are acting as aerial base stations under the UAV-assisted cellular paradigm? How can a real-world prototype of an open-source, 3GPP-compliant flying base station be built, and what hardware/software design decisions and components are required?

Q3. How can UAV-enabled cellular systems accommodate heterogeneous 5G service classes arising from wide range of vertical industries?

Q4. To what extent do 5G and beyond systems present substantial synergies with respect to its innovations with better radio hardware, cloudification, and virtualization technologies, and what kinds of integration challenges appear while integrating UAVs as aerial UEs of existing cellular network in Cellular-assisted UAV paradigm? Have we made enough progress in R&D for aerial UEs to become a reality?

Q5. Is a single UAV enough for all kind of mission? If not, why?

Q6. What are the communication challenges and benefits of a multi-UAV mission? When working with many UAVs, what special considerations must be made for effective communication?

Q7. What kind of cellular technologies support UAV-to-UAV communication in a swarm of multiple UAVs?

Q8. How do we foresee current technological advances in UAVs and 5G translating to future 6G systems? Where do we find these technological enablers?

To provide an overview of emerging real-life use case as a response to answer Q1, in this **Chapter 1**, Section 1.7 presents a thorough overview of diverse application scenarios in which UAV-cellular integration finds its direct application to accomplish the mission. The following subsection outlines the main contributions and high level organization of this thesis.

1.6 Contributions and Outline of the thesis

Chapter 2 describes the UAV-assisted cellular paradigm from the viewpoint of unique air-to-ground (A2G) channel model, architectural unification and prototyping framework of UAV base station to enable on-demand cellular connectivity. In a nutshell, the material presented in this chapter offers a thorough answer to Q2.

Chapter 3 provides a resource slicing and coexistence framework for UAV-assisted 5G RAN for simultaneous and effective multiplexing the three heterogeneous slice service types (eMBB, uRLLC and mMTC) over the common UAV-BS radio resources. A segregated, light-weight, two-phase slicing optimization model consisting of (i) resource optimizer (RO) module

and (ii) scheduling validator (SV) module, is proposed for dynamic resource slicing policy for computationally-constrained UAV-BS platform. The answer to Q3 is presented in this chapter.

Chapter 4 presents cellular-assisted UAV paradigm, in which UAVs are realized as aerial UEs that cohabit alongside ground-based UEs. Even while cellular-connected UAVs are becoming increasingly common, there are still a number of obstacles and operational problems that need to be explored before they can reach their full potential. In this chapter, we discuss several integration challenges that must be overcome in order to implement cellular-connected UAVs. Furthermore, it highlights most important technology advancements in the 5G era and beyond, as well as the continuing efforts in design development and field trials that support these claims. The answer to Q4 is presented in this chapter.

Chapter 5 presents collaborative multi-UAV deployment forming a swarm of cellular-connected UAVs to perform the mission. It discuses the 3GPP sidelink technology for inter-UAVs communications and provide a comprehensive characterization of Cellular-U2X (Cellular UAV-to-Everything). The answer to Q5, Q6 and Q7 are detailed in this chapter.

Chapter 6 highlights several novel 6G enabling technologies, and presents ongoing standardization activities, regulatory frameworks and socio-economic issues. The answer to Q8 is presented in this chapter.

Finally, we conclude the thesis in **Chapter 7** and provide future research directions. The high level organization of this thesis is shown in Fig. 1.7.

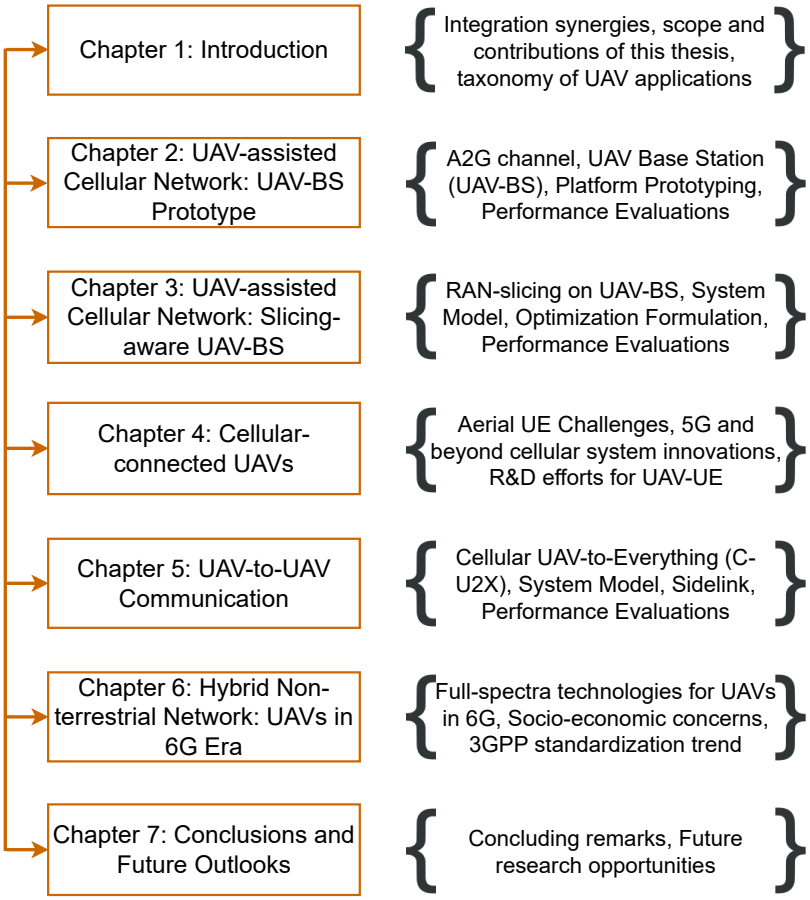

Figure 1.7: High level organization of this thesis

1.7 Taxonomy of UAV Applications

Before investigating deeper into the UAV-cellular integration challenges, 5G and beyond innovations and experimental synergies, an overview of real-world applications and use cases are presented in this section. The 5G mobile networks have greatly emphasized its design and development goals to foster service-oriented realizations from an early stage of evolution. Service-oriented 5G vision has attracted vertical industries, over-the-top (OTT) service providers to deliver their services to end users through 5G infrastructure [32]. Hence, the ultimate goal of integrating two different ecosystems (UAV and cellular ecosystem) must create value added services not only for mobile operators, but also satisfy the need of 5G and beyond vertical industries to serve their end users. In this subsection, some of the attractive researched domains with varying demands and goals are highlighted. A bird's-eye view of this subsection is presented in Fig. 1.8.

Earth and Environment Observation

As an innovative and efficient platform for gathering data, UAVs have become a preferred choice over traditional geomatics mechanisms of data acquisition. UAVs could autonomously fly in a defined trajectory and could precisely capture real-time measurements of the ongoing geophysical processes for abnormal hazards, such as volcanoes, landslides, sea dynamics, earthquakes, etc. Furthermore, the UAVs are equipped with various sensors to capture atmospheric temperature, pollutant levels in the air, carbon emissions, terrestrial biomass characterization, precipitation distribution in industrial zones, etc. As an efficient mechanism, the deployment of a fleet of UAVs, equipped with onboard sensors can perform the sensing for the presence of pollutant levels or any hazardous chemicals in the target areas [33, 34].

In a disaster situation, first 48 to 72 hours are very crucial to perform any kind of mitigation to the damage or outage and to restore the normal state of the environment. The response time is the key in saving lives in the affected regions. The major problems in these initial hours are: lack of proper communication infrastructure, massive or often unpredictable losses of lives and property. Thus, the situation forces the first responder teams to implement and improvise the search and rescue (SAR) mission to be conducted quickly and efficiently. Latest advancements of UAVs and sensor networks are capable to meet this need in terms of disaster prediction, assessment and fast recovery. UAVs can gather the information (e.g., situational awareness, early warnings, persons movement) during disaster phase and these information are helpful for first responder teams to react efficiently. UAVs can re-establish the communication infrastructure (*i.e.,* UAV-assisted paradigm) destroyed at the time of disaster.

Civil and Commercial Services

Government constructions and public infrastructures such as highways and railways are greatly benefited by these flying platforms for efficient surveillance, land surveying, tracking workers and employees, on-site construction and demolition [35–37]. Furthermore, UAV-based delivery systems are gaining wide popularity in logistics domain to achieve faster and cost effective good delivery service [38]. Such a system handles consumer orders, manages autonomous flight and status tracking using real time control. Google's Wing project and Amazon Prime Air are the some of the efforts to realize such a use case of UAVs. In precision agriculture, UAVs are capable of observing the agricultural fields for health monitoring, spraying pesticides and perform hyper spectral imagery. Such activities by humans are time consuming and prone to risks. Unmanned aircrafts are well suited for such use cases enhancing productivity and cost efficacy. The cellular

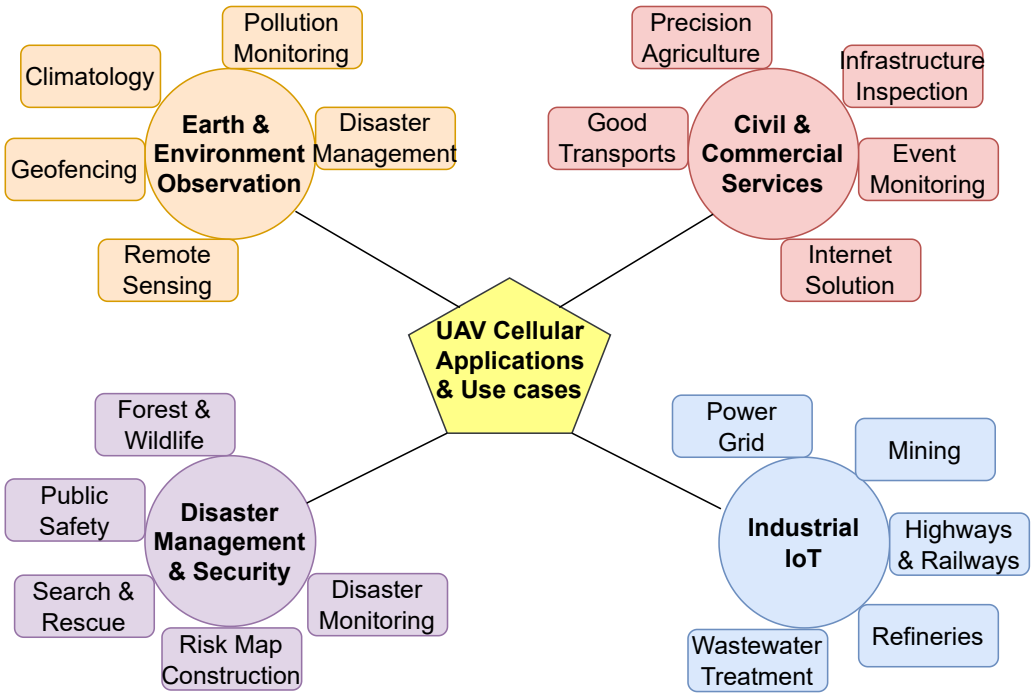

Figure 1.8: Taxonomy of UAV cellular applications, civil and industrial use cases

operators have started envisioning UAVs as backup wireless infrastructure (flying base stations or relays) in the absence of terrestrial communication infrastructure to boost network capacity [39]. Google's Loon project aims to provide ubiquitous Internet services & wireless connectivity to both remote and rural areas by employing high altitude platform (HAP) UAVs as balloons.

Some emerging technologies such as augmented reality (AR) and virtual reality (VR) combined with capabilities of UAV open up novel possibilities [40]. Real life videos from high altitude or high quality aerial photographs bring a great look and feel experience for users. Also, in the enterprise markets, the VR technology clients can accelerate buyer's decisions by presenting them best scenery and viewing of the real estate. AR- and VR-enabled UAVs are also used for virtual tour of the real environments, 3D models of buildings, graphical overlays of maps, streets, gaming, etc.

Disaster management & Security

UAVs are an effective means of surveillance and monitoring of areas stricken by a natural disaster. For instance, autonomous UAVs are sent to landslide, fire, earthquake and flooding areas to help with assessing the risks, the damages and support first responders teams as well as providing connectivity to isolated people [41–43]. Similarly, low cost UAVs revolutionize the conservation and management of forest and wildlife ecosystem by assisting in counting animal populations, tracking illegal activities, etc. UAVs are also an effective means of surveillance and control for the homeland security and public safety [44–46]. In case of anti-terroristic operations, UAVs are used to develop and prepare for situational awareness of threat, carrying out pre-emptive strikes or reconnaissance mission. UAVs assist in speeding up the rescue and recovery (search and rescue) missions in certain disastrous and crime control situations in a target area.

Industrial IoT platforms (IIoT)

Industry 4.0 is an emerging paradigm embracing next generation industrial developments with the ideas of using Internet of Things (IoT) to industrial automation, cyber physical systems, smart production and service systems. This industrial revolution is a gateway to boost economy and operational excellence under the umbrella term of "Smart Factory".

UAVs have already begun to become a vital component of Industrial IoT platforms [47, 48]. Practical usage of UAVs in industrial settings include monitoring terrains of manufacturing sites or regions that are impenetrable for humans due to hazardous exposures. The manual on-site inspection carried out by humans are time-consuming and often include very challenging terrains with inaccessible/unsafe zones. Such human-driven inspections pose threats to human lives. On the bright side, not only industrial UAVs can penetrate complex and inaccessible areas, but also are equipped with a multitude of sensors with cognitive computing to facilitate on-demand real-time bidirectional communication with industrial control stations. UAVs used in industrial settings can measure many parameters for the region under study via onboard sensors, such as electric and magnetic field strength, humidity, temperature, pressure in the atmosphere, methane or toxic pollutants. The communication could occur the same way as an IoT sensor sending signals to the Supervisory Control and Data Acquisition (SCADA) system.

1.8 Conclusions

The popularity of UAV is growing day-by-day and it is considered as a preferred technology to cater to a wide variety of emerging real-world use cases. UAVs can be autonomous, intelligent, adaptive and highly mobile. From communication and networking perspective, UAVs play an important role in cellular domain. The cellular ecosystem can benefit from UAV technology. UAVs can be efficiently integrated to existing cellular networks as a flying base station or a relay or an aerial UE. In this chapter, we outline four types of integration synergies of UAV and cellular system. Owing to the implicit benefits of cellular networks in terms of ubiquitous accessibility, large coverage, scheduled and safe information exchange protocols, UAVs are well suited and find their applicability in many real-world applications such as earth and environmental observation, civil infrastructure and surveillance, defence and security, industrial IoT platforms, etc. Integrating UAVs to 5G and beyond cellular systems proves to be a win-win situation for both the parties. The detailed taxonomy of various application domains with emerging use cases as well as the technical synergistic challenges of UAV integration with cellular network are discussed. Furthermore, the chapter presented the scope of the thesis and the neat outline delineating contributions from each of the chapter.

Chapter 2

UAV-assisted Cellular Network: UAV-BS Prototype

2.1 Introduction

An integration paradigm of UAVs with cellular network in which the airborne UAVs are realized as flying communication infrastructures to provide agile, on-demand communication services to the ground UEs[1] is referred as *UAV-assisted cellular network*. In particular, an airborne UAV equipped with 5G base station (BS) functionality (*i.e.,* UAV-BS) is not only capable to establish a distance-efficient line-of-sight (LOS) link for ground UEs due to its self-organizing maneuverability [49], but also, serves as a cost-effective platform to supplement to the network load of terrestrial BS infrastructure in addressing high spatio-temporal dynamics of the communication demand during flash-crowd, hotspots or temporary events [50–52]. In general, on-demand mitigation to dead-zones/coverage holes (*i.e.,* coverage expansion) or uninterrupted service offering to hotspots (*i.e.,* capacity expansion) are two most commonly discussed use cases of *UAV-assisted 5G cellular network*. A lot of research efforts have been produced by industry and academia in order to validate the true potentials concerning above use cases that claim an all-wireless airborne network in the sky is far less disruptive and takes far less time than ground-based infrastructures. In this backdrop, this chapter presents a deeper investigation towards UAV-BS, focusing on unique air-to-ground channel, design goals, proof-of-concept (PoC) implementation platform and improvements in communication performance through adaptive placement of UAV-BS. It should be noted that, in contrast to several existing works, the goal of this chapter is to examine the implementation and experimental prototyping aspects of UAV-BS, rather than to investigate numerous scientific difficulties of this paradigm, encompassing all active fields of research.

The following sentence reminds the reader of the fundamental question (Q2 in Section 1.5) that this chapter attempts to raise and discuss potential answers to.

> **Q2.** What are the special difficulties introduced by the propagation medium when UAVs are acting as aerial base stations under the UAV-assisted cellular paradigm? How can a real-world prototype of an open-source, 3GPP-compliant flying base station be built, and what hardware/software design decisions and components are required?

[1] In this thesis, UE and user are used interchangeably.

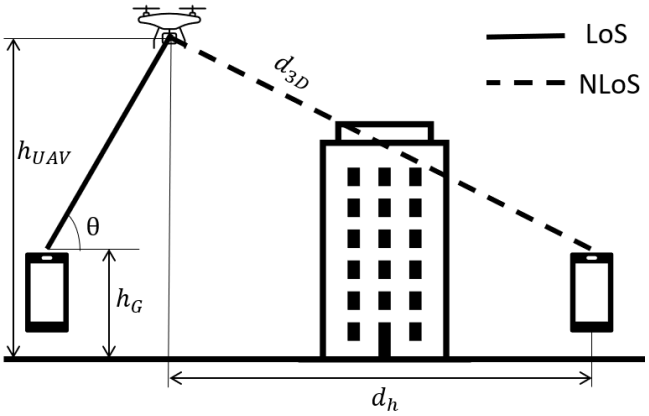

Figure 2.1: Geometry of Air-to-Ground propagation

2.2 Air-to-Ground (A2G) Channel

In wireless communication networks, the propagation channel is the medium between the transmitter and the receiver. As the medium properties largely define the physical limitations of wireless networks' performance (e.g., range, achievable throughput, latency) and directly impact the technology design choices, channel characterization and modeling become a crucial first step toward achieving the ambitious 5G and beyond performance goals.

The propagation medium between the UAV-BS infrastructure (air) and the ground UEs (ground) are characterized by unique properties different from those defined by ground BS to ground UE. The air-to-ground (A2G) propagation medium from UAV-BS to ground UE implies a high probability of line-of-sight (LOS) propagation (this is especially important for higher frequencies such as mmWaves and THz). This results in higher link reliability and lower transmission power required to ensure the targeted link budget [53]. Even for non-line-of-sight (NLOS) links at lower frequencies, power variations are less severe than in terrestrial communication networks due to the fact that only the ground-based side of the link is surrounded by the objects that affect the propagation [54]. Figure 2.1 illustrates A2G propagation channel and introduces the main geometrical parameters as well as drawing the important distinction between LOS and NLOS channels.

2.2.1 Propagation Basics

The transmitter radiates electromagnetic waves in several directions. Waves interact with the surrounding environment through various propagation phenomena before they reach the receiver. As illustrated in Figure 2.2, different phenomena such as specular reflections, diffraction, scattering, penetration or any combination of these can be involved in propagation [55]. Moreover, the blockage must be considered (see Figure 2.1). Therefore, multiple realizations of the transmitted signal, often termed as Multipath Components (MPC) arrive at the Rx with different amplitudes, delays and directions. The resulting signal is the linear coherent superposition of all copies of the transmitted signal, which can be constructive or destructive depending upon their respective random phases.

Typically, radio channels can be represented as a superposition of several separate fading

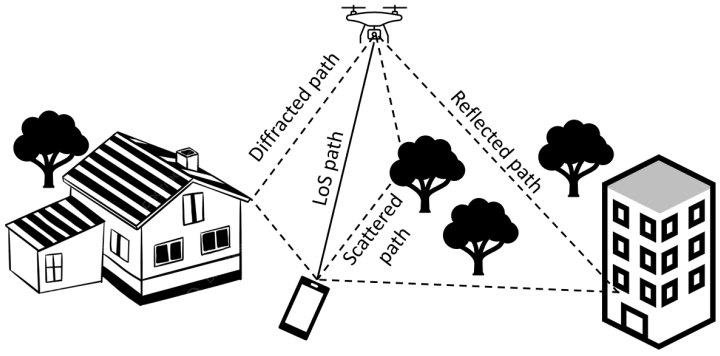

Figure 2.2: Air-to-ground propagation phenomena

mechanisms:

$$H = \Lambda + X_{sh} + X_{SS}, \tag{2.1}$$

where, Λ is the distance-dependent Pathloss (PL), X_{sh} is the Shadow fading (also known as shadowing) consisting of large-scale power variations caused by the environment, and X_{SS} is the Small-Scale fading (alternatively, fast fading). Next, let us describe models of the components presented in (2.1) separately.

2.2.2 Channel Model

There exist several channel models not drawing an explicit distinction between LOS and NLOS channels. However, the most common channel modeling approach consists of the four following steps:

- Define the link state (LOS/NLOS);
- Generate pathloss accordingly;
- Generate Shadow fading;
- Generate SS fading.

Line-of-sight modeling: In the case when the distinction between LOS and NLOS links is made, the LOS probability P_{LOS} modeling becomes critical. In this chapter, we describe a popular approach suggested by ITU[2] [57]. In [57], the LOS probability is given by

$$P_{LOS} = \prod_{n=0}^{m} \Big[1 - \exp\big(-\frac{[h_{UAV} - \frac{(n+1/2)(h_{UAV}-h_G)}{m+1}]^2}{2\Omega^2}\big)\Big], \tag{2.2}$$

where we have $m = floor(d_h\sqrt{\varsigma\xi} - 1)$, d_h is the horizontal distance between the UAV and the ground node, h_{UAV} and h_G are the terminal heights, ς is the ratio of land area covered by buildings compared to the total land area, ξ is the mean number of buildings per km^2, and Ω is the scale parameter of building heights distribution (assumed to follow Rayleigh distribution). In some cases, it is more convenient to express the LOS probability as a function of incident or

[2]Note that another popular model suggested by 3GPP in [56] is not applicable since it considers an aerial user connected to an elevated terrestrial BS.

elevation angle (e.g., in [54]). This representation can be found in [58].

It is worth noting that, the NLOS probability is computed from the LOS probability by the following equation.

$$P_{NLOS} = 1 - P_{LOS}. \tag{2.3}$$

Pathloss modeling: Pathloss is the distance-dependent attenuation experienced by radio signal while it propagates through the media. The simplest PL model assumes an LOS link between the transmitter and receiver, and propagation in free space. In this case, the received signal power is given as [59]

$$P_R = P_T G_T G_R \left(\frac{\lambda}{4\pi d}\right)^2, \tag{2.4}$$

where P_T is the transmitted power, G_T and G_R are the transmit and receive antenna gains, respectively, λ is the carrier wavelength, and d is the distance between the Tx and Rx[3]. Note that the Pathloss exponent (PLE) η (the power of the distance dependence) in this equation is 2 for free-space propagation. So that the path loss can be expressed for a generalized case as

$$\Lambda = \left(\frac{4\pi d}{\lambda}\right)^{\eta}. \tag{2.5}$$

Unfortunately, the signals in real-life A2G wireless communications do not always experience free space propagation. In the majority of literature, the well-known log-distance PL model with free-space propagation reference is used for PL (in dB) modeling:

$$\Lambda(d) = \Lambda_0 + 10\eta \log(d/d_0), \tag{2.6}$$

where Λ_0 is the PL at reference distance d_0 (Λ_0 can be specified or calculated as free space pathloss $\Lambda_0 = 20 \log\left[\frac{4\pi d_0}{\lambda}\right]$).

Finally, pathloss can be predicted based on a combination of LOS and NLOS components [60–62]:

$$\Lambda = P_{LOS} \cdot \Lambda_{LOS} + (1 - P_{LOS}) \cdot \Lambda_{NLOS}, \tag{2.7}$$

where $\Lambda_{LOS,NLOS}$ are the path loss for the LOS and NLOS cases, respectively, P_{LOS} denotes the probability of having an LOS link between the UAV and the ground node. The PLE values for Λ_{LoS} and Λ_{NLoS} can be found in Table 2.1 [54]. Note that these results are valid for the indicated frequency ranges and environments. Additionally, atmospheric absorption and rain attenuation can also lead to significant power loss for mmWaves and THz frequency bands.

Shadowing and Small-scale fading modeling: Apart from pathloss, large obstacles (such as buildings, vegetation, and vehicles) can cause position-specific random variations of received power. Typically, these variations are changing relatively slowly (in the order of a few tens or hundreds of wavelengths). This channel component is called Shadow fading. At any distance d, Shadow fading X_{sh} measured in dB is usually modeled as a normal random variable with a variance σ, which takes into account random variations of the received power around the pathloss curve. In Table 2.1, the standard deviation for the Normal distribution $\mathcal{N}(0, \sigma^2)$ describing Shadow fading can be found.

Small-scale fading describes the random fluctuations of the received power over short distances, typically a few wavelengths, due to constructive or destructive interference of MPCs

[3]For simplicity of notation, $d = d_{3d}$ in Figure 2.1

Table 2.1: Parameters of Pathloss and Shadow fading models

Scenario	Frequency, GHz	η	Λ_0, dB	σ, dB	Reference
		2.54-3.037	21.9-34.9	2.79-5.3	[63]
		2.2-2.6			[64]
		2.01			[65]
Suburban,		4.1		5.24	[66]
Urban, Open		2-2.25			[67]
field	0.968	1.6	102.3		[68]
	5.06	1.9	113.9		[68]
	0.968	1.7	98.2-99.4	2.6-3.1	[69]
	5.06	1.5-2	110.4-116.7	2.9-3.2	[69]
Urban (LOS)	28	2.1		3.6	[70]
Urban (NLOS)	28	3.4		9.7	
Urban (LOS)	38	1.9-2		1.8-4.4	
Urban (NLOS)	38	2.2-2.8		4.1-10.8	
Urban (LOS)	73	2		4.2-5.2	
Urban (NLOS)	73	3.3-3.5		7.6-7.9	

impinging at the receiver. Different distributions are proposed to characterize the random fading behavior of the signal envelope, suitable for different wireless systems and propagation environments. The Rayleigh and Rice distributions, both based on a complex Gaussian distribution, are the most commonly used models. Considering a large number of MPCs with amplitudes and random phases, the signal envelope of small-scale fading thus follows a Rayleigh distribution [59]. For A2A and A2G channels, where the impact of LOS propagation is high, the Ricean distribution [59] provides a better fit. Of course, other distributions such as the Nakagami[71], chi-squared (χ^2) and non-central χ^2 [61, 72], and Weibull distributions might also be employed. The family of χ^2 distributions is attracting our attention since many of the distributions listed above are particular cases of it.

Small-scale fading models apply to narrow-band channels or taps in tapped delay line wide-band models. Due to the stochastic nature of these signal variations, fading is usually modeled using statistical approaches and its models are obtained through measurements or through geometric analysis and simulations. The most popular type of small-scale models is Geometry-Based Stochastic Channel Models (GBSCM) [55].

2.3 Research Challenges

While there are several research issues associated with UAV-assisted cellular communication, we aim to highlight some notable challenges that must be considered before successful roll-out of system encompassing UAVs as part of aerial network infrastructure [10].

Optimal Positioning: It is clear that proximity to the user is helpful for enhancing the quality of service (QoS) provided to the user due to the greater SINR and LOS likelihood [25]. UAVs take use of their great relocating flexibility to position themselves in appropriate areas in order to provide the user with a higher QoS. However, making optimal placement selections in airborne networks is not simple. First, both the user and the UAVs are mobile during the operation, resulting in a time-varying channel. In other words, a little user or UAV or both

movement invalidates a superior serving position. Second, users with varying QoS requirements create trade-offs in which the best placement option cannot be reached with fine temporal granularity. In an ideal circumstance, for instance, a better serving position would be determined in each transmission time interval (TTI) when user scheduling occurs, however this is extremely difficult from a realistic viewpoint. Third, the precise deployment of unmanned aerial vehicles (UAVs) must be based on accurate radio maps, which may not be available in an unpredictable environment. This will result in a considerable amount of time spent constructing the radio map based on the various user locations.

Cooperative Control: Due to the rising complexity of missions and the limiting capabilities of a single UAV, a multi-UAV system (UAV fleet or UAV swarm) is becoming the obvious choice for accelerating mission completion. Multi-UAV deployment with cooperative route planning and control is essential for cooperatively optimizing user services and preventing UAV collisions [73]. This could take one of two forms: (a) centralized control, in which a centralized entity is responsible for pre-computing the time-dependent flight paths for UAVs and assigning them to each UAV on mission; or (b) decentralized control, in which each UAV runs its own movement control and reacts autonomously to the behavior of other UAVs in the fleet. A decentralized category offers greater benefits in autonomous UAV behavior as a result of a collaborative planning and optimization process that reaches an agreement among them.

Wireless Backhaul: In terrestrial infrastructure, the backhaul is frequently a high-speed, multi-gigabit, dedicated fiber link distributed from the BS site to the core network. When UAVs are working as the aerial base stations, this link is wireless and suffer from numerous constraints in terms of gathering user data and deliver them to the core network. Recently, Millimeter wave has been proposed as an enabler to answer the speed need in the backhaul, although such an implementation increase the complexity owing to high atmospheric absorption loss, high frequency range of operation, and need of directional antennas for transmission [74].

Energy constraints and Recharging: In every case where a UAV ecosystem is used, the amount of energy available is one of the most important factors to think about in order to provide continuous, high-quality service [10]. UAVs are energy-constrained machines that runs largely on battery or solar power. There has been a flurry of studies lately looking into the feasibility of gasoline fuel that might last for days at a time with no interruptions. For the most part, this will rely on the mass and dimensions of the UAVs involved in the communication operation. UAVs have a total energy consumption that takes into account not just the mission's demands but also the UAV's own weight and any extra payload it carries during landing and takeoff. The restricted onboard energy still substantially inhibits the practical implementation of longer mission, despite the availability of energy harvesting technology and effective storage units. Iterative recharging and mission integration is considered by the authors in [75] and [37] for efficient UAV operation over extended periods of time.

Interference Management: When more than one aerial BS is active, it causes interference not just between itself but also with the ground-based stations [76]. Additionally, non-serving UAV base stations may be negatively impacted by uplink interference originating from terrestrial user transmissions. As a result, there has to be appropriate interference mitigation mechanisms in place to reduce the possibility of interference between UAVs and terrestrial BS.

While each of the aforementioned research challenges can lead to distinct but related sub-

problems, in this chapter, we are primarily concerned with determining the optimal positioning of the UAV-BS. Unlike many previous research that are based on mathematical modeling and system simulations, we want to *explore and evaluate UAV-BS optimum placement using a proof-of-concept (PoC) prototype platform that we created from scratch.* As a result, the next section provides *a full overview focusing on the design and construction of a real-world UAV-BS prototype platform.*

2.4 UAV-BS Prototype Platform

While integration of 5G and UAV ecosystem to design an all-wireless airborne UAV-BS network in the sky is perceived as a transformational way to make wireless connectivity more efficient and dependable, the real-world PoC implementations that focuses on joint design of aerial robotics and cellular communication capabilities are lacking. On a broad viewpoint, *FlightStack* and *CommStack* are two fundamental interacting entities in the UAV-BS framework. *FlightStack* refers to the autopilot firmware and associated programs that closely manage the UAV hardware to keep it aloft in the air, while being controlled back by ground operator. *CommStack* refers to the "5G and beyond" radio access network (RAN) protocol stack that enables base station features on the UAV. The performance and manageability of UAV-BS would be significantly improved by a single framework combining the UAV and cellular ecosystem as opposed to leaving the *FlightStack* and *CommStack* extremely isolated in the architecture. We envision a middleware that, in contrast to previous prototypes [25], integrates the *FlightStack* and *CommStack*, while keeping them independent and modular.

2.4.1 Related Works on Prototyping

UAV-BSs are cost-effective implementation than terrestrial BS, thereby making them suitable for applications like temporary connectivity, unpredicted crowd, on-demand services. It is feasible to exploit and maintain LOS links that could lead to improvements in a given communication objective. However, realizing UAV-BS in real-world operation requires various pieces to come together, and its design and implementation puts forward complex challenges to solve. There are numerous works in literature that analytically models and optimizes number of UAV-BSs required to serve multiple UEs, 3D dynamic positioning for optimal communication services etc [73, 77, 78]. However, real-world implementations to experimentally capture challenges along with benefits offered by UAV-BS are scarce. Additionally, unification of two different ecosystems (*i.e.,* both UAV and cellular) to realize UAV-BS, brings forward hardware and software integration challenges encompassing *CommStack* and *FlightStack*.

A real-world implementation of a UAV-based LTE-relay is pursued in [79] and the authors present preliminary results on its autonomous placement to serve a ground UE that is far-away from terrestrial BS. The practical experiment includes a single terrestrial BS, a single UAV-relay and a single UE. The LTE-relay places itself in an optimal location the improve the throughput of the ground UE. In [80], a quality-aware placement of UAV-BS is presented that on-the-fly repositions itself for improving UE network performance in real-time. The prototype is implemented using open-source 4G/5G software stack, Openairinterface [81] with USRP B200min-i SDR and PX4 autopilot. Similarly, the authors in [25] presents SkyRAN, an on-demand, dynamic airborne LTE infrastructure to optimize communication service offerings to ground UEs. SkyRAN testbed uses Openairinterface and DJI Matrice 600 Pro UAV realize the UAV-BS. In [82], the authors intended to quantify the performance gain that is achievable by using UAV-mounted access point in order to create an on-demand WiFi network in a region of interest.

Table 2.2: UAV Hardware and All-Weight-Up (AWU)

Component Name	**No. of Units**	**Weight (grams)**	**Total weight (grams)**
TMotor U7-V2.0 KV280	4	317	1268
22 x 6.6 Carbon Fiber Propeller	4	45	180
Pixhawk 4 mini Autopilot	1	25	25
6S 22000 mAh, 22.2V LiPo Battery	2	2500	5000
Gryphon Dynamics X8 800 Frame	1	990	990
TMotor Flame 70 Amp 6S ESC	4	55	220
CommStack	1	500	500
Total takeoff weight			**8183**

In aforementioned implementations, the authors did not emphasize the joint design of robotics and wireless components, rather kept them functionally decoupled from each other. In other words, the communication devices are mounted as a payload on the UAV platform that carries them. The work in [83] presents "SkyCell", a real-time implementation of UAV-BS that makes an attempt to unify the flight control and cellular stack in order to guide the UAV trajectory with the help of an exploration-exploitation algorithm. However, the authors did not show any comparison of UAV-BS placement with respect to available placement options *e.g.,*. at centroid of UE location cluster or prioritized traffic-aware placement.

2.4.2 Main Contributions

Differently from above existing works, in this chapter, we present a proof-of-concept (PoC) implementation of UAV-BS platform. The prototype not only features high-level mission APIs that unifies *CommStack* and *FlightStack* functions to configure communication missions, but also position itself to improve the radio connection quality to the connected UEs on the ground terrain. The developed prototype exploits unification of robotics and networking components to improve the system performance as compared to decoupled UAV-BS designs present in existing literature. The main contributions in summary are:

- Joint development of CommStack and *CommStack* and *FlightStack* functions (Section 2.4.3);
- Design and development of a middleware for above unification, and implementation of features encompassing autonomous mobility, fail-safe flight behavior during UAV-BS mission (Section 2.5);
- Open-sky performance evaluation using the prototype (Section 2.6).

2.4.3 Our Prototype

Fig. 2.3 shows the real-world UAV-BS prototype developed. The UAV is designed considering the required flight time and maximum supported communication payload [84]. The custom-built UAV platform is assembled entirely using commercial off-the-shelf (COTS) hardware component. The dimension of the platform is 960 mm, spanning between two opposite motors. It can carry a total takeoff weight of nearly 15.704 Kg when all the motors operate at 85% throttle for a flight time of 35.68 minutes. The components and endurance calculation of the UAV are given in Tables 2.2 and 2.3.

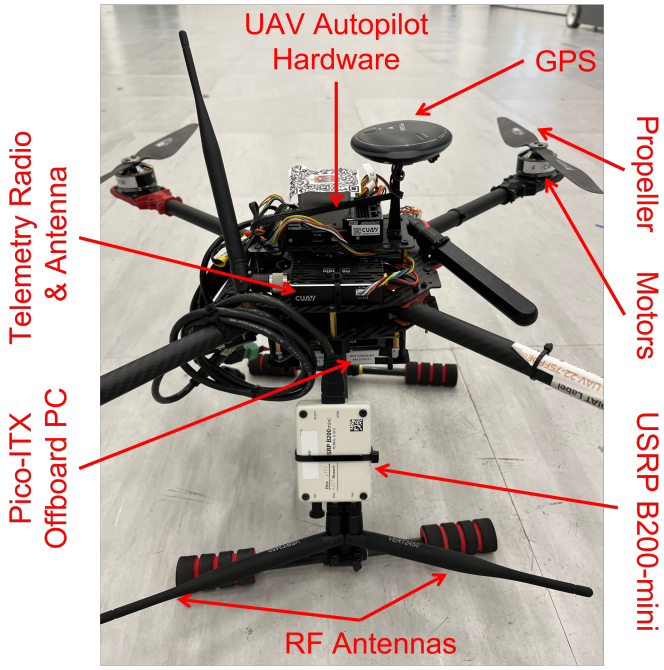

Figure 2.3: UAV-BS Prototype Platform

Table 2.3: UAV-BS Endurance Calculations

Throttle (%)	Motor thrust (grams)	Total thrust of UAV	Motor current (in Amp)	Total current (in mAh)	Endurance (in minutes)
55	1956	7872	8.5	566.67	77.65
60	2264	9056	10.6	706.67	62.26
65	2615	10460	13.2	880	50
75	3218	13124	1.6	1240	35.48
85	3926	15704	25.7	1713.33	25.68

2.4.4 Design Components and Schematics

The design components and schematics of the UAV-BS prototype is shown in Fig. 2. The UAV is equipped with a companion computer (also known as "offboard") that is connected with the autopilot through UART connection. The offboard hosts the application software *i.e.,* the *CommStack* for base station. The RF unit is connected to the offboard via USB3 port and *CommStack* sends the signal samples over the air via the antenna connected to the RF. The middleware that glues between the *CommStack* and *FlightStack* is a vital part of UAV-BS. The middleware is fully implemented in software and installed on the offboard computer. From functionality point of view, it is the combination of "NetController" (set of APIs managing *CommStack* features), "DroneController" (set of APIs managing *FlightStack* and autopilot navigation features) and "AppController" (high-level APIs managing the applications or services as part of the UAV-BS mission). The segregation of functionalities in different controllers allows flexible implementation, modular design and improved manageability while keeping a unified view of all the control functionalities within UAV-BS middleware.

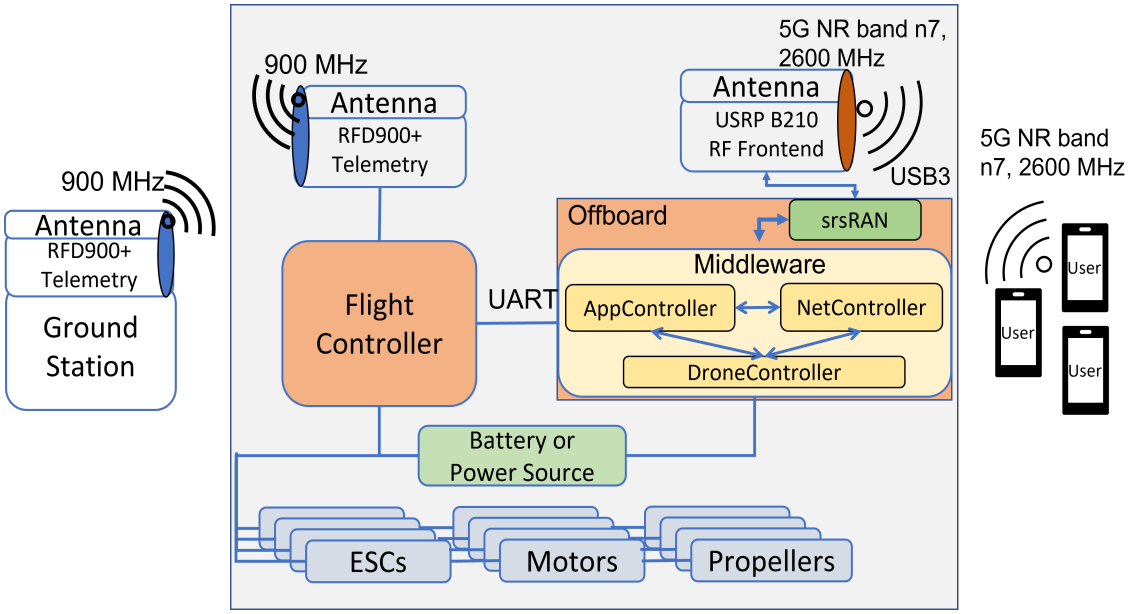

Figure 2.4: Design and Schematics of UAV-BS prototype

UAV and *FlightStack*

For flight controller, we used Pixhawk 4 mini, an open-source flight controller to control the UAV during flight mission supporting MAVLink protocol control. UAVs are equipped with GNSS integrated modules that allows us to a precision accuracy of xx meters. To improve the accuracy, we used RTK upgrade to standard GPS. (Centimeter level accuracy). The telemetry control of the UAV occurs through 900 MHz RFD900+ radios. Two battery packs of 22000 mAh are used to achieve a flight time of 60+ minutes when all the UAV motors operate at 60% throttle. The offboard used is a PICO-TGU4 compact PICO-ITX board containing 11th generation Intel core i5, x86 processor with 32 GB LPDDR4 onboard RAM memory, 256 GB SSD storage. The offboard draws a current of 3 A at 12 V. The offboard is enclosed with a light-weight enclosure case for safety and keeps track of UAV GPS locations, altitude, velocity, and other navigation metrics. The offboard provides waypoint updates for the UAV to visit. We associate radio measurement readings with geographic positions.

CommStack

To realize the 5G base station, we used USRP B200-mini SDR card with 5G frequency band n7 (2680 MHz). It is connected to a pair of Vert 2450 antennas for Tx and Rx processing from USRP device. USRP B200-mini is a low-cost, open-source SDR with 1x1 transceiver chains based on Xilinx Spartan-6 FPGA, operating between frequency range 70 MHz to 6 GHz. The SDR and offboard are connected through USB 3.0 connector. On the software side, the 5G base station radio protocol (*i.e., CommStack*) runs on Ubuntu 20.04 LTS. *CommStack* is realized using srsRAN [85], release 22.04, which is available as open-source repository in public GitHub domain. Main parts of srsRAN are srseNB, srsEPC. srsRAN supports 3GPP rel-15 compliant 5G protocol stack that runs on commodity x86 based Linux offboard. The *CommStack* is configured to run in FDD/TDD mode, 10 MHz bandwidth of NR band n7.

Ground User/UE

The UE used is Samsung A42 5G smart phone with Sysmocom SJA2 programmable SIM card.

Middleware Message Flow

The envisioned implementation of middleware is based on message-passing based inter-process communication between srsRAN (*i.e., CommStack*) and PX4 autopilot (*i.e., FlightStack*). ZeroMQ, a message-passing networking library is used for above purpose. Depending upon the nature and direction of the message flow, we describe following operational flow during mission.
FlightStack $\rightarrow$ ***CommStack***: PX4 sends periodic GPS info to srsRAN. This is unidirectional message flow. We used srsRAN as subscriber and PX4 as publisher (implemented as ZeroMQ PUB-SUB socket). Periodicity of message flow is kept at 1 Hz *i.e.,* 1 GPS update per second. This ensures that the base station is aware of precise GPS location (latitude, longitude) during mission at all the time.
CommStack $\rightarrow$ **Ground UEs**: The srsRAN offers communication services to the ground UEs (smartphones). Important real-time communication metrics such as UE-specific RSSI values, downlink and uplink signal strengths are stored on the offboard computer. Above requirements necessitate to implement srsRAN as a publisher and offboard as a subscriber of the communication metrics. Periodicity of message flow is kept at 1 Hz *i.e.,* 1 update per second. These logs are critical to implement innovative data-driven algorithms for UAV-BS. Potential benefits are leveraged by AI/ML-based learning algorithms and optimization. Using these communication metrics/logs, the offboard computer determines an effective position in 3D space where the UAV-BS should be placed during mission that improves a given communication objective. Let us call this effective position as "next_setpoint".
CommStack $\rightarrow$ ***FlightStack***: The *CommStack* sends this "next_setpoint" to PX4. PX4 fly to the location pointed by next_setpoint. From implementation point of view this is realized by asynchronous socket (ZeroMQ Request-Reply).

2.5 Middleware Controller

The middleware controller forms a vital component of the UAV-BS platform. Unlike several existing works in the literature [25, 80], this work designs a middleware that interacts with both *FlightStack* and *CommStack*. This middleware can be tailored for RAN-aware intelligent decision making and resource management in UAV-BS. This modular deign and separation of responsibilities offer advantages to the network operator in managing multiple UAV-BSs.

Precisely, the middleware is a software module/agent that acts as a broker between *FlightStack* and *CommStack*. This is deployed on the offboard computer with an interface towards *FlightStack* and another interface towards *CommStack*. As shown in Fig. 2, the middleware is functionally subdivided into three distinct components as described below.

2.5.1 DroneController

This component of the middleware takes care of interfacing and message exchanges with the *FlightStack*. DroneController objectives are to ensure offboard flight control mode operation is flight-safe and the waypoint input provided by UAV-BS is properly sanitized and validated. In our implementation, DroneController uses MAVROS [86] as main drone API, unit testing with GoogleTest and CppCheck [87] for static code analysis. The communication interface between

FlightStack and DroneController makes use of ZeroMQ socket library [88] and parsing JSON data functionality with defined message protocol format. An example of DroneController control module use case to depict the flight-safe features are shown in Fig. 2.5.

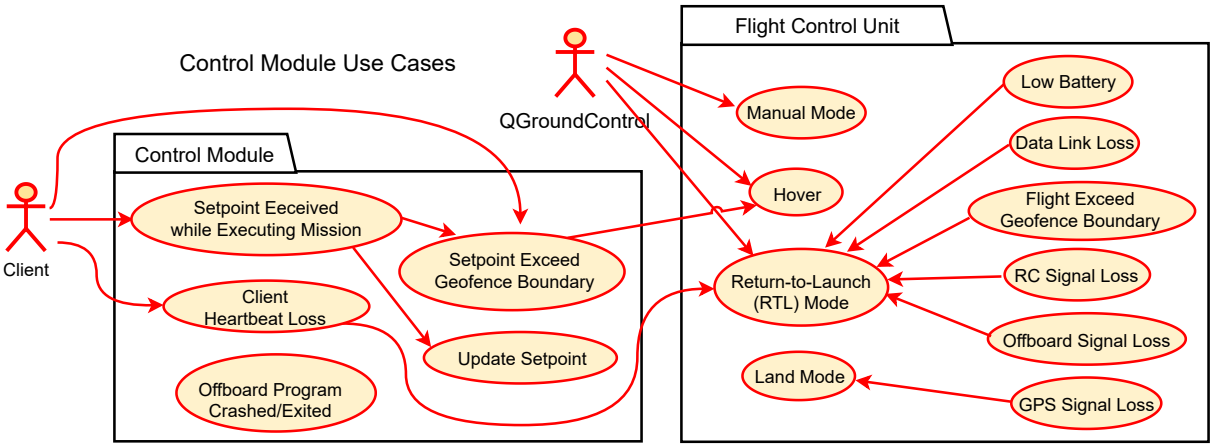

Figure 2.5: DroneController flight-safe implementation

2.5.2 NetController

The NetController is the RAN side controller that takes care of the network-related decision making and optimizations by frequently exchanging messages with *CommStack*. It gathers the radio measurements, communication signal strengths (RSRP, SINR etc.) for individual ground UEs. These data are utilized by the NetController to employ suitable optimization procedures to meet desired application quality of service (QoS). With respect to the adaptive positioning of the UAV-BS, we use a light-weight, lookahead-based exploration technique to do short flights to the 10 neighbors of current UAV-BS position. These 10 neighbors are the adjacent grids (4 directions, 4 diagonal directions, up and down) of 1m x 1m square grids. The neighbor that generates optimal performance is then added to the flight path and this procedure continues until the UAV-BS reaches the global optimum.

2.5.3 AppController

AppController is considered as driver for business logic and custom implementations defined by the network operator. For example, envisioning a service-oriented 5G vision, vertical industries or communication service providers (also referred as tenants) define high-level network objectives for the UAV-BS, and NetController along with DroneController tune parameters internally to meet those objectives. For example, AppController would expose APIs to tenants/vertical industries for creation of network slices on the UAV-BS serving UEs belonging to heterogeneous 5G services.

2.6 Performance Evaluation

The UAV-BS test-bed is deployed in an outdoor environment of 1200 m^2 area. The performance results are based on 10 test flights within the outdoor space and averaging the results for overall performance analysis. Four Samsung A42 5G smartphones (UEs) are deployed on the ground and one UAV-BS node is used to serve all the ground UEs. Our goals in the experiments are to use

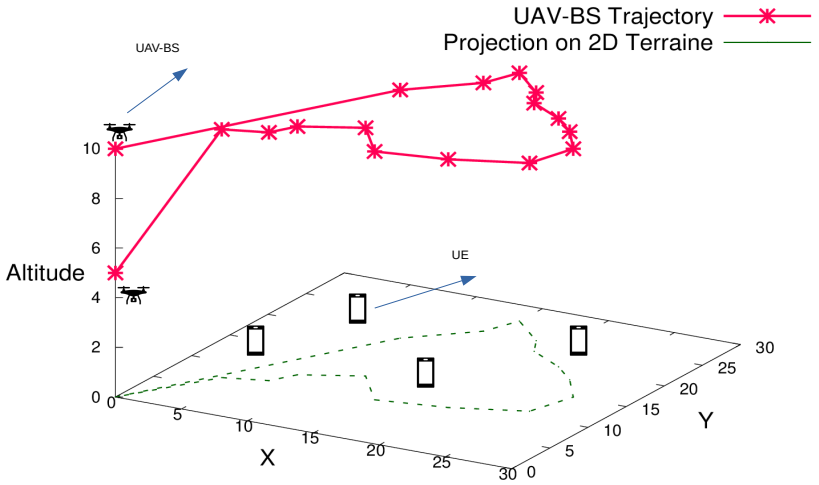

Figure 2.6: UAV-BS trajectory in 3D space and its projection in horizontal terrain

UAV-BS to experimentally validate dynamic UAV-BS positioning for improved communication quality. Note that, our aim in this section is not to propose a new dynamic UAV-BS placement algorithm, rather leverage the developed prototype to assess the communication performance with the help of known/existing UAV-BS placement algorithms using real-world outdoor flight experiments.

2.6.1 Experiment #1: Arbitrary Placement

In this experiment, four UEs are placed statically at random positions inside the test region and the UAV-BS is initially placed at 10 m height at one corner. The UAV then follows a random flight for a duration of 60 seconds within the test region and returns back to similar position at a height of 5m. Fig 2.6 depicts the trajectory followed by the UAV and experimental setup. Note that, for positioning, our experiment utilize the GPS coordinates obtained from the GPS sensor attached to Pixhawk autopilot and the UAV-BS navigates as per real-time GPS locations obtained from GPS sensors. For easy reference in Fig. 2.6, the starting GPS coordinate is assumed to be at origin (0,0) and all other positions are relative to origin. In this experiment, the UAV-BS does not take into account any UE-specific measurement reports to optimize its trajectory, rather performs random flights in order to establish the need of dynamic UAV-BS positioning to improve the communication quality intended for ground UEs.

Fig 2.7 shows the variation in aggregated throughput perceived by all the UEs due to random flight taken by UAV-BS. There are two main observations that can be derived from this figure. First, the aggregate user throughput is highly bursty in nature and not all the positions in the UAV-BS trajectory (*e.g.,* at 20s) result in optimal communication performance. This observation is inline with many results shown in existing literature that use analytical models. Second, the number of optimal positions are limited *i.e.,* few maxima positions exist. Therefore, a UAV-BS positioning algorithm would need to exploit the current UAV-BS position and amount of extra reposition distance needed to optimally serve the ground UEs.

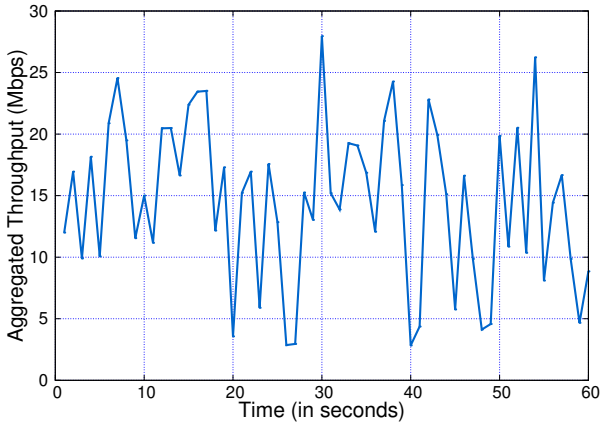

Figure 2.7: Aggregated downlink throughput by the ground UEs

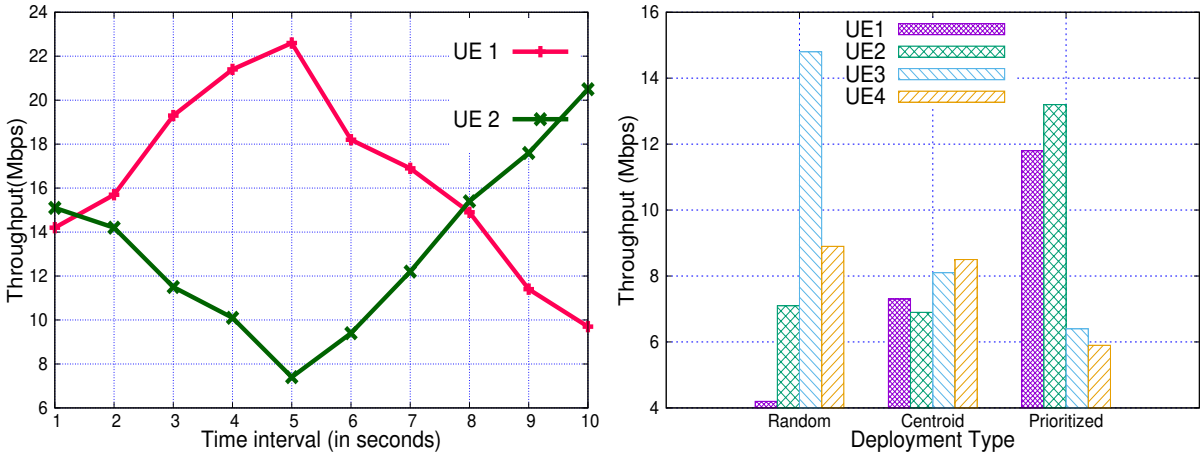

(a) (b)

Figure 2.8: (a) Variation of throughput (b) Throughput vs different deployment type

2.6.2 Experiment #2: UE Location-based Placement

Motivated from above experiment, we exploit the ground UE location information in order to guide the UAV-BS to choose better serving locations. Two ground UEs (Samsung A42 smartphones), UE1 and UE2 are placed 30 meter apart inside the outdoor arena test-bed and one UAV-BS is placed at the center of both UEs. The UAV-BS is slowly moved in a straight line to UE1 and then fly back towards UE2. The variation in the downlink throughput for both the UEs are presented in Fig. 2.8a. It is evident that when the UAV-BS was at the center (*i.e.,* at barycenter or centroid when number of UEs are more than two), both UEs were able to generate nearly same throughput. The movement of UAV-BS towards UE1 results better signal conditions for UE1 than UE2, thereby improving the achievable throughput for UE1 and degrading the throughput for UE2. Similarly, form the figure, we can observe that the movement of UAV-BS towards center position equalizes the throughput received for both UEs.

2.6.3 Experiment #3: Traffic-aware (Prioritized) Placement

In this experiment, in addition to the ground UE location information, we also take into consideration the traffic demand from the ground UEs. In order to be able to offer fair services, the UAV-BS need to reposition itself in an optimal location that improves the overall quality of signal or throughput. Four Samsung A42 smartphones are deployed inside the outdoor arena at random locations and one UAV-BS is deployed to serve them. Using iperf3, continuous UDP/TCP traffic are generated from these UEs. The UAV-BS use a weighted average estimation combining both the outstanding traffic from the UE and its current location (distance from UAV-BS) in order to derive the optimal location to serve. In other words, the UAV-BS prioritizes its movements towards a UE that has highest weighted average. To evaluate the performance for such preferential treatment among ground UEs, we present the comparison among three UAV-BS placement options. "Random" denotes a placement strategy were the UAV-BS placement is agnostic to user traffic demands and UE location on the ground. "Centroid" denotes a placement strategy were the UAV-BS placement is agnostic to user traffic demands, but takes into account the current UE location information while deriving the optimal location. "Prioritized" denotes a placement strategy were the UAV-BS placement is aware to both user traffic demands and current UE location information.

Fig 2.8b presents the overall comparison of all the placement options of UAV-BS. It is evident that, the choice to consider traffic demand from the UEs along with the current location information within the optimal positioning framework significantly improves the user throughput and fairness to users. The "Centroid" option primarily drive UAV-BS trajectory aiming at offering a fair communication performance to all the ground UEs involved. Hence, in Fig 2.8b, all the UEs are able to achieve more or less same throughput guarantees. The "Prioritized" or traffic-aware placement option is suitable is cases where the network operator wish to emphasize certain class of UEs to be benefited from UAV-BS placement. For example, a vertical industry or over-the-top (OTT) service provider may rent the UAV-BS infrastructure as a tenant of the 5G services and demands preferential treatment over other existing vanilla customers. This lays the foundation and motivation towards a network slicing based UAV-BS design that can slice/partition its available radio/transport/core network resources and utilize dynamic positioning to improvise service offering to a group of end users. Chapter 3 describes the UAV-BS with network slicing capabilities for heterogeneous 5G service classes encompassing eMBB, uRLLC and mMTC users.

2.7 Conclusions

In this chapter, we presented essential modeling parameters of airborne A2G channel propagation including pathloss, shadowing and fading behavior. Various research challenges are introduced concerning UAV-BS adaptive positioning, cooperative control, backhaul and interference. We introduce and describes the framework and real-world test-bed of UAV-BS that unifies UAV *FlightStack* and cellular *CommStack* for high-level communication missions. The implementation is realized with open-source 4G/5G stack, srsRAN and Pixhawk flight management firmware. It is equipped with a software middleware based on MAVROS API with neat interfaces to handle the tasks and interactions with flight or RF processing blocks. This framework is used to validate the performance benefits with respect to the flexible positioning of UAV-BS to achieve UE-specific QoS targets. We performed real-world flight tests that demonstrate the gains for different UAV-BS placement choices. We believe that, this study will motivate further research and exploration in regards to prototyping in UAV-assisted cellular communication.

Chapter 3

UAV-assisted Cellular Network: Slicing-aware UAV-BS

3.1 Introduction

Existing 5G mobile networks have greatly emphasized its design and development goals to foster service-oriented realizations from an early stage of evolution. Besides legacy broadband services in 4G, inherent support for enhanced mobile broadband (eMBB), ultra-reliable low-latency communication (uRLLC), and critical massive machine-type communication (mMTC) are identified as key pillars in its development ecosystem [89]. Service-oriented 5G vision has attracted vertical industries, over-the-top service providers to deliver their services to end users through 5G infrastructure [32]. To meet aforementioned requirements in 5G and beyond cellular systems, mobile network operator (MNO) leverage *network slicing* as a key enabler where multiple service-specific logical networks (called 'slices') are created and customized to fulfill QoS defined by the *tenant* [90]. A tenant is often referred as a *slice owner* and described as an entity that requests communication services from the MNO. The MNO is referred as the *slice provider* who allocates a portion of infrastructure resources (*radio bandwidth, power, computation, fiber*) to tenant. This is a win-win situation for both tenant and MNO, because, (i) the tenant deploys the services without owning and managing any real infrastructures, (ii) MNO is benefited from a revenue model (monetizing on QoS) by renting slices to tenant those wish to support a particular group of customers, or market segment.

Envisioning architectures and systems that support future UAV-enabled communication system in 5G and beyond networks, our work investigates and evaluates a UAV-BS platform empowered with network slicing capabilities. Fig. 3.1 highlights the fundamental radio slicing architecture of UAV-assisted 5G RAN serving three heterogeneous class of ground UEs. Each tenant issues a service request for a desired slice configuration indicating the slice service type (eMBB or uRLLC or mMTC), QoS of the supported users, time bounds for slice life cycle maintenance. The MNO performs an admission control check verifying the availability of enough channel resources (by adopting a slicing policy) and then dynamically allocates a portion of radio bandwidth to support instantiation of slice request. To enable above operational flow of tenant-MNO, a slice management and orchestrator (SMO) component manages the slice life-cycle from slice request to slice commissioning and slice decommissioning. An intelligent controller (*i.e.,* a near real-time RAN intelligent controller (RIC) design of O-RAN alliance [91]) interfaces with each UAV-BS agent control/user plane to provision intelligent radio resource allocation for UAV-BS satisfying the per-slice need. The closed-loop signaling and feedback from UAV-BS agent to the near-time

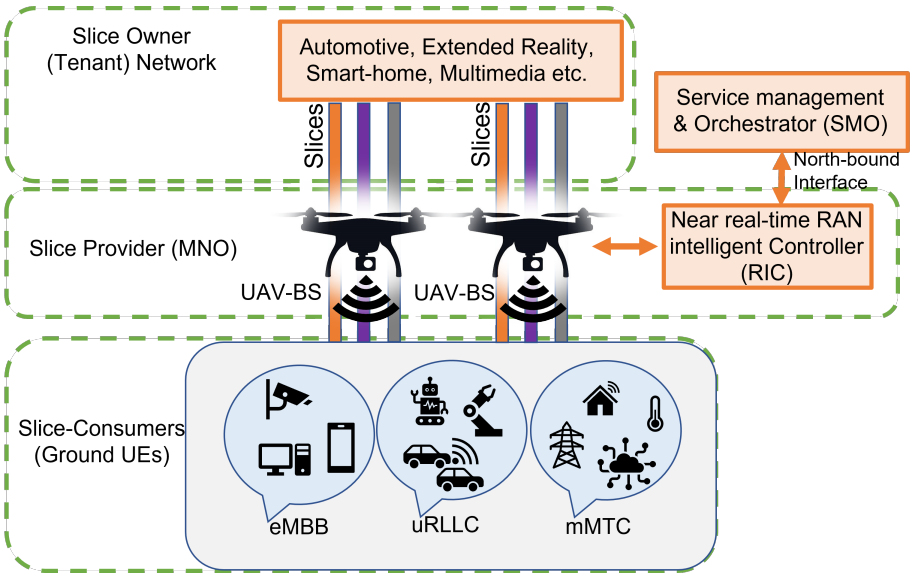

Figure 3.1: RAN Slicing of UAV-assisted 5G network.

RIC concerning the changing arrival and traffic demands from UEs not only ensures an adaptive slicing policy at UAV-BS with high multiplexing gain, but also enables it to optimally position itself to improve the service for ground UEs. In the interest of meeting emerging enterprise needs from industry verticals, flexibility of 5G networks built into UAVs give rise to a *slice-aware UAV-assisted RAN* ecosystem which could exploit the best of both worlds, cellular and UAV. This remains our primary focus in this chapter.

The following sentence reminds the reader of the fundamental question (Q3 in Section 1.5) that this chapter attempts to raise and discuss potential answers to.

Q3. How can UAV-enabled cellular systems accommodate heterogeneous 5G service classes arising from wide range of vertical industries?

3.1.1 Challenges

The coexistence of eMBB, uRLLC and mMTC services on the same UAV-BS radio resources leads to a very challenging downlink scheduling problem due to underlying trade-off of end-user requirements in terms of coverage, traffic demand, data rates, latency, reliability etc along with the UAV-specific constraints. Efficiently allocating the resources among slices ensuring a fair-share for each tenant is of paramount importance when users belonging to different slices compete for same set of finite channel resources. Several important contributions in intelligent slicing optimization, resource scheduling, architectures, end-to-end life-cycle management and orchestration (MANO) are already demonstrated and studied extensively in past few years [90, 92–97] for terrestrial 5G network. Only very few works have been pursued in the context of UAV-assisted network scenario [98–101] and largely unexplored in regards to realize a slicing-ready system for airborne UAVs. Note that, slicing policies and optimization formulations of a terrestrial 5G network may not be directly applied for airborne UAV-BS due to two major challenges. First, UAVs are constrained platforms in terms of finite computation, on-board battery power, thereby demanding a light-weight slicing-ready solution that makes it suitable for

flying platforms. Second, the benefits of flexible positioning of UAV-BS impacting the system performance of heterogeneous network slices need further study.

3.1.2 Chapter Contributions

Motivated by the above challenges, our work considers a framework of resource slicing of UAV-assisted 5G RAN as depicted in Fig. 3.1 in which heterogeneous and differentiated 5G services (*i.e.,* eMBB, uRLLC, mMTC slices) requested by multiple tenants are multiplexed in common radio interface of UAV-BS. In this chapter, we focus on the analysis of channel sharing among the three types of heterogeneous slice services when a single UAV-BS is in charge of connecting them to the 5G network.
Specifically, our main goals in this work are the following:

- *We present a resource slicing and coexistence framework for UAV-assisted 5G RAN for simultaneous and effective multiplexing the three heterogeneous slice service types (eMBB, uRLLC and mMTC) over the common UAV-BS hardware.* A probabilistic mixture of different UE types and data traffic demands are considered to evaluate the performance gains;

- *We propose a segregated, light-weight, two-phase slicing optimization model consisting of (i) resource optimizer (RO) module and (ii) scheduling validator (SV) module, that assists in dynamic resource slicing policy for computationally-constrained UAV-BS platform.* We show that, it not only guarantees the agreed QoS to all the required/mandatory users, but it also maximizes the acceptance of the additional/optional users whenever there is a provision to do so within system capacity limits;

- *We show preliminary results on how the proposed model can be used to identify an effective positioning of the UAV-BS.* The positioning can be chosen in a way to be either 'slice-specific' (in which users belonging to a specific slice service type are prioritized) or 'balanced' (in which users of all the slice service types are treated with equal priority).

3.2 Related Works

Given the broad literature already existing for 5G RAN slicing and our contributions to this field, we split the literature review into three subsections: (i) slicing on terrestrial BS and UAV-BS; (ii) mathematical modeling of RAN slicing; and (iii) UAV-BS positioning.

3.2.1 Slicing on terrestrial BS and UAV-BS

In the presence of heterogeneous slices' requests, an important issue is how to schedule the radio resources among slices in an adaptive manner. The work in [102] proposes a two-level scheduler where at first level, PRBs are abstracted as virtual resource blocks (vRB) and assigned to the UEs; in a second level, the mapping from vRB to PRB is executed where a resource mapper is in charge for resource optimization. Similar two-level architecture is used in [103] to share the radio resources that can dynamically adjust the assigned number of PRBs to time-varying slice demands. Different works analyzed the possibility of sharing RAN resources by focusing mainly only on two different slice types [103–106]. In [104], the authors studied the co-scheduling problem of eMBB and uRLLC traffic based upon the puncturing technique, *i.e.,* the technique that enables the BS to allocate zero power to the eMBB in order to let the uRLLC transmit.

Here, radio resources are scheduled among eMBB and uRLLC users in time-slot and mini-slot granularity, respectively. In [106], a deep reinforcement learning (DRL)-based framework is proposed for the resource scheduling task among eMBB and uRLLC. First, the eMBB users get the requested resources, and then the uRLLC users are distributed among the available channels to minimize the intersections with the eMBB users and satisfying the stringent uRLLC reliability.

Only few limited works have been pursued in the context of UAV-assisted 5G network slicing [98–101, 107–111]. In [98], the authors studied the co-existence of two slices in a UAV-relay network: eMBB slice for payload transmission and uRLLC slice for stringent UAV control and non-payload communications (CNPC). They adopted a distributed learning approach to obtain user locations and wireless channel gain. Here, the authors proposed a Lyapunov-based optimization framework to decompose the original problem into several repeated optimization sub-problems to satisfy eMBB coverage and rate fulfillment along with uRLLC requirement of CNPC link. However, they neither consider interference among slices, nor sporadic arrival of uRLLC traffic from end users impacting eMBB slice performance. Our work addresses above shortcomings (a) by taking into account the mutual interference in terms of radio resource overlap among users when different slices are served by UAV-BS, and (b) factoring eMBB rate degradation caused by sporadic arrival of uRLLC traffic (detailed in Section 3.3.2).

Furthermore, the majority of related works focuses on standalone optimization in which either a single service class (eMBB or uRLLC or mMTC separately) [99, 100, 107] or mixed type scenarios with joint optimization including two service classes *e.g.,* eMBB with uRLLC [98, 112], or eMBB with mMTC [108, 109, 113] are considered. In [99], the authors used UAV to deliver uRLLC services to out-of-coverage area by jointly optimizing the UAV deployment guaranteeing minimum sum-rate for latency-sensitive users along with transmit power control. In [107], the authors focused on UAV energy limitation and realized a time-dependent mixed-integer-non-convex problem formulation to optimize the eMBB user traffic performances while minimizing UAVs' total transmission power. On the mMTC side, the authors in [100] focused on data collection optimization from massive machine-type communication devices (MTCDs) and they proposed a path planning algorithm and an optimal hovering location that maximizes the data collection efficiency from mMTC networks. Differently from prior works, we focus on UAV-BS providing communication services to users belonging to all three service classes (detailed in Section 3.3.1).

3.2.2 Mathematical modeling of RAN slicing

The main approach in the mathematical modeling for RAN slicing has been to formulate the resource allocation problem using a Mixed Integer Linear Programming (MILP) or Mixed Integer Non-Linear Programming (MINLP) models. Such models belong to NP domain [93] and compute intensive due to heterogeneous traffic requests, service classes and presence of interference. A reasonable alternative to reduce model complexity is to rely on models that explicitly calculate SINR and limits the number of interfering nodes as demonstrated in [114, 115]. A binary quadratic non-convex optimization problem is proposed in [115] to minimize the inter-slice interference and to ensure slide-isolation. The authors reduced the model complexity by considering only two interfering nodes in SINR derivation. The NP-hardness of resource scheduling is presented in [116, 117], where an approximation algorithm is used to render tractable solution.

In our work, we leverage a segregated, light-weight, two-phase slicing optimization model in order to reduce the model complexity in resource-constrained devices such as UAVs (detailed in Section 3.4). The two-phase iteration of optimization passes is not a new concept. The works [104, 106, 118] already present a good evidence in its applicability for light-weight mod-

els. In [106], a two-phase approach is proposed for eMBB and uRLLC scheduling based on optimization-aided Deep Reinforcement Learning (DRL) based framework. In [104], the co-scheduling problem among eMBB and uRLLC traffic has been decomposed into two smaller sub-problems on time slot basis for eMBB and on a mini-slot basis for uRLLC. Above two works only considers two service classes. In [118], a non-convex MILP problem has been decomposed in two sub-problems with a two-sided matching algorithm solving user association, and a whale optimization and Lagrangian relaxation solving resource assignment. Above work does not consider any interference in channel model. In this work, differently from above, the formulated two-phases slicing optimization encompasses interference in channel model as well as inclusion of three service classes.

3.2.3 UAV-BS Positioning

The UAV-BS is able to dynamically adapt its position in 3D space according to UE locations on ground to improvise a given communication metric [77, 100, 101]. For instance, the placement decision is driven to maximize user coverage [119], or a backhaul-aware link utilization [120]. Besides above analytical works on UAV-BS placement decision, measurement-driven (*e.g.,* ray-tracing or radio environment map) methods [25] are also demonstrated to show higher improvements to communication services. However, 'how the performance of resource slicing for heterogeneous 5G service classes is affected through different UAV-BS position' is not addressed in literature. Note that, our aim in this work, is not to propose a new path-planning or positioning algorithm for UAV-BS, rather evaluating on *how the performance of slicing framework responds to different positioning of UAV-BS*. Hence, to address this gap, we seek answer to a fundamental question: *whether a careful decision of UAV-BS positioning can improve the slice performance?* In Section 3.6.3, we showcase that a careful decision on UAV-BS positioning can lead to optimal service offerings for slice tenants. Hence, based on our results, future works could explore path-planning and trajectory algorithms to maximize the UAV-assisted services slicing performance.

3.3 System Model

We consider a downlink scheduling system of UAV-assisted 5G RAN in which a single UAV-BS (U) is deployed to provide services to three types of heterogeneous slices *i.e.,* eMBB slice, uRLLC slice and mMTC slice. As shown in Fig 3.1, each UE belongs to one or more slice service type and obtains physical resource blocks (PRBs) from the UAV-BS to meet its slice-specific application requirements. In order to show the dynamic behavior of slicing policy to allocate resources with maximal multiplexing benefit and opportunity of MNOs for lucrative service offering, we further classify the eMBB and mMTC slice users into two categories: (i) Optional and (ii) Non-optional (mandatory). The slicing policy aims to serve all the non-optional users and maximizes the acceptance of the optional users within system capacity limits. Note that, for uRLLC slice service type, we have only non-optional user category, because of their tight QoS requirements in terms of high reliability and low latency. More formally, we define $\mathcal{G} = \{g_1, \dots g_{N_\mathcal{G}}\}$ as the set of ground users that can belong to one of the three service type request: $\mathcal{G}_U \subseteq \mathcal{G}$ as the uRLLC ground users, $\mathcal{G}_M \subseteq \mathcal{G}$ as the mMTC ground users, $\mathcal{G}_E \subseteq \mathcal{G}$ as the eMBB ground users, such that $\mathcal{G}_U \cup \mathcal{G}_M \cup \mathcal{G}_E = \mathcal{G}$ and $\mathcal{G}_U \cap \mathcal{G}_M \cap \mathcal{G}_E = \emptyset$. Moreover, we define $\mathcal{G}_M^O \subseteq \mathcal{G}_M$ as the optional mMTC ground users and $\mathcal{G}_E^O \subseteq \mathcal{G}_E$ as the optional eMBB ground users. For a complete glossary of mathematical notations used in the document, refer to Table 3.1.

Table 3.1: Glossary of Mathematical Notations

Name	Description
$\mathcal{F} = \{f_1, \dots f_{N_\mathcal{F}}\}$	Set of available channel resources, with $\lvert\mathcal{F}\rvert = N_\mathcal{F}$
$\mathcal{G} = \{g_1, \dots g_{N_\mathcal{G}}\}$	Set of ground users, with $\lvert\mathcal{G}\rvert = N_\mathcal{G}$
$\mathcal{G}_U \subseteq \mathcal{G}$	Set of uRLLC ground users, with $\lvert\mathcal{G}_U\rvert = N_{\mathcal{G}_U}$
$\mathcal{G}_M \subseteq \mathcal{G}$	Set of mMTC ground users, with $\lvert\mathcal{G}_M\rvert = N_{\mathcal{G}_M}$
$\mathcal{G}_E \subseteq \mathcal{G}$	Set of eMBB ground users, with $\lvert\mathcal{G}_E\rvert = N_{\mathcal{G}_E}$
$\mathcal{G}_M^O \subseteq \mathcal{G}_M$	Set of optional mMTC ground users, with $\lvert\mathcal{G}_M^O\rvert = N_{\mathcal{G}_M^O}$
$\mathcal{G}_E^O \subseteq \mathcal{G}_E$	Set of optional eMBB ground users, with $\lvert\mathcal{G}_E^O\rvert = N_{\mathcal{G}_E^O}$
$\texttt{class}(g_j)$	The class of ground user g_j
$\texttt{pos}(g_j)$	The position of ground user g_j
$\texttt{pos}(u_i)$	The position of UAV u_i
$\texttt{pot}(g_j)$	The probability of transmitting for uRLLC ground user g_j. (We assume that $\texttt{pot}(g_j) = 1$, $\forall g_j \in \mathcal{G}_E$)
$\texttt{nrc}(g_j)$	The number of channel resources requested by eMBB ground user g_j
$\texttt{dr}(g_j)$	The minimum data rate expected by ground user g_j
$\texttt{rel}(g_j)$	The minimum reliability expected by ground user g_j
$\texttt{lat}(g_j)$	The minimum latency expected by ground user g_j
$S_{u_i,g_j}^{f_k}$	Signal power received at UAV u_i from ground user g_j using frequency f_k.
p_{LoS}	Probability of LoS connection between UAV-BS and ground UE
θ	User-UAV incident angle w.r.t. ground surface
a, b	Environment-dependent constants as per [77]
$\eta(h, d)$	Total pathloss at height h and 2D distance d
G_t, G_r	Transmit and receive antenna gains
$\tilde{H}$	Fading channel
$t_{g_j}^{f_k}$	Binary scheduling variable for channel allocation. Equal to 1 if channel f_k assigned to user g_j, 0 otherwise
$\text{SINR}_{g_j}, R_{g_j}$	SINR and data rate of user g_j
$Q^{-1}\{\cdot\}$	Inverse of the Q-function
$\mathbb{E}\{\}$	Statistical expectation operator
ϵ	Minimum guaranteed uRLLC reliability
r	Coding rate for uRLLC

3.3.1 Coexistence of eMBB with uRLLC and mMTC

The UAV-BS provides communication services to the ground UEs through downlink fading wireless channel. In the frequency domain, the radio bandwidth is split into physical resource blocks (PRBs). Each PRB spans 12 consecutive subcarriers supporting scalable numerologies with subcarrier spacing of $2^\mu \cdot 15$ kHz ($\mu = 0, 1, 2, ..., 4$), defining the $\mathcal{F} = \{f_1, \dots f_{N_\mathcal{F}}\}$ available channel resources. In the time domain, the UAV-BS considers a scheduling time slot (referred as transmission time interval or TTI in short) of 1 ms for eMBB slice users. The UAV-BS allocates PRBs for eMBB slice users at the beginning of each TTI. Such resource allocation policy is not

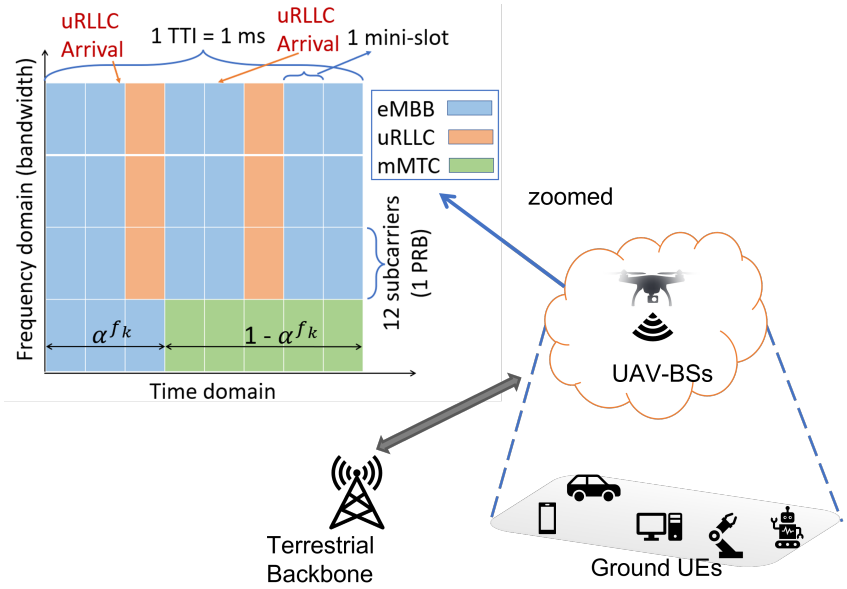

Figure 3.2: An illustrative example of simultaneous coexistence of eMBB with uRLLC via puncturing. eMBB traffic are scheduled at beginning of each TTI, whereas uRLLC traffic on arrival can be overlapped over eMBB in next mini-slot.

different from legacy LTE eNodeB (4G BS) scheduler. On the other hand, the uRLLC traffic is sporadic with short packet size. For the uRLLC slice users, each TTI is further split into M mini-slots of duration τ *i.e.,* $M \times \tau = 1$ TTI.

Due to the tight latency limits, uRLLC traffic that appears during an ongoing eMBB transmission cannot be delayed until the conclusion of one TTI when both eMBB and uRLLC traffic are multiplexed sharing the same set of PRBs. This is the case when both types of traffic are sharing the same PRBs. Because of this, the uRLLC traffic is scheduled promptly in next available mini-slots. This is accomplished by overwriting (also referred as preemption) a portion of the ongoing eMBB transmission using *puncturing* in the mini-slot granularity [104, 121]. Fig. 3.2 provides a visual representation of this scenario. This results in a varied level of scheduling granularity based on the kind of slice service type, with users of uRLLC slices being scheduled in mini-slots (sub-ms) and users of eMBB slices being planned in TTIs (1 ms), respectively. 3GPP Rel-15 proposes a preemption/punctured indication (PI) information element (IE) to be signaled by the gNB (5G BS) scheduler for multiplexing eMBB with uRLLC traffic [122].

In order to resolve the ambiguity in terminology among different scheduling granularity that arise due to flexible 5G numerology across time and frequency domain for various class of user traffic, we refer to “channel resource", in this work, as the minimum block that can be allocated to any ground user. A channel resource for eMBB and mMTC ground users span 1 TTI in time domain and 12 subcarriers in frequency domain *i.e.,* 1 PRB. A channel resource for an uRLLC ground user span 1 mini-slot in time domain and 12 subcarriers in the frequency domain. In summary, to realize effective multiplexing of heterogeneous slice traffic, we make following assumptions for simultaneous coexistence:

- If a uRLLC user is sharing the same PRB of an eMBB user, we need to take in account the random uRLLC traffic arrival pattern at UAV-BS (in any mini-slot) with a probability of transmission that preempts existing eMBB transmission. Let $\texttt{pot}(g_w)$ be the probability

of transmission of uRLLC user g_w during an ongoing eMBB slot. The data bits lost during puncturing is re-transmitted and recovered in future TTIs.

- If an mMTC user is sharing the same PRB of an eMBB user, we need to decide the fraction of channel resource that is associated to the mMTC user. As shown in Fig. 3.2, we therefore indicate with $\alpha^{f_k} \in [0, 1]$ the fraction of the channel resource f_k dedicated to eMBB transmission. $(1 - \alpha^{f_k})$ is the remaining fraction for mMTC transmission. It is worth noting that, this orthogonal fractional sharing of eMBB with mMTC mitigates the potential overlap issue between mMTC and eMBB user, but incur a proportional data rate degradation for eMBB and mMTC users depending on the value of α^{f_k}. Refer to Section 3.3.2 that presents how it is parameterized in the model.
- One mMTC user and one uRLLC user cannot share the same channel resource, *i.e.,* their scheduling allocations by UAV-BS is orthogonal.
- A channel resource cannot be shared by more than one uRLLC user. This setting is to prevent the risk of overlap and increase reliability. The PER might be adversely affected when multiple uRLLC users are scheduled in the same channel resource [123].

3.3.2 Signal and Slice Resource Model

Signal Model

The air-to-ground (A2G) propagation model from UAV-BS to ground UE is modeled by using a probabilistic pathloss channel (large-scale fading) including both line-of-sight (LoS) and non-LoS component along with small-scale fading and shadowing. We denote p_{LOS} as the probability of the LoS connection between UAV-BS and ground UE, and given by [77],

$$p_{\text{LoS}} = \frac{1}{1 + a \exp\left(-b\left[\frac{180}{\pi}\theta - a\right]\right)}$$

where θ is the elevation angle (*i.e.,* user-UAV incident angle w.r.t. ground surface), a and b are environment-dependent constants as per rural, sub-urban or urban deployment as mentioned in [77]. θ is computed as $\tan^{-1}\left(\frac{h}{d}\right)$ in which h is flying altitude of UAV-BS and d is horizontal 2D distance between UAV-BS and ground UE. The probability of non-LoS channel is denoted by $p_{\text{non-LoS}}$, and is computed as $(1 - p_{\text{LoS}})$. The total pathloss $\eta(h, d)$ is given by,

$$\eta(h,d) = 20\log\left(\frac{4\pi f_c}{c}\right) + 20\log\left(\sqrt{h^2 + d^2}\right) + [p_{\text{LoS}} \cdot \eta_{\text{LoS}}] + [p_{\text{non-LoS}} \cdot \eta_{\text{non-LoS}}]$$

The received signal power S_{g_j} for any user g_j from UAV-BS u_i using frequency f_k ($S : \mathcal{G} \times \mathcal{F} \rightarrow \mathbb{R}$) is given by,

$$S_{g_j} = P_t \cdot G_t \cdot G_r \cdot \eta(h,d) \cdot \left|\tilde{H}\right|^2 \tag{3.1}$$

where P_t is UAV-BS transmit power, G_t and G_r are the transmit and receive antenna gains, respectively, and $\tilde{H}$ denotes the multipath fading component. Considering the obstructions of LOS component due to tall buildings or other obstacles in urban/suburban environment, we assume that the multipath fading component behaves like Rician shadowed fading. By modeling

the channel using Rician shadowed distribution, we can compute the impact of shadowing severity on the system performance when we have weak LOS component. Moreover, we can use the special case of same distribution (Rician-K or Nakagami-m) to evaluate the system performance when we have strong LOS component. The channel gain of a Rician shadowed fading channel $\tilde{H}$ can be obtained using the $\kappa - \mu$ shadowed fading distribution by substituting $m = 1$ and $\kappa = K$ (Rician-K parameter), as

$$\tilde{H} = \left[X + Z\, w\right]^2 + Y^2\,, \tag{3.2}$$

where X and Y are mutually independent Gaussian random variables with $\mathbb{E}\{X\} = \mathbb{E}\{Y\} = 0$, $\mathbb{E}\{X^2\} = \mathbb{E}\{Y^2\} = \sigma^2$ where $\mathbb{E}\{\cdot\}$ is an expectation operator, Z is a Nakagami-m random variable with $\mathbb{E}\{Z^2\} = 1$, the parameter $w = \frac{K}{K+1}$, where K represents the power contributions by LOS path to the remaining multipaths. For a special case with Rician $K = 0$, and Nakagami $m = 1$, the PDF of $\tilde{H}$ reduces to Rayleigh distribution which can incorporate the scenarios where the non-LOS signal component is dominant.

Slice Resource Model

In this subsection, we characterize the signal-to-interference-plus-noise ratio (SINR) using received signal model presented in Eqn. 3.1 for different types of slice users. Using the analysis and assumptions presented in subsection 3.3.1 for coexistence of different slice users, we formulate SINR expressions in a way to adhere towards slice-specific QoS. We hence introduce a scheduling variable $t : \mathcal{G} \times \mathcal{F} \rightarrow \{0, 1\}$ to represent the allocation of time-frequency channel resources to different users:

$$t_{g_j}^{f_k} \;=\; \begin{cases} 1 & \text{if channel } f_k \text{ assigned to user } g_j \\ 0 & \text{otherwise} \end{cases} \quad .$$

For an eMBB slice user g_j, the $\text{SINR}_{g_j} : \mathcal{G} :\rightarrow \mathbb{R}$ is expressed as,

$$\text{SINR}_{g_j} = \sum_{f_k \in \mathcal{F}} \frac{S_{g_j} \cdot t_{g_j}^{f_k}}{\sum_{g_w \in \mathcal{G}_E \setminus g_j} \left(S_{g_w} \cdot t_{g_w}^{f_k}\right) + \sigma^2} \tag{3.3}$$

where σ^2 is the noise power and $t_{g_j}^{f_k}$ is the binary variable associated if the channel resource is used for data transmission.

The SINR for uRLLC user g_j is given by,

$$\text{SINR}_{g_j}^{f_k} = \frac{S_{g_j}^{f_k} \cdot t_{g_j}^{f_k}}{\sigma^2} \tag{3.4}$$

where $S_{g_j}^{f_k}$ is the received signal power and σ^2 is the noise.

The SINR for mMTC user g_j is given by,

$$\text{SINR}_{g_j} = \sum_{f_k \in \mathcal{F}} \frac{S_{g_j} \cdot t_{g_j}^{f_k}}{\sum_{g_w \in \mathcal{G}_M \setminus g_j} \left(S_{g_w} \cdot t_{g_w}^{f_k}\right) + \sigma^2}\,. \tag{3.5}$$

Above SINR expressions on physical layer characterization impel medium access control (MAC) and above layers to look after specific needs for users belonging to heterogeneous slices. For example, the eMBB slice users demand a minimum required guaranteed data rate and

URLLC slice users demand a minimum required reliability and latency constraints. For eMBB slice user, using SINR Equation (3.3) and following Shannon's rate computation, the data rate $R : \mathcal{G} \times \mathcal{F} \rightarrow \mathbb{R}$ [bit/sec] is defined as:

$$R_{g_j} = \log_2(1 + \text{SINR}_{g_j}) \cdot \sum_{f_k \in \mathcal{F}} t_{g_j}^{f_k} (\alpha^{f_k} - \sum_{g_w \in \mathcal{G}_U} t_{g_w}^{f_k} \texttt{pot}(g_w)) \; . \tag{3.6}$$

The term $(\alpha^{f_k} - \sum_{g_w \in \mathcal{G}_U} t_{g_w}^{f_k} \texttt{pot}(g_w))$ in Equation(3.6) contributes to the data rate degradation of an eMBB user when a mMTC or uRLLC user are scheduled over ongoing eMBB transmission. We define a data rate-oriented QoS requirement for the eMBB slice, where the slice tenant specifies a minimum channel ergodic capacity $\texttt{dr}(g_j)$ to be guaranteed for the eMBB slice user, *i.e.,* $R_{g_j} \geq \texttt{dr}(g_j)$. Similarly, the rate achieved by the mMTC user is given by,

$$R_{g_j} = \log_2(1 + \text{SINR}_{g_j}) \cdot (1 - \sum_{f_k \in \mathcal{F}} t_{g_j}^{f_k} \alpha^{f_k}) \; . \tag{3.7}$$

A uRLLC user does not share the assigned channel resource with another uRLLC user. The QoS of uRLLC slice traffic is primarily modeled by a maximum allowed latency $\texttt{lat}(g_j)$ and guaranteed reliability threshold of $\texttt{rel}(g_j)$. Due to its short packet size, the achievable data rate of uRLLC falls in the finite blocklength coding regime. For block error rate (BLER) ϵ, blocklength or the number of channel uses n, the coding rate r (bits per channel use) with Additive White Gaussian Noise (AWGN) channel, is given by [124], [125, eq(1)]

$$\begin{aligned} r =& \frac{1}{2}\log_2(1 + \text{SINR}_{g_j}^{f_k}) - \sqrt{\left(1 - \frac{1}{(1 + \text{SINR}_{g_j}^{f_k})^2}\right)/2n} \\ & Q^{-1}(\varepsilon)\log_2 e + \frac{O(\log_2 n)}{n}, \end{aligned} \tag{3.8}$$

where $Q^{-1}\{\cdot\}$ is the inverse of the Q-function represented by $Q(w) = \int_w^\infty \frac{1}{\sqrt{2\pi}} e^{-t^2/2} dt$. This result can be extended for a complex Gaussian channel model as,

$$r \approx \log_2(1 + \text{SINR}_{g_j}^{f_k}) - \sqrt{\frac{V}{n}} \cdot Q^{-1}(\varepsilon), \tag{3.9}$$

where for complex Gaussian channel model, V that measures the channel dispersion. It is defined as,

$$V = \left(1 - \frac{1}{1 + (\text{SINR}_{g_j}^{f_k})^2}\right) (\log_2 \; e)^2 \, . \tag{3.10}$$

For sufficient large n (*i.e.,* $n \geq 100$) in (3.9), the guaranteed reliability for uRLLC traffic can be represented in terms of BLER as,

$$\epsilon \approx \mathbb{E}\left\{ Q\left(\frac{\log_2(1 + \text{SINR}_{g_j}^{f_k}) - r}{\sqrt{V/n}}\right)\right\}. \tag{3.11}$$

Equation (3.11) presents the QoS requirement in terms of reliability of uRLLC slice users where the uRLLC slice tenant necessitates the channel resources to be scheduled ensuring this minimum guaranteed reliability, *i.e.,* $\epsilon \leq \texttt{rel}(g_j)$. Similarly, the latency requirement of uRLLC

slice traffic $\texttt{lat}(g_j)$ is the minimum number of mini-slots required to successfully transmit a message. Note that, there is a strict constraint on serving all the uRLLC requests that appeared in any mini-slot m (with duration τ) of the given $i-th$ time slot. Within this specific period of τ, the payload $B_u^{m,i}$ requested by serving uRLLC users $U_u^{m,i}$, for $u \in U$, need to be transferred successfully, and hence satisfying the latency constraint[4] $B_u^{m,i} U_u^{m,i} \leq r_u^{m,i} \tau$ [104]. These minimum required QoS constraints $\texttt{rel}(g_j)$ and $\texttt{lat}(g_j)$ for uRLLC traffic are demanded by the slice tenant and the goal is to ensure that minimum required QoS in terms of latency and reliability for uRLLC slice traffic are fulfilled.

Parameterization of α

The split variable α^{f_k} regulates the coexistence behavior eMBB and mMTC users. Note that, its value can be tuned to prioritize a specific user category. In our work, we derive α^{f_k} by conditioning on the achievable data rates of eMBB and mMTC users. More precisely, α^{f_k} is proportional to the number of eMBB slice users assigned to a particular channel resource with respect to the total amount of eMBB and mMTC users assigned to that channel resource (weighted on the data rate). Hence, it is defined as follows.

$$\alpha^{f_k} = \frac{\sum_{g_j \in \mathcal{G}_E} \texttt{dr}(g_j) t_{g_j}^{f_k}}{\sum_{g_j \in \mathcal{G}_E \cup \mathcal{G}_M} \texttt{dr}(g_j) t_{g_j}^{f_k}} \,. \tag{3.12}$$

3.4 EASIER: Solution Framework

Airborne UAV-BSs are constrained computational platforms where, unlike terrestrial base stations, the limitations on the size, weight, and power (SWaP) demand utmost consideration for the design of lightweight and resource-efficient optimization algorithms. In general, the implementation of a computationally-efficient algorithm that is able to realize a dynamic scheduling behavior across different time scales when users of heterogeneous services coexist is a hard problem, as shown in Section 3.2. A feasible solution must consider the number of active slices, user locations and their spatio-temporal traffic demands per slice. Furthermore, the relation between allocation choices and required QoS could be represented by functions that are highly non-linear or that can not even be written in a closed-form.

For this reason, in this section, we introduce a modular and customizable resource slicing optimization framework for UAV-BS known as gEneral rAn Slicing optImizEr fRamework (*EASIER*). The aim is to propose a general optimization framework that can fit different application/service scenarios, signal propagation models, available computational power, and can deal with the trade-off between outcome accuracy and used resources. The functional blocks of the *EASIER* framework are shown in Fig. 3.3. Here, the framework takes as input the position of the available UAV-BS (U), the set of ground UEs belonging to different slices ($\mathcal{G}$), the users' QoS requirements depending on the slice type and tenant's service level agreement (SLA), and it calculates as output the dynamic assignment of radio resources to ground UEs.

[4]The $\texttt{lat}(g_j)$ basically consist of two parts: propagation latency and the handling latency. The propagation latency in the given constant time-slot t_{slot} is the probability of successfully transmitting the message (P_{prop}) without any need of re-transmission i.e., $\frac{t_{slot}}{P_{prop}}$. Moreover, the handling latency is caused due to the message arrival rate and managing the message queues, which forms a message-handling process. In this work, we are defining latency as the minimum mini-slots required for reliable communication, which is SINR-dependent. Evaluation of handling latency does not fall in the scope of this work. Our main goal is to maximize the number of admissible slice UEs guaranteeing the QoS requirements of all three considered slice service types.

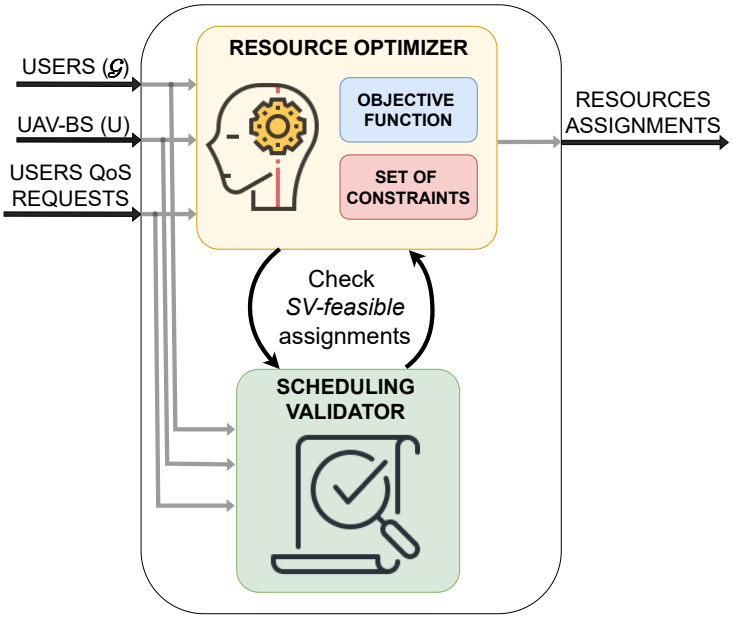

Figure 3.3: *EASIER*: modular components and architecture

To deal with the problem complexity, we propose to split the optimization framework into two main parts as follows:

- *Resource Optimizer (RO)* that is in charge of finding assignment of channel resources to slice users by respecting a *set of constraints* and guided by a given *objective function*.
- *Scheduling Validator (SV)* that is a support module in charge of validating whether the channel resource assignment decisions made by the RO module are feasible or not, according to QoS requirements specified by tenant.

This general and intuitive idea of viewing the optimization framework as the interaction of two components has been already investigated in the operational research field. It is possible to find several works in the literature with mathematical models where a subset of the requirements on the feasible region is not explicitly defined with a set of functions, but it is delegated to an *oracle* of different nature, such approaches falls in the category of Logic-based Benders Decomposition (LbBD) [126–129]. The main idea of LbBD is to combine a Master Problem, defined with a mathematical programming model where the feasible region has a combinatorial nature, with an auxiliary sub-problem that has no limitations on the kind of optimization problem (the oracle), to which the only information requested is whether a certain solution is admissible or not. In our design, in fact, the RO finds the solutions for the assignment of channel resources to slice users and delegates to the SV module to verify the quality of the assignment proposed by RO. Thanks to this tasks subdivision, the *EASIER* framework could implement a *NoSV* version in case the SV module is unavailable or it is too heavy to compute. In this case, the RO will optimize its objective function being unaware of the full correct validity of the result. The abstraction and separation of the RO and the SV modules bring multiple advantages in the design of resources assignment algorithms, as described below.

Modularity and Isolation: the framework modularity is of paramount importance when addressing a complex problem. The modular organization favors the framework design and implementation due to its inner flexibility and the ability to accelerate the modules' innovation. Two

segregated modules: the resource optimizer (RO) and the scheduling validator (SV) allow isolation and permit development independently of each other. Once the interconnections are agreed upon by the different modules, the design and implementation can be carried autonomously as multiple *black boxes*. The module isolation enables the development of different versions for the same module that fit various needs. This is the case of the proposed *EASIER* framework, where different versions of the RO and the SV modules will be proposed in forthcoming Sections to address different optimization targets.

Offline and online verification and optimization: As discussed in Section 3.2.2, finding a solution for the resource scheduling in UAV-enabled 5G RAN slicing is a hard task. Different solutions can be found to solve these problems and they can be subdivided into two categories: offline and online. In offline algorithms, the solution starts with the full knowledge of the system variables to solve the problem; in this case, depending on the definition of the algorithm and its implementation, a fast and/or accurate solution is found. On the other side, an online algorithm does not know apriori the system variables and needs to find, or approximate, them during its execution. The proposed framework supports both the two categories due to the split between the decision process conducted by RO and its validation performed by SV. In this case, in fact, an offline solution will establish an iterative approach where the RO proposes a solution that is evaluated by the SV, and thereby performs validation of a specific assignment of slice user to a channel resource. If any resultant assignment decision proposed by RO respects all the QoS required by all the slice users involved, then the SV does not perform any additional validation. Otherwise, if at least one of the QoS metrics is not satisfied as per the agreed SLA with slice tenant, one new constraint is added at the RO level. In this way, RO module utilizes the periodic feedback responses from SV module to shrink the solution space and converge to an effective assignment decision that respects the slice users' QoS requirements. With the same method, but with an online approach, the evaluation of the quality of a scheduler assignment that is performed by the SV can be learned during the multiple executions of the assignment task and receiving feedback from the ground UEs.

The advantages described so far, allow the EASIER framework to be easily applied also to a multi-UAV-assisted 5G RAN case to improve the covered area and the QoS offered to the connected users. In this case the RO module will be in charge of avoiding multiple assignments of the same UE to multiple UAV-BSs, while the SV module will validate the channel allocations, considering also the inter UAV-BSs interference.

In this work, we propose the *EASIER* framework that focuses on *modularity*, *isolation* and *offline verification and optimization* for single-UAV-assisted 5G RAN scenarios. Future works on *online verification and optimization* are envisioned to include continual learning and reinforcement learning control system approaches to address the dynamic resource assignment problem in 5G slicing with on-line optimization solutions in multi-UAV-assisted 5G RAN scenarios.

3.5 EASIER Implementation and Optimization

This Section describes the *EASIER* framework's implementation in depth, based on the considerations made in Section 3.3 on channel modeling and slice coexistence. The suggested framework is modular and consists of a mathematical model that may be adjusted to meet various demands. The model consists of two main parts:

1. A basic model (`Resource Optimizer`) - The objective function of this model is obtained as a weighted sum of two different objective functions, one that gives priority to assignments with a high number of accepted users and another that gives priority to assignments with a

high probability of respecting the users' requests. On the other hand, the set of constraints ensures that we have a feasible resource allocation.

2. Additional set of optional constraints (`Scheduling Validator`) - These constraints are included if we want to ensure that the quality of service requested by the users is respected.

In the following two subsections, we describe both parts in detail.

3.5.1 Resource Optimizer (RO)

In this section we describe the mathematical model used as a Resource Optimizer. The mathematical model uses a set of *assignment* variables t, where with t is a binary vector of size $N_{\mathcal{G}} \cdot N_{\mathcal{F}}$. The vector t represents a possible assignment of the scheduling variables:

$$t_{g_j}^{f_k} = \begin{cases} 1 & \text{if channel } f_k \text{ assigned to user } g_j \\ 0 & \text{otherwise} \end{cases} .$$

The model associated to the Resource Optimizer is the following:

$$\max \phi(t) = \gamma\phi_{ou}(t) + (1-\gamma)\phi_{ovl}(t) \tag{3.13}$$

$$\sum_{f_k \in \mathcal{F}} t_{g_j}^{f_k} = \texttt{nrc}(g_j) \qquad \forall g_j \in \mathcal{G}_E \setminus \mathcal{G}_E^O \tag{3.14}$$

$$\sum_{f_k \in \mathcal{F}} t_{g_j}^{f_k} \leq \texttt{nrc}(g_j) \qquad \forall g_j \in \mathcal{G}_E^O \tag{3.15}$$

$$\sum_{f_k \in \mathcal{F}} t_{g_j}^{f_k} = 1 \qquad \forall g_j \in (\mathcal{G}_U \cup \mathcal{G}_M) \setminus \mathcal{G}_M^O \tag{3.16}$$

$$\sum_{f_k \in \mathcal{F}} t_{g_j}^{f_k} \leq 1 \qquad \forall g_j \in \mathcal{G}_M^O \tag{3.17}$$

$$t_{g_j}^{f_k} = 1 \qquad \forall j = k = 1, \ldots, N_{\mathcal{G}_U} \tag{3.18}$$

$$t_{g_j}^{f_k} = 0 \qquad \forall g_j \in \mathcal{G}_M, k = 1, \ldots, N_{\mathcal{G}_U} \tag{3.19}$$

$$t_{g_j}^{f_k} \in \{0, 1\} \qquad \forall g_j \in \mathcal{G}, f_k \in \mathcal{F} \tag{3.20}$$

The objective function $\phi(t)$ is defined as a weighted sum of two functions: $\phi_{ou}(t)$ and $\phi_{ovl}(t)$. In order to strike the balance between above two determining functions $\phi_{ou}(t)$ and $\phi_{ovl}(t)$, $\gamma \in [0, 1]$ is used as a weighting factor. Generally speaking, function $\phi_{ou}(t)$ (where the subscript "ou" stands for optional users) is designed in a way to provide a high value to assignments that accept large number of optional slice users. On the other hand, the role of function $\phi_{ovl}(t)$ (where the subscript "ovl" stands for overlapping resource) is to give the priority to the assignments favoring good QoS for the accepted slice users. In Sections 3.5.1 and 3.5.1 we present an in-dept analysis of the different variants of $\phi_{ou}(t)$ and $\phi_{ovl}(t)$ used in our framework and in Section 3.6, we experimentally show that a careful choice on the weights used to penalize one overlap can significantly improve the overall QoS of the accepted slice users.

Equations (3.14) and (3.16) ensure that each non-optional ground UE is assigned to the required number of channel resources. Equations (3.15) and (3.17) limit the maximum number of optional users that can be assigned, based on the required number of channel resources. Equation (3.18) exploits the fact that a channel resource can be associated to at most one uRLLC

If $g_j, g_{j'} \in \mathcal{G}_E$ or if $g_j, g_{j'} \in \mathcal{G}_M$:

$$w_{g_j g_{j'}} = \frac{1}{\min\{\frac{1}{\mathtt{dr}(g_j)} \log_2(1 + \frac{S_{g_j}}{S_{g_{j'}}+\sigma^2}), \frac{1}{\mathtt{dr}(g_{j'})} \log_2(1 + \frac{S_{g_{j'}}}{S_{g_j}+\sigma^2})\}} \ . \tag{3.21}$$

If $g_j \in \mathcal{G}_E$ and $g_{j'} \in \mathcal{G}_M$:

$$w_{g_j g_{j'}} = \frac{1}{\min\{\log_2(1 + \frac{S_{g_j}}{\sigma^2}) \frac{1}{\mathtt{dr}(g_j)+\mathtt{dr}(g_{j'})}, \log_2(1 + \frac{S_{g_{j'}}}{\sigma^2}) \frac{1}{\mathtt{dr}(g_j)+\mathtt{dr}(g_{j'})}\}} \ . \tag{3.22}$$

If $g_j \in \mathcal{G}_E$ and $g_{j'} \in \mathcal{G}_U$:

$$w_{g_j g_{j'}} = \frac{1}{\frac{1}{\mathtt{dr}(g_j)} \log_2(1 + \frac{S_{g_j}}{\sigma^2})(1 - \mathtt{pot}(g_{j'}))} \ . \tag{3.23}$$

user. This implies that, without loss of generality, we can impose to assign each of the first $N_{\mathcal{G}_U}$ channel resources to uRLLC users. Equation (3.19) ensures that no mMTC user is assigned to a channel resource that is already associated to a uRLLC user. Equations (3.20) defines the binary t variable. An assignment t is said to be *RO-feasible* if it satisfies the constraints (3.14)-(3.20).

We now proceed to describe in detail the RO objective function that guides the channel resource assignment decision, given the aforementioned constraints. The choice to mix two objective functions is due to the fact that evaluating the quality of an assignment is not straightforward and primarily depends on two factors:

- *Presence of Optional Users-* The objective function should prioritize assignment decisions that improves acceptance of optional users *i.e.,* to maximize the number of optional users to be served. Moreover, heterogeneous optional users with varying priority and QoS objective can help in comparing among different situations in which the objective function produce QoS-aware assignments.

- *Improving the Slice-specific SLA-* In practice, it is possible to obtain several assignments where the same set of users are accepted. Therefore, it is beneficial to favor, among these assignments, the one that guarantees highest level of service towards for the accepted slice users.

Each component of the objective function is defined in a way to give the priority to one of the two conflicting goals: $\phi_{ou}(t)$ rewards solutions with an high quantity of optional users, while $\phi_{ovl}(t)$ pushes toward solutions that provides an higher level of service to the accepted users. In the following two sections we describe the variants used for $\phi_{ou}(t)$ and $\phi_{ovl}(t)$.

$\phi_{ou}(t)$ Variants

The generic formulation of this function is in charge of prioritizing assignment with an higher number of optional users. It is given by:

$$\phi_{ou}(t) = \sum_{f_k \in \mathcal{F}} \sum_{g_j \in \mathcal{G}_M^O \cup \mathcal{G}_E^O} p_{g_j} t_{g_j}^{f_k} \ , \tag{3.24}$$

where p_{g_j} is the profit associated to serving optional user g_j. In principle, the value of p_{g_j} should be defined by the slice tenant and is proportional to the importance/priority of the slice user g_j. For simplicity, our experiments consider $p_{g_j} = 1$ for all $g_j \in \mathcal{G}_M^O \cup \mathcal{G}_E^O$ *i.e.,* for all optional UEs.

$\phi_{ovl}(t)$ Variants

Measuring the exact value of the required data rate (or similar QoS indicators) can in principle lead to a highly non-linear function. For this reason, function $\phi_{ovl}(t)$ uses a simpler (but easier to compute) *proxy measure* of the desired QoS, *i.e.,* a weighted sum of the number of *overlaps* in each channel resource. More precisely, we mean by *overlaps* as the number of pairs of users (regardless of their slice type) that are associated to same channel resource in a given assignment. For example, if four users are associated to the same channel resource, they contribute to a total of six overlaps (one for each pair of users).

This function is therefore in charge of penalizing solutions with an higher number of overlaps. It is given by,

$$\phi_{ovl}(t) = \sum_{f_k \in \mathcal{F}} \sum_{g_j \in \mathcal{G}} \sum_{g_{j'} \in \mathcal{G}} -w_{g_j g_{j'}} t_{g_j}^{f_k} t_{g_{j'}}^{f_k} \tag{3.25}$$

where each term $w_{g_j g_{j'}}$ is positive. If two users g_j and $g_{j'}$ are associated to same channel resource f_k, the objective function is decreased with quantity $w_{g_j g_{j'}}$. Note that, the choice of how the penalization weights are calculated has a strong influence on the quality of feasible solution obtained. For the penalization weights, we propose the following two options:

- *Uniform weights-* This option simply aims at counting the number of times a pair of users is associated to the same channel resource:

$$w_{g_j g_{j'}} = 1 \ . \tag{3.26}$$

- *Rate-dependent weights-* The main limitation of the uniform weights option is that it does not take into account the relative position and the characteristics of each ground user. This options attempts to make the function ϕ_{ovl} behave as an effective proxy measure of the slice-specific QoS. Such a goal is achieved by assigning a weight $w_{g_j g_{j'}}$ inversely proportional to the minimum between the data rates obtained by the two users g_j and $g_{j'}$ if no additional user is assigned to the channel resource. To take into account the effective required QoS, the two values are weighted on the required data rates $\texttt{dr}(g_j)$ and $\texttt{dr}(g_{j'})$. The main limitation of this option is that, it overestimates the data rates if more than two ground users are assigned to the same channel resource. Equations (3.21), (3.22) and (3.23), highlight the derivation of data rate dependent weights depending upon slice service type to which the pair of users belong to.

3.5.2 Scheduling Validator (SV)

This module verifies whether an allocation decision proposed by RO respects the requirements as per the tenant's SLA or not. It relies on $\texttt{pot}(g_j)$ to estimate the degradation of the data rate due to puncturing of eMBB slice traffic by random traffic arrival from uRLLC user. Similarly, α^{f_k} is used to decide how much fraction of the channel resource are shared by eMBB and mMTC user. SV needs following user information to be able to asses the validity of one assignment: $\texttt{class}(g_j)$, $\texttt{pos}(g_j)$, $\texttt{pot}(g_j)$, $\texttt{dr}(g_j)$, $\texttt{lat}(g_j)$, $\forall g_j \in \mathcal{G}$. More formally, let $\mathcal{S}$ be the collection of

all subsets of $\mathcal{G}$. The SV can be viewed as a mapping $SV : \mathcal{S} \rightarrow \{\texttt{TRUE}, \texttt{FALSE}\}$ that takes as input a subset of users $\mathcal{G}' \subseteq \mathcal{G}$ that are assigned to a channel resource and returns boolean `TRUE`, if the assignment respects all the requirements of the users in $\mathcal{G}'$, `FALSE` otherwise.

In addition to the modular organization of the optimization framework, a clear advantage achieved from segregated RO-SV module is flexible and dynamic tuning of the "validation" logic of the SV module according to desired QoS of slice users. In this work, we rely on a SINR-driven QoS validation for determining channel resource assignment of eMBB, uRLLC and mMTC slice users. Depending on the way how the SINR values are treated in the SV "validation" logic, following two approaches can be devised. Note that, our focus is not to compare following two proposed approaches showing superiority over one another, rather to justify its suitable use depending on the available computational resource, assumptions on the perfect channel state estimation, type of propagation environment etc.

Instantaneous SINR (`SV-Inst`)

This approach is suitable for accurate modeling and validation of the slice-specific QoS. Such an approach is statistically reliable and requires a significant amount of sampling and therefore, it requires a non-negligible computing time. The instantaneous channel statistics is defined in Equation (3.2) and uses instantaneous SINR values to evaluate the desired data rate for eMBB and mMTC slice users, by using Equations (3.6) and (3.7), respectively. For uRLLC slice users, Equation (3.11) evaluates the reliability (BLER) in closed-form and also validate the same using computer simulations.

Average SINR (`SV-Avg`)

In contrast to instantaneous SINR, a reasonable alternative would be to compute the SINR value by assuming that, the channel envelope of the transmitted signals has a fixed expected value: $\mathbb{E}\{\tilde{H}\} = 1$. This simplification results in lower number of samples and less computing time that may be considered as a viable choice in computationally-constrained flying platforms. Using this simplification, Equation (3.1) for the received signal power S_{g_j} consists of only constant terms and therefore, the QoS metrics are derivable applying a closed-form formula.

How to include the SV feedback to the RO

An important advantage of such a definition of the SV is that it does not depend on the specific channel resource used. Hence, the collection of possible assignments $\mathcal{S}$ can be partitioned into two sets. Let, $\mathcal{S}_{\texttt{F}} \subseteq \mathcal{S}$ represents the collection of assignments to a channel resource that do not respect all the slice-specific QoS requirement. A symmetric definition can be given for set $\mathcal{S}_{\texttt{T}} \subseteq \mathcal{S}$ that corresponds to collection of assignments to a channel resource meeting all the QoS requirements. In other words:

$$\mathcal{S}_{\texttt{F}} = \{\mathcal{G}' \subseteq \mathcal{G} : \mathcal{G}' \text{ is RO-feasible and } \mathcal{S}(\mathcal{G}') = \texttt{FALSE}\}$$
$$\mathcal{S}_{\texttt{T}} = \{\mathcal{G}' \subseteq \mathcal{G} : \mathcal{G}' \text{ is RO-feasible and } \mathcal{S}(\mathcal{G}') = \texttt{TRUE}\}$$

To obtain an SV-feasible assignment, the following set of so-called *no-good constraints (or cuts)* [129, 130] needs to be added to the mathematical model:

$$\sum_{g_j \in \mathcal{G}'} t_{g_j}^{f_k} \leq |\mathcal{G}'| - 1 \quad \forall \mathcal{G}' \in \mathcal{S}_{\texttt{F}}, f_k \in \mathcal{F} \; . \tag{3.27}$$

The following lemma shows that adding the set of constraints (3.27) to RO is sufficient to have an *SV-feasible* assignments.

***No-good constraint* in Equation** (3.27) **guarantees *SV-feasible* channel resource assignments.**

Proof. To forbid an unfeasible assignment, it is sufficient to forbid that, for each channel resource f_k and for each unfeasible assignment $\mathcal{G}' \in \mathcal{S}_{\mathtt{F}}$, it is not possible to assign all the ground users $g_j \in \mathcal{G}'$ to f_k. This is equivalent to impose that at most $|\mathcal{G}'| - 1$ of them must be assigned together. □

The execution flow of the EASIER framework is depicted in Figure 3.4. If the Solution Validator is not used, the EASIER framework reduces to solving the model (3.13)-(3.20) once. On the other hand, if the SV is active, an assignment needs to be validated by the Scheduling Validator (either the `SV-Inst` or the `SV-Avg`), in therms of mathematical model, this reduces to add one violated inequality (3.27), After the inequality is added, the problem is solved again, until the current assignment is considered feasible by the Scheduling Validator. The set $\mathcal{S}_{\mathtt{F}}$ is exponential in size. So its enumeration can be potentially time consuming. In our implementation, the size of the instances considered makes it possible to enumerated a-priori all the element of $\mathcal{S}_{\mathtt{F}}$ and all the inequalities (3.27) are added one-the flight when needed to the constraints of the RO model (3.14)-(3.20).

3.6 Experimental Setup and Evaluations

In this section, we present a comprehensive analysis and evaluation of the solutions provided by the proposed framework. We assess the performance for different optimization settings and compare the results. All the mentioned models are implemented in C++ using IBM ILOG CPLEX 12.8.0 as MILP solver. The experiments are executed on a x86, single core, Intel Xeon E5-4620 processor at 2.2 GHz CPU frequency and 4 GB RAM.

3.6.1 Optimization Diversity

Multiple versions of the EASIER framework can be evaluated using different mathematical models that are used to produce RO-feasible assignments. They can be classified into two categories: `SV-Oblivious` and `SV-Aware`.

SV-Oblivious

The assignment decisions resulted from this approach are not based on SV and are obtained by solving the following mathematical model:

$$\max \sum_{f_k \in \mathcal{F}} \sum_{g_j \in \mathcal{G}} \sum_{g_{j'} \in \mathcal{G}} -w_{g_j g_{j'}} t_{g_j}^{f_k} t_{g_{j'}}^{f_k}$$
$$s.t. \quad (3.14) - (3.20).$$

We can see that as objective function, we use equation (3.13) with $\gamma = 0$ and $\mathcal{G}^O = \emptyset$ (*i.e.,* all users are mandatory or non-optional). As ϕ_{ovl} (see equation (3.25)), we test both the uniform ($\mathtt{NoSV}_U$) and the data rate-dependent ($\mathtt{NoSV}_{DR}$) weights (equations (3.26) and (3.21)-(3.23) respectively).

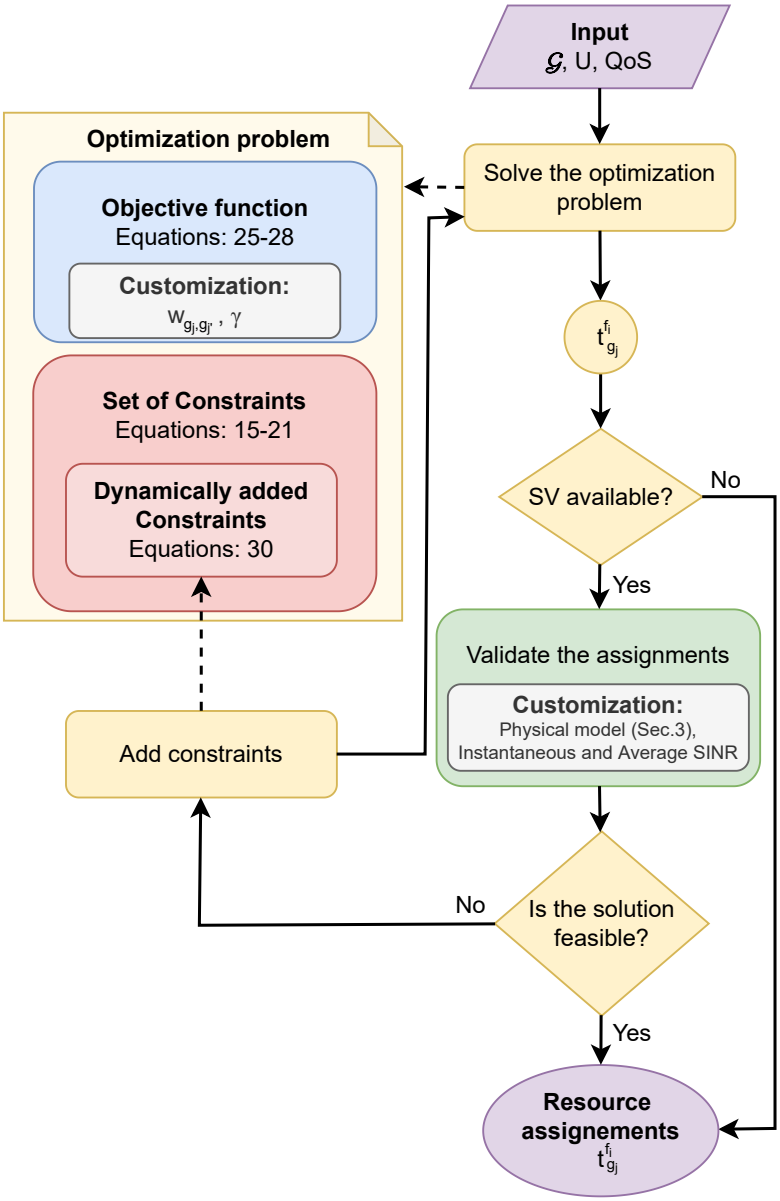

Figure 3.4: *EASIER*: the execution flow

SV-Aware

The assignment decisions in this case are obtained by solving following mathematical model:

$$\max \gamma \sum_{f_k \in \mathcal{F}} \sum_{g_j \in \mathcal{G}^O_M \cup \mathcal{G}^O_E} t^{f_k}_{g_j} +$$
$$(1-\gamma) \sum_{f_k \in \mathcal{F}} \sum_{g_j \in \mathcal{G}} \sum_{g_{j'} \in \mathcal{G}} -w_{g_j g_{j'}} t^{f_k}_{g_j} t^{f_k}_{g_{j'}}$$
$$s.t. \quad (3.14) - (3.20), \ (3.27).$$

Above model is obtained after adding the set of no-good constraints (3.27) in addition to constraints (3.14)-(3.20). The set of no-good constraints are obtained by either using the in-

Table 3.2: Optimization Diversity

Option	SV Channel Estimation	p_{g_j}	$w_{g_j,g_{j'}}$	γ	$\mathcal{G}$
$\texttt{NoSV}_U$	-	0	1	0	$\mathcal{G}^O = \emptyset$
$\texttt{NoSV}_{DR}$	-	0	Eqn. (3.21) (3.22) (3.23)	0	$\mathcal{G}^O = \emptyset$
$\texttt{SV-Avg}_U$	Average SINR	1	1	$1 - 10^{-6}$	$\mathcal{G}^O = \mathcal{G}$
$\texttt{SV-Inst}_U$	Instantaneous SINR	1	1	$1 - 10^{-6}$	$\mathcal{G}^O = \mathcal{G}$
$\texttt{SV-Avg}_{DR}$	Average SINR	1	Eqn. (3.21) (3.22) (3.23)	$1 - 10^{-6}$	$\mathcal{G}^O = \mathcal{G}$
$\texttt{SV-Inst}_{DR}$	Instantaneous SINR	1	Eqn. (3.21) (3.22) (3.23)	$1 - 10^{-6}$	$\mathcal{G}^O = \mathcal{G}$
$\texttt{SV-Avg}_X$	Average SINR	1	0	1	$\mathcal{G}^O = \mathcal{G}$
$\texttt{SV-Inst}_X$	Instantaneous SINR	1	0	1	$\mathcal{G}^O = \mathcal{G}$

stantaneous SINR (`SV-Inst`) or the average SINR (`SV-Avg`) approach. As objective function, we used equation (3.13) with $\gamma = 1 - 10^{-6}$ and $\mathcal{G}^O = \mathcal{G}$ (*i.e.,* all users are optional). Such a choice for the gamma coefficient implies that the objective function becomes a so-called *lexicographic* objective function, where we first maximize ϕ_{ou} and as secondary objective, we minimize the weighted number of overlaps ϕ_{ovl}. As ϕ_{ovl} (see equation (3.25)), we used both uniform (options $\texttt{SV-Avg}_U$ and $\texttt{SV-Inst}_U$), data rate-dependent (options $\texttt{SV-Avg}_{DR}$ and $\texttt{SV-Inst}_{DR}$) weights and no $\phi_{ovl}(t)$ (options $\texttt{SV-Avg}_X$ and $\texttt{SV-Inst}_X$). Table 3.2 summarizes how the coefficients of ϕ_{ou} and ϕ_{ovl} changes according to the options used.

The basic idea of the `SV-Oblivious` options is to test the performances of an algorithm that is not able to directly check the feasibility of an assignment in terms of respecting required data rates, and therefore aims at admitting *"as best as possible"* all the slice users. On the other hand, the `SV-Aware` options serve the primary goal of accepting the maximum number of slice users while guaranteeing their required QoS metric as set by slice owners (*i.e.,* tenants). To maximize only the number of accepted users imposed in the objective function, often leads to a situation where several different assignments can all provide the optimal solution. The secondary objective function, $\phi_{ovl}(t)$ can therefore help in selectively pruning the vast solution space and finding, among all the assignments that accommodates maximum number of users, the one that attempts to improve the data rates of the accepted users.

3.6.2 Evaluation Scenario

We consider a cellular wireless fading channel environment where a standalone UAV-BS is deployed in a coverage area of 200 $m \times 200$ m and operates with 20 MHz radio bandwidth. Three heterogeneous slice service types (eMBB, uRLLC and mMTC) are supported by the UAV-BS and the slice users are randomly distributed in the coverage area as per Poisson point process (PPP) [131]. The total number of slice UEs ranges between 30 and 45, with 20% eMBB, 20% uRLLC, and 50% mMTC UEs. An example instance deployment can be visualized in Fig. 3.5. Each TTI spans 1 ms in time domain and 12 subcarriers in frequency domain. To facilitate latency-sensitive uRLLC traffic, each 1 ms TTI is further split into 8 equally-spaced mini-slots of 125 μs each [104]. The uRLLC traffic for user g_j arrive randomly in mini-slots with a rate of $\texttt{pot}(g_j) = 0.25$. In this work, we consider the BLER for uRLLC slice traffic, $1 - \texttt{rel}(g_j) = 10^{-5}$ where $\texttt{rel}(g_j)$ is the reliability demanded by the slice tenant. The list of all experimental parameters is shown in Table 3.3.

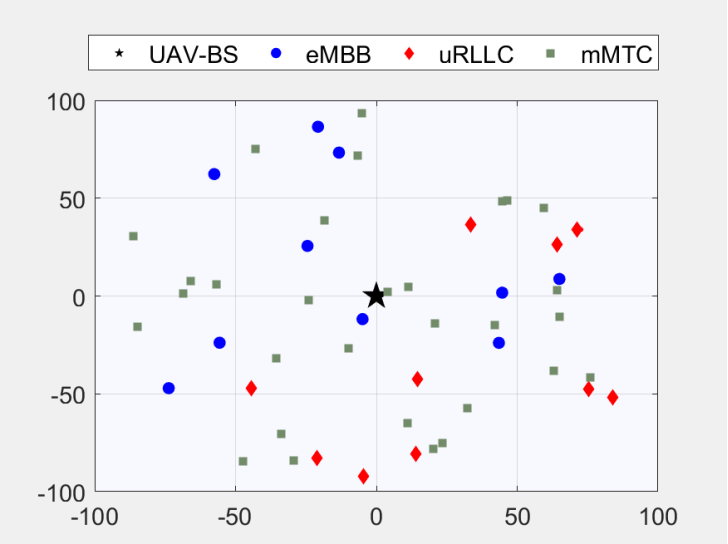

Figure 3.5: An example deployment with one UAV-BS positioned at origin $(0, 0)$ flying at 50 meters altitude in 200 $m \times 200$ m. Ground UEs of three slice service types (10 eMBB, 10 uRLLC and 30 mMTC) are deployed randomly within the area.

Table 3.3: Simulation Parameters

Parameter	**Value**
Slice service Type	[eMBB, uRLLC, mMTC]
UAV-BS transmission power	1 Watt
Coverage area	200 $m \times 200$ m
Ground UE distribution	Random (PPP)
UAV-BS altitude	50 meters
A2G environment variable $[a, b]$	[9.61,0.16]
Scenario	Urban
Antenna gain $[G_t, G_r]$	[6, 6] dB
Total radio bandwidth	20 MHz (100 PRBs)
$[N_{\mathcal{G}_E}, N_{\mathcal{G}_U}, N_{\mathcal{G}_M}]$	[10, 3, 20]
Noise power density	-174 dBm/Hz
A2G fading channel	Rician
# of subcarriers per channel resource	12
Sub-carrier spacing (KHz)	15 and 30
uRLLC traffic arrival rate ($\texttt{pot}(g_j)$)	0.25
SLA: Minimum eMBB rate	2.5 Mbps
SLA: uRLLC reliability	10^{-4} BLER
SLA: uRLLC latency deadline	1 mini-slot *i.e.*, 125 μs
SLA: Minimum mMTC rate	250 Kbps

3.6.3 Results and Discussions

To assess the performance, we first examine whether addition of the Scheduling Validator has a positive effect in terms of quality of the obtained assignments. Secondly, we verify how it can be used to identify a better positioning of the UAV-BS.

		SV-Oblivious		**SV-Aware**					
				SV-Avg			**SV-Inst**		
		$\texttt{NoSV}_U$	$\texttt{NoSV}_{DR}$	$\texttt{SV-Avg}_X$	$\texttt{SV-Avg}_U$	$\texttt{SV-Avg}_{DR}$	$\texttt{SV-Inst}_X$	$\texttt{SV-Inst}_U$	$\texttt{SV-Inst}_{DR}$
eMBB	**%Accept**	100	100	88	90.3	92.9	95	94.5	98.4
	%Sat	53	99.4	100	100	100	100	100	100
mMTC	**%Accept**	100	100	88.2	88.5	86.9	92.5	92.3	91.3
	%Sat	62.9	77.2	100	100	100	100	100	100

Table 3.4: Comparison between SV-Oblivious and SV-Aware resource assignment - Accepted and Satisfied per-slice users. Each value is the average of 50 simulation environment randomly deploying 50 ground UEs in an area of 200 $m \times 200$ m.

Impact of Scheduling Validator (SV)

To the best of our knowledge, there are no algorithms available in the literature that solve the class of problems proposed including a generic Schedule validator like the one we propose in this work. Therefore, aim of this section is to shows the effectiveness of SV module during channel resource assignment to heterogeneous slice users. Table 3.4 summarizes the benefits obtained when SV module is working in conjunction with RO module in segregated RO-SV optimization framework described in Section 3.5. For a given class of slice users, we present two rows that denotes (i) the percentage of accepted users (%Accept) and (ii) the percentage of slice users where the slice-specific SLA are satisfied (%Sat). We benchmark our framework against the `SV-Oblivious` policy, that tries to accommodate all the slice users by considering them as mandatory (*i.e.,* non-optional). Such policy does not always guarantee that slice-specific SLA are met for an accepted user. On the other hand, `SV-Aware` slicing policy (either `SV-Inst` or `SV-Avg`) ensures that slice-specific SLA for an accepted user is always met. This hard enforcement tends to lower the user acceptance ratio as compared to corresponding values obtained through `SV-Oblivious` slicing policy. We can observe that, the value of %Accept for `SV-Oblivious` options is always 100% as it aims to provision service to all slice users, but %Sat are less. In `SV-Avg` and `SV-Inst`, the row values in %Accept are less than 100%, however all these accepted users have met their corresponding slice-specific SLA *i.e.,* resulting a value of 100% in row %Sat.

Per-slice SLA Satisfaction

In this subsection, we compare and contrast among two variants of `SV-Aware` slicing policies in terms of user acceptance and SLA satisfaction rate. This can be done by focusing on the two vertical parts of `SV-Aware` in Table 3.4. For the instances considered, `SV-Inst` allows to satisfy approximately 5% more users than `SV-Avg`, without deteriorating the required slice-specific SLA, showing clearly an advantage over the averaged SINR-based, simplistic `SV-Avg` option. If we consider the second indicator %Sat, as expected, we have always a value of 100% for `SV-Inst`, because the no-good constraints are obtained following the same computation. It is interesting to notice that, all the slice-specific SLA of the accepted users are satisfied for `SV-Avg`, showing the ability of this option to provide reliable assignments. Finally, if we consider the `SV-Oblivious` option, a significant percentage (around 20% for the DR option) of the accepted users do not have the required data rate, clearly showing the limitation of not using a SV module in conjunction

with RO module.

As second part of the analysis, Fig 3.6 shows the variation in the user acceptance ratio of eMBB slice service type for both `SV-Inst` and `SV-Avg` options. `SV-Inst` is able to squeeze-in more slice users than `SV-Avg` irrespective of the eMBB demanded data rate. Note that, when eMBB slice users demanded data rate increase, the `SV-Aware` options undergo a degradation in user acceptance rate. This is because, more number of radio resources are allocated per every eMBB user to maintain data rate threshold, thereby reducing the total amount of users to be served. Fig. 3.7 presents a comparison between `SV-Inst` and `SV-Avg` with varying UAV-BS operating altitude from 25 meters to 200 meters. The figure plots the average percentage of users accepted for both schemes with 95% confidence interval. Note that, `SV-Inst` performs better than `SV-Avg` option by squeezing more users that shows the importance of channel responsiveness in our `SV-Aware` proposal.

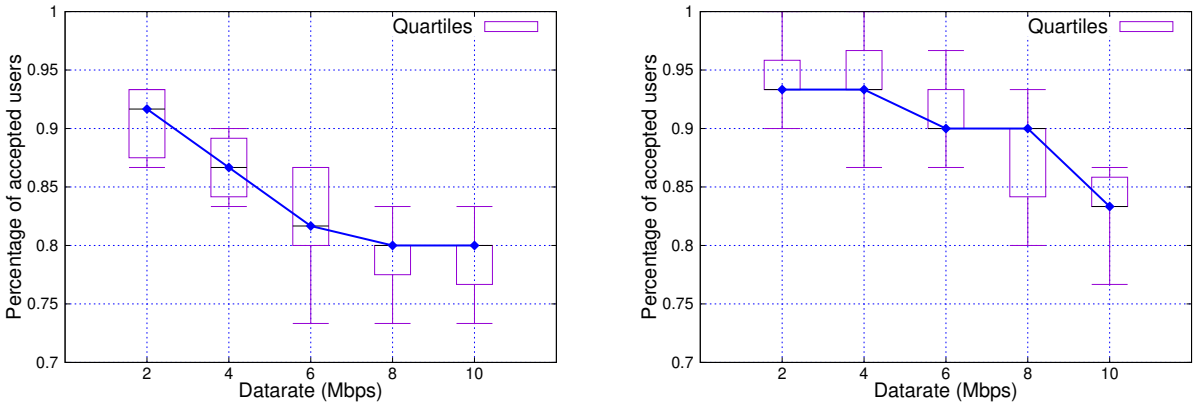

Figure 3.6: Percentage of accepted eMBB users w.r.t. varying data rate for (a) SV-AVG and (b) SV-INST

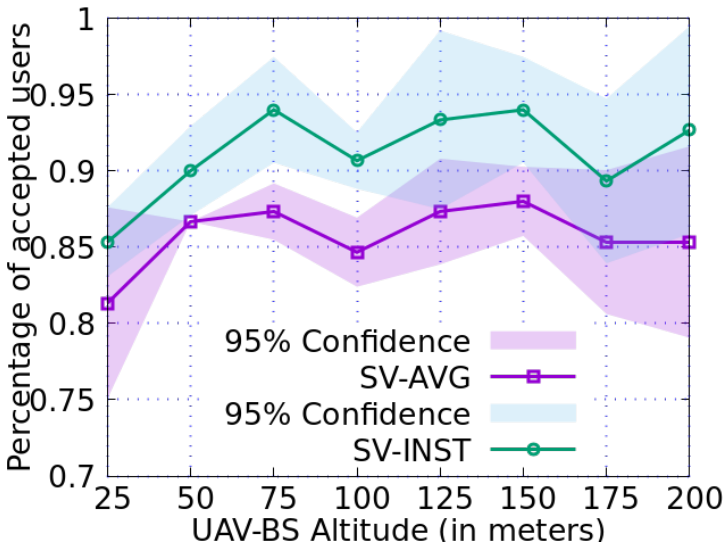

Figure 3.7: Percentage of accepted eMBB users with respect to varying UAV-BS altitude for SV-AVG and SV-INST

UAV-BS Positioning

UAV-BSs are capable of self-positioning in order to improve SLA metrics for ground UEs. To show the importance of a careful positioning of the UAV-BS, we present in Fig. 3.8a, a map that shows the percentage of accepted slice users changes in accordance with hypothetical different UAV-BS positions. In this scenario of 200 $m \times 200$ m, we uniformly placed 10 eMBB, 20 mMTC, and 3 uRLLC ground users. We placed the UAV-BS at different positions on a grid 4×4 centered on the geographical terrain considered for the experimentation, with a distance in the x,y directions of 40 m. Finally, we interpolated the 4×4 results in order to have a smoother heatmap, as showed in Figure 3.8a. In the experiment, the `SV-Inst` slicing policy has been used and we analyze the percentage of accepted slice users. We can notice from Fig. 3.8a the importance of the correct placement of the UAV-BS in order to maximize number of users that satisfy the demand from slice-specific SLA. Indeed, the proposed *EASIER* framework became crucial in future path planning algorithms for the UAV-BS by flexible placement decisions in a dynamic environment, where position of the ground UEs are continuously changing. We can observe that how the ground users' position impacts the overall system performance.

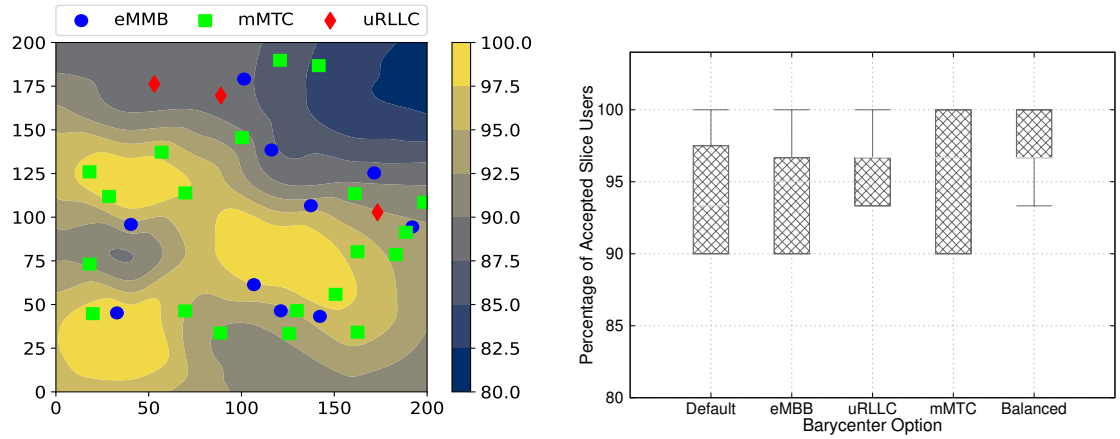

(a) (b)

Figure 3.8: (a) Heatmap denoting the percentage of accepted slice users according to positioning of UAV-BS in 200 $m \times 200$ m. (b) Box-and-whisker plot showing percentage of accepted users for different barycenter choices of positioning UAV-BS.

Motivated by the flexible placement opportunity and its influence on individual slice performance, we expanded the prior experiment to study and analyze different UAV-BS placement policies. A frequently adopted approach to solve the problem of the positioning of UAV-BS is to compute a *barycenter* given by a weighted sum of the slice user locations. Let $\texttt{pos}_x(g_j)$ and $\texttt{pos}_y(g_j)$ be the coordinate over the x- and y-axis of ground user g_j, the *barycenter* (x_B, y_B) of a set of users $\overline{\mathcal{G}}$ consists of the following coordinate:

$$(x_B, y_B) = \left(\frac{\sum_{g_j \in \mathcal{G}} \texttt{pos}_x(g_j)}{|\overline{\mathcal{G}}|}, \frac{\sum_{g_j \in \mathcal{G}} \texttt{pos}_y(g_j)}{|\overline{\mathcal{G}}|}\right) \tag{3.28}$$

We therefore investigate three types of policies to automatically identify the positioning of the UAV-BS:

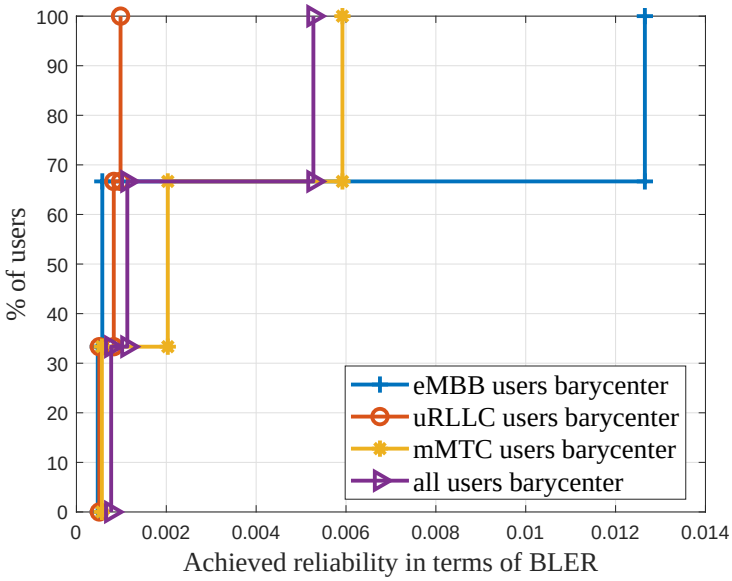

Figure 3.9: Improved reliability performance resulted from placing UAV-BS at uRLLC barycenter vs. other barycenters

- *Default positioning* - In this case, the UAV-BS is placed at the center coordinate of the geographical terrain *i.e.,* at origin $(0, 0)$ at fixed altitude of 50 meters.
- *Slice-specific positioning* - In an heterogeneous user environment with non-uniform QoS demands, an optimal positioning of UAV-BS can be exploited to prioritize service offering to a particular slice tenant. For example, considering a need, where the eMBB slice users need more priority over other class of slice users (*e.g.,* uRLLC or mMTC), the UAV-BS may choose to optimal position itself to maximize the SINR/rate for eMBB users. Similarly, the UAV-BS may position itself to reduce the latency for uRLLC user. We therefore introduce three types of barycenter: uRLLC-centric $(x_B, y_B)_u$, eMBB-centric $(x_B, y_B)_e$ and mMTC-centric $(x_B, y_B)_m$ obtained after applying Equation (3.28) with $\overline{\mathcal{G}}$ equal to $\mathcal{G}_U$, $\mathcal{G}_E$ and $\mathcal{G}_M$, respectively.
- *Balanced positioning* - In this case, the UAV-BS positions itself in a designated barycenter determined by giving equal weights (weighted-average) on all classes of slice users. This is obtained by imposing $\overline{\mathcal{G}} = \mathcal{G}$.

To study and evaluate above positioning variants, our simulation environment randomly generates 10 sets of positioning samples and compute for each positioning, the number of slice users accepted. We report the box-and-whisker plot for each choice of barycenter in Fig. 3.8b. Both Fig. 3.8a and Fig. 3.8b show that the positioning can significantly affect the overall number of accepted users. The balanced approach seems to be the one that allows in general to satisfy an higher number of slice users. On the other hand, we know that for each random environment it is possible to accept all the users. This observation implies that even a simple spatial grid search based on the proposed model leads to a substantial improvement with respect to a benchmark formed by the different barycenters. However, in the future it could be beneficial to include also the positioning in the optimization process.

In Fig. 3.9, we demonstrate the percentage of uRLLC slice users accepted when the UAV-BS is positioned at different barycenter. We can observe that, among all the choices of barycenter,

the positioning of UAV-BS at the uRLLC barycenter favors uRLLC slice users in obtaining improved BLER performance. *This is an inherent benefit exploited by airborne UAV-BS when a particular slice service type (uRLLC in this case) has to be prioritized over another slice service type (eMBB and mMTC).* A similar justification is equally valid for prioritizing eMBB and mMTC slice service types when demanded from slice tenants. In general, such 'prioritized slice' decisions are taken on the basis of a strategic business need of the tenant.

3.7 Conclusions

In this chapter, we present a slicing framework known as *EASIER* in which differentiated 5G services (*i.e.,* eMBB, uRLLC, mMTC slice service types) requested by several tenants are multiplexed in common radio interface of UAV-BS. To ensure slice-specific requirements and to maximize the number of admissible slice users without violating their QoS requirements, *EASIER* is decomposed into a two-phase slicing optimization model: RO and SV, that permits the development of the different modules independently of each other. The RO finds the solutions for the assignment of channel resources to slice users and delegates to the SV module to verify the quality of the assignment proposed by RO. We show that it meets the QoS for all the non-optional users and maximizes the acceptance of the optional users. Moreover, we show that *EASIER* exploits the dynamic positioning of UAV-BS offering preferential treatment to slice-specific requirements as well as slice users improvising overall performance.

Chapter 4

Cellular-connected UAVs

4.1 Introduction

"Cellular-assisted UAV paradigm" refers to communication scenarios in which the UAVs are integrated as new aerial UEs of existing cellular network coexisting with ground UEs. Literally, the name of this paradigm "cellular-assisted" signifies that, in this case, the cellular network extends help towards UAV ecosystem to achieve its mission. In broad literature, such paradigm is also referred as cellular-connected UAVs or 5G-connected UAVs, drone UEs, UAV-UEs etc. In this chapter, we use the term "cellular-connected UAV" to avoid any terminology confusion.

The aerial communications and networking of cellular-connected UAVs pose several challenges to thoroughly investigate. For instance, a reliable and low latency communication for efficient control of the UAV is of utmost importance. Existing cellular infrastructures are primarily designed and developed to offer enhanced communication services for the terrestrial users. Also, the geographical terrains with limited coverage from ground BS may not provide the required connectivity services to the cellular-connected UAVs, thereby demand promising solutions for successful adoption of this technology.

Various studies and research efforts have shown tremendous potential for the support and operation of low altitude UAVs using cellular networks [132]. The benefits of cost-effective cellular spectrum in terms of low latency and high throughput connectivity services, make it a suitable candidate for integration of UAVs. Moreover, this technology is scheduled, robust, secure and offers reliable services. In terms of the security aspects of data communication, existing mobile networks already encompass the needful security and authentication features in their protocol layers. A work item to study and evaluate LTE as a potential candidate for UAV operation is carried out in 3GPP Rel-15, and the results are summarized in TR 36.777 [19]. In addition to existing cellular spectrum bands (600 MHz - 6 GHz), 5G ecosystem is also considering the use of spectrum in millimeter wave (mmWave) bands (24-86 GHz). As a foundation of cellular operations, the licensed spectrum provide scheduled, reliable and wide area connectivity that can potentially be leveraged for UAV operations in BVLoS range. There are a lot of challenges to be tackled in order to make the cellular-connected UAVs as an attractive solution for a plethora of emerging use cases. In the following section, we highlight the primary design challenges and perspectives to be considered for cellular-connected UAVs, as well as the studies and solutions already available.

The following sentence reminds the reader of the fundamental question (Q4 in Section 1.5) that this chapter attempts to raise and discuss potential answers to.

Q4. To what extent do 5G and beyond systems present substantial synergies with respect to its innovations with better radio hardware, cloudification, and virtualization technologies, and what kinds of integration challenges appear while integrating UAVs as aerial UEs of existing cellular network in Cellular-assisted UAV paradigm? Have we made enough progress in R&D for aerial UEs to become a reality?

4.2 Integration Challenges

4.2.1 Three Dimensional (3D) Coverage Model

Preliminary

The existing radio access technologies are not primarily suited for supporting flying radio devices as their deployments are mainly focused to optimally serve the ground UEs (or terrestrial UEs). The base stations (eNodeBs) are typically designed and developed to provide optimal performance to the ground users. The current eNodeBs are downtilted to serve above purpose. Down-tilting the antennas produces radiation patterns that are not useful to serve aerial UEs, which are expected to be positioned at different altitudes with respect to the ground surface. The inherent assumptions made for the ground UEs are quite different from aerial UEs. The aerial users typically fly higher than the BS antenna height and therefore, need 3D coverage suitable for varying UAV altitude [133]. The BS antennas of LTE networks may provide weak channel gain by using their antenna side lobes. In the 3D space, the coverage criterion of UAVs are functions of BS antenna height, UAV altitude, antenna pattern, and association rules. Hence, the network model for aerial users coexisting with ground users necessitates a 3D coverage model [134].

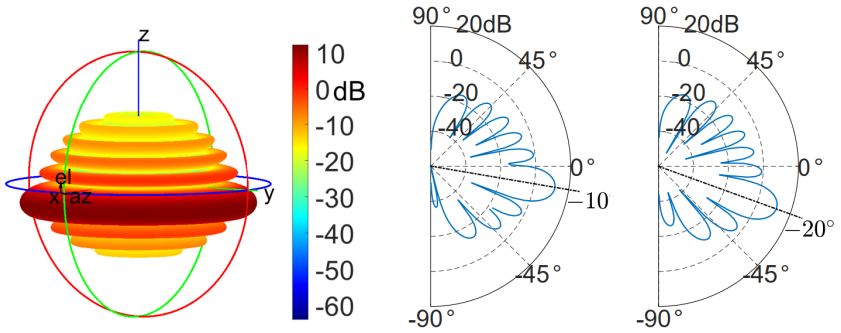

Figure 4.1: Power gain and elevation pattern of ground BS [135]

Associated Works and Illustrative Results

In [135], the authors present 3D coverage and channel modelling of cellular-connected UAVs in the downlink and uplink directions. The BS antenna pattern tremendously impacts the coverage distribution that affects the UAV operation and mobility. As the down-tilt angle increases, the ground BS offers smaller gains to UAV above the BS height, thereby impacting the uplink and downlink coverage probabilities. In Fig. 4.1 (a), the power gain pattern is illustrated for a synchronized uniform linear antenna array (ULA) with 10 co-polarized dipole antenna elements

and BS down-tilt angle $\theta_{tilt} = -10°$. (b) and (c) are the 2D elevation pattern for BS with down-tilt angle for $\theta_{tilt} = -10°$ and $\theta_{tilt} = -20°$, respectively.

4.2.2 UAV-Ground Channel

Preliminary

One of the primary design challenges in realizing the cellular-connected UAVs is to ensure harmonious coexistence mechanisms between ground users and aerial users [71]. Proper UAV-ground interference management is central to realize this coexistence. Also, the interference patterns in ground BS to UAVs communication link experiences remarkable difference than that of link between ground BS to ground UE [136]. The higher altitude of UAVs than base stations results in LoS links, which are more reliable than the link with ground users. Additionally, they exploit large macro diversity gains being served from several BSs. On the other hand, the dominant LoS links create more uplink/downlink interference as compared to ground users, thereby making the interference management (ICIC) highly difficult. Other relevant effects to take into account are fading, shadowing and path-loss. Existing ICIC mechanisms may be well suited for current cellular designs, but fail to handle UAV interference management, which involves many BSs and impose limitations due to high complexity.

Therefore, there is a need for efficient interference management techniques for harmonious coexistence of ground users and UAVs. There are several works in literature [134, 137, 138] that investigate this problem considering downlink and uplink interference.

The communication channel mainly involves two types of links, namely Ground-to-UAV (G2U) link and UAV-to-Ground (U2G) link. In cellular-connected UAV, the G2U link serves the downlink purpose of control and command for proper UAV operations, whereas U2G link serves the uplink purpose of payload communication. Rayleigh fading is the commonly used small-scale fading model for terrestrial channel model, whereas due to the presence of LoS propagation characteristics, Nakagami-m and Rician small-scale fading are usually preferred for U2G channels. The large-scale fading is affected because of the 3D coverage region and varying altitude of UAV. The large-scale fading models used can be based on a free-space channel model or altitude/angle dependent channel model or probabilistic LoS models:

- Free-space model - In free-space channel model, there is no effect of fading and shadowing with very limited obstruction. This model is typically suited for rural regions where the LoS assumption holds valid between high altitude UAVs and ground station. However, in urban environment, the low altitude UAVs may encounter non-LoS links, therefore need other approaches to properly map with the propagation environment.

- Altitude/Angle dependent model - In this case, the channel parameters such as shadowing and path loss exponents are functions of UAV altitude or elevation angle. These models find their applicability in urban or sub-urban regions depending upon the deployment. However, if the altitude does not change or UAVs fly horizontally, altitude dependent models may not be found suitable. The elevation angle based models are mostly used for theoretical study purpose and existing literatures are also limited in this regard.

- Probabilistic LoS model - The models based on this approach are typically suited for urban environment where the LoS and NLoS link between UAV and ground are considered, due to buildings, obstacles or blockages. Moreover, the LoS and NLoS components are separately modelled based on their occurrence probability in urban environment. The nature of urban

environment with respect to building heights and density are key factors that statistically determine the LoS and NLoS propagation characteristics.

Associated Works and Illustrative Results

The study item of 3GPP TSG on the enhanced LTE support for aerial vehicles [16] highlights the channel modelling between ground base station and UAV flying at different altitudes. The study includes the modelling of small scale fading, path loss, shadowing and LOS probability (P_{los}) for three 3GPP deployment scenarios, namely Urban-Micro (UMi), Urban-Macro (UMa) and Rural-Macro (RMa). The LoS probability is specified by:

- 2D distance between UAV and ground station (d)
- Altitude of UAV (h_u)

The existing terrestrial communication channel model can be directly used for low UAV altitude (height below certain threshold H_{low}) to model the LoS probability. For altitude greater than a certain threshold H_{high}, 3GPP suggests to use 100% LoS probability. For height in between H_{low} and H_{high}, the LoS probability is a function of d and h_u. Hence, for the three deployment scenarios, P_{los} is given by,

$$P_{los} = \begin{cases} UE\_P_{los}, & \text{if 1.5 meter } \leq h_u \leq H_{low} \\ f(h_u, d), & \text{if } H_{low} \leq h_u \leq H_{high} \\ 1, & \text{if } h_u \geq H_{high} \text{ and } h_u \leq 300 \text{ meter} \end{cases}$$

UE_P_{los} is the LoS probability for ground mobile terminal in conventional terrestrial communication in Table 7.4.2 of [139]. $f(h_u, d)$ is given by,

$$f(h_u, d) = \begin{cases} 1, & \text{if } h_u \leq l1 \\ \frac{l1}{h_u} + exp(\frac{-h_u}{p1})(1 - \frac{l1}{h_u}), & \text{if } h_u > l1 \end{cases}$$

The variables $l1$ and $p1$ are given as the logarithmic increasing function of UAV height h_u as specified in [16]. The values of H_{low}, H_{high}, $p1$ and $l1$ are also defined with respect to different 3GPP deployment scenarios. Table B-2 and B-3 in [16] provides detailed path-loss and shadowing standard deviation, respectively.

4.2.3 System Operations & Mobility

Preliminary

UAVs are inherently mobile in nature and section 1.7 highlights many use cases of cellular-connected UAVs that implicitly demand BVLoS [140]. The mobility and handover characteristics of terrestrial cellular users are quite different from the 3D aerial mobility of cellular-connected UAVs. With increase in height, the radio environment changes and mobile UAVs face connectivity challenges. In this case, the performance of the system depends on the handover rates, including failed and successful handovers and radio link failures. Radio link failures occurs when the UAV is unable to maintain a successful connection with the serving cell. This could be because of the problematic RACH or expiry of timers or after a certain maximum number of retransmissions is reached [141].

In cellular-connected UAV, the protocol operations and regulatory needs of UAVs as aerial users are quite different from the ground user. Hence, the network must first detect if the user device is aerial or not [142]. This detection can be driven by the ground BS by estimating:

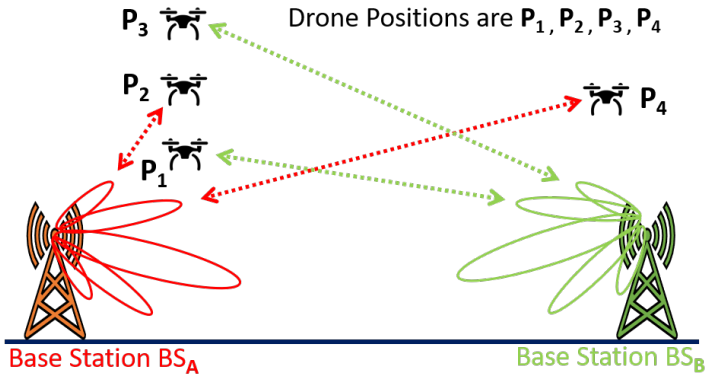

Figure 4.2: UAVs being served from side lobes [143]

- the elevation angle of the reference signal;
- vertical location (altitude) or velocity of user device;
- path loss/delay spread measurement of user devices.

Associated Works and Illustrative Results

The handover characteristics vary significantly between ground UEs and aerial UE due to the nature of cell selection, as shown in Fig. 4.2. In [143], the authors demonstrated the impact of UAV flight path on handovers. The results show that UAVs are prone to frequent handovers, and ping-pong handovers, due to varying altitude and speed. Even smaller flight distances can have a large impact on handover rate. Also, the handover frequency increases when flight altitude increases. Table 4.1 summarizes the number of handovers occurring per minute for UAV, as compared to terrestrial users. Scenario1 is equivalent to a ground user having one handover per minute. However, in scenario4, UAVs, at an altitude of 150m, experiences 5 handovers per minute. Many of the handovers are unnecessary and generate high signalling overhead. Handover decisions are mainly made depending upon received RSRP (Referenced Signal Referenced Power) values from different BS antennas. Ground users are benefited by this approach, because the radio transmission power are directed to ground from the main lobes of the antenna, thereby improved radio power and every received RSRP is well separated from others. However, the aerial users are served primarily by the antenna side lobes, whose RSRP tends to be very similar to the radio power from other surrounding BS. Hence, the UAV connects with more cells (distant cells), as there is a small difference in the RSRP values resulted from BS antenna side lobes.

Hence, integration of cellular-connected UAVs with future 5G and beyond networks necessitates enhanced solutions for cell selection and handovers that seamlessly cover changing altitudes of UAVs and support their 3D mobility patterns.

4.2.4 Trajectory Optimization

Preliminary

UAV trajectory or flight path refers to the path through which UAV completes its mission for a specified use case. It involves a pair of locations that need to be covered, considering communication requirements of payload and CNPC links. The flying direction of UAV is usually optimized

Table 4.1: Rate of handovers with varying UAV altitude [143]

Scenario	Height (Meters)	#Handovers/Minute
1	10	1.0
2	50	1.9
3	100	4
4	150	5

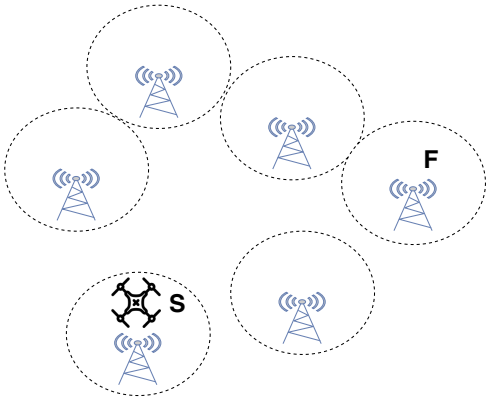

Figure 4.3: UAV trajectory with cellular discontinuity

to meet the application requirements, based on some cost function involving BS locations, association sequence and mission type [144–146]. A UAV trajectory is optimized to minimize the UAV flight time by ensuring that the UAV is always connected to at least one BS, often with some discontinuity tolerance limit [147]. An optimization of flight path with above assumption is known as communication-aware trajectory design.

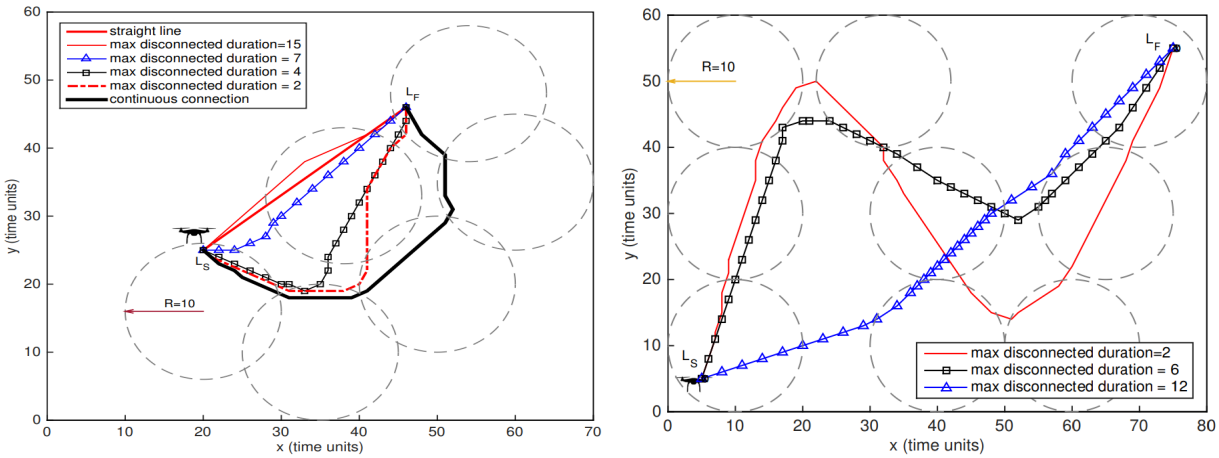

(a) UAV trajectory with first cell layout

(b) UAV trajectory with second cell layout

Figure 4.4: UAV trajectory for two different layouts with varying discontinuity threshold [147]

The rural and unpopulated areas with poor or no cellular connectivity impact UAV trajectory, as the persistent connection controlling the UAV might be interrupted. Additionally, UAVs operations in mmWave bands of 5G suffer from greater path loss and blockages leading to

Table 4.2: Reference works on trajectory optimization for cellular-connected UAVs

References	Key considerations for Optimization	Approach Taken	Goals of Optimization
[147]	Discontinuity duration	Dynamic Programming based approximate solution with low complexity	Minimize the UAV trajectory distance without staying out of coverage for certain threshold
[145]	Ensuring connectivity to one ground BS at any instance of time, thereby targeting minimum SNR during mission	Graph connectivity-based approach	Minimize the UAV's mission completion time by optimizing the trajectory
[144]	Wireless transmission latency, flight time, interference	Deep reinforcement learning algorithm based on echo state network (ESN) cells	Maximize the energy efficiency, minimize the wireless transmission latency and interference on ground network, minimize the time needed to reach destination

interrupted connections during mission path. Fig. 4.3 demonstrates the need for communication-aware trajectory design in cellular-connected UAVs consisting of many ground BSs and a single UAV. Assume that the UAV has to cover a path from start position S to final position F. As shown in the figure, the coverage from all the ground stations does not fully meet the connection requirement and may suffer from discontinuity. Following are two main observations that complicate this mission path and must be accounted in the communication-aware trajectory design:

- The flight path may not be a linear or straight path from S to F, although it is distance-optimal. The UAV must exhibit persistent connection with cellular networks during flight path, thereby making it non-linear or curved.
- The optimal path may pass beyond cellular coverage and hence, proper tolerance limits have to be applied before the UAV connection is interrupted. The cases, where the discontinuity duration exceeds beyond the acceptable tolerance limit, the UAV fails to accomplish the given mission being unable to maintain a successful connection to cellular network.

Associated Works and Illustrative Results

Table 6.1 highlights the existing literature for UAV trajectory optimization. The authors in [147] formulate an approximate optimum trajectory finding problem for cellular-connected UAVs without exceeding a given discontinuity tolerance limit between a pair of locations. The problem is solved by a dynamic programming approach having low computational complexity and is shown to achieve close to optimal results. Fig. 5.9 demonstrates the UAV trajectory for two different cellular layouts with respect to a discontinuity threshold. It is clear that, the UAV respects this threshold limit to generate the flying coordinates for trajectory. Threshold value of zero (*i.e.,* continuous connection) generates a trajectory that must pass through the cellular coverage, as shown by a dark black line in Fig. 4.4a. When the threshold value is 15 time units (shown by a red line in Fig. 4.4a), then the trajectory tries to minimize the distance covered and nearly follows a straight path for distance optimization. Similar justifications are also valid for second cellular layout shown in Fig. 4.4b.

4.2.5 Security Challenges

Preliminary

Cellular-connected UAVs are usually equipped with a multitude of sensors that collect and disseminate data. This provides numerous opportunities to expose them to vulnerabilities. These flying platforms are prone to cyber physical attacks, with an intention to steal, control and misuse the UAV payload information by reprogramming it for undesired behaviour. For instance, in business use case such as goods delivery, the attacker can gain physical access to the customer package as well as to the UAV device. Existing information security measures are not well suited for cellular-connected UAVs, because these measures do not take into account possible threats imposed on numerous on-board sensors and actuator measurements of UAVs [148, 149]. An attacker can manipulate the UAV's communication and control system, thereby making it very difficult to bring it back online. Thus, it is crucial to develop new protection methodologies to avoid aforementioned intrusions and hacking procedures [150].

Associated Works and Illustrative Results

Inspired by the efficacy of the AI and ML-empowered approaches, in [150], the authors presented various security challenges focusing from the viewpoint of three different cellular-connected UAV applications. They are - (i) UAV-based delivery systems (UAV-DS), (ii) UAV-based real-time multimedia streaming (UAV-RMS) and (iii) UAV-enabled intelligent transportation systems (UAV-ITS). In order to solve this challenge, the authors proposed an artificial neural network (ANN) based solution approach which adaptively optimizes the network changes to safeguard the resource and UAV operation.

- UAV-DS: These systems are vulnerable to cyber-physical attacks where the delivery of goods is compromised. The malicious intruder takes control of the UAV with an intention to destroy, steal or delay the transported goods. Even the UAVs can be physically attacked to acquire the goods being transported along with physical UAV assets.

- UAV-RMS: UAV-enabled VR, online video transmission and online tracking are some of the use cases in this type of application. An attacker can manipulate the identity of the UAV and transmit disrupted information to the control station using their identities. In a large-scale deployment of UAVs, the control station must process the multi-media files incurring a large delay and burdening high utilization of computational resources.

- UAV-ITS: This application ensures road safety, traffic analysis to monitor accidents, track compromised vehicles, etc. Such benefits are achieved by a swarm of cellular-connected UAVs cooperating to capture needful data during mission. An attacker can choose to send an unidentified UAV to join the swarm of UAVs to steal the information or initial self-collision to disrupt the UAV-UAV communication. Such attacks can bring serious consequences to the entire mission.

In [149], the authors have presented a brief survey of state-of-the-art intrusion detection system (IDS) mechanisms for networked UAVs. It highlights existing UAV-IDS approaches and areas that need attention for building a secure UAV-IDS system.

4.3 Synergies of 5G innovations for Cellular-connected UAVs

By design, cellular-connected UAVs are expected to be controlled and managed remotely by a Ground Control Station (GCS). Depending upon the UAV application and use case, the UAVs carry out different missions, which require unique networking characteristics. In general, these networking requirements are very tightly coupled with the use case and hardware infrastructure support. Especially, multi-UAV systems comprising many functional and coordinated UAVs, establishing the reliable and secure communication path as well as the design and development of efficient reconfigurable network architectures is a challenging issue.

The key innovations of 5G and beyond systems are the cloudification and virtualization of network resources through Software Defined Networking (SDN), Network Function Virtualization (NFV), Service Function Chaining (SFC), network slicing, and physical layer improvements. SDN segregates the control functions and forwarding functions of a device. It allows softwarization of the control functions, thereby making the network programmable. NFV transforms the traditional network services into software based solutions (Virtual Network Functions i.e., VNFs) that can be dynamically deployed on a general purpose hardware platforms. SFC is a chain of simple and smaller network functions that must follow an execution sequence to realize a complex and large network function. Future 5G-centric networking applications and services are driven by programmable network architectures, where softwarization and cloudification of network functions are the key enablers. Therefore, the above-mentioned 5G innovations are envisioned as a part of the cellular-connected UAV applications and will be detailed in this Section. Specifically, Section 4.3.1 focuses on the envisioned network architectures for cellular-connected UAVs. The hardware and physical layer improvements are discussed in Section 4.3.2.

4.3.1 Network Architectures

Based on the key enablers of future 5G-centric networking applications, the cellular-connected UAV network architectures can be summarized in the following groups. They are (i) NFV Oriented, (ii) MEC Oriented, (iii) IoT Oriented, (iv) Service Oriented (SOA). In next subsection, we highlight the respective architectures and existing works. Table 4.3 shows the glossary of related works for each of these network architectures.

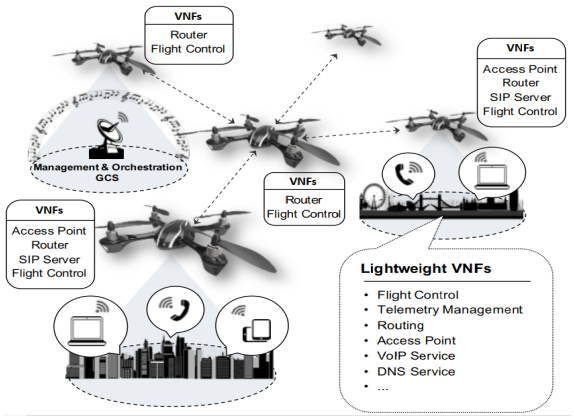

Figure 4.5: NFV based achitecture for UAVs [151]

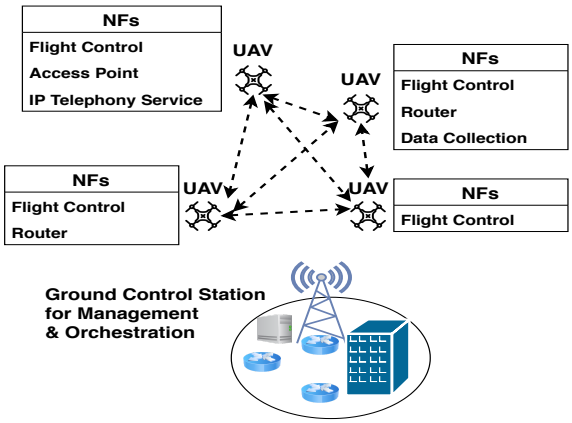

Figure 4.6: UAVs with diverse network functions

Table 4.3: Envisioned Network architectures of cellular-connected UAV

Technology	Principle	Benefits
NFV-Oriented [151], [152], [153]	Decouples the hardware and software that exists in traditional vendor network setting	• Greater flexibility for NF deployment • Dynamic service provisioning • Easily deployable and well scalable • Efficient allocation to general purpose hardware
MEC-Oriented [154], [155], [156]	The cloud computing capabilities are placed close to edge of mobile network	• Significant reduction in data exchange cost • Computational offloading to local servers • Improvement of QoE for end users
IoT-Oriented [157], [158], [44], [48]	Connecting massive number of diverse, smart devices to 5G/B5G cellular network	• Assists efficient decision making on huge data • Extracting meaningful information for end users • Control automation without human intervention • Information sharing and communication
Service-Oriented [159], [160], [161]	Network services are provided over a communication protocol that is independent of vendors or product	• Improves the modularity of application • Transforms monolithic networking application into a set of microservices • Each microservice is a basic unit of functionality

NFV Oriented Architectures

In [151], the authors present the feasibility of an agile, automated and cost-effective UAV deployment architecture carrying out heterogeneous missions with the help of NFV technology. This work proposes an adaptable way to achieve a reconfigurable UAV management system, which is capable of carrying out missions with varying objectives. For example, some UAVs could incorporate a VNF that provides access point connectivity services, another VNF for network layer routing functionalities, a third VNF for flight control system that can be easily upgraded as per the changing needs of the mission. The work is validated by a prototype built upon open-source technologies. The high-level architecture of such a system is shown in Fig. 4.5. As shown in the figure, the communication infrastructure formed by a set of UAVs, where the mission planner used a MANO NFV framework (defined by ETSI), installed at ground station to flexibly deploy a set of VNFs over the set of UAVs. Overall design of such a system consists of the following components:

- Management and Orchestration (MANO):- It is located with the GCS and realized by Open Source MANO (OSM) Release TWO. It contains all the necessary functionalities of service orchestration and VNF manager as per ETSI NFV reference architecture [162]. OpenStack Ocata is used for VIM. Both OSM and VIM were deployed in mini-ITX computer having 4 Gb Ethernet ports, 8 GB RAM, Intel Core i7 2.3 GHz, 128 GB SSD with DPDK support.
- UAV hardware and software:- It provides the infrastructure support for execution and deployment on light-weight VNFs. It is realized by Parrot AR.Drone 2.0 carrying single

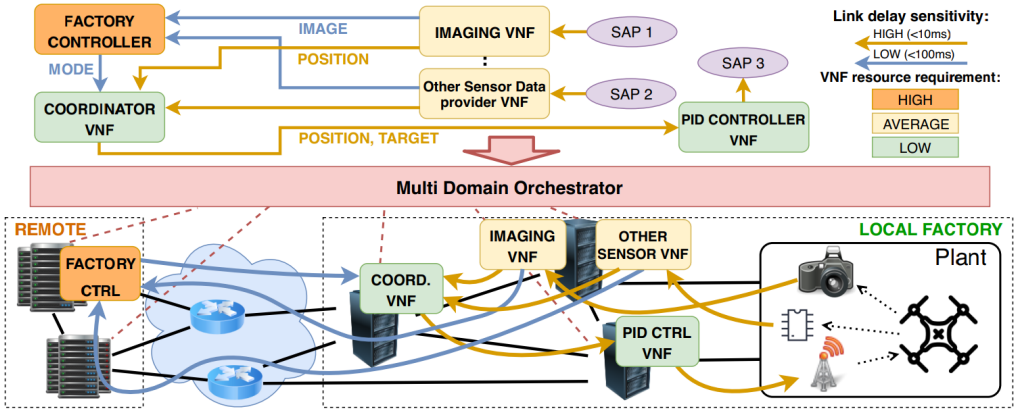

Figure 4.7: Deployment on multi-domain UAV services [153]

board Raspberry Pi 3 Model B.

- Mission Planner:- It is located at the GCS and defines the nature and characteristics of different network services or network functions (NFs) to be deployed along with their placement policies. It also interfaces with MANO component to call for the light-weight VNF deployment on set of UAVs.

In order to carry out routing of VNFs to different target UAVs, LXC Linux containers on Ubuntu OS are used. Each routing VNF requires resources of 1 vCPU, 128 MB RAM and 4 GB storage.

The authors in [152] have presented a practical NFV based approach to support UAV multi-purpose deployment, which can be rapidly configured according to the need of the civilian mission. They have considered the UAVs to provide infrastructure and hardware that enable agile integration of network functions at deployment time by a network operator. As shown in Fig. 4.6, a set of UAVs could be used for providing communication infrastructure (virtual access points) in case of disaster or can be used in SAR operation in a remote area. The mission specific UAV behaviours are softwarized as network functions and installed to UAV infrastructure (hardware) at the time of deployment. Some network functions pertaining to mandatory features of any UAV such as flight control and telemetry are installed on all UAV hardware, irrespective of the mission. The implementation of the system prototype and the light-weight VNF is done using open-source software technologies. The orchestration and life-cycle management of light-weight VNF is done by OSM Release FOUR. OpenStack Ocata version is used for realizing the virtual infrastructure layer (VIM). The virtual machine environment runs mini-ITX computer which consists of Intel Core i7 2.3 GHz processor, 4Gb Ethernet ports, 16 GB RAM, 128 GB SSD. The UAV hardware platform consists of DJI Phantom 3 carrying a Raspberry Pi 3 Model B computing board and serves the platform for execution of light-weight VNFs needed for specific mission.

A software based service architecture running on a distributed cloud environment is demonstrated in [153]. In this demonstration, an Industry 4.0 application controlling the indoor drones is considered for study. The application is implemented using SFC orchestrated by a multi-domain orchestrator known as ESCAPE. The orchestrator is able to setup and configure VNFs onto the physical UAV boards according to mission's policies and requirements. The proposed implementation is shown in Fig. 4.7. The deployment occurs when the service requests are triggered to ESCAPE as per requirement. OpenStack is used for running the cloud environment and

few laptop hosts are used as edge execution machines by Docker platform. High level commands such as take-off, land, fly are used for controlling the UAV behaviour from factory controller.

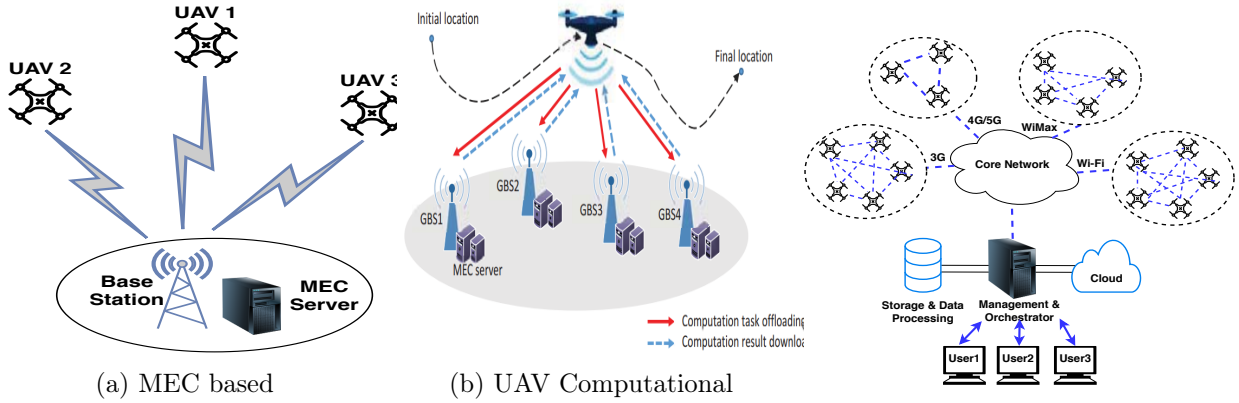

(a) MEC based Architecture [154]

(b) UAV Computational Offloading [155]

(c) UAV-based IoT Platform

Figure 4.8: Network Architectures of Cellular-connected UAV

MEC Oriented Architectures

In general, UAVs possess physical constraints in terms of computational capability, storage and battery capacity. MEC has been identified as one of the promising techniques to deal with the limitations of low computational capability and restricted battery capacity of flying UAV. Some examples of resource-intensive tasks are trajectory optimization, object recognition, AI processing in crowd-sensing. Due to the limited onboard resources of the UAVs, computation of above resource intensive tasks are not very efficient. Hence, in such case, edge-cloud based network architectures provide substantial improvements for operations of cellular-connected UAVs.

In [154], the authors presented a UAV-enabled MEC architecture applicable for cellular-connected UAVs. Fig. 4.8a illustrates this architecture, where the UAV has some computational task to be executed. This task can be offloaded to the MEC server located with the ground station and, after the computation, obtained results can be sent back to UAV for their exploitation. Depending upon the volume of the offload, there can be two modes of operation: (i) partial mode, and (ii) binary mode. In partial offload mode, the whole task is split into two parts. One part is executed locally and the other part is executed by the MEC server (e.g., face recognition use case). In binary offload mode, each task is executed as one unit, irrespective of whether it is done locally or at the MEC server (e.g., channel state information (CSI) estimation). Both of these offload modes have advantages and drawbacks. The selection of the suitable mode depends on the nature of computational task being performed, UAV structure and characteristics.

Considering the use case of trajectory optimization and computational offloading in cellular-connected UAV, the work in [155] presents a novel MEC setup, where the UAV needs to offload some of its processing task to the ground station. The UAV flies from an initial location to a destination location and offload the task to selected ground base stations during the trajectory. The goal of the MEC setup is to minimize the total time for UAV mission considering the maximum speed and ground station capacity constraints. This setup is shown in Fig. 4.8b.

In reference work [156], the authors proposed a 5G network slicing concept extend to video monitoring with UAVs having MEC facilities. The surveillance area is divided into multiple zones and a set of UAVs are assigned the task to monitor a specific zone. The MEC enabled UAVs could offload the captured data and video streams with acceptable quality and performance.

IoT Oriented Architectures

In [157], the authors envision a heterogeneous UAV network architecture, where UAVs are used to deliver value-added IoT services from the sky. The UAVs are considered as key enabler of IoT framework that are deployed by following a specific vision. Each UAV is equipped with various IoT sensors or camera to gather data. The deployment spans across a large area, where UAVs are grouped to form UAV clusters (because of close geographical proximity or mission type or altitude). A fixed UAV is designated as cluster head (CH), and is mainly responsible for disseminating collected data to the other UAVs or orchestrator via core network. The core network performs the intelligent decisions and employs algorithms for efficient processing the data gathered from UAV sensors. The high level architecture schematic of this proposal is shown in Fig. 4.8c.

In [158], the authors presented the network architecture of a UAV-enabled IoT framework developed for disaster mitigation. In this case, the UAV not only acts as a flying base station in emergency situation, but also behaves as a cellular-connected UAV for information dissemination in scenarios such as wildfire or environmental losses. The framework consists of three main components, (i) ground-IoT network, (ii) connectivity of UAV and ground-IoT network and (iii) data analytics.

The authors in [44] demonstrated a UAV-based IoT framework for crowd surveillance application which collects the data and performs facial recognition to track and identify suspicious activities in a crowd. The fleet of UAVs are managed by a centralized orchestrator component.

Service Oriented Architectures (SOA)

The work in [159] demonstrates the design and development of a UAS Service Abstraction Layer (USAL) for UAV which implements different types of missions with minimal re-configuration time. USAL contains a set of predefined useful services that can be configured quickly according to the requirements of civil mission. The architecture is service oriented, and the service abstraction layer provides the re-usability of the system. The mission functionalities are split into smaller parts and are implemented as independent services. USAL replies on a middleware that manages the services and their communication needs. USAL may contain a large number of services, however, all of them need not be present. Depending upon the mission, suitable services can be loaded and activated to meet the objective of mission.

In [160], the authors presented Dronemap Planner, a service-oriented cloud based UAV management system, which performs overall management of UAVs over Internet and control their communication and mission. It virtualizes the access mechanism of UAVs via REST API or SOAP. It uses two communication protocols: (i) MAVLink and (ii) ROSLink. The objective of designing such a system is to provide seamless control to monitor UAVs, offload compute intensive tasks to cloud platform, and dynamically schedule the mission on demand. The cloud computing model creates an elastic model that scales well with the numbers of UAVs as well as with the offered services. Fig 4.9 shows the schematic of system architecture developed in this study.

4.3.2 Hardware and Physical layer consideration

The performance of cellular-connected UAVs in 5G networks significantly depends on the underlying physical layer signal processing. In this section, we highlight the candidate physical layer techniques that influence the UAV communication. The key techniques are massive MIMO

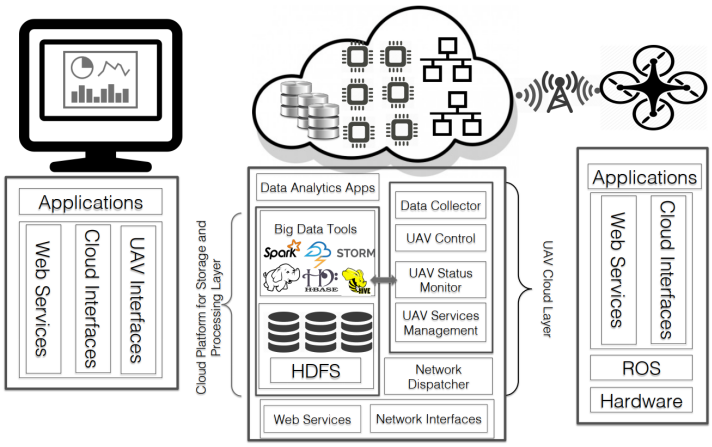

Figure 4.9: Service Oriented System Architecture of UAV [160]

Table 4.4: Candidate waveforms for 5G

Scheme	Description
Generalized Frequency Division Multiplexing (GFDM)	It is a block-based modulation approach where the available bandwidth is either divided into several narrow bandwidth subcarrier or few subcarriers with high bandwidth for each.
Universal Filter Bank Multi-carrier (UFMC)	Multicarrier signal format to handle loss of orthogonality at receiver end. It uses sub-band short duration filters.
Filter Bank Multicarrier (FBMC)	It uses a preamble burst based approach to ensure flexible resource allocation.
Biorthogonal Frequency Division Multiplexing (BFDM)	It uses a relaxed form of orthogonality where transmitter and receiver are bi-orthogonal. In other words, the transmitted and received pulses have to be pairwise orthogonal. BFDM is more robust than OFDM.

(Multiple Input Multiple Output) antenna, mmWave communication (3-300 GHz), beamforming and beam division multiple access (BDMA), as well as some new modulation schemes. In 4G LTE, Orthogonal frequency division multiplexing (OFDM) and Orthogonal frequency division multiple access (OFDMA) are predominantly used for multiplexing and multiple access method. 5G/B5G networks is considering new waveforms to support efficient air interface [163]. These new waveforms are superior than OFDM and no longer require strict orthogonality and synchronization. Table 4.4 provides a brief categorization of different waveforms for 5G from implementation perspective.

5G NR

5G new radio (NR) is a new radio interface and radio access network which is designed and developed for advanced cellular connectivity. It utilizes novel modulation schemes and access technologies that help the underlying system to cater to high data rate services and low latency requirements. The first version of 5G NR started in 3GPP Rel-15. 5G NR supports the frequency ranges in sub 6 GHz or in mmWave range (24.25 to 52.6 GHz). It has greater coverage and enhanced efficiency because of beamformed controls, MIMO and access mechanisms. 5G NR is expected to cater to three broad categories of services i.e., (i) extreme mobile broadband (eMBB), (ii) ultra-reliable low latency communication (URLLC) and (iii) massive machine type

communication (mMTC). Specifically, the expectations for each of the mentioned scenarios are:

- For eMBB use case scenario, the data rate is promised as 100 Mbps and three time more spectral efficiency than 4G systems. It will be able to support a device that moved with a maximum speed of 500 km/h.
- For URLLC use case scenario, the goal is to achieve 1 ms latency with reliability 99.999%. It means, the reliability of the wireless link will not be met, if more than one data unit out of 10^5 data units does not get delivered within 1 ms.
- For mMTC use case scenario, the density of devices that 5G will be able to handle will reach nearly 1000000 per square kilometer.

URLLC ensures strict latency and reliability requirements for the application. 5G NR focuses on framing, packetization, channel coding and diversity enhancements for achieving URLLC. One of the most vital scenarios of URLLC is the remote piloting of cellular-connected UAVs in BVLoS range. Package delivery, remote surveillance and border patrolling are some of the use cases that demand UAV operations in BVLoS range. Due to the changing altitude, velocity and distance between remote UAV and ground station, the URLLC requirements may vary. URLLC is the key use case scenario to enable BVLoS UAV operations, which assist in safe UAV piloting to avoid crashes, obstacles etc. Cellular-connected UAVs can benefit from 5G NR design as it offers dominant uplink data transmissions from UAV to ground BS, especially for many demanding use cases pertaining to streaming, surveillance, imaging etc. The downlink data transmission requirement is much smaller in contrast to uplink. Moreover, the sub 6 GHz and millimetre wave spectrum could potentially be used for the downlink and uplink respectively, considering the asymmetric traffic requirements.

Massive MIMO

Massive MIMO is a promising technology that consists of a large number of controllable antenna arrays. It is supported by 3GPP in Rel-15 for 5G NR. 5G will exploit full benefits of MIMO by leveraging the uncorrelated and distributed spatial location of cellular-connected UAVs, as well as ground users. Massive MIMO enhances the signal strength, where multiple data streams can include unique phase and weights to the waveforms to be constructively generated at the UAV receiver [164, 165]. It minimizes the interference to other cellular-connected UAV receivers.

The work [164] presents an evaluation of a massive MIMO system for cellular-connected UAVs. It demonstrates that, massive MIMO assists in harmonious coexistence of cellular-connected UAVs with ground users, supports large uplink data rates and results in consistent CNPC link behaviour. The test uses 20 MHz bandwidth in sub-6GHz licensed spectrum operating in TDD mode. Massive MIMO-enabled systems are useful to restrict the impact of interference to the existing terrestrial users. Such system requires frequent and accurate CSI updates.

Millimeter-wave communications

Millimeter-wave (mmWave) spectrum has been extensively investigated in UAV cellular communication that offers high bandwidth services using frequency spectrum above 28 GHz. The channel between cellular-connected UAVs and ground BS is typical LoS dominant and mmWave having high bandwidth are favourable for communications. However, the mmWave signals are

affected by any kind of blockage, which poses several implementation challenges. Therefore, efficient beamforming and tracking are needed for cellular-connected UAV operation.

The work [166] presents a simulated study to showcase the feasibility of using 28 GHz 5G link for public safety use case. The results claim that, it is feasible to achieve 1 Gbps throughput with sub ms latency using mmWave links when the grounds base station is situated close to the mission area. In [167], the authors conducted an analysis on the air-to-ground channel propagation for two different mmWave bands at 28 GHz and 60 GHz using ray tracing simulations. During experiment, the UAV speed was kept at 15 m/s and limited to a flight distance of 2 km. A total of four scenarios are validated such as urban, sub-urban, rural and over-sea. It is observed that, received signal strength (RSS) follows the two ray propagation model as per UAV flight path at higher altitudes. This two-ray propagation model is impacted in urban scenario due to high rise scattering obstacles.

Beamforming and BDMA

Beamforming is a technique by which a beam (signal element directed to the users) is transmitted from the ground base station and directed to a specific user to minimize interference to other neighbouring users and maximizes the useful signal for the given user. In 5G NR, the antennas can create and exploit beam patterns for the specific cellular-connected UAV. This is of great importance, because of aerial mobility of UAVs and high LoS channel conditions from ground BSs. Beam division multiple access (BDMA) is capable to handle large number of users and to enhance the communication system capacity. In this case, a separate beam is allocated to each user. This access technology is dependent on the user positioning, location and speed of user movement.

Beam forming requires the base station to have more than one transceiver RF chain and the user (both aerial and ground) to have single RF transceiver. In order to support a greater number of users, the beam should be split. The key challenge is to find a way to group users that are served by a single beam without causing interference to other users at the same time. Strategies like angle of departure (AoD) or angle of arrival (AoA) help to measure the steering angle from BS to mitigate interference to some extent.

In [168], the authors presented a study on using steerable directional transmitters on UAVs to evaluate the co-existence of cellular-connected UAVs with ground user. This work jointly optimized the flight path and antenna steering angle to improvise uplink throughput while minimizing interference to other neighbour base stations. The proposal is validated by a testbed setup involving 2×2 MIMO where wide beam transmitters are employed half-power beams at 60° on azimuth and elevation planes and 6 dBi forward gain. Fig. 4.10 shows the performance variation with respect to the throughput in presence of both ground users and aerial users. The results show that such techniques are of utmost importance when the ground and aerial users coexist at such scale.

NOMA

Non-orthogonal multiple access (NOMA) is a promising candidate technology for 5G wireless communication, as it leads to higher spectrum utilization than orthogonal multiple access methods (OMA). NOMA has been widely explored in UAV-assisted wireless communications, where

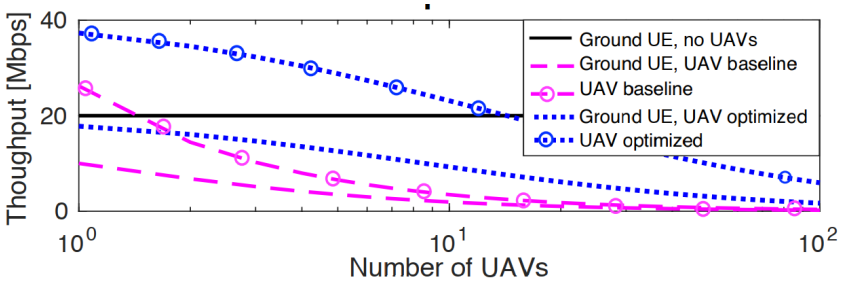

Figure 4.10: Coexistence performance of aerial UE and ground UE, 700 MHz in rural setting [168]

UAV is deployed as a flying BS to serve the ground users [169]. Few studies [170, 171] also investigated the applicability of NOMA in cellular-connected UAV network.

OFDMA and single-carrier (SC)-FDMA are conventional orthogonal multiple access methods (OMA) adopted as a natural choice of 4G LTE/LTE-Advanced wireless systems. The basic principles of OFDMA is to transmit the different user signals over different frequency resources, not to produce mutual interference among users. Cellular-connected UAVs coexisting with ground users benefit from such orthogonal multiple access methods, because the UAVs within a given coverage can avoid any interference to ground users by transmitting in those resource blocks that are not assigned to any ground users. Thus, the resource blocks can be allocated within the coverage area in a non overlapping manner. However, increased user density and the frequency reuse result in poor spectrum performance from such OMA methods, due to resource block scarcity. On this advent, NOMA methods allows the cellular-connected UAVs to reuse the resource blocks. In other words, NOMA is capable to serve many users at the same time/frequency resources. NOMA employs two techniques for multiple access:

- Power domain: Multiple access is based on different power levels.
- Code domain: Multiple access is based on different codes.

NOMA with interference cancellation (IC) is an appealing solution to the cellular-connected UAVs because the UAVs can reuse the resource blocks that are allocated to ground users. Moreover, at high altitude, UAVs experience stronger LoS channel condition than ground users, so that BS can use IC to decode strong signal from UAVs, then subtract it to decode ground user signal [146].

4.4 Existing Prototypes and Field Trials

Experimental assessment and prototyping are time consuming and relatively complex, because they must take into consideration the deep technical aspects of any realistic deployment. There are several ongoing efforts from industry and academia that focus on experimental frameworks for cellular-connected UAVs. These efforts provide more practical insights about the underlying behaviour and complexities involved in integration of UAVs into cellular networks. Field trials and measurement campaigns are a cost-effective and powerful step towards the prototyping, as they help investigating the solutions to potential research problems. In the following subsections, we shed some light on these efforts and classify them into two broad groups such as (i) experimental testbeds and (ii) field trials.

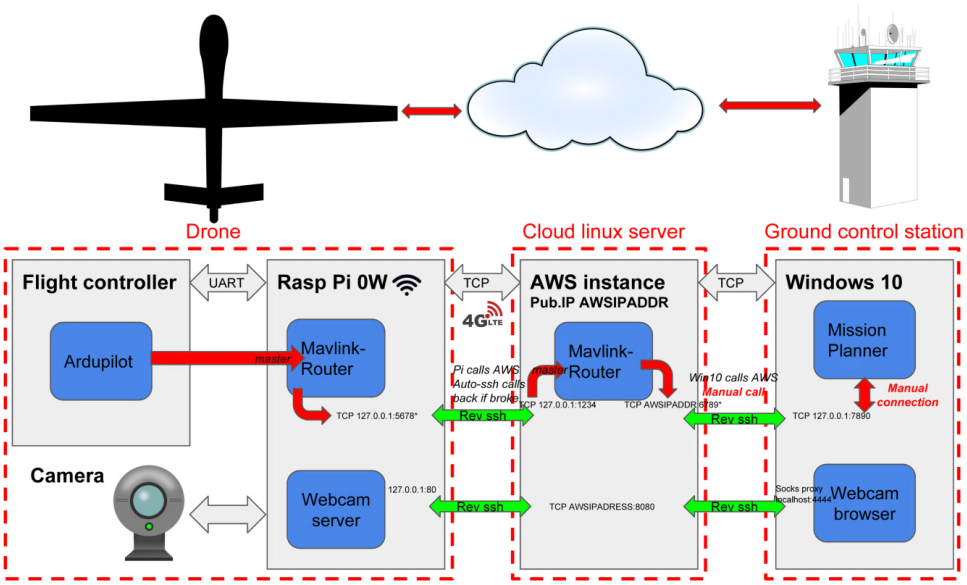

Figure 4.11: Prototype design and configurations in [172]

4.4.1 Experimental Testbeds

There is hardly any complete real-world testbed that fully characterizes the challenges and benefits of cellular-connected UAVs. The literature in this regard is scarce. However, several ongoing efforts are being actively pursued by researchers from both industry and academia to advance the working prototypes. It is worth mentioning that, realization of working prototypes of cellular-connected UAV mainly differ with respect to (i) the main objective for which they are built, and (ii) the features being implemented, which are also dependent on the main objective. For example, one prototype may completely focus its prototype development on investigating 5G/B5G network support to efficient UAV operations. Another prototype may prioritize its development on achieving a fail-safe, reliable communication with desired QoS guarantees. Furthermore, each prototype may utilize different hardware and software flight stacks to realize the goal. The chosen hardware and software platforms may be open-source or proprietary in nature. Hence, the existing efforts tend to be very specific to the goal being pursued, thereby providing unique characteristics or behaviours to the prototype being developed. There are no formal development guidelines available so far in order to harmonize available features for these prototyping efforts.

An ideal view of cellular-connected UAV prototype is still missing. This ideal prototype can be thought of possessing a non-trivial list of mandatory features and should be adaptable to varying needs of the mission. Our current work attempts to foresight such an ideal prototype and enumerates the list of encompassing features. Table 4.7 illustrates a feature-oriented comparison of existing testbed works in literature with the desirable set of features from an ideal prototype point of view. Note that, this list of features is not exhaustive, rather provides a use-case driven analogy to consolidate the basic set of mandatory features. New features may arise in future with evolution of emerging use cases for cellular-connected UAVs.

In this subsection, we aim at investigating the existing efforts to design and develop working prototypes for realizing some UAV operations over LTE/4G/5G/B5G cellular network infrastructure along with their implemented features. They are presented as follows.

An open-source 4G connected and controlled self-flying UAV is demonstrated in [172], defining a new, light-weight, secure and open-source class of cellular-connected UAV. This work utilizes

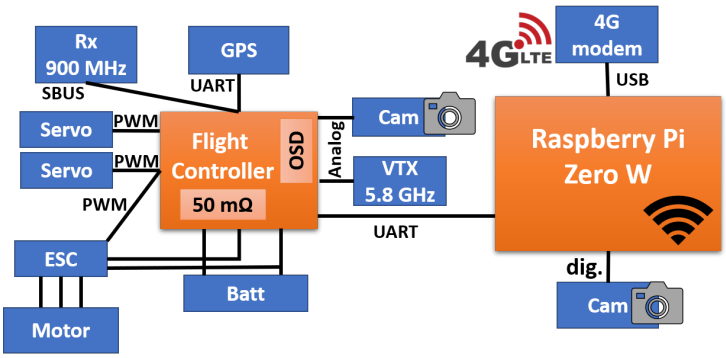

Figure 4.12: Schematic of the avionics components in [172]

open-source hardware and software stack to design and develop fully autonomous and fail-safe flight behaviour. This work provides a comprehensive and detailed discussion on the possible hardware and software options for flight controllers, radio receivers, sensors, microcontrollers and 4G cellular modems. Fig. 4.11 summarizes the hardware and software components used in the prototype development. The detailed hardware avionics schematics and equipment models are highlighted in Fig. 4.12 and Table 4.6, respectively. The performance of the prototype is tested for endurance, terrain alignment, autonomous flying behaviour, wind speed and real-time video quality. The important accomplishments of this work are summarized as follows.

- The entire prototype setup is done by open-source hardware and software components with Commercial off-the-shelf (COTS) components.
- The UAV shows longest demonstrated flight time i.e., over one hour.
- This work provides clear, concise and step-to-step guidelines for entire prototype design and development along with the programming of individual pieces. This also includes an online manual (wiki) and supplementary information.
- The prototype shows self-healing internet architecture and utilizes the fail-safe protocols for the lost links in communication.
- The UAV cellular to ground control is secure by encryption and can pass through several firewalls.
- As compared to other UAV industry verticals, the significant advantages are light weight (UAV weighs nearly 300 grams) and longer flight time ($>$ 1 hour).

A working prototype of LTE controlled drone was demonstrated in [173] proving the control of UAV via LTE connection and then tested as a 3D measurement platform. The goal of this prototype development was to investigate and evaluate LTE as a potential candidate of communication infrastructure for controlling a UAV. The experimental goals are to provide answer to below mentioned questions.

- whether existing LTE network infrastructure is an efficient means of controlling UAVs?
- whether the LTE connection is good enough in terms of providing low latency, jitter and bit error rate?

Table 4.5: A feature-oriented comparison of prototypes of cellular-connected UAVs from viewpoint of idealistic baseline

References → Features ↓	**Short Description**	**[172]**	**[173]**	**[174]**	**[175]**
Cellular Network	Cellular network generation type to which the prototype is connected and tested	4G LTE	4G LTE	GSM/ GPRS	3G/4G LTE
Open-source	Constituent hardware and software components of the prototype being developed	✓	✓	✓	✓
Autonomous	Whether the UAV can fly autonomously without human intervention (self-flying nature)	✓	✗	✗	✗
Fail-safe	Ability to be resistant against lost link and return to home after UAV control is interrupted	✓	✗	✗	✗
Encrypted Comm	Use of encryption mechanism to secure the message exchanges from potential attackers	✓	✗	✗	✗
BVLoS Capable	Being able to command and control the UAV, even not in the direct view of the remote pilot	✓	✓	✗	✗
QoS-Aware	UAV successfully fulfils the application demands such as packet loss, latency, rate and jitter	✗	✓	✗	✗
Internet Connectivity	Being able to control and steer UAV from persistent Internet connection	✓	✗	✓	✓
Ground Control	UAV being remotely controlled by GCS for command and control, or payload communication	✓	✓	✓	✓
Light-weight	Light-weight of UAV to enhance the prototype performance	✓	✗	✗	✗
Terrain Following	UAV maintains a fixed altitude and follows in unknown terrains like mountains	✓	✗	✗	✗
Flight Longevity	Higher flight time of UAV indicating energy efficiency and negligible interruption during missions	✓	✗	✗	✗
Endurance	Robustness and integrity of UAV in extreme environment	✓	✗	✗	✗
Energy Efficient	Consumption of very less power to maintain persistent flight operation to accomplish the mission	✓	✗	✗	✗
Network Virt.	Capability in terms of hardware platform independency and softwarization of UAV functions	✗	✗	✗	✗
Adaptable	Being responsive and ability to reconfigure as per changing requirement in minimum time	✗	✗	✗	✗
AI/ML-Powered	Ability to leverage efficient AI/ML approaches to self-learn and apply the learnt knowledge	✗	✗	✗	✗
Swarm Cooperation	Ability to coordinate information via UAV-to-UAV links in a multi-UAV deployment scenario	✗	✗	✗	✗

- whether the bit rate is sufficient to perform the use case of live video streaming in BVLoS range?

The prototype is tested with respect to above mentioned goals and found that LTE is an efficient technology for UAV operations in BVLoS range satisfying the required the bit rate, latency

and jitter. However, this prototype has several shortcomings and may not be considered as a full-fledged cellular-connected UAV testbed. Many features are either missing or not considered to keep the prototype simple in this development, thereby leaving enough scope for further enhancements. Some of the important features worth highlighting which are lacking in the prototype are listed below.

- The design did not consider cellular network coverage holes and discontinuity problem which may lead to failure of UAV operation. Flight fail safe mechanism is lacking.
- The UAV mission specific investigation with respect to trajectory, interference from neighbouring base stations, handover criteria are missing from the design.
- The QoS delivered by the UAV application must take into account diverse real-world use cases in presence of obstacles and variation of signal strength. Such study is missing.
- It did not consider the factors and performance penalties when UAV coexist with other ground UEs.

The work presented in [174] proposes an arduino-based low-cost, flexible control subsystem for controlling UAVs and ubiquitous UAV mission management by GSM/GPRS cellular networks. The ground control station transmits control signals to UAV present in LoS or beyond LoS over GSM or GPRS cellular network, through which, it is shown that is possible to connect to Internet, send/receive text messages or voice calls utilizing a GSM antenna and a SIM card. The experimental setup includes the following components: (i) UAV is an IRIS+ quadcoptor by 3DRobotics, (ii) Pixhawk autopilot, (iii) Arduino Mega ADK Rev. 3 microcontroller board, (iv) GSM/GPRS module by Arduino GSM shield with Quectel M10 modem, (v) Mission Planner, an open source software for ground control station software. The field tests are conducted by sending basic control commands from smartphone or laptop to UAV and they are successfully executed by the UAV. The subsystem initialization time is high, but occurs only once when the subsystem is powered ON. Fig. 4.13 shows the high level system schematics of the working prototype. Following are the key observations drawn from above experiment.

- Communication via GPRS using a Mission Planner software has faster response time.
- The Internet connectivity of GRPS is very fragile which make the GSM text message mode to be an efficient way for command and control message exchange.

Table 4.6: List of avionics components used in [172]

Component	**Model**
Flight Controller	Omnibus F4 Pro
GPS	BN-220
Radio Rx	TBS Nano
Camera & Video Tx	TX05
Computer	Raspberry Pi Zero W
4G Modem	Verizon USB730L
4G Antenna	TS9

A flexible open-source long-range communication solution for UAV telemetry based on cellular data transfer service is presented in [175] which is implemented on Raspberry Pi 3 model B (also known as rpi3) and Gentoo Linux control. The UAV is equipped with a Huawei 3372h dongle to get the cellular data services.

Table 4.7: Glossary of experimental prototyping for cellular-connected UAVs

Reference Work	Network	GCS Software	Mobility	Fail-Safe	Autonomous	Encrypted	QoS-Aware	Internet Connectivity	Open-source
[172]	4G LTE	Mission Planner	Flying	✓	✓	✓	✗	✓	✓
[173]	4G LTE	Mission Planner	Flying	✗	✗	✗	✓	✗	✓
[174]	GSM/GPRS	Mission Planner	Flying	✗	✗	✗	✗	✓	✓
[175]	3G/4G LTE	Mission Planner	Static	✗	✗	✗	✗	✓	✓

4.4.2 Field Trials

In this subsection, various efforts on field trials and measurement campaigns of cellular-connected UAVs are discussed. Authors in [176] conducted a field measurement in a commercial LTE network for cellular-connected UAV operation. An LTE smartphone mounted on a consumer grade DJI Phantom 4Pro radio controlled quadcopter is used to gather the UAV flight results. The smartphone has TEMS Pocket 16.3 installed for wireless measurement and analysis. The field trial results include distribution and measurement of signal quality metric such as Reference Signal Received Power (RSRP), Reference Signal Received Quality (RSRQ), Signal to Interference and Noise Ratio (SINR) in the serving cell and neighbouring cells with respect to UAV movement. The results show the feasibility of UAV operations in commercial LTE network and also highlight the implementation challenges for dynamic radio environment. The simulations are also conducted to supplement the field trial results in terms of network performance involving a higher number of cellular-connected UAVs. Following observations are drawn from the experiments.

- The aerial propagation conditions are close to free space propagation and hence, the aerial UEs experience stronger RSRP than the ground UEs.
- The RSRQ and SINR at higher altitude is lower than the corresponding ground UE because of the strong downlink interference from neighbour non-serving cells to the aerial UE.
- The uplink throughput for aerial UE is observed to be better than ground UE due to free space propagation condition. Note that, this uplink performance also depends upon many other factors like scheduling mechanism and network load.
- In the downlink command and control traffic, higher altitude results in lower spectral efficiency due to increased interference and higher physical resource block (PRB) utilization.
- Considering the mobility of aerial UEs at higher altitudes and LoS propagation conditions, a greater number of radio link failures (RLF) occur due to poor SINR and large interference.

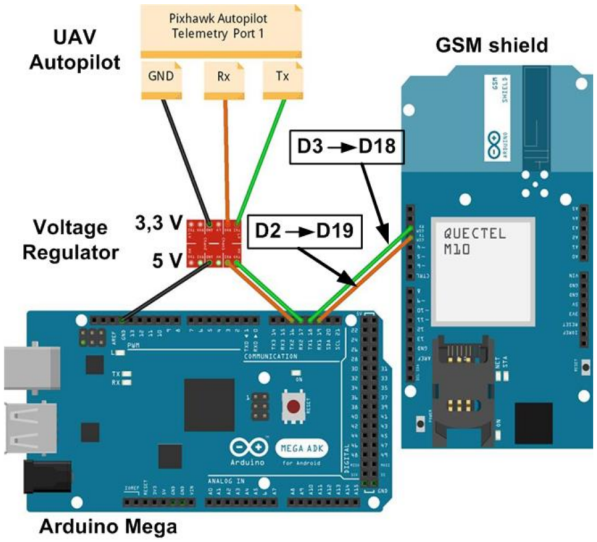

Figure 4.13: High level shematics of the prototype setup in [174]

Also, they may connect to far-away cells instead of the closest cell.

In [177], the authors demonstrated an experimental platform where UAVs are connected to a commercial 5G NR base station for radio link measurements. The 5G BS is developed by Magenta Telekom in Austria and operates between 3.7 and 3.8 GHz frequency, using 100 MHz band. It has 64×64 massive MIMO setup with beam forming capabilities. An Asctec Pelican quadcopter is flown near this BS and the test measurements are performed by a Cellular Drone Measurement Tool (CDMT). This UAV carries a non-standalone Wistron NeWeb mobile test platform based on Qualcomm Snapdragon X50 5G modem. It supports sub-6 GHz 5G NR using 4×4 MIMO and 256-QAM. The goal of the study is to investigate the communication behaviour and performance characterization of flying UAV when connected to a commercially operated 5G base station. The communication aspects for 5G-connected UAV measured in this test are 5G connectivity, RSRP, SNR, throughput and number of handovers. The UAV flight includes both vertical lift-off and horizontal trajectory. Following observations are drawn from above testbed driven study of 5G connected UAV.

- The UAV connectivity to 5G cannot be always guaranteed and fall back to 4G network. This situation is even worse at higher altitudes with more handovers towards 4G network.
- The UAV is able to receive enough data rate (several hundred Mbps) from 5G NR based deployment, which is adequate for many applications and use cases.
- The handovers to 4G network could be reduced by deploying a larger number of 5G NR base stations, and downlink rate would be improved. However, the experiment did not yield much benefit in the uplink as compared to 4G. The authors assume that uplink rate analysis needs further investigation.

Qualcomm also tested the UAV operation in commercial LTE networks in September 2016 and produced a trial report in May 2017 on LTE unmanned aircraft system [178]. The focus of this test was to understand the operation of low altitude UAV platforms being supported by terrestrial cellular networks. The overall test encompasses both field trials and simulations. The field trials aim to capture datasets by performing hundreds of flights and then complemented

Table 4.8: Comparison of existing works on field trials and measurement campaigns

Reference Work	Cellular Network	Trial Environment	Performance Metric
[176]	4G LTE	Suburban	RSRP, RSRQ, SINR, downlink latency, resource utilization
[177]	5G New Radio	Rural	RSRP, SNR, Throughput, 5G connectivity
[178]	4G LTE	Mixed Suburban	Cellular connectivity for low altitude UAVs
[179]	4G LTE	Rural	RSRP, RSRQ, SINR, Effect of altitude on UAV
[168]	4G LTE	Rural, Suburban, and Urban	Throughput degradation, Interference, Uplink signal power
[180]	4G LTE-A	Unknown	RSRP, RSRQ, SINR, PCI, UL/DL throughput, EARFCN
[181]	4G LTE	Rural	Cellular-connected UAV identification
[182]	4G LTE	Urban	Channel propagation models
[183]	4G LTE	Rural	RSSI, RSRP, RSRQ, uplink/downlink throughput

by extensive system level simulations to understand the performance of UAV operation. The flights and measurements were performed by custom designed 390QC quadrotor drone. Note that, these results are collected in a suburban/residential zone which was having good cellular coverage, hence, cannot be generalized for other zones like urban or rural areas. Moreover, the performance results are approximate in nature rather than accurate. The key results obtained from the trail report are summarized as follows.

- The aerial UEs experience higher received signal strength than ground UEs despite of the down-tilted BS antennas. This is because of the better free space propagation condition at higher altitude.
- The SINR in the downlink for aerial UEs is lower as compared to ground UEs due to the interference experience from neighbour cell.
- The UE transmit power is more for ground UEs than aerial UEs in the uplink, because good free space propagation condition at higher altitude enhances the interference energy from neighbour cell. The field results depicted that aerial UEs experience nearly three times more interference than ground UEs in 700 MHz band.
- Handover performance in terms of lower handover frequency and success rate of handovers is superior for aerial UE than ground UE due to signal stability at high altitude.
- The optimization in the power control scheme are applied by simulation and was shown to eliminate the excess uplink interference.

The work in [179] presents the field trial done at a small airport in vicinity of Odense, Denmark and results were collected in an LTE network operating in 800 MHz and the UAV altitude is maintained between 20 to 100 meters. The cellular network data was collected by a Samsung Galaxy S5 smartphone which was placed inside the flying UAV cavity. It was equipped with Qualipoc software for reporting the radio measurements. The UE was programmed to use

a 20MHz carrier with centre frequency at 810 MHz. The measurement field had no obstruction between UAV and BS and was an open area to prevent significant signal attenuation and reflected paths. For every second interval, the software radio reports include RSRP and RSRQ. The goal of the experiment was to understand the effects of altitude on the radio performance of an aerial user. It is observed that the SINR degrades when the UAV flies high. The steepest degradation is seen in height variation between 20-40 metres indicating that the increase in interference is more prominent at lower altitudes, and smaller variations at higher altitudes due to improved gain. The study reveals that, expanded radio horizon at higher altitudes, high LoS probability and clearance of first Fresnel zones are key radio factors in modelling the path loss between aerial users and ground stations.

In [168], the authors experimentally evaluated the terrestrial users' performance in the presence of UAV as aerial users on LTE testbed. The performance measurements are conducted to measure the throughput degradation. The LTE network is considered to operate over 2300 MHz carrier frequency with 20 MHz operational bandwidth spanning an area of 160000 square feet. The setup includes 2 eNodeBs, 4 LTE cells each having 2×2 MIMO capability. The downlink and uplink bitrates are kept as 150 Mbps and 50 Mbps, respectively. The UAV hovers at a height of 50 meters. To analyse the performance, both ground UE and aerial UE generate uplink traffic at full buffer capacity for one minute in each experiment run. It is observed that the ground UE suffers a throughput degradation up to 21.75 Mbps because of the inter-cell uplink interference by aerial users. The average reduction in throughput is nearly 52% i.e., equivalent to 11 Mbps.

The work in [180] presents the experimental evaluation of cellular-connected UAVs communication performance connected to an LTE-Advanced network running 3GPP Release 13. An Asctec Pelican quadrocoptor carrying a smartphone (Sony Xperia XZ2 H8216) flies in the coverage of an LTE-A network within the premises of University of Klagenfurt campus. The experiment is performed in open-field and obstacle-free areas ensuring LoS link with at least one BS. The UE supports LTE carrier aggregation and a 2×2 MIMO antenna setup is used. The base station has a transmit power of 20 Watt and 256 QAM and 64 QAM in downlink and uplink, respectively. The UE was able to report various LTE parameters such as RSRP, RSRQ, SINR, serving PCI, TCP uplink and downlink throughput, EARFCN etc. The UAV followed a straight path spanning 300 meters with a speed of 3 meters/second. The broad goal of this experimental study was to understand the impact of varying UAV altitude on achievable throughput and performance measurement of handovers by aerial user without any specific change in the network. The keys findings are as follows:

- The achievable throughput of UAV is sufficient enough to cater to many applications and use cases. At an altitude of 150 metres, the UAV's average throughput is 20 Mbps and 40 Mbps in the downlink and uplink, respectively.

- The number of handovers increase with increasing height of UAV. The reason for high handover frequency is the high RSRP and high interference values from neighbour base stations.

In [181], the authors used machine learning algorithms in order to identify the cellular-connected UAVs in the network based on LTE radio measurements. The measurement was conducted in a rural location of Northern Denmark where the airborne aerial UAV users are realized by mounting a QualiPoc android smartphone on commercial UAV attached to an 800 MHz LTE carrier. The height is maintained at 4 different levels and UAV is flown in 4 rectangular routes. This work claims the use of supervised learning algorithms for efficient detection of aerial

users in the network solely based on LTE radio measurements with small number of training samples.

Authors in [182] focuses on aerial communication field trial, where a radio scanner is attached to construction lift and radio signal was measured with heights up to 40 metres in urban scenario. The measurement was carried out in three LTE carriers such as 800, 1800 and 2600 MHz in northern Denmark. The experimental study aims at providing propagation models of UAVs connected to cellular networks. The key findings from the trials are as follows:

- Increase in the received power from neighbour sources even in height of 40 meters that contributes to heavy interference for the aerial user.
- The observed path loss approximated to free space path loss after a UAV height of 25 meters.

The authors in [183] have demonstrated the feasibility of UAV operation via commercial cellular network for high data connectivity in low altitude and BVLoS operations throughout different times of the day.

Table 4.8 presents a comparative analysis of different existing works in literature with respect to field trials and measurement campaigns. Existing field trials vary greatly in several aspects, such as type of environment, deployment scenario, modelling platform, goal of experiment, performance metric, etc.

4.5 Conclusions

In this chapter, we provided a comprehensive study on the Cellular-assisted UAV communication paradigm (Cellular-connected UAV) where UAV is integrated to 5G and beyond cellular systems as a new aerial UE. The technical synergistic challenges of UAV integration with cellular network are discussed first. The varying altitude of UAV necessitates a 3D wireless coverage model for base stations, because the current design of terrestrial base station is highly optimized for ground users. Typically, the UAVs fly higher than base station creating LoS links that are prone to be interfered from other neighbouring base stations. Proper interference management becomes challenging and critical in terms of harmonious coexistence between aerial UEs and ground UEs simultaneously. UAVs are highly mobile and mainly served by the side lobes of existing base stations. This produces a peculiar cell association and increased handover rates, completely different than that of ground users. The mobility of UAV in 3D space necessitates enhanced cell selection and seamless handover patterns to optimize its operation.

Then, we focus on the promising network architectures and physical layer improvements in 5G and beyond systems considering the hardware and software design challenges of Cellular-connected UAVs. Based on the principles of softwarization and cloudification of networking resources, the network architectures involving cellular-connected UAV solve several practical limitations with respect to performance and scalability issue. 5G and beyond hardware (NR) and software upgrades by cellular network operators along with the technical advancements by UAV manufacturers suitably caters to application specific latency, rate and reliability demands arising from the use cases, thereby improving overall performance of applications using cellular-connected UAVs. The key innovative 5G technologies are elaborated enabling the seamless integration and support of UAV communication over cellular spectrum. In order to characterize the design performance benefits and study the realistic deployment issues, we also highlighted the efforts to develop working prototypes as well as the field trials and simulations.

Chapter 5

UAV-to-UAV Communication

5.1 Introduction

A real-world mission often necessitates the coordination of numerous UAVs to complete a specified goal. For example, in a surveillance operation over a broad geographical region, using many UAVs to collect surveillance data would be more quicker. When numerous UAVs share mission duties, the capabilities/features or dimensions of the UAVs are also simplified. Moreover, the failure of one or two UAVs during a flight has no significant impact on mission performance. If the surveillance duty had been performed by a single UAV, the whole operation would have failed if that UAV malfunctioned. Obviously, when numerous UAVs coordinate an operation, certain significant benefits are realized in terms of mission completion time, resilience to UAV failures, and the division of larger missions into smaller components. In this chapter, a "swarm" or "fleet" of cellular-connected UAVs, or simply "swarm", refers to a network of many cellular-connected UAVs that cooperate together as a team/group to fulfill a given mission objective [184]. The group of UAVs in the swarm "collaborate together" by making necessary formations and flight configurations that optimizes their integrated capabilities [185]. To exchange information with another UAV member in the swarm, the UAV members must use a wireless communication channel. In general, providing secure and reliable UAV-to-UAV (U2U) communications among swarm UAVs is important for any successful operation. The primary focus of this chapter continues to be a thorough exploration of various U2U linkages, network models, technological enablers, and to evaluate the performance of U2U links.

The following sentences remind the reader of the fundamental questions (Q5, Q6 and Q7 in Section 1.5) that this chapter attempts to raise and discuss potential answers to.

Q5. Is a single UAV enough for all kind of mission? If not, why?

Q6. What are the communication challenges and benefits of a multi-UAV mission? When working with many UAVs, what special considerations must be made for effective communication?

Q7. What kind of cellular technologies support UAV-to-UAV communication in a swarm of multiple UAVs?

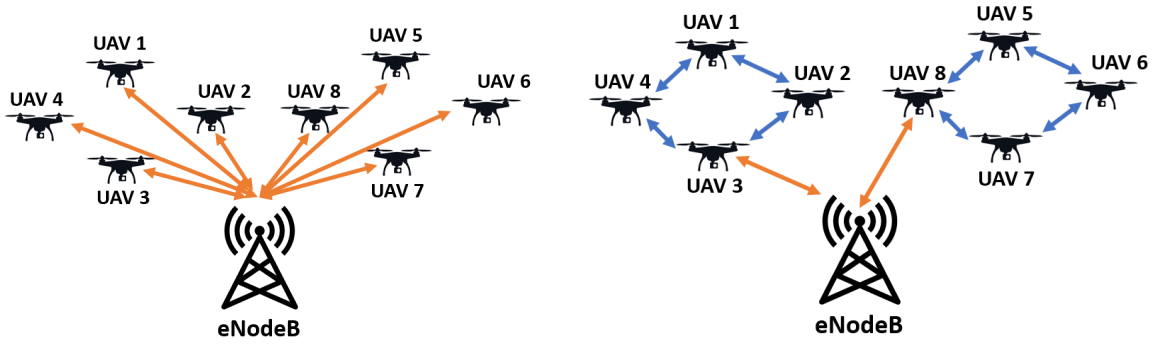

(a) Centralized (b) Decentralized

Figure 5.1: Cellular-connected UAV swarm architecture

5.1.1 Network Architecture

The network architecture to manage the swarm of cellular-connected UAVs [186] can be subdivided in two broad classes (as shown in Fig. 5.1): Centralized and Decentralized.

Centralized Architecture (Fig. 5.1a)

This type of architecture is also known as infrastructure-based architecture because the cellular base station (BS) acts as a command center for guiding and controlling the fleet of UAVs. Each UAV transmits the surveillance and monitoring information to the BS via UAV-to-Infrastructure (U2I) links. There are no direct point-to-point links between two UAVs within the swarm. Massive MIMO, a vital technology component of emerging 5G standards, is a viable solution for supporting centralized swarm model of cellular-connected UAVs coexisting with cellular ground UEs [164, 187].

Decentralized Architecture (Fig. 5.1b)

In this architecture, not all the UAVs are connected to the BS for control and communication. A UAV can communicate directly with another peer UAV within the swarm to exchange information. Such peer-to-peer links are key enabler to establish U2U communication. Hence, in addition to the U2I links, this architecture also supports U2U links for robust swarm functioning.

5.1.2 U2U Technology Enablers

We split the enabling technologies for U2U communications into two main groups:

Non-3GPP Technologies

This group includes Flying Adhoc networks (FANETs), wireless mesh networks (WMNs), Bluetooth, Zigbee, WiMAX etc. In a swarm of multiple UAVs, U2U communication is a difficult and complex item when it comes to frequency regulations and security in the airspace traffic management. This is the reason why most of existing U2U communication technologies use unlicensed frequency spectrum (e.g., LoRa, Wi-Fi, Zigbee etc), which is not a very reliable and safe means of maneuvering for UAV swarms. Also, unlicensed bands have limited operational range, high latency and cannot guarantee the QoS requirement for the mission.

3GPP Technologies

The aforementioned limitations of non-3GPP can be efficiently mitigated in licensed cellular spectrum by integrating the UAVs to 3GPP cellular communication technology (*e.g.,* LTE, 4G/5G and beyond systems). The performance of UAV communication and collaboration in swarm can be greatly improved by 5G and beyond cellular ecosystems. Ultra-reliable low latency communication (URLLC) is one of key 5G technical innovations which guarantees strict QoS constraints on end-to-end delay and reliability of the network applications, which makes it a suitable candidate for time-critical U2U communication.

5.1.3 U2U Challenges

The swarm of UAVs exhibit unique characteristics that are very different from terrestrial, vehicular or slow-moving networks: intermittent links, varying altitude, dynamic topology and mobility. In order to be able to achieve the mission objective correctly, the swarm of cellular-connected UAVs remain connected for information sharing in many real-world applications and use cases. This demands a distributed network configuration and communication strategy to cater to the real time challenges in swarm operation [9]. In general, the swarm of UAVs must have reliable and effective wireless communication mechanisms. Having said above, the intra-swarm (inter-UAV) U2U links are highly critical for ensuring autonomous and self-organizing network behaviour.

Many recent studies investigated the possibility to setup cellular D2D communication systems in both static and vehicular environments, e.g. by addressing the issue of device discovery, resource allocation and interference mitigation with the BSs [188, 189]. In addition, all releases of 3GPP after release-12 included standardization items for Vehicle-to-Everything(V2X) scenarios. We propose 3GPP sidelink technology (PC5 radio interface) for inter-UAVs communication and data flow scheduling within the swarm nodes. The application of sidelink for U2U communications in swarm of cellular-connected UAVs has not been investigated in literature.

In this chapter, **four** main contributions are presented as follows.

- Introducing sidelink as a potential enabler of U2U communication in swarm of UAVs. Through numerical results, we compute the average link quality improvement when the UAV swarm uses U2U links, hence assessing the usage of sidelink technology for aerial communications. (Section 5.3)

- A novel, cooperative multi-hop communication model, based on the C-U2X (Cellular UAV-to-Everything) is presented for efficient UAV data flow scheduling within the swarm. The model design aims at optimizing the C-U2X communication via a interference-aware data flow scheduling. The model is mathematically presented as Multi-Channel Flow Optimization Problem (MCFOP) that computes the optimal data flow scheduling for a swarm of cellular-connected UAVs in a "centralized" way. We prove that the problem itself is NP-hard, and for this reason we introduce an optimization model where the objective function consists of a linear and a quadratic part. The proposed model is able to optimize simultaneously both the routing of the information and the allocation of different sub-channels. (Section 5.4)

- We extend above model to the distributed scenario without any central authority (in our case, the BS) and propose two distributed algorithms for channel allocation and transmission scheduling. Specifically, we describe an extension of the popular auction-based Consensus-Based Bundle Algorithm (CBBA) to produce a conflict-free assignment of transmission opportunities to the UAVs. The performance analysis demonstrates that the Dy-

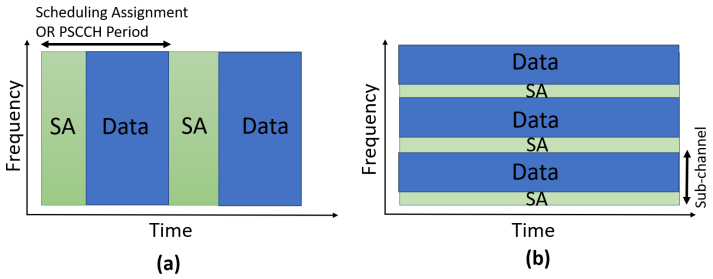

Figure 5.2: Resource Pool Structure: Mode (a) 1,2 (b) 3,4

namic CBBA (D-CBBA) algorithm is able to face the dynamicity of multi-hop UAV networks by executing almost 80% of the data transmissions without causing harmful interference in the multi-hop network. Moreover, D-CBBA greatly overcomes the basic CBBA and the greedy schemes, while it approaches the optimal results produced by the centralized MCFOP solution. (Section 5.5)

- Evaluation of a sidelink-assisted multi-hop communication model to establish connectivity to out-of-coverage UAVs during mission. (Section 5.6)

5.2 Related Works

We split the literature review into three Sections that discuss different aspects of our work. In Section 5.2.1 we provide a brief overview of sidelink technologies and standardization efforts from the 3GPP. In Section 5.2.2 we review the state of the art concerning cellular-connected UAVs and UAV-to-X communications. Finally, in Section 5.2.3 we discuss channel scheduling algorithms. Given the lack of studies focusing on our specific research problem (i.e. scheduling in cellular UAV swarms), we broaden the review to other multi-hop wireless networks.

5.2.1 Sidelink technology and 3GPP Standardization Efforts

Sidelink defines a competent cellular technology which enables direct transmission between devices with or without involvement of cellular BSs. This technology is investigated by 3GPP starting from release-12 as D2D Proximity Service (ProSe) feature to support public safety networks. More specifically, dedicated physical layer channels such as Physical Sidelink Shared Channel (PSSCH), Physical Sidelink Control Channel (PSCCH), Physical Sidelink Broadcast Channel (PSBCH), Sidelink Control Information (SCI) have been created with the specific purpose to support sidelink transmission, synchronization and device discovery. Each sidelink channel is split into a time-frequency resource grid structure: in time domain, 1 ms subframes and in the frequency domain, a set of contiguous resource blocks (RBs). A subchannel defines a group of RBs in the same sub-frame. The number of RBs in subchannel can vary depending upon the configuration. Both sidelink mode 1 and 2 share the same resource structure where direct communication is performed by scheduling the time-frequency resources from the resource pool that comprises of repeating sequence of hyperframes called Scheduling Assignment (SA) or PSCCH period. Each SA period owns resources for control (carried via PSCCH) and data (carried via PSSCH). PSCCH carries the SCI (Sidelink Channel Information) containing details about the modulation and coding scheme, the RBs used, resource reservation interval.

A Transport Block (TB) contains a full packet to be transmitted via PSSCH. In mode 3 and 4, the SA is transmitted using specific RBs in subchannel and TB transmission can occupy the adjacent or non-adjacent RBs in the same subframe. Figure 5.2 shows both type of resource pool structure. Sometimes, more than one device may occasionally select the same resources from the shared pool leading to resource conflict. Hence, such selections are coordinated using proper collision resolution methods. The current scheduling algorithm is a sensing-based semi-persistent scheduling [190] where each node can choose the time-frequency resources to use. The algorithm does not provide any coordination among the competing nodes; the nodes have to apply a sensing-based mechanism to identify the least used time-frequency resources.

Sidelink has already been shown to be useful in Vehicle-to-Everything (V2X) and maritime communication [191, 192]. Release-14 of 3GPP included many additional standardization items for V2X that encompasses Vehicle-to-vehicle (V2V), Vehicle-to-infrastructure (V2I), Vehicle-to-Network (V2N). 3GPP release-15 and release-16 include further safety related enhancements to V2X communication (eV2X) like automated and remote driving, platooning of vehicles [193, 194].

Among others, two main components of sidelink technology have been extensively revised by standardization bodies and investigated by the research community, *i.e.,* the (a) device discovery and the (b) resource allocation. The discovery corresponds to the ability to locate another device, which is in proximity, by using sidelink (PC5) radio interface, and it can be done directly by the UE or at the core network level. The notion of proximity can be extended to the quality of radio channel experienced between communicating UE pairs, signal quality, delay, throughput, network load, etc. Regarding the resource allocation, two sidelink resource allocation modes for public safety [191] are available in 3GPP release-12, respectively *i.e.,* mode 1 (scheduling performed by eNodeB) and mode 2 (devices autonomously manage the resource scheduling). Mode 1 and 2 are primarily used for prolonged battery life at cost of higher latency. In release-14, standardization of C-V2X introduced two additional resource allocation modes [192] designed to cater reliable and latency sensitive communication *i.e.,* mode 3 (in which scheduling is managed by network) and mode 4 (out-of-coverage vehicles autonomously select the resources using a distributed sensing-based semi-persistent scheduling (SPS) scheme).

The work in [195] highlighted the use of sidelink as one of the key candidate technology for enabling U2U communication in 5G and beyond (6G) networks. Authors in [196] analyzed the sidelink resource allocation for mode 1 C-V2X where the BS is in charge of scheduling the resources for the D2D communication. However, mode 1 and 3 envisage the continuous transmission of channel state information (CSI) to the BS. Due to the dynamic nature of UAV wireless networks, this mode is infeasible for multi-hop communication. On the contrary, mode 2 and 4 enable the autonomous selection of the resources for data transmissions over sidelink channels. Mode 4 uses as resource scheduling the Semi-Persistent Scheduling with Listen-Before-Talk (LBT) strategy. However, this method is found to be unable to cope with high network load [192]. To this aim, the authors in [197] showed that a congestion control mechanism can mitigate the channel degradation.

5.2.2 Cellular UAV-to-X communication

The realization of a swarm of cellular-connected UAVs has not been demonstrated so far experimentally and related literature, in this regard, is unavailable. Even though it is foreseen and inclusion of U2U communications in the next 3GPP releases to support new UAVs applications is gaining high attention [198], very few works have considered the U2U communication being supported by the cellular spectrum. A preliminary study was introduced in [199] to motivate the use of sidelink for establishing efficient intra-swarm U2U communication for extending the

connectivity for out-of-coverage UAVs during mission. Moreover, the majority of the works considers single-hop communications only. For what concerns the use of sidelink, in [29], the authors investigated U2U communication in a scenario where the UAV pairs share a portion of uplink spectrum resources of ground users in an underlay manner. The study aims at improving the link performance of both U2U and uplink by adopting tools from stochastic geometry.

The same authors extended the analysis in [200] where UAV pairs share the same spectrum in uplink with ground users considering both underlay and overlay spectrum sharing settings. Note that, above two reference works split the spectrum resources allocated to uplink of cellular ground users, thereby requiring additional interference handling mechanisms. In underlay setting, same spectrum serves both U2U and cellular uplink transmission, hence it is prone to mutual interference from other U2U and ground user uplink transmission. In overlay, the achievable rate is compromised, because the spectrum resources are dedicated separately (non-overlapping) for U2U and cellular uplink. In [30], the authors propose to optimize the cellular UAV-to-X communications: with given routing information, the uplink sum-rate is maximized, while the quality of the sidelink communication is handled by imposing a constraint on the minimum transmission rate for each sidelink.

5.2.3 Multi-hop multi-channel scheduling

Due to the multi-hop multi-channel nature of the communications inside the UAV swarm, channel scheduling algorithm must be designed in order to optimize the wireless resources used during the U2U communications. Resource allocation in dense UEs scenarios has been studied in [201] in order to establish a set of device-to-device multi-hop multi-path (MHMP) communications in 5G networks. Here the authors studied the sharing of downlink channel for distributed video content delivery. The proposed optimization problem is derived from the definition of the channel quality and then the channel scheduling is modelled to ensure the maximum channel capacity in the communications. In [202], the authors defined a Non Linear Integer Programming (NLIP) model for channel assignment to minimize mutual interference in different wireless links.

The works aforementioned do not take into consideration the time dimension of the problem and the actual transmissions on the wireless links. In a scenario of a multi-radio multi-channel multi-hop cognitive cellular network, the authors in [203] defined a joint scheduling and routing optimization problem using a mixed integer non-linear programming (MINLP), but the impact of interference was been taken into account. Similarly, the study in [204] presents a framework of frequency sharing in multi-hop OFDM networks for a chain topology.

However, none of the aforementioned works analyzed the scheduling problem in a multi-hop scenario for a cellular-connected UAVs network. In this work, we focus on the implementation of a distributed channel scheduler for Mode 4 over 5G sidelink communication that is able minimize the collision among the UAVs transmissions, focusing on the peculiarities of aerial communications, such as Line-of-Sight (LoS) transmission links and multi-hop communications. In Table 5.1, we highlight similar works found in the literature that align with different aspects of the contributions made in this work.

5.3 Preliminary Study on the C-U2X Sidelink

In this Section, we provide preliminary results about the application of sidelink. First, in Section 5.3.1, we discuss challenges and unique characteristics of aerial sidelink communications with respect to the well-investigated terrestrial scenarios. Then, in Section 5.3.2, we derive the proba-

Table 5.1: Summary of similar works and contributions

Reference Work(s)	Focus of the study	Contributions/Solutions
[192]	LTE V2X	An overview of LTE-V standard for sidelink V2V communication, Comparison of LTE-V with other short-range solutions like 802.11p or DSRC. Proposed a modified sensing-based semi-persistent scheduling for efficient channel resource selection.
[191]	LTE V2X	Adances of D2D sidelink for enhanced V2X communication. Performance analysis semi-persistent scheduling for D2D modes 3 and 4 via system-level simulations.
[193]	3GPP NR V2X	Performance evaluation to assess the gains of the new control channel design of 5G NR.
[194]	Cellular V2X	A comprehensive overview of 3GPP Release 16 NR SL design for NR V2X, the network architecture, security, and protocol enhancement.
[29], [200]	Cellular U2U	Performance analysis of U2U communication under-laying cellular uplink resources of ground UEs, Single-hop transmission path, Stochastic geometry based analysis.
[203]	Traditional Cellular	Multi-hop, multi-channel joint resource scheduling and routing formulated as MINLP problem to enhance network throughput.
[204]	Traditional Cellular	Multi-hop, sub-channel scheduling exploiting the frequency sharing among hops to achieve higher spectral efficiency, Mathematical modeling and optimization.
This work	Cellular U2X	*Characterization of U2U sidelink and multi-hop resource (sub-channel) scheduling among UAVs for data transmission in a cellular-connected UAV swarm, Performance evaluation and complexity analysis of both centralized and distributed algorithm.*

bility of successful transmission for U2I and U2U links showing numerical results demonstrating the advantages of using U2U links for swarm formation.

5.3.1 Envisioning Sidelink for U2U

D2D-enabled ProSe technology over PC5 interface is already revolutionizing the data transmissions for terrestrial Machine Type Communications (MTC) [191, 192]. Indeed, adaptation of terrestrial sidelink is primarily targeted for direct communication among ground UEs. In cellular UAV-swarms, nearby devices flying in proximity and joining the same mission can take advance of the sidelink feature to forward data towards the BS as well as to exchange control data among them. At the same time, aerial UAVs pose additional complications and novel opportunities for U2U communication which are briefly summarized as follows.

Dimensionality of Environment **-** Terrestrial UEs mostly operate in 2D area where the height of the receiver is typically a few meters. In addition, these devices move horizontally and are surrounded by the 2D coverage of cellular BS. Vice versa, UAVs are flying entities that operate in a 3D space with varying altitude, and the latter produces a non-negligible impact on the coverage criterion and the average U2U link quality.
Propagation Medium **-** UAVs are airborne devices staying at a much higher altitude than the terrestrial UEs or automotive vehicles. With increase in the height above ground, radio environment changes drastically. Usually UAVs fly much above the BS antenna height. Hence, the UAVs may experience dominant LoS probability from different ground BSs that contribute to high interference at the UAV receivers. Additionally, due to the relative velocity of UAVs

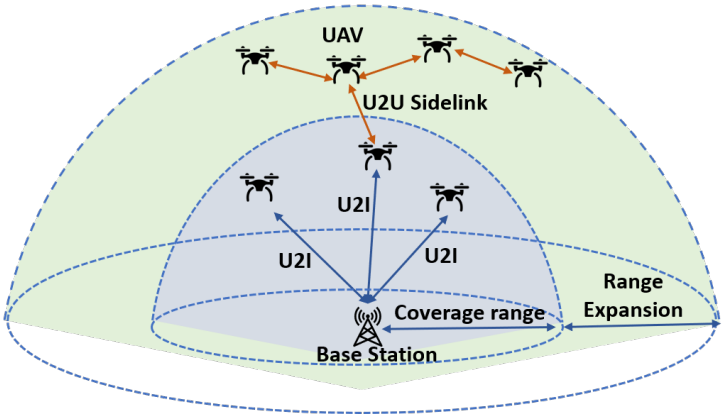

Figure 5.3: System Diagram

during mission, there exists a space-time correlation effect on the U2U link.

Path Planning Optimization -. The UAVs mostly plan their path and optimize the trajectory in a 3D space depending on the mission objective and on coverage/connectivity constraints. Vice versa, terrestrial UEs do not consider path planning as an optimization objective because their movements are often not tied to any real-time mission, or because the overall trajectories are known by the users/drivers but not by the devices. The path awareness may constitute an advantage for the sidelink deployment, since the scheduling of data transmissions on U2U links may take into account the current and future positions of the UAVs and hence the evolution of the wireless links.

Energy Constraints - Energy saving constitutes already an issue for battery powered terrestrial UEs. However, it becomes a vital bottleneck in case of aerial UAVs where the flight autonomy is extremely limited. As a result, network-intensive sidelink mechanisms e.g. related to device discovery or computationally-intensive resource allocation strategies must be carefully evaluated for the case of cellular UAV swarms.

5.3.2 Communication Link Characterization

In the following, we study and analyze both U2I and U2U communication links taking into consideration the shared nature of the sidelink mode 4 channels. The U2I links leverage cellular (Uu) radio interface to connect UAVs to the BS for high payload services in uplink and essential CNPC in downlink. The U2U links are used to disseminate periodical safety critical and payload information via sidelink (PC5) radio interface with D2D ProSe communication. These links provide support to robust and reliable communication for multiple UAVs.

We investigate the for considering an architecture depicted in Fig. 3. For modeling the UAVs and the BSs for the network deployment in a swarm of cellular-connected UAVs, tools from stochastic geometry, spatial statistics and point processes are used. These tools not only result in tractable approach for estimating rate and coverage of the deployment, but also assist in deriving important insights concerning the adopted model. We consider a multiple deployment realization in which each realization consists of an evaluation environment with multiple terrestrial base stations and multiple UAVs being served by those base stations. We assume that the base stations are deployed by a single operator in 2D space and their locations are modeled as per Matern hard core point process type II (MHCPP-II) with density $\lambda_b = 0.01$ per square meters [206]. We model the UAV distribution as per Poisson Point Process (PPP) with altitude $H_u = 100$ meters and

Table 5.2: Glossary of Environmental Parameters

Parameter	Value
Reference Pathloss	$28 + 20 \cdot log10(f_c$ in GHz)
Pathloss exponent (LoS)	2.2
Pathloss exponent (NLoS)	$4.6 - 0.7log10(H_u)$
Small scale fading	Nakagami-m fading model
LoS probability	ITU model, Eqn.4 of [205]
Height of UAV (H_u)	100 meters
BS Density per m^2 (λ_b)	0.01
UAV Density per m^2 (λ_u)	0.05
Noise Figure	7 dB
Thermal Noise	-104 dBm/Hz
Antenna Gain	Omnidirectional with 6 dB
UAV Transmit Power	24 dBm

density $\lambda_u = 0.05$ per square meters. The UAVs are assumed to be positioned in 3D coordinate system and connected to their serving BS according to strongest received signal strength. For accuracy, both UAV-to-Ground and UAV-to-UAV channel includes large-scale fading along with small-scale fading and shadowing. Table 5.2 summarizes the essential parameters about the propagation environment used in the experiment.

In Fig. 5.4, we demonstrate SINR distribution for U2U and U2I links. As shown in Fig. 5.4a, U2U link performance is improved as compared with U2I links. Considering 0 dB as a baseline for SINR comparison, nearly 80% of UAVs experience good SINR coverage (more than 0 dB) for U2U links whereas 20% of UAVs experience good SINR more than 0 dB for U2I links. Hence, sidelink can improve the link throughput to support data transmission services. In Fig. 5.4b, we show the variation of instantaneous UAV SINR values for both U2U and U2I links. Overall range of SINR dispersion for both type of links with five number summary (minimum, first quartile, median, third quartile, and maximum) is presented in the box plot shown in Fig 5.5. UAVs are provided with good coverage by the U2U links as compared to the U2I links.

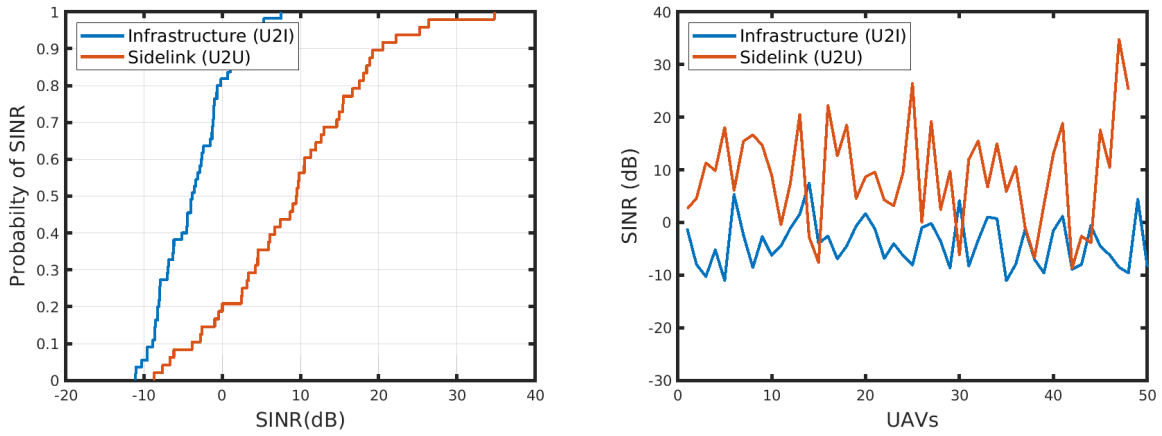

(a) CDF of SINR

(b) Instantaneous SINR distribution

Figure 5.4: Coverage comparison of sidelink (U2U) with infrastructure (U2I) links

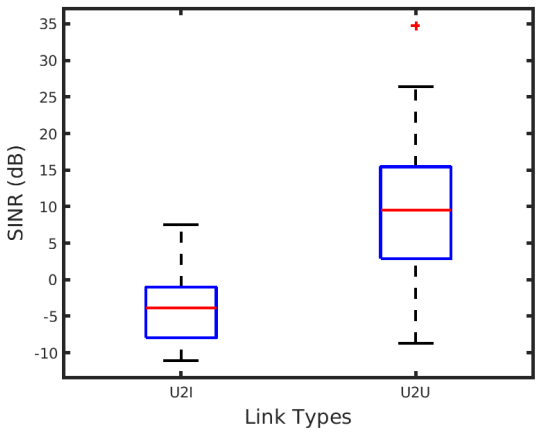

Figure 5.5: Box plot showing SINR dispersion

5.4 Data Flow Scheduling in Swarm of cellular-connected UAVs

5.4.1 Scenario Description

We consider a generic video monitoring mission depicted in Figure 4, in which a swarm of cellular-connected UAVs must monitor a target region and stream back the sensing data to the BS. To this aim, we assume that the entire region is divided into small zones or Points of Interests (PoIs), marked as stars in the Figure. The PoIs are assumed to be static and their positions are known to the UAVs before mission execution. The UAVs have to hover over the PoIs and to transmit the video streams in real-time towards the BS, by using a combination of U2I and U2U links. The focus of this chapter is on the cellular communication issues; hence, we abstract from details of the specific application in use, by the meaning of the PoIs and by the multimedia aspects. However, it is worth remarking that the target scenario can fit the characteristics of several applications of UAV swarms, i.e. related to environmental or crowd monitoring. To meet the mission's objectives, UAVs must fly around the target PoIs, possibly beyond the supported communication range from the BS, thus incurring in potential disconnections and reducing the overall throughput of the monitoring system. This case is shown in Figure 4b and corresponds to a random and non-cooperative deployment of the UAVs where swarm connectivity constraints are not taken into account. On the opposite, Figure 4c depicts a fully cooperative deployment where some UAVs serve as relays (*i.e.,* UE relays) to extend the cellular coverage, hence ensuring a fully-connected swarm deployment.

Broadly speaking, the optimal deployment of a swarm of cellular-connected UAVs for monitoring mission requires to simultaneously address two research issues:

- *Positioning*, *i.e.,* how to place the UAVs so that the maximum number of PoIs is covered while ensuring that each UAV is always connected to the BS via direct or multi-hop links;
- *Scheduling*, *i.e.,* how to allocate the data flows on the available radio time-frequency resources (*i.e.:* sub-channels) so that the expected number of packets successfully received at the BS is maximized.

In this chapter, the two problems are addressed sequentially. First, the positions of the UAVs are computed by the BS. Then, the scheduling algorithms are executed. We rely on state-of-art solutions for the positioning problem since this is not the main focus of this work; interested

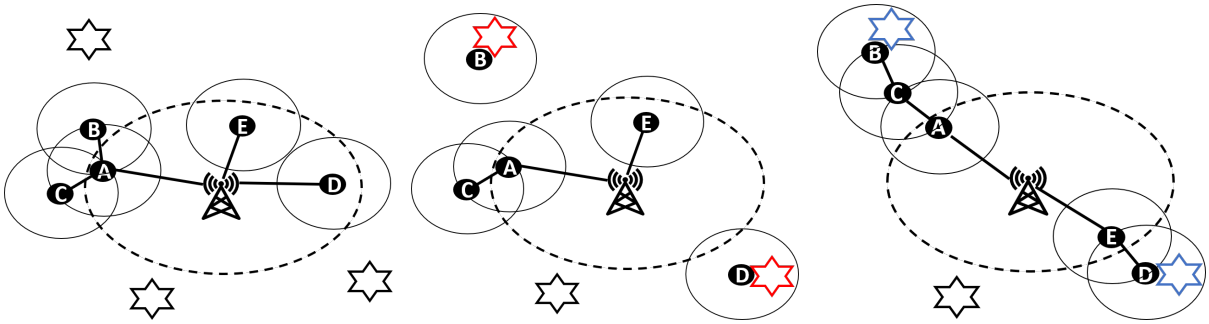

(a) Initial scenario (b) Non-cooperative planning (c) Spatio-temporal cooperation

Figure 5.6: Dynamic aerial network formation and coverage constraints

readers can refer to our previous study [207] related to UAV swarm coverage and connectivity using centralized and distributed approaches. In the following, we formally model the scenario and introduce the objective function of the scheduling problem.

5.4.2 System Model

Let $\mathcal{U} \triangleq \{u_1, u_2, \ldots, u_{N_U}\}$ be a swarm of N_U cellular-connected UAVs in a 3D Cartesian coordinate system. Without loss of generality, we denote as D_{comm} the maximum range (as distance) for U2U communications. Similarly, with indicate with R_{comm} the maximum range for U2I communications. The swarm topology is modeled as a *layout graph* $\bar{G} = (\bar{V}, \bar{E})$ representing the relative positions of the UAVs. The set $\bar{V}$ contains one node for each UAV and for the BS: $\bar{V} = \{\langle u_1 \rangle, \ldots, \langle u_{N_U} \rangle, \langle B \rangle\}$. The set $\bar{E} = \bar{E}_{UAV} \cup \bar{E}_B$ contains the U2U links and U2I links enabled by the communication ranges. More specifically, we indicate with $e = \{\langle u_i \rangle, \langle u_j \rangle\} \subseteq \bar{E}_{UAV} \subseteq \bar{V} \times \bar{V}$ the U2U link between UAVs $\langle u_i \rangle$ *and* $\langle u_j \rangle$, placed at distance lower or equal than D_{comm}. Similarly, we indicate with $e = \{\langle u_i \rangle, \langle B \rangle\} \subseteq \bar{E}_B \subseteq \bar{V} \times \langle B \rangle$ the link between UAV $\langle u_i \rangle$ and the BS, when their distance is lower or equal than R_{comm}. Each edge $e \in \bar{E}$ is associated to an integer transit time τ_e, corresponding to the delay (in terms of number of time slots) required to transmit a data packet over link e. The graph is assumed to be connected when the mission starts. The mathematical notations used to define our system model are summarized in Table 5.3.

In the following, we model the characteristics of the data sources and traffic load. We assume a finite number of subchannels $\mathcal{R} \triangleq \{r_0, r_1, r_2, r_3, \ldots, r_{N_{\text{subc}}}\}$ (where r_0 is the buffering channel). Also, we assume a slotted time model, with a *finite* time horizon $\mathcal{T}$, divided into N_T time slots of equal length t_{slot}: $\mathcal{T} \triangleq \{t_1, t_2, \ldots, t_{N_T}, t_{N_T+1}\}$. As described in Section 5.3, sidelink transmissions rely on a basic time subdivision with subframe of length 1 ms, hence $t_{\text{slot}} = 1\ ms$. Let N_Z be the number of target PoIs. Let $\mathcal{U}_{z_j} \subseteq \mathcal{U}$ be the subset of UAVs that are involved in the data flow related to the target area z_j.

During the entire mission, we assume that N_{z_i} data packets are generated for PoI z_i, with a uniform data rate of N_g packets per second (constant over the PoIs). Let $\text{dt}_{z_i}^{t_w}$ be the data packet generated at time t_w for PoI z_i. We indicate with $\text{DT}_{z_i} \triangleq \{\text{dt}_{z_i}^{t_1}, \text{dt}_{z_i}^{t_2}, ..., \text{dt}_{z_i}^{t_{N_{z_i}}}\}$ the overall set of data packets generated at the target PoI z_i, and with $\text{DT} \triangleq \bigcup_{z_i \in \mathcal{Z}} \text{DT}_{z_i}$ the set of all the packets generated over the scenario during the entire mission. For ease of disposition, we use $\text{dt} \in DT$ to refer to a generic packet when there is no need to explicit the region and the time slot.

In order to model the scheduling of the data transmissions in the cellular UAV swarm, we

Table 5.3: Glossary

Notation	Definition
D_{comm}	Range of U2U communication
R_{comm}	Range of U2I communication
$\mathcal{U} \triangleq \{u_1, u_2, \ldots, u_{N_U}\}$	Swarm of N_U cellular-connected UAVs
$\mathcal{Z} \triangleq \{z_1, z_2, \ldots, z_{N_Z}\}$	Set of N_Z target point of interests (PoIs)
$\mathcal{T} \triangleq \{t_1, t_2, \ldots, t_{N_T}, t_{N_T+1}\}$	Time horizon
N_{z_i}	Data packets generated for PoI z_i
$\mathcal{U}_{z_j} \subseteq \mathcal{U}$	The subset of UAVs involved in data flow related to target area z_j
$\mathcal{R} \triangleq \{r_0, r_1, r_2, r_3, \ldots, r_{N_{\text{subc}}}\}$	Set of subchannels
r_0	Buffering channel
$\bar{G} = (\bar{V}, \bar{E})$	Layout graph of swarm
A_A	Set of *assignment* arcs
A_{BUF}	Set of *buffering* arcs
A_{TR}	Set of *transmission* arcs
A_B	Set of *base* arcs
$\text{rss}(a)$	The signal strength received at the destination UAV belonging to arc a
τ_e	Delay (number of time slots required to transmit a data packet) over link e
$\mathcal{W}_a$	The probability of successful transmission through arc a
N_0	Noise figure
φ_a	1 if arc $a \in A$ is selected, 0 otherwise
$\mathcal{U}_{z_j} \subseteq \mathcal{U}$	The subset of UAVs that are involved in the data flow
$\text{dt}_{z_i}^{t_w}$	The data packet generated at time t_w for PoI z_i
$\text{DT} \triangleq \bigcup_{z_i \in \mathcal{Z}} \text{DT}_{z_i}$	Set of all the packets generated over the scenario
$\delta^+(v)$, $\delta^-(v)$	The outgoing and incoming arcs of vertex v, respectively
$\delta^+_{r_j}(v)$, $\delta^-_{r_j}(v))$	The outgoing and incoming arcs using sub-channel r_j, respectively
$\delta^+_{\text{dt}}(v)$, $\delta^-_{\text{dt}}(v))$	The outgoing and incoming arcs related to data packet dt, respectively

introduce the concept of *multi-graph* $G = (V, A)$, a time-expanded directed version of the graph $\bar{G}$ that allows to model the transmissions of the data packets from the targets PoIs towards the BS during the time horizon considered. The set of vertexes $V = V_D \cup V_{UAV} \cup \langle B \rangle$ includes the following elements (in addition to B, the BS):

- $V_D = DT$ contains one vertex for each packet $\left\langle \text{dt}_{z_i}^{t_k} \right\rangle$ generated during the mission;
- V_{UAV} consists of tuples $\langle u_i, t_k \rangle$, $\forall u_i \in \mathcal{U}$, and $\forall t_k \in \mathcal{T}$. Item $\langle u_i, t_k \rangle$, $\forall u_i \in \mathcal{U}$ indicates that UAV u_i is using a subchannel in time slot t_k.

We indicate with $V(t_k) = \{v = \langle u_i, t_{k'} \rangle : k = k'\} \subseteq V$ the subset of vertices associated to time slot $t_{k'}$.
Similarly, the set of arcs $A = A_A \cup A_{BUF} \cup A_{TR} \cup A_B$ consists of the following elements:

- $A_A = \{\left(\left\langle \text{dt}_{z_i}^{t_k} \right\rangle, \langle u_i, t_k \rangle\right), \forall \text{dt}_{z_i}^{t_k} \in DT, \forall u_i \in \mathcal{U}_{z_j}, k = 0, \ldots, N_T\}$ is the set of *assignment* arcs, associating the data packets produced by a PoI to a UAV that is covering that region;
- $A_{BUF} = \{(\langle u_i, t_k \rangle, \langle u_i, t_{k+1} \rangle)_{r_0,\text{dt}}, \forall r_j \in \mathcal{R}, u_i \in \mathcal{U}, \text{dt} \in DT, k = 0, \ldots, N_T\}$ is the set of

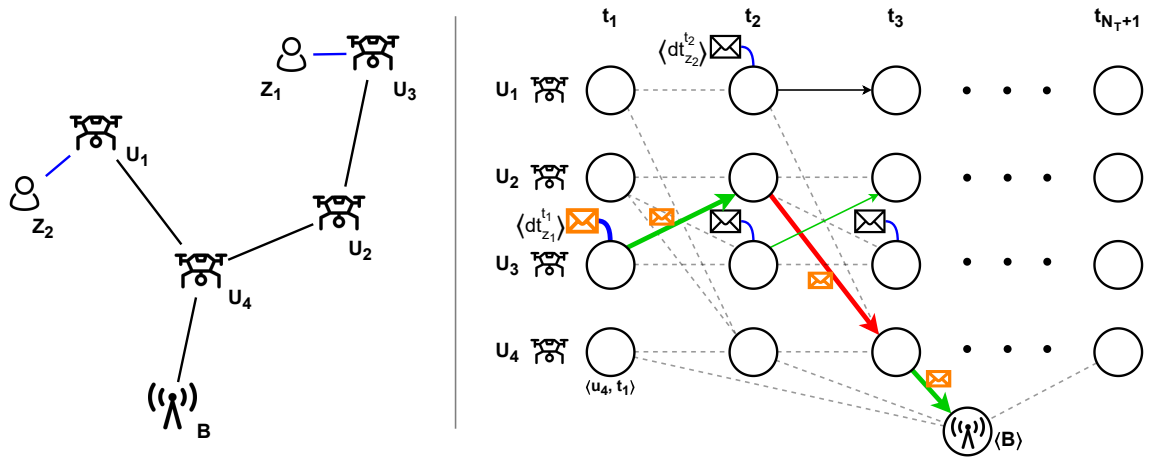

Figure 5.7: Illustration of the multi-graph construction. On the left, we have the scenario with 4 UAVs (U_1,U_2,U_3,U_4) and 2 PoIs (Z_1,Z_2), while the derived multi-graph is depicted on the right. For ease of drawing, not all the labels are showed. The V_{UAV} vertexes consist of tuples $\langle u_i, t_k \rangle$, the BS node $\langle B \rangle$, and the packets $\langle \mathrm{dt}_{z_j}^{t_k} \rangle$. The colored arrows depict the different channels that are used for transmitting, while the black one shows the buffering of the packet $\langle \mathrm{dt}_{z_2}^{t_2} \rangle$ at UAV u_1. The thick arrows depict the path performed by the packet $\langle \mathrm{dt}_{z_1}^{t_1} \rangle$ (colored in orange).

buffering arcs used to represent the possibility for a UAV u_i to delay the transmission of data packet dt at time t_k;

- $A_{TR} = \{\left(\langle u_i, t_k \rangle, \langle u_{i'}, t_{k+\tau_{ii'}} \rangle\right)_{r_j,\mathrm{dt}}, \forall r_j \in \mathcal{R} \setminus \{r_0\}, \forall \{\langle u_i \rangle, \langle u_{i'} \rangle\} \in \bar{E}_{UAV}, \forall \mathrm{dt} \in DT, k = 0, \ldots, N_T\}$ is the set of *transmission* arcs used to represent the transmission of the data packet from u_i to $u_{i'}$ with subchannel r_j.
- $A_B = \{(\langle u_i, t_k \rangle, \langle B \rangle)_{r_j,\mathrm{dt}}, \forall r_j \in \mathcal{R} \setminus \{r_0\}, \forall \{\langle u_i \rangle, \langle B \rangle\} \in \bar{E}_B, \forall \mathrm{dt} \in DT, k = 0, \ldots, N_T + 1\}$ is the set of *base* arcs denoting the communication of UAV u_i to the BS B;

We indicate with $\delta^+(v)$ (resp. $\delta^-(v)$), the outgoing (resp. incoming) arcs of vertex v. Similarly, we indicate with $\delta^+_{r_j}(v)$ (resp. $\delta^-_{r_j}(v)$), the outgoing (resp. incoming) arcs using sub-channel r_j and with $\delta^+_{\mathrm{dt}}(v)$ (resp. $\delta^-_{\mathrm{dt}}(v)$), the outgoing (resp. incoming) arcs related to data packet dt. Fig. 5.7 depicts an example of multi-graph construction for a small-scale scenario.

5.4.3 Problem Formulation

Given the multi-graph formulation introduced in the previous Section, the scheduling of data transmission over the cellular UAV-swarm can be modeled as the problem of determining the optimal sequence of arcs (which correspond to networking actions in our modeling) so that the overall probability of successful transmission is maximized. To this purpose, we introduce the following variable:

$$\varphi_a = \begin{cases} 1, & \text{if arc } a \in A \text{ is selected} \\ 0, & \text{otherwise} \end{cases} . \tag{5.1}$$

Let $\mathcal{W}_a$ denote the probability of successful transmission through arc a, with $a \in \{A_{TR} \cup A_B\}$, i.e. the arc corresponds to a transmission on a U2U or on a U2I link. We model $\mathcal{W}_a$ as follows:

$$\mathcal{W}(a) = \begin{cases} 1 & \text{if } \mathrm{SINR}_a^{\mathrm{SL}}[dBm] > k_2 \\ 0 & \text{if } \mathrm{SINR}_a^{\mathrm{SL}}[dBm] < k_1 \\ (\mathrm{SINR}_a^{\mathrm{SL}}[dBm] - k_1)/(k_2 - k_1) & \text{otherwise} \end{cases} \tag{5.2}$$

where the constants k_1 and k_2 can be extrapolated from the SINR range in Fig. 5.4a of Section 5.3.2. Here, $\mathrm{SINR}_a^{\mathrm{SL}}$ is derived in Section 5.3.2 and specifies the SINR value at the destination UAV. Its value can be expressed as:

$$\mathrm{SINR}_a^{\mathrm{SL}}[W] = \frac{\varphi_a \cdot \mathrm{rss}(a)}{\sum_{v \in V(t_k)} \sum_{a' \in \delta^+(v)_{r_j}} \varphi_{a'} \cdot \mathrm{rss}(a') + N_0} \tag{5.3}$$

$$\mathrm{SINR}_a^{\mathrm{SL}}[dBm] = 10 \cdot log_{10}(1000 \cdot \mathrm{SINR}_a^{\mathrm{SL}}[W]) \tag{5.4}$$

where N_0 refers the received power noise, and $\mathrm{rss}(a)$ is the signal strength received at the destination UAV belonging to arc a. For a single data packet dt, the overall probability can be computed as:

$$\prod_{a \text{ used by dt}} \mathcal{W}(a) \tag{5.5}$$

It is worth noting that, when the data packet is being delivered over a multi-hop an end-to-end link, the overall packet delivery probability will be constrained by the most unreliable link included in the routing path. Due to the iterative behavior of our optimization model, some cases may result in sub-optimal results of the overall probability induced by the link unreliability experienced in the path. However, we show that, this trade-off does not cause significant performance degradation (*e.g.,* the packer delivery ratio (PDR)) as shown in Fig. 5.9. During the "positioning" phase, the UAVs form a multi-hop path from PoI towards the base that would ensure communication range constraint. Although the "transmission scheduling" phase follows after “positioning”, their estimated locations in the multi-hop chain ensure an end-to-end link being able to deliver the data packet across the chain towards the base. If the SINR experienced through the arc is above certain threshold, the link is active for data transmission and transmit with a probability. We aim at maximizing the probability of successful transmission through a given arc from the channel conditions experienced (*i.e.,* SINR) between transmitter and receiver. In the scheduling problem, we want to determine the optimal φ_a so that the expected number of packets successfully received by the BS is maximized, considering all the traffic produced in the scenario, *i.e.,*:

$$\underset{\varphi_a}{\mathrm{argmax}} \sum_{\mathrm{dt} \in \mathrm{DT}} \prod_{a \text{ used by dt}} \mathcal{W}(a). \tag{5.6}$$

Maximizing the value of Eqn. (5.6) leads to an highly nonlinear problem. Hence, we relax the objective function to be able to reformulate the problem and solve it with optimization tools.

5.4.4 Centralized Solution

We propose a mathematical model that aims at finding an effective communication schedule by tuning as parameters the path associated to each data packets in the multi-graph presented in Section 5.4.2, *i.e.,* the φ_a values. More precisely, the optimal solution to the scheduling problem can be obtained by solving the following Multi-Channel Flow Optimization Problem (MCFOP):

$$\min \sum_{a,\in A} b_a \varphi_a + \sum_{a,a' \in A} c_{a,a'} \varphi_a \varphi_{a'} \tag{5.7}$$

$$\sum_{a \in \delta^+(v)} \varphi_a \leq 1, \qquad \forall v \in V_D \tag{5.8}$$

$$\sum_{a \in \delta^+_{r_j}(v)} \varphi_a \leq 1, \qquad \forall v \in V_{UAV}, r_j \in \mathcal{R} \tag{5.9}$$

$$\sum_{a \in \delta^-_{r_j}(v)} \varphi_a \leq 1, \qquad \forall v \in V_{UAV}, r_j \in \mathcal{R} \tag{5.10}$$

$$\sum_{a \in \delta^+_{\mathrm{dt}}(v)} \varphi_a - \sum_{a \in \delta^-_{\mathrm{dt}}(v)} \varphi_a = 0, \qquad \forall v \in V_{UAV}, r_j \in \mathrm{DT} \tag{5.11}$$

$$\varphi_a + \varphi_{a'} \leq 1, \qquad \forall v \in V_{UAV}, \; \forall a \in \delta^+(v) \setminus A_{BUF}, \; a' \in \delta^-(v) \setminus A_{BUF} \tag{5.12}$$

$$\varphi_a \in \{0,1\}, \qquad \forall a \in A \tag{5.13}$$

The objective function presented in (5.7) is an approximation of the real objective function $\max \sum_{\mathrm{dt} \in \mathrm{DT}} \prod_{a \text{ used by dt}} \mathcal{W}(a)$ and it consists of a linear and a quadratic term. The two terms play two different roles in the search for the optimal solution. The linear term allows to find the shortest routing to the BS. On the other hand, the quadratic term introduces a penalty whether a pairs of arcs a and a' appears together in the solution. In principle, the objective function is written in a generic way that allows to penalize any pair of arcs in the multi-graph G. However, in our implementation, we fixed the values of $b_a = \frac{1}{\mathcal{W}(a)}$, while $c_{a,a'} = 10^2$ if the distance between arcs a and a' is lower than a given threshold D_{interf}, and they have the same time period and same subchannel. In this way the objective function (5.7) first aims at minimizing the number of times we have a transmission with a potential interference. Secondly, for two solutions with the same number of conflicts, it prefers a solution maximizing the total sum of probabilities of having a successful communication.

Constraint (5.8) ensures that each data source (*i.e.,* PoI) is associated to at most one UAV. Constraints (5.9) and (5.10) ensure that a UAV transmits and receives at most one data packet on the same subchannel during the same subframe period. Constraint (5.12) ensures that each UAV can only either receive or transmit in a given time t. Finally, Constraint (5.11) creates a *flow* for the data frames from the source to the BS. In other words, if a node receives a data packet at a given time t, it must either keep it via *buffering* arcs or sent it to another UAV or to the BS via *transmission* or *base* arc.

Complexity of the MCFOP

In this subsection, we prove the complexity of the MCFOP by restriction from the shortest weight-constrained path [208]:

Theorem 5.4.1. The MCFOP is NP-hard.

Proof. Given a graph $G = (V, A)$, a set of non-negative length l_a and a non-negative weight w_a for each arc $a \in A$, two specified vertices $s, t \in V$ and positive integers K and W. The Shortest

weight-Constrained Path (SCP) searches for a simple path in G from s to t with total weight W or less and total length K or less. The SCP is NP-hard [208]. For a given instance of SCP, let us consider the following restriction of the MCFOP: we fix $N_T = T$, $N_{subc} = 1$, we use G as layout graph, where $\bar{E}_{UAV} = \{\langle s \rangle\}$, t is the base station ($\langle B \rangle = t$) and $\tau_a = t_a$. The linear costs are given by w_a, i.e., $b_a = w_a$ and there are no quadratic costs, i.e., $c_{a,a'} = 0$. With the given transformation, MCFOP compute a SCP of minimal cost with total length less than T, therefore MCFOP is also NP-hard. □

5.5 Dynamic Consensus-Based Bundle Algorithm

The centralized solution assumes a complete knowledge of the UAVs positions and a continuous exchange of control messages between the central BS and the UAV swarm. Given the unfeasibility of such assumptions, and the computational cost of the centralized solution, in this Section we propose a distributed method for channel sharing and transmission scheduling, based on popular auction-based algorithms. Indeed, Consensus-Based Bundle Algorithm (CBBA) [209] is a well-known auction-based method for decentralized task allocation among some agents. CBBA proceeds in repeated iterations of two phases, (1) Bundle construction and (2) Consensus phase. In the first phase, an agent creates task bundle by winning the bid over the other agents. In the second phase, a mutual consensus is applied on the winning bids of agents in order to perform the conflict resolution among the agent-task pairs. The algorithm is shown to converge in real-time and produces a conflict-free assignment of agents to tasks [209]. We model the UAVs as agents and the Transport Blocks (TBs) as tasks that the agents can use to transmit its data. The UAVs must be assigned to different TBs in order to avoid mutual interference.

To this purpose, the task allocation algorithm must produce a conflict-free assignment of N_{task} tasks among N_U UAVs to minimize simultaneous transmissions over the shared channels. Let $\mathcal{U}$ be the set of UAVs and $\mathcal{K}$ the set of available tasks. In our modeling, $\mathcal{K} = \{k_1, k_2, \ldots, k_{N_{\text{task}}}\}$ represents the pool of TBs that UAVs can reserve to transmit their data. Assume that the time $\mathcal{T}$ is subdivided into superframes $\mathcal{T}^i_{\text{supf}} = \{t_{0+N_{\text{supf}} \cdot i}, t_{1+N_{\text{supf}} \cdot i}, \ldots, t_{(N_{\text{supf}}-1)+N_{\text{supf}} \cdot i}\} \subset \mathcal{T}$ of length N_{supf}, where $t^s_k = t_{k+N_{\text{supf}} \cdot i}$ that represents the k-th time slot inside every superframe. The task $k_j \in \mathcal{K}$ is hence defined as a pair $\langle t^s_k, r_y \rangle$, with $r_y \in \mathcal{R} \setminus \{r_0\}$ being an available subchannel (see Figure 5.8). The number of tasks is given by: $N_{\text{task}} = N_{\text{supf}} \cdot N_{\text{subc}}$. The CBBA algorithm envisages the possibility for each agent to perform L_t tasks during the algorithm execution. Initially, we assume this value to be homogeneous among the UAVs and equal to the packet generation rate from the PoIs (N_g). How to remove the assumption is discussed later in this Section.

During the first phase, the CBBA algorithm keeps track of the following lists: (*i*) the winning bid list $\mathbf{y}_i$ of length N_{task} containing the bid of the winning agent; (*ii*) the winning UAV list $\mathbf{z}_i$ of length N_{task} containing the the winning UAV for each specific TB in the resource pool; (*iii*) and a bundle $\mathbf{b}_i$ that contains the list of the TBs obtained by UAV i. Let c_{ij} be the score function, defining the reward for UAV i using the TB k_j for the transmission. We define the score function as follow:

$$c_{ij} = \begin{cases} 1 & \text{if } \text{rss}_j \leq \text{rss}_{\min} \\ \frac{1}{1+(\text{rss}_j - \text{rss}_{\min})} & \text{otherwise} \end{cases} \tag{5.14}$$

where rss_j is the estimation of the received signal strength detected at the TB of task k_j in the previous superframes, while $\text{rss}_{\min}$ is a system threshold on the rss under which the sub-channel is detected as idle. The aim of the distributed assignment algorithm is to maximize the value of $\sum_{u_i \in \mathcal{U}} \sum_{k_j \in \mathcal{K}} c_{ij} \cdot \text{x}_{ij}$, i.e. to minimize the simultaneous transmissions of different UAVs on the

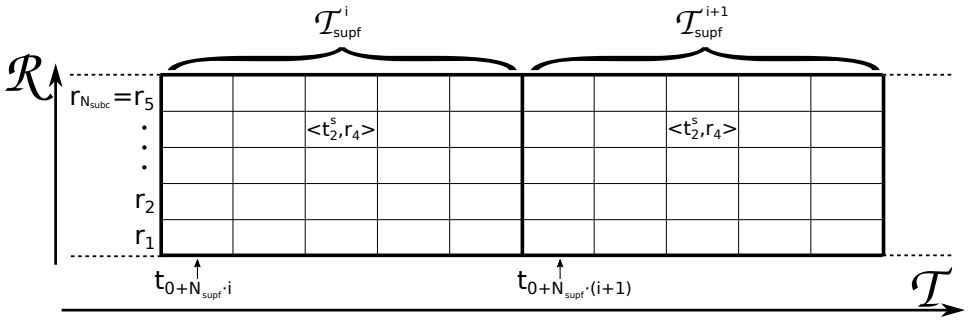

Figure 5.8: Tasks definition: in this example, two consecutive task pools are depicted, $\mathcal{T}^{i}_{\text{supf}}$ and $\mathcal{T}^{i+1}_{\text{supf}}$, where $N_{\text{subc}} = 5$ and $N_{\text{supf}} = 5$.

same TB. Here, x_{ij} is 1 if UAV i uses the TB k_j, and 0 otherwise. Algorithm 1 shows the first phase of the bundle construction. The bundle construction is executed at each t^s_0, i.e. at the beginning of each superframe.

Algorithm 1: Bundle Construction

Input: $\mathbf{y}_i$, $\mathbf{z}_i$, $\mathbf{b}_i$

1 **while** $|\boldsymbol{b}_i| < L_t$ **do**
2 $\quad h_{ij} \leftarrow \mathbb{I}(c_{ij} > y_{ij}) \quad \forall k_j \in \mathcal{K}$
3 $\quad J_i = \text{argmax}_j(c_{ij} \cdot h_{ij})$
4 $\quad \mathbf{b}_i \leftarrow \mathbf{b}_i \cup \{k_j\}$
5 $\quad y_{i,j} \leftarrow c_{i,J_i}$
6 $\quad z_{i,j} \leftarrow i$
7 **end**

In Algorithm 1, we assume that at time t_0 the elements in the sets $\mathbf{y}_i$ and $\mathbf{z}_i$ are initialized to 0, and $\mathbf{b}_i$ to $\emptyset$, $\forall u_i \in \mathcal{U}$. The algorithm starts with checking the $\mathbf{b}_i$ set that must contain L_t elements, i.e. the requested packets to transmit (line 1). Inside the while loop, the algorithm chooses the best task whose score function is greater then the winning bid (lines 2 and 3). Here, the $\mathbb{I}$ function returns 1 if the argument is true, 0 otherwise. Finally, the bundle $\mathbf{b}_i$ is updated with the winning task, and consequently the sets $\mathbf{y}_i$ and $\mathbf{z}_i$ (lines 4 - 6).

Each UAV broadcasts a beacon message every T_{beacon} seconds, in order to exchange control information used for the consensus phase performing conflict resolution. This message contains the winning bids list $\mathbf{y}_i$, the winning agents list $\mathbf{z}_i$, and the list $\mathbf{s}_i$, with $|\mathbf{s}_i| = N_U$, indicating the timestamp referring the last received beacon from the other UAVs. At every beacon reception from UAV u_j, the UAV i activates the conflict resolution phase that consists in the execution of a set of check rules listed in [209] for every element in $\mathbf{z}_j$. Each rule serves to update the conflicts on the task assignment, by allocating the tasks to the UAVs with the greatest bid.

The Algorithm 1 described so far considers a static number of tasks for each UAV u_i, given by the value of L_t. However, the need of transmission opportunities within cellular UAV swarms may change dynamically as a consequence of varying traffic loads, new mission requirements, interference effects, etc. For this reason, let L^i_t be the number of tasks for each agent $u_i \in \mathcal{U}$ and at each time slot t_k. In the following, we introduce a variant of the CBBA algorithm, named *Dynamic-CBBA* (D-CBBA), that takes into account the presence of $L^i_t(t_k)$ terms for each UAV/time slot. The algorithm works similar to the legacy CBBA algorithm and is composed of a sequence of a bundle construction phases followed by a conflict resolution phase. However,

differently from the legacy CBBA, we need to add a decision rule to the decision table defined in [209], in order to deal with the variability of assigned tasks. This rule is defined in Table 5.4.

Table 5.4: D-CBBA extra decision rule

Agent i thinks $z_{i,j}(t_k)$ **is**	**Agent i thinks** $z_{i,j}(t_{k+1})$ **is**	**Action**
i	i	$L_t^i(t_{k+1}) < L_t^i(t_k)$ $\Downarrow$ ResetWorst

The action "ResetWorst" resets both the winning bid and the agent, i.e. $y_{i,j} = 0$ and $z_{i,j} = 0$ of the worst task belonging to the winning bundle $\mathbf{b}_i$ at time t_k, i.e. k_w with $w = \text{argmin}_j\, c_{ij}$ where $\text{x}_{iw} = 1$. This new rule allows to release the resource when it is no longer needed by the UAV. For the D-CBBA algorithm, we define the number of tasks to assign to the UAV u_i as $L_t^i(t_k) = \text{queue}_i(t_k) + \text{hist}_i(t_k)$, where $\text{queue}_i(t_k)$ indicates the packet queue size of UAV u_i at time slot t_k, while $\text{hist}_i(t_k)$ is the number of packets received during the last N_{supf} time slots. In this way, the UAV will be able to obtain enough TBs to transmit the packets from the transmission queue plus an estimation of packets that the UAV will receive during the next superframe. It is worth mentioning that the value of $L_t^i(t_k)$ must be less or equal than the number of available tasks N_{task}.

5.5.1 Computational complexity

The computational complexity of the bundle construction phase, i.e. Algorithm 1, is defined by the main loop of line 1, that is executed $\mathcal{O}(L_t)$ times. Inside the loop, the research of the best task is $\mathcal{O}(N_{\text{task}})$ due to the linear research of the argmax value (line 3). Given that the maximum value that L_t can get in our D-CBBA algorithm is N_{task}, the total computational complexity of the bundle construction phase is $\mathcal{O}(N_{\text{task}}^2)$.

The second phase, i.e. the conflict resolution, is activated at each UAV u_i upon reception of a beacon message form UAV u_j. During this phase, the elements of $\mathbf{z}_j$ are visited and, for each element, the table check is executed. We recall that $|\mathbf{z}_j| = N_{\text{task}}$. The rules defined in CBBA [209] are executed in constant time, $\mathcal{O}(1)$, while the action "ResetWorst" defined in Table 5.4 is $\mathcal{O}(N_{\text{task}})$ due to its argmin search over all the possible tasks. In conclusion, also the the second phase has a computational complexity of $\mathcal{O}(N_{\text{task}}^2)$.

5.5.2 Positioning Algorithm

We assume that the positioning algorithm is computed in a centralized way by the BS before the starting of the mission. The goal is to maximize the the coverage of PoIs from the UAVs. To this aim, we assume that a Minimum Spanning Tree (MST) algorithm is used, where the vertexes are the PoIs and the BS, while the weights of the arcs are defined as the Euclidean distance between the vertexes. The Prim's algorithm is executed to compute the tree. Finally, the UAVs are placed on the edges at a maximum distance of D_{comm} in order to ensure that the swarm is fully connected.

Table 5.5: Simulation Parameters

Component	Model
N_U	10
M	10 km
N_{Z}	4
N_{supf}	20
N_{subc}	3
N_g	400
D_{comm}	1000 m
D_{interf}	1200 m
T_{beacon}	0.2 s
rss_{min}	-105 dBm
BUF_{max}	500

5.5.3 Performance Evaluation

The simulation setup considers a swarm of cellular-connected UAVs performing video monitoring tasks of N_Z target regions. The monitoring regions are placed randomly in a map scenario of size $M \times M$ square meters. There are N_U UAVs statically placed using the MST algorithm with an inter-UAV distance of at most D_{comm} meters. The BS is placed at the center of the scenario. The simulation parameters are reported in Table 5.5. The UAVs that are positioned at the PoIs represent the end nodes of the MST and are in charge of generating sensing data with a rate of N_g packets per second.

We compare these scheduling algorithms in the performance evaluation:

- *Centralized Solution with Limited Interference*: This is the algorithm presented in Section 5.4.4, by considering an interference radius equal to D_{interf} meters. It is abbreviated as Centralized (Lim. Int.) in the plots.
- *Centralized Solution*: this is the above mentioned algorithm after removing the assumption on the limited interference radius.
- *CBBA*: This is the state-of-the-art distributed algorithm with the application described in Section 5.5 and a static number of tasks. Specifically, we set $L_t = N_g$.
- *D-CBBA*: This is our extension of the *CBBA* algorithm with varying number of tasks for UAVs, described in Section 5.5.
- *Greedy Algorithm*: This is a basic scheme where each UAV randomly selects the TBs for data transmission, without any explicit cooperation with other peers. It is used here as baseline for distributed resource allocation.

The centralized solution is evaluated with mathematical optimization framework by solving the optimization problem stated in Equation 5.7 and Equations 5.8-5.12. This model is implemented in C++ using IBM ILOG CPLEX 12.8.0 [210] as MILP solver. All experiments are executed on a single core of an Intel Xeon E5-4620 at 2.2GHz with 4GB of available memory. The distributed solution is evaluated via extensive simulations. The Packet Delivery Ratio (PDR) is used as key performance metric.

Figures 5.9a and 5.9b depict the PDR with respect to the varying rate of packet generation (N_g) and number of sub-channels (N_{subc}), respectively. As expected, the PDR is negatively correlated with the data generation rate and positively correlated with the number of available

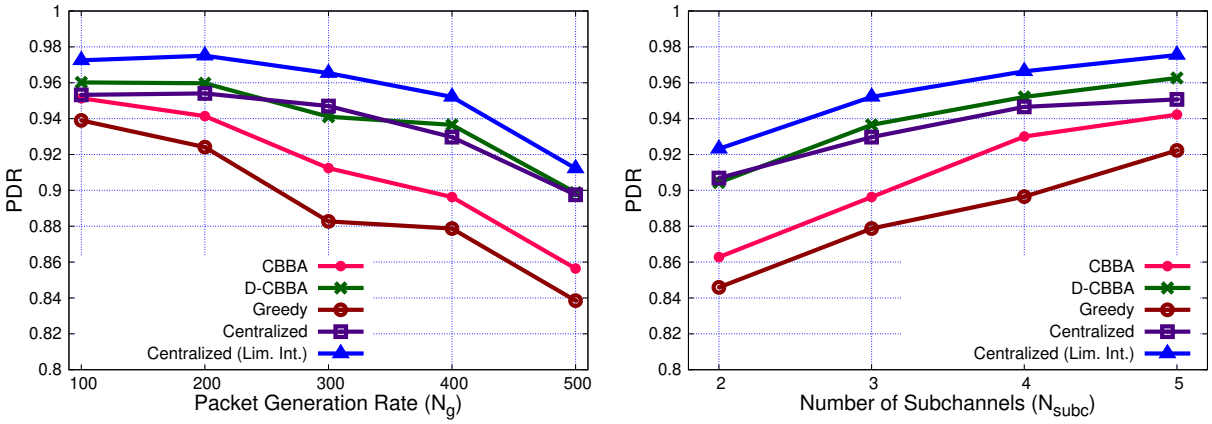

(a) PDR varying with rate of packet generation (N_g)

(b) PDR varying with number of subchannels (N_{subc})

Figure 5.9: Variability of PDR

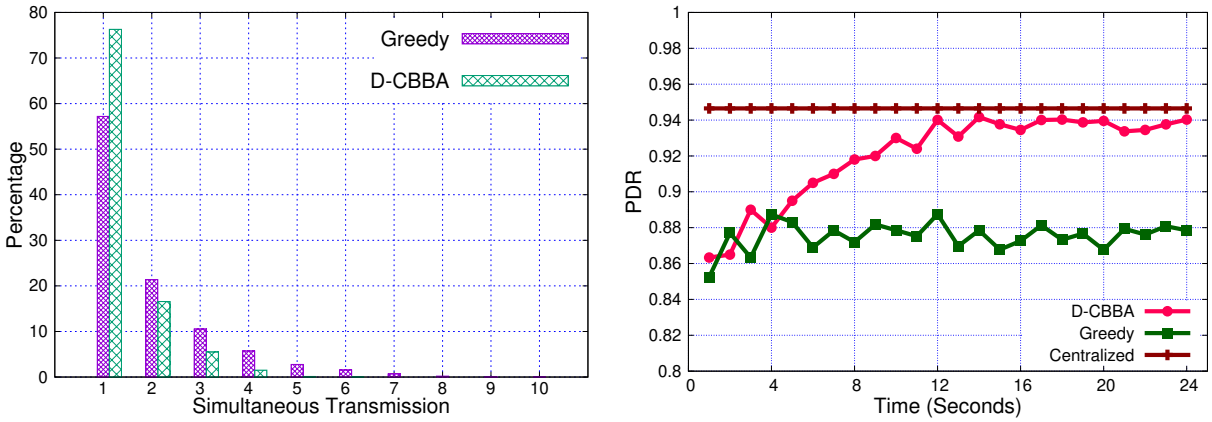

(a)

(b)

Figure 5.10: (a) Percentage of simultaneous transmissions for Greedy and D-CBBA, (b) Comparison of the algorithm convergence time.

sub-channels. When increasing the packet generation ratio, in fact, the network becomes more and more congested; as a result, it becomes challenging to allocate idle TBs to only one UAV. Vice versa, the interference decreases when expanding the pools of available sub-channels from which the UAVs can pick up the TBs.

From these Figures, we can observe the difference between the two centralized solutions and more specifically the impact of the approximation introduced in Section 5.4.4 to make the problem tractable. The centralized solution with limited interference adds the assumption of a limited interference radius, equal to D_{interf} meters; it is easy to notice that the assumption produces a PDR equal to 98%. If we keep the same transmission scheduling but remove the assumption of limited interference radius, we can notice an additional loss of around 2% in the performance. This is mainly due to packet collisions occurring on links covering long distances and hence with reduced SINR values.

Moving the analysis to the distributed solutions, we can appreciate the differences between the D-CBBA, the CBBA and the Greedy algorithm. The Greedy algorithm perform worse than

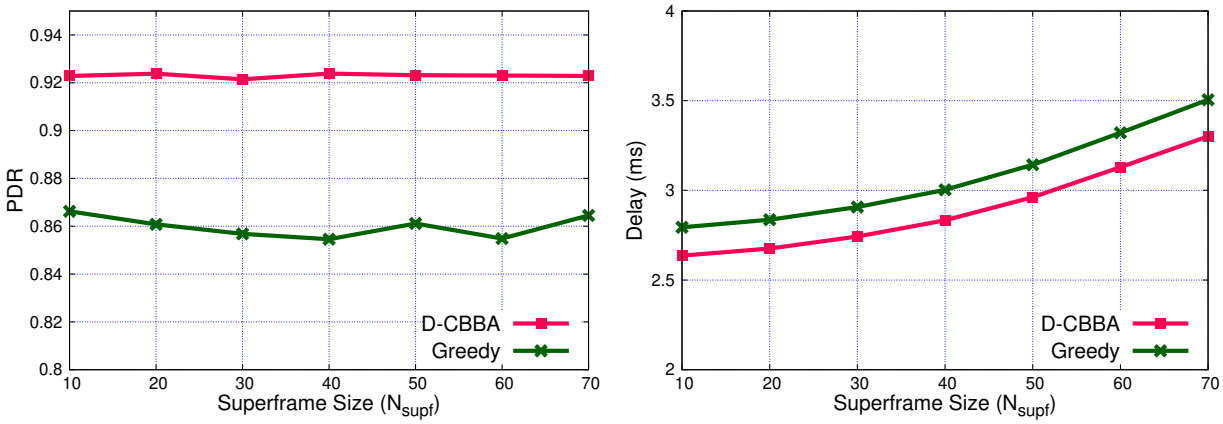

(a) PDR Variation

(b) Delay Variation

Figure 5.11: PDR and Delay varying with superframe size (N_{supf}).

the other schemes with a PDR value close to 0.8 with $N_g = 500$ and $N_{\text{subc}} = 3$. This is due to the lack of coordination among the UAVs that select the RBs in a pure random basis. Differently, both CBBA and the D-CBBA schemes introduce coordination among the UAVs; in particular, the D-CBBA self-adapts to the network requests, thus it reserves only the resources needed at each superframe. We can notice that D-CBBA performs similar to the centralized solution, where the transmissions are coordinated by the central BS. The choice of the score function c_{ij} (Equation 5.14) has a fundamental impact on the performance of CBBA algorithms. In this case, UAVs that are close to each other are able to avoid the selection of the same TBs for the transmission. However, when the network becomes crowded, due to the increasing traffic load or the small number of available channels, the CBBA algorithm is able to avoid interference between close UAVs, hence reducing the impact on the SINR on the receiver UAVs. Furthermore, the dynamic choice of the L_t^i value in the D-CBBA algorithm allows a more adaptive scheme, where the UAVs reserve only the exact amount of resources needed.

Figure 5.10a confirms the analysis described so far. Indeed, the Figure shows the number of simultaneous transmissions and hence it reflects the ability of the algorithms in avoiding potential concurrent access to the shared resources. The D-CBBA algorithm is able to successfully complete more than 75% of data transmissions without generating interference, while the Greedy algorithm can barely reach 60%. Fig. 5.10b evaluates the convergence time of the D-CBBA algorithm. The system reaches a steady state nearly at 12 *sec* where the PDR stabilizes to a value around 0.94. The algorithm, in fact, exchanges control messages every T_{beacon} seconds in order to reach the consensus on the data transmission scheduling decisions. On the contrary, the Greedy algorithm does not exchange messages and behaves in the same manner for the entire duration of the simulation.

Finally, Figures 5.11a and 5.11b investigate the impact of the superframe size N_{supf} on the PDR and end-to-end delay. The two algorithms behaves similarly, with an increasing trend of the end-to-end delay. Indeed, for larger superframe size, there may be unused TBs which introduce additional delays in the packet transmission. On the other side, the PDR is not affected by the variation of the superframe size. Again, we can appreciate the ability of the D-CBBA algorithm to adapt to the network conditions when choosing the number of requested tasks, i.e. the number of transmissions inside each superframe. Such value depends, indeed, on the estimated number of packets that should be sent during the next superframe, and therefore, the scheme adapts to

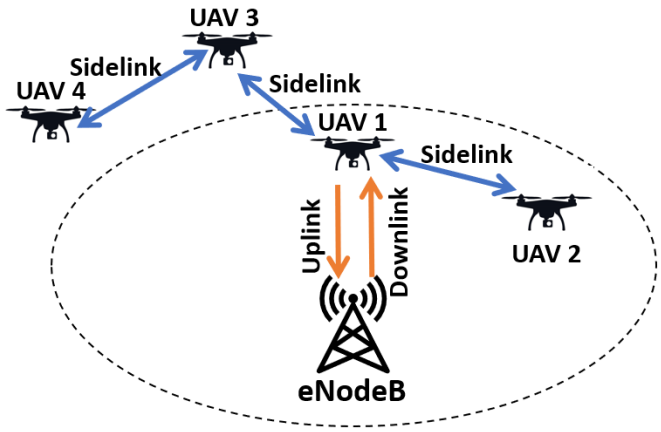

Figure 5.12: "Sidelink" in a multi-hop fashion to enhance coverage

its size.

5.6 Multi-hop U2U Packet Routing

As the coverage of cellular infrastructure is finite, during any mission, swarm of UAVs tend to fly beyond the cellular coverage that results in signal degradation. This results in UAVs being unable to transmit back essential information to the central base station (BS). However, multi-hop links connecting a UAV to another UAV extend the connectivity and coverage of network infrastructure. In the multi-hop pattern, some UAVs act as relaying nodes to transmit messages to the next UAV. Such type of multi-hop connectivity is demonstrated in Fig. 5.12 employing sidelink interface. UAV4 can send necessary information to the central BS (i.e., eNodeB) by forming a multi-hop link through UAV3 and UAV1. Once the information has reached to UAV1, cellular Uu radio interface is used to transmit the data to eNodeB via uplink. Similarly, needful timing synchronizations can be propagated from eNodeB to UAV1 in the downlink, which, in turn, propagates to UAV3 and UAV3 propagates to UAV4. "Sidelink" is a promising candidate in D2D paradigm that enables direct communication between two devices with or without the involvement of cellular infrastructure. Using sidelink, the communication range can be extended beyond the cellular coverage where in-coverage devices can act as communication anchors for other far-away devices. Sidelink Mode-4 can be used to take care of such out-of-coverage scenario where all the UAVs involved in the mission are not within cellular coverage.

Sidelink transmission and reception for existing vehicular communication (C-V2X) has two modes of resource allocation. (i) Mode-3 (Network-assisted), in which the network infrastructure (eNodeB) takes charge of distributing and allocating channel resources for the devices. This mode is preferred when the communicating devices are in-coverage. (ii) Mode-4 (Autonomous), in which the devices autonomously select the channel resources, not requiring any intervention from the infrastructure. This mode is preferred when the two communicating devices are out-of-coverage region. Another important novelty in Mode-4 is the introduction of a distributed, sensing-based semi persistent scheduling (SB-SPS) protocol, which is used by the vehicles in V2X to autonomously select their radio resources for transmission in the absence of cellular coverage [211].

Existing works

Sidelink is being actively studied for Cellular Vehicle-to-Everything (C-V2X) and maritime communication platforms including Vehicle-to-Vehicle (V2V) platooning, remote and automated driving [192, 193]. Sidelink is currently extensively investigated in vehicular communication domain for V2V communication in 5G where this communication link is exploited to transfer safety-critical or periodic content awareness messages to avoid collisions with pedestrian users or other vehicles. However, for aerial flying platforms, the performance evaluation of sidelink-assisted UAV-to-UAV communication in a UAV swarm are still lacking.

In [191, 212], the authors presented sidelink scheduling to minimize the resource selection collisions and its trade-off with different scheduling parameters, such as resource reservation interval and resource selection window. Similarly, in [213], the authors studied a mutual beneficial resource allocation for both vehicular and cellular users maximizing the sum-rate and fairness for cellular users. In [214], the authors modified the classical sensing-based scheduling algorithm to cope with non-periodic traffic from latency-sensitive applications. In their proposal, they showed improved performance with respect to decreased packet collisions. However, none of above works consider multi-hop for relaying the information. This condition is vital for aerial flying platforms (*i.e.,* drones) which tend to fly beyond the coverage range of the base station during mission.

Existing works on multi-hop D2D data relaying are primarily focused on the terrestrial users or vehicles. In [215], the authors proposed a multi-hop network model to extend the limited cellular connectivity to far-away users in public-safety scenarios. The authors in [216] studied the interference and outage performance analysis in order to intelligently allocate the radio resources to maximize the user's coverage and throughput. Above works do not address the unique characteristics of UAV networks and coverage situations. In this section, we aim to use multi-hop connectivity to extend the communication coverage for far-away flying UAVs using cellular sidelink interface.

Section 5.6.1 elaborates the sidelink channel structure and semi-persistent scheduling mechanism. Then, Section 5.6.2 describes application of AODV routing within UAV swarm. The performance analysis of U2U routing over multi-hop links is presented in Section 5.6.3.

5.6.1 Channel Resource Structure & Scheduling

Sidelink uses the single carrier frequency division multiple access (SC-FDMA) scheme, where the time-frequency orthogonal resource blocks are organized. Each channel resource is divided into subframes of 1 ms interval in time domain and a set of sub-channels in the frequency domain. A sub-channel is a group of one or more resource blocks (RBs) in the same subframe. A resource block is 180 KHz (12 sub-carriers of 15 KHz each) wide in frequency domain. The sub-channels are used to carry both data and control information. Usually, the data is transmitted in transport blocks (TBs), where one TB contains the full packet to be transmitted. A device willing to transmit the TB must also transmit the associated sidelink control information (SCI) message that occupies 2 RBs. The SCI is vital for the receiving device in order to correctly decode the transmitted TB and hence, must be positioned prior to the TB. Hence, a sub-channel consists of an SCI (control) followed by a TB (data) part.

Mode-4 Sensing-based Semi Persistent Scheduling (SPS)

Sensing-based SPS (SB-SPS) is a distributed scheduling protocol by 3GPP that enables the devices to autonomously select radio resources for sidelink transmission without relying on the

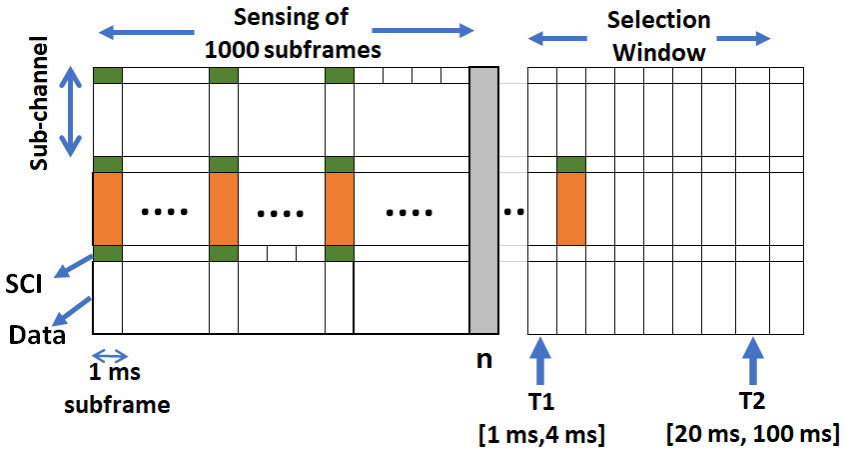

Figure 5.13: Mode-4 Sensing-based Semi Persistent Scheduling

infrastructure assistance [211]. The device selects the resources for a random number of consecutive packet transmissions. Two parameters are predefined for the autonomous resource selection using sidelink transmissions: (a) resource reservation interval (RRI) and (b) re-selection counter (SL_{ctr}). The RRI depends on the number of packets transmitted per second. For example, assuming 10 packets generated by the application, the RRI would be 1 second/10 = 100 ms. For a given value of RRI, the value of SL_{ctr} is determined as per Table. 5.6.

Resource Reservation Interval	Re-selection Counter
100 ms	[5, 15]
50 ms	[10, 30]
20 ms	[25, 75]

Table 5.6: RRI and corresponding SL_{ctr} values

For example, for RRI = 100 ms, then the SL_{ctr} can take any value between 5 and 15. Assuming the SL_{ctr} value is chosen as 8, the packets would then be transmitted at x, $x+1*RRI$, $x + 2 * RRI$, $x + 3 * RRI$ upto $x + 7 * RRI$ where x is the subframe where the transmission began. Fig. 5.13 illustrates the main principles of SB-SPS scheme, which are the following:

1. Assume a packet arrives at subframe "n" and has to be transmitted by maximum latency $T2$ where $T2 \in [20ms, ...100ms]$. As a subframe spans for 1 ms, it is equivalent to say that the packet has to be sent within $T2$ ms. Assuming $T1$ subframes ($T1 \leq 4$) for packet processing, the device has to effectively select a sub-channel within $[n + T1, n + T2]$ time period. This interval $[T1, T2]$ is called "selection window".

2. Now, suppose a sub-channel in subframe N is selected for transmission. Then, the later transmissions would occur in subframe $N + 1 * RRI$, $N + 2 * RRI$, $N + 3 * RRI$ upto $N + (SL_{ctr} - 1) * RRI$ where SL_{ctr} value is randomly chosen as per Table 1 for a given RRI. The SL_{ctr} value behaves like a counter that is decremented after each transmission. The procedure to select a specific subframe and subchannel is explained in the following:

   (a) The device keeps monitoring/sensing the sidelink received signal strength indicator (S-RSSI) for past $S_{\text{win}} = 1000$ subframes (1 second). This sensing information is used to select the resources for transmissions within the selection window $[T1, T2]$.

However, the resources that are occupied with other device transmission are excluded, i.e.: sub-channels in which the device senses a defined signal threshold of S_{th}.

(b) In case the number of available sub-channels is below 20% of the total sub-channels within $T1$ and $T2$, this step is repeated again, after further increasing S_{th} by 3 dB. We keep increasing S_{th} by 3 dB until 20% sub-channel availability criteria is fulfilled.

(c) Once 20% of sub-channel resources are identified, the MAC layer randomly chooses a candidate sub-channel in a subframe for first transmission. This is the N, which we pointed out in step 2.

3. Once SL_{ctr} reaches 0, a new resource allocation is performed with probability $1^{\vee}p_{RK}$, where p_{RK} is known as the resource keep probability. This probability value is chosen in the range of $[0, 0.8]$.

5.6.2 Routing protocols for Sidelink-based multi-hop networks

The scenario described in previous section in order to extend the cellular connectivity service envisages the use of multi-hop communication among the UAVs in the swarm. However, the standard sidelink implementation and its distributed channel access method, the SB-SPS, do not include any routing mechanisms for multi-hop data transmissions. The routing protocol is the specific module in the communication stack that is in charge of finding the multi-hop routes for the data packets in order to reach correctly from the source to destination node.

Multiple routing protocols can be found in literature for the specific case of Flying Ad-Hoc Networks (FANETs). FANETs are characterized by an infrastructure-less scenario, where the flying nodes need to cooperate with each other in order to reach to a mutual agreement determining the best packet routes for the multi-hop communications. Different routing protocols have been proposed for FANETs and they can be broadly classified into two classes: proactive and reactive.

The proactive ones, like Optimized Link State Routing (OLSR) or Destination-Sequenced Distance Vector (DSDV), use periodic broadcast messages that are injected in the network to constantly keep the routing table updated. In this way, whenever a packet needs to be routed from a source to its destination, the routing path is already calculated, and therefore the data packet can be directly send over the network. On the contrary, the reactive routing protocols, such as Dynamic Source Routing (DSR) or Ad-Hoc On-Demand Distance Vector (AODV), calculate the routing path only when it is requested. Hence, there are no periodic control messages sent in the network, and they are used only when needed. However, this kind of protocols has the drawback that the route discovery can delay the data transmission, due to the time needed for the route discovery process. Moreover, hybrid solutions have been proposed in literature to include the positive aspects of both proactive and reactive methods.

Owing to highly dynamic swarm network topology, the most promising method for the UAV swarms is represented by the routing protocols that belong to the "reactive" class, as they possess the capability to cope with the frequent route changes. In this work, we study and analyze the behavior of the AODV routing protocol over the sidelink U2U communications. However, we want to stress the fact that our main contribution is represented by the adaption of the sidelink mechanism for FANET, which is independent from the routing protocol used.

The AODV routing scheme has a reactive behavior on the route discovery. AODV uses a broadcast route discovery mechanism where the path discovery process is initiated when a source node needs to send data packets to a destination node, and it has no routing information in its routing table. Thus, the source node broadcasts to the network a route request control message,

called AODV-RREQ that is flooded into the network in order to reach the destination node. During the route discovery process, each intermediate node that receives the AODV-RREQ control packet, uses the control message to save the new route towards the source node. Once the AODV-RREQ reaches the destination node, the new route is established and every node in the traversal path knows how to reach the source node. At this point the destination node can send a route reply control message, called AODV-RREP, to inform the source node that the path has been established. This control message is no more flooded into the network, but it follows a direct path toward the source node.

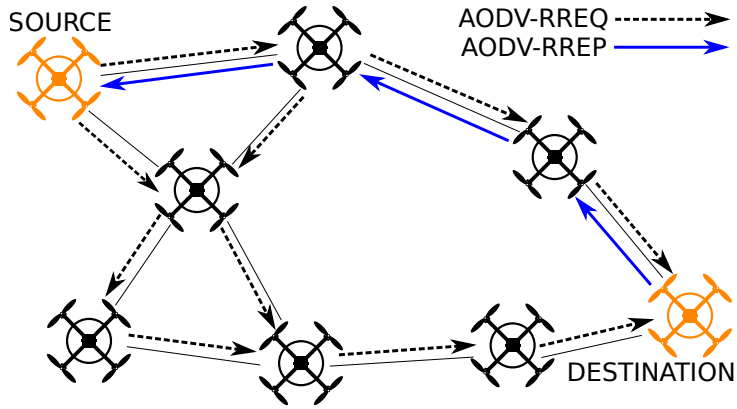

Figure 5.14: The AODV route discovery. SOURCE starts a route discovery for DESTINATION. The AODV-RREQ message reaches all the nodes, while the AODV-RREP follows a direct path.

A graphical example of the route discovery process is demonstrated in Figure 5.14. After the route discovery, the data packets can travel through the network using the “found" path. Route maintenance is needed to keep only the active routes. In this case, whenever a node loses connectivity to its next hop, the node invalidates its route by sending an AODV-RERR control message to all nodes that potentially received its AODV-RREP. More details about the AODV protocol and route maintenance can be found in [217].

5.6.3 Sidelink Evaluation with AODV routing

Our experimental platform is based on OMNeT++ simulator tool[5] that supports OpenCV2X[6] Mode-4 framework [218]. OpenCV2X is an open-source, 3GPP Release-14 compliant, C-V2X implementation with Mode-4 support. In order to include the routing protocol, we merged it with the INET framework[7] that contains, among the others, the implementation of the AODV routing protocol. In order to study and evaluate different realistic network deployment layouts, we conducted the experiments for three different scenarios, which are shown in Fig. 5.15: (i) Chain layout, (ii) Grid layout, and (iii) Dynamic Ad-hoc layout.

We consider the Packet Delivery Ratio (PDR) as the key performance metric in order to analyze the ability of the SB-SPS distributed scheduling algorithm to support the multi-hop communication for cooperative UAV swarm. The PDR is defined as the ratio of data packets that are actually received to those that were originally sent by the sender. Table 5.7 summarizes the simulation parameters used for the experimental study. In the following subsections, we highlight each deployment scenario considered for the experimental assessment.

[5]https://omnetpp.org/
[6]http://www.cs.ucc.ie/cv2x/
[7]https://inet.omnetpp.org/

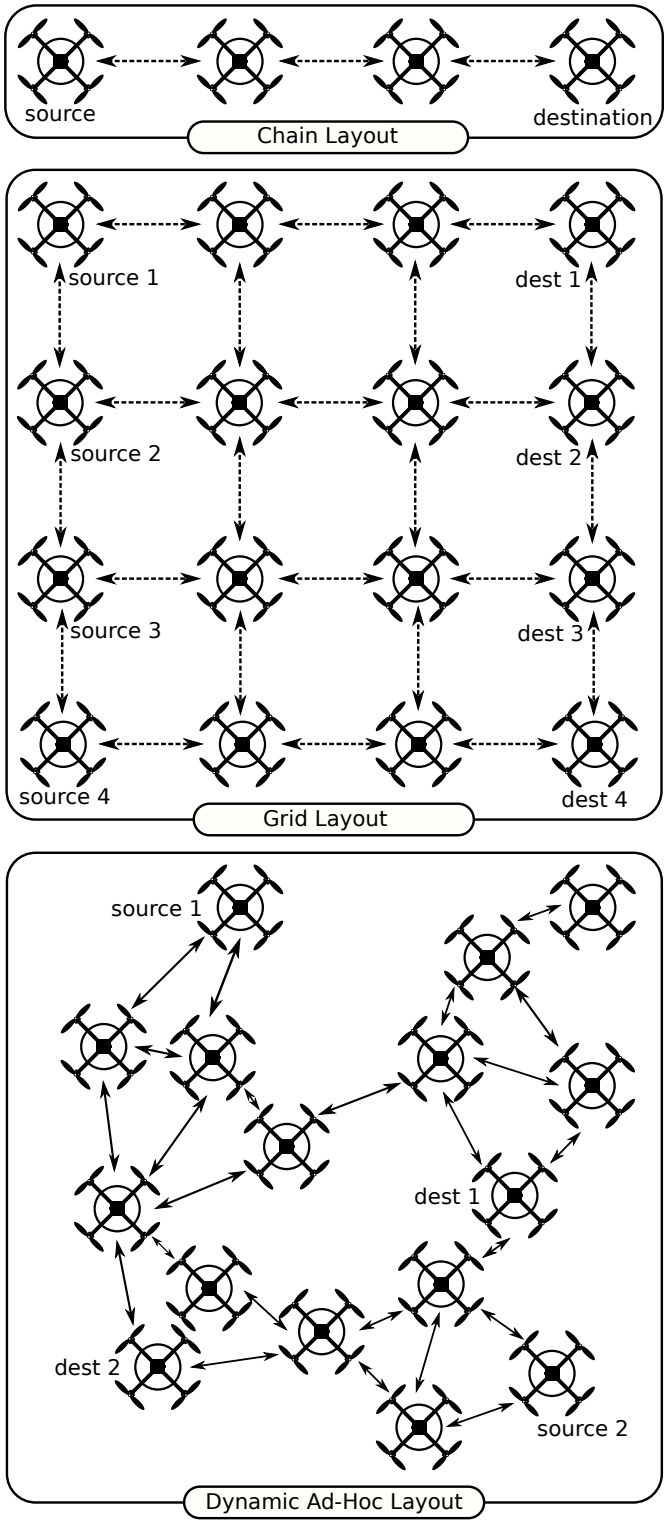

Figure 5.15: The sets of experimental scenarios used for evaluation.

Chain Layout

This first scenario demonstrates a simple chain layout in which a variable number of UAVs $u_1, u_2, \ldots u_{N_U}$ are placed at fixed positions in a chain topology. Each UAV is at a distance of

Table 5.7: Simulation Parameters

Parameter Name	**Value**
Number of UAVs (N_U)	20
Number of fixed UAVs (N_F)	9
Distance between static UAVs (d_{U2U})	1 km
Transmission Frequency (f_{tx})	10 pps
Resource Reservation Interval (RRI)	100 ms
Resource Keep Probability (p_{RK})	0.5
Sensing Window (S_{win})	1000 ms
Number of Sub-channels	3
Sub-channel Size	16
Transmission Power	23 dBm
UAV Speed	10-20 m/s

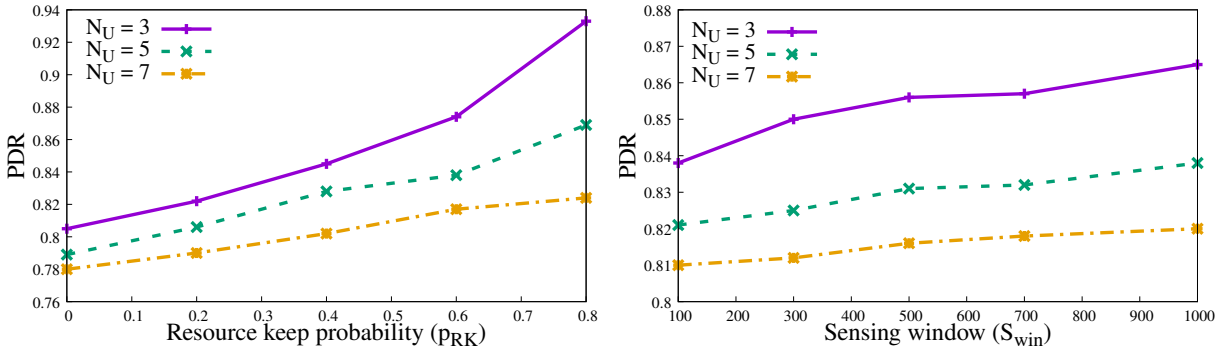

(a) (b)

Figure 5.16: Chain Scenario - PDR index (a) by varying p_{RK}, (b) by varying S_{win}.

d_{U2U} from its neighbors. There is only one data flow from UAV u_1 to UAV u_{N_U}. This static placement is intended to make sure that the data packets transmitted by UAV u_i is received only by u_{i-1} and UAV u_{i+1}. Here, the UAV u_1 transmits with a frequency of f_{tx} packets per second (pps) and the packets pass through all the chained nodes to reach the destination UAV u_{N_U}.

In this scenario, we analyze the effect of the resource keep probability (p_{RK}), and the length of the chain (u_{N_U}) on the network performance, as shown in Fig. 5.16a. The length of the chain negatively impacts on the total PDR because the higher the number of hops traversed by the packets, the higher is the probability of the packet lost in the network. It is interesting to note the effect of the probability of resource keep p_{RK} on the multi-hop network model. The performance increases with increasing probability p_{RK}, reaching values close to 1 for small UAV chains. This is because of the static placement and configuration of the UAVs. In such layout, the SB-SPS algorithm is able to stabilize the channel resource scheduling scheme for the data transmission, and therefore avoids potential channel resource collisions during the data transmissions. Furthermore, we want to study the impact of the sensing window size on the performance of the system. The sensing window is used by the scheduler to understand which sub-channels are used less. Fig. 5.16b depicts the study of S_{win} parameter, where we observe that an increase of the sensing window enables the SP-SBS to perform better, due to a more

accurate sub-channel selection.

Grid Layout

In the previous chained layout, there was only one transmitting UAV, one receiving UAV and the other intermediate UAVs that act as relays for data transmission. In current scenario, we create different multi-hop transmission chains in order to see how the scheduler is able to perform in a noisier environment. Thus, we create a grid scenario with $N_U = M_U \times M_U$ UAVs, where M_U is the side of the square grid. Then, we generate M_U data flow, so that the packets in each data flow need to go through $(M_U - 1)$ hops. Figs. 5.17a and 5.17b present the results of this experiment. In Fig. 5.17a, we study the PDR trend varying with the probability of resource keep *i.e.,* p_{RK}. It is easy to notice the effects that a noisy environment has on the transmission performances. With only $N_U = 9$, the PDR drops dramatically around $PDR = 0.5$ and further drops to a value around $PDR = 0.2$ with $N_U = 25$. We recall here that, the AODV routing protocol activates the route discovery procedure only at the beginning of the experiment. This is because the grid topology remain fixed during time and the route discovery happens only once. Therefore, there is no overhead due to the AODV control messages and only data packets are present in the network. Similar to the chain scenario, we observe an improvement in the performance at high values of p_{RK}. Fig. 5.17b depicts the effect on the PDR in response to a varying sensing window size S_{win}. Also in this layout, having larger sensing window, permits the distributed scheduler to gain a better understanding of the sub-channels occupation.

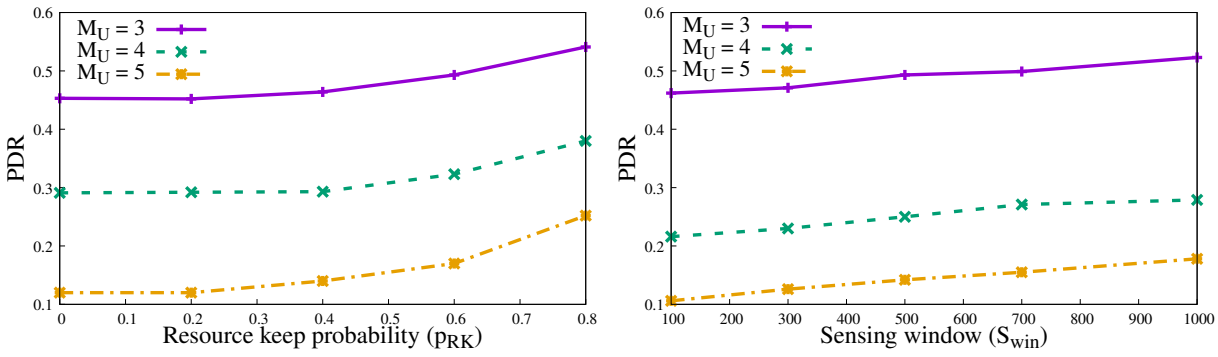

(a) (b)

Figure 5.17: Grid Scenario - PDR index (a) by varying p_{RK}, (b) by varying S_{win}.

Dynamic Ad-hoc Layout

In this scenario, we analyze the SP-SBS scheduling protocol on a UAV swarm that moves in a region of 5 $km \times 5$ km. In this experiment, the UAVs move with a *random waypoint* mobility pattern at fixed velocity between 10 and 20 meters per second. In order to ensure the swarm connectivity, we select $N_F \ll N_U$ UAVs and place them at fixed positions so that the whole scenario is covered. Specifying a mobility model that guarantees the connectivity inside the UAV swarm is out of scope of this work. We deploy $N_U = 20$ UAVs and generate 4 data flows between two UAVs randomly chosen inside the swarm. Fig. 5.18a shows the analysis of both p_{RK} and S_{win} parameters. Here, we can observe a difference with the static cases described earlier. Note that, the use of bigger sensing window S_{win} deteriorates the system performances. This

is due to the high mobility of the UAVs inside the swarm that makes the sensing information inside a long window outdated. On the contrary, the p_{RK} value still has a positive impact on the delivery ratio, as it helps in achieving a cooperative consensus for the use of the shared resources.

Lastly, Fig. 5.18b shows the performance of the swarm varying with transmission frequency f_{tx} and RRI interval. A different value of f_{tx} influences the three values of RRI to behave differently. For low values of f_{tx}, the $RRI = 100\ ms$ has superior performance due to low request of transmission from UAVs. For medium values of f_{tx}, the $RRI = 50\ ms$ became the best solution. Finally, $RRI = 20\ ms$ generates an optimal performance with high frequency of data transmission. It shows the importance of the reservation resource index in the network performance. It is evident that an adaptive selection of the RRI value is needed in dynamic multi-hop environments, in order to maximize the performance of the SB-SPS algorithm.

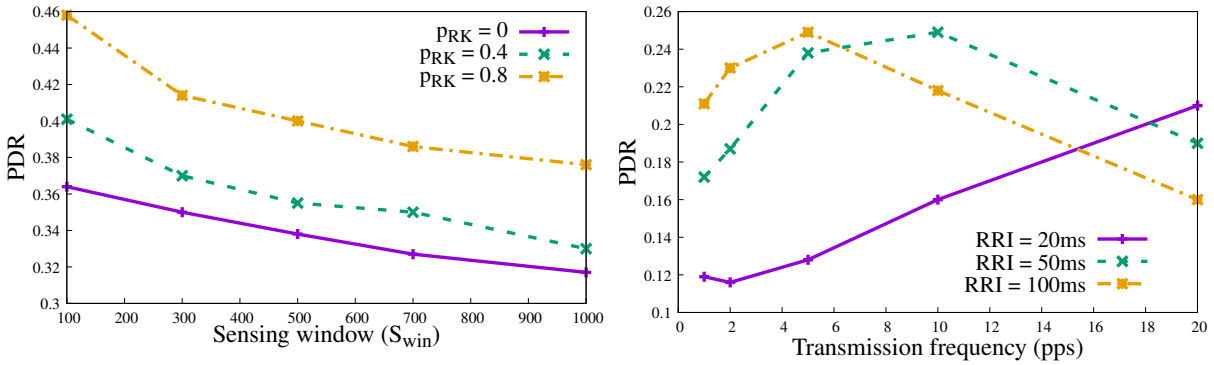

(a) (b)

Figure 5.18: The evaluation of the UAV swarm scenario varying both p_{RK} and S_{win} is depicted in Figure 5.18a. The impact of the RRI parameter on the performance is shown in Figure 5.18b.

Remarks

UAV seamless connectivity and reliability is very important for aerial swarm networks during any mission. This chapter presented a potential candidate cellular technology "sidelink" for establishing efficient intra-swarm U2U communication for extending the connectivity for out-of-coverage UAVs during mission. A multi-hop network model is proposed that leverages mutual cooperation with neighbor UAVs to preserve ubiquitous coverage during mission. Three different sidelink-assisted multi-hop network deployments have been studied and performance benefits have been presented considering key scheduling parameters of sensing-based distributed scheduling algorithm. As part of future work, we aim to consider various data transmission models with periodic and non-periodic traffic, and evaluate the performance for aerial swarm network.

5.7 Conclusions

In this chapter, the problem of cooperative and communication-aware UAV positioning and channel scheduling is investigated in order to carry out the data transmission from a set of target points towards cellular BS. The range of UAV radios are finite and hence, they tend to fly beyond the BS coverage in a typical mission. Considering the limited coverage, we studied a cooperative, multi-hop sidelink-assisted design of C-U2X communication model that optimizes

the scheduling decisions of data transmission employing sidelink sub-channels. The model is validated using both centralized and distributed algorithms. The formulated problem is solved in centralized manner by mathematical optimization framework. A distributed auction-class of algorithms, D-CBBA is proposed to generate efficient sub-channel scheduling decision for maximizing data transmission from PoIs to central BS. Our experimental assessment demonstrates that the distributed algorithm potentially enhances the cellular infrastructure coverage via multi-hop communications over the 5G sidelink. Moreover, we presented a multi-hop network model is proposed that leverages mutual cooperation with neighbor UAVs to preserve ubiquitous coverage during mission. Three different sidelink-assisted multi-hop network deployments have been studied and performance benefits have been presented considering key scheduling parameters of sensing-based distributed scheduling algorithm.

Chapter 6

Hybrid Non-terrestrial Network: UAVs in 6G Era

6.1 Introduction

While the fifth generation (5G) mobile systems are being deployed all over the world, academia and industry are already focusing on the demands and constraints that novel futuristic use-cases will require from beyond 5G (6G) systems. Insistence for high data rates, low latency, massive connectivity, ultra-reliability, and high devices density are key requirements reinforcing novel services for virtual/augmented reality (VR/AR), autonomous cyber-physical systems, intelligent industrial automation, smart infrastructures, multi-sensory holographic teleportation, real-time remote healthcare, high-performance precision agriculture, reactive disaster management, and space connectivity [219, 220].

To cope with such strict requirements, the initial directions undertaken by communication practitioners can be summarized into four main research lines *i.e.*, (*i*) new ways of using the spectrum and, consequently, (*ii*) new paradigms of designing the radio, (*iii*) highly reconfigurable, intelligent and autonomous network architectures, and (*iv*) larger network connectivity areas, extended to near-Earth and deep-space. The mentioned research directions can be assembled into a novel mobile communication paradigm that will represent researchers' challenges for the next years: the 6G [221]. The real potential would be unleashed only by extending connectivity links to space network (*i.e.*, satellites, high-altitude platforms), thus generating an *integrated space-air-ground communication network*. Towards the fulfillment of this grand vision, the objective of this chapter is to explore the synergistic trends of UAVs within 6G systems, with a special focus on *(i)* global ubiquitous coverage, *(ii)* full-spectra usage, *(iii)* diverse applications and use-cases, and *(iv)* enabling technologies, as summarized in Figure 6.1.

The following sentence reminds the reader of the fundamental question (Q8 in Section 1.5) that this chapter attempts to raise and discuss potential answers to.

> **Q8.** How do we foresee current technological advances in UAVs and 5G translating to future 6G systems? Where do we find these technological enablers?

The need to reach a **global ubiquitous coverage** establishes the connectivity of the future via universal and seamless accessibility. Through inter-working of ground, air and space network segments, the convergence advantages from different segments can be exploited to sup-

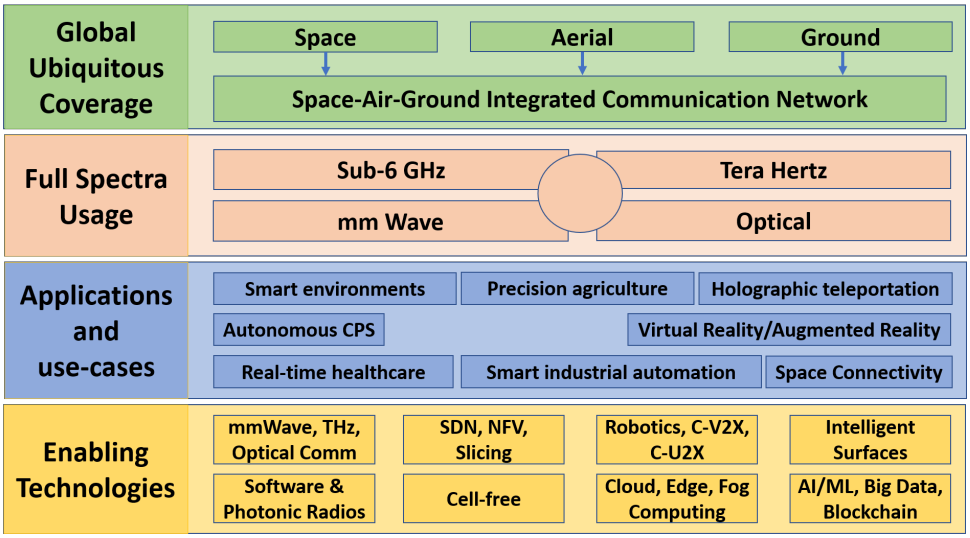

Figure 6.1: Synergy of UAV networking with 6G vision.

port multifarious UAV applications and services in an efficient and cost-effective manner. To this aim, 6G envisions **full spectra usage** through new spectrum-use methods with multi-band high-spread spectrum, as well as high frequency bands including Sub-6 GHz, Millimetre Wave (mmWave), Terahertz (THz), and even optical frequency band to allow high date rate transmission links. The aforementioned **diverse applications and use-cases** that would benefit from the introduction of UAVs into 6G systems have shifted the vertical industries towards data-driven dynamic and intelligent service models to offer "fully immersive experiences" and "anything or everything-as-a-service" paradigms.

Such innovative models and paradigms are then requiring novel **enabling technologies** that are developed with attractive potentials. The key drivers include Artificial Intelligence (AI) and Machine Learning (ML), Blockchain and big data technologies for information security, automatization, and network intelligence. Also, new technologies like those in mmWave, THz and optical frequency bands are expected to provide higher spectral efficiency, as well as cell-free communications to ensure seamless connectivity and handovers, and intelligent reflecting surfaces for proactive radio signal control. Furthermore, the need for softwarization and programmability of network service deployment has pushed advances in slicing, network function virtualization (NFV), software-defined networking (SDN) and cloud technologies. Finally, photonics radios are expected to offload the complex signal processing to photonics chip and spectrum mining, while Cellular Vehicle (UAV)-to-everything (C-V2X or C-U2X) paradigm is an enabler to connected robotics for intelligent device access and autonomous provisioning.

6.2 Integrated Space-Aerial-Ground Communication Network

The integration of heterogeneous networks, such as '5G with satellites' or '5G with UAVs', is already a part of the standardization process for 5G by 3GPP. Due to the enormous potential of UAVs, it is anticipated that they will soon become an essential technology enabler of the airspace. Global deployment of these UAVs is anticipated as the technology develops and the necessary rules are put in place. Their inherent mobility in three dimensional space and portability makes them useful in a wide variety of contexts, including package delivery, pollution control, farming,

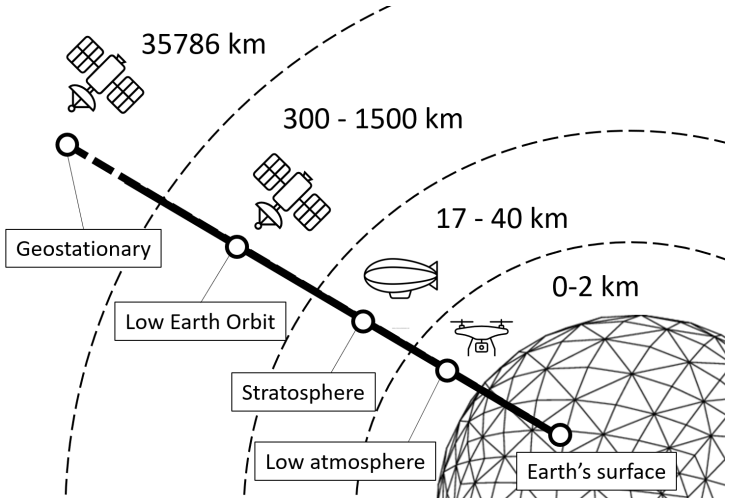

Figure 6.2: Platforms of Non-Terrestrial Networks: GEO, LEO, HAP, and UAV [223]

and search-and-rescue missions. 6G wireless systems envision to bring transformational changes to global ubiquitous coverage that establishes the connectivity of the future via universal and seamless accessibility for a variety of different Radio Access Technologies (also known as multi-RATs) [222]. There are continuing discussions to build and construct network architecture that combines cross-layer, high and low altitude platforms and space satellites into conventional cellular networks in order to inject more capacity and improve coverage for underserved regions in a cost-effective way [31]. Motivated by this necessity, this section details workable strategies for integrating space-air-ground networks and provides insight into studies that have embraced the multi-dimensional and inter-operational network, key to the 6G concept. This section describes the three different parts of the network and places special emphasis on the "aerial" segment as an enabling layer between the ground and the space, as seen in Figure 6.2.

The links that connect the ground (terrestrial) network with aerial ones make it possible to communicate ground-to-aerial (G2A) and aerial-to-ground (A2G), which complements the wireless broadband access provided by the ground infrastructure. This kind of cross-layer interworking is the most advanced approach in terms of the implementation of already existing solutions that have been standardized. 3GPP Rel-15 anticipates UAVs having the ability to handle high transmission rates (10 Gbps), tight latency (one millisecond round trip delay), user traffic offloading, and upgrades to radio access technologies. In addition, 3GPP Rel-17 outlines the requirements and key performance indicators (KPIs) for a variety of use cases including dependable and beyond visual line of sight (BVLoS) operations using UAVs.

Space Segment

Satellites and other means of long-distance communication fall under the "space" category. Satellite communication backbone (SATCOM) is centered on earth expanding to different orbital depths of the universe. Typical SATCOM backbone network consists of low earth orbiting (LEO), middle earth orbiting (MEO) and geosynchronous earth orbiting (GEO) satellites delivering data to the "ground" network segment. SATCOM allows satellites in various orbits to provide varying service quality. SATCOM connections are reliable and secure, with the added benefit of being able to reach every corner of the globe. However, significant barriers to entry in this market include high costs associated with infrastructure, long propagation distances, and

slow connections. Space-to-aerial (S2A) and aerial-to-space (A2S) transmission lines are an effective cross-layer inter-working method for transferring information from satellites to "aerial" and then to "ground" segment. LEO and GEO satellites, which operate at 2000 and 35000 km altitudes, respectively, are the two most often utilized systems for S2A/A2S communications, providing cost-effective and backhaul-aware transmissions to HAPs.

Aerial Segment

The aerial segment is a key layer in implementing the multi-dimensional and inter-operational network of 6G vision because to its capacity to efficiently bind the other two levels, which are separated by thousands of kilometers. In this market category, commercial multirotors, fixed-wing UAVs, balloons, and airships serve as high or low altitude platforms (HAPs or LAPs). HAPs work with decreased transmission latency, cheaper cost, simple mobility in emergency scenarios, and broad coverage with high elevation angles, in contrast to SATCOM. Existing works demonstrate the cooperation between SATCOM and HAP for robust beamforming or boosting communication confidentiality. LAPs serve as a connecting connection to ground devices in cases when HAPs are not desired owing to their expensive cost in common civilian applications (e.g., temporary hotspots, sporting events). The LAPs could then bridge the link to HAPs and then to the space segment, enabling end-to-end communication from the ground device to the space network.

The following points elaborate on certain elements of planned 6G communication for airborne RAN.

- **Aerial Internet:** UAVs deployed as aerial base station (UAV-BS) can extend Internet services to remote/rural areas and under-served regions of interest with poor or no connectivity.

- **Emergency and Temporary Network:** UAVs offer high capacity links for wireless coverage required for temporary events e.g., political rallies, sports event, exhibitions, hotspots, etc. Additionally, for cell-edge or resource constrained user, it provides extra capacity and fair communication services by optimally placing itself in a better serving position.

- **Aerial Backhaul:** UAVs can serve the backhaul demands arising from ground infrastructure and also extend to locations without any wired backhaul solutions. It decreases the cost of traditional fiber-like deployments.

- **Sensing:** UAVs can be used to harvest data from ground sensor devices. While such data collection is dependent on efficient placement before the data collection begins, an online optimization on UAV placement that copes with the dynamic environment by learning or discovering the uncertain environment during flight is much more promising. An optimal trajectory path that maximizes the metric associated with data collection accelerate the sensing performance.

- **Caching, Computing, Control (3C):** In latency-critical applications, UAVs with edge computing functionality can exploit closeness to the user and provide rapid deployment solution for content distribution applications. The practicality of deploying edge servers on satellites is limited due to cost, latency and hardware calibration. However, UAVs perform as the best candidate in such requirements, thus bringing content and computational resources close to the origin of requests (users).

6.3 Full-Spectra Candidate Technologies in 6G for UAVs

Candidate technologies such as mmWave or sub-6 GHz are widely studied, and their performance is already evaluated for 5G communication systems. While these technologies mark key advancements towards higher spectral efficiency, 6G wireless network necessitates further exploration of access networks and communication links to meet its multifarious vision. Specifically, we have envisioned massive MIMO, mmWave, THz, Sidelink, Free Space Optics (FSO), and Visible Light Communications (VLC) as the main technologies for 6G scenario. Following subsection summarizes each technology in terms of (*i*) main features, (*ii*) standardization progress, (*iii*) integration with UAVs, and (*iv*) main advantages and drawbacks.

6.3.1 Massive Multiple Input Multiple Output (MIMO)

Technology overview

Massive MIMO is a compelling sub-6 GHz physical layer wireless access technology and a key enabler of multi-antenna multi-user cellular communication possessing with three main features *i.e.*, (*i*) array gain that helps in coverage extension, (*ii*) spatial multiplexing serving many terminals in same resource block and (*iii*) supporting high mobility via time division duplex (TDD) and channel reciprocity. Moreover, for aerial and space LoS communication, massive MIMO performs well along with rich scattering. In urban environments, antenna array mounted on high-rise buildings provide ubiquitous coverage for UAVs.

Standardization progress

3GPP release 13 and 14 specifies a beam-based NR (new radio) air-interface in which 16 to 32 antenna elements are used as massive MIMO. Release 15 further enhances to 64+ antenna elements to support more complex and efficient processing for capacity extension.

Integration with UAVs

In case of cellular-connected drones controlled by a central base station, massive MIMO facilitates reliable A2G and G2A transmission links. Unlike ground UEs, drones move in 3D space, the flight dynamics tend to change to antenna polarization and gains with time, thus making the continuous connectivity very vulnerable. Furthermore, UAVs possess less multi-path propagation and hence, result in frequent polarization mismatch events. Massive MIMO is instrumental in solving issues pertaining to 3D UAV mobility by exploiting more antennas for robust signal processing [187].

Advantages and drawbacks

Massive MIMO offers high throughput communications for UAVs to quickly cover large geographical regions. The primary challenge in massive MIMO based deployment is the design of efficient MAC layer and interference management. Moreover, the antenna array geometry of the ground station, flying speed, and altitude of UAVs complicate the propagation environment, as well as the spectrum management for drones.

6.3.2 Millimetre Wave (mmWave)

Technology overview

The mmWave frequencies will play a key role in 6G vision because of the availability of high bandwidth (in $30-300$ GHz range) supporting high data rate (nearly 10 Gbps) aerial communication. Shorter mmWave wavelengths are also beneficial for UAV operation, resulting in smaller circuits and antennas. In terms of security and interference, mmWave frequencies are immune to channel disturbances because of highly directional beams and high resolutions that make the signal interception really hard.

Standardization progress

The standardization activities by IEEE and 3GPP for mmWave are still in their initial stages and 3GPP/IEEE compliant standardization proposals towards solving current challenges of mmWave are also missing. There have been some contributions by 3GPP RAN1 group with focus on the mmWave waveform designs and MIMO performance such as interference analysis in the range between $24.25-86$ GHz, cyclic-prefix (CP) types over 6 GHz etc.

Integration with UAVs

mmWave is considered as a preferred candidate for UAV-assisted cellular networks (*e.g.*, flying base stations, relays) than lower microwave frequencies because of notable coverage and capacity enhancements for ground users.

Advantages and drawbacks

The key advantages of mmWave-based communications are attributed to availability of higher channel bandwidth that translates to higher data rates, smaller wavelength that encodes more information in less time, presence of narrow beams that are preferred for secure and sensitive message transmission with better interference control schemes. Despite of several advantages, primary challenges for mmWave frequencies are related to beam misalignment, high path loss and atmospheric attenuation. Moreover, harsh weather conditions (*i.e.*, rain, absorption by water vapors, oxygen) degrade the mmWave channel.

6.3.3 Terahertz (THz)

Technology overview

6G requires specific applications to handle large amount of data as well as very high throughput per devices (Gbps to Tbps), and per area efficiency (bps/km^2). In this context, THz technology is envisioned to surpass the gap between the mmWave and optical communications band.

Standardization progress

In 2017, IEEE 802.15.3d-2017 is published as the first wireless communication standard operating at carrier frequencies around 300 GHz [224]. It focuses on fixed point-to-point links, and refers to applications as intra-device communication, kiosk downloading, complementary links in data centers and backhaul/fronthaul links. Furthermore, at IEEE 802.15, the THz Interest Group is actively working towards identification of further additional applications, which would require a

further amendment of the current standard. In terms of spectrum for THz communications the radio regulations allow the use of spectrum beyond 275 GHz.

Integration with UAVs

At higher altitudes above 16 kilometers, the impact of environmental moisture is not significant and therefore, THz is mainly envisioned HAPs. Furthermore, THz is a suitable alternative for environments with high UAV mobility. High mobility UAVs are less affected by Doppler effect in a high carrier frequency setting like THz. THz communications can establish high-speed communication links through the selection of the optimal beam pattern. THz MIMO-OFDM system between two UAVs can be used to estimate the UAV position and orientation. As a result, millimeter-level positioning accuracy has been shown to be reachable if the transmitter-receiver separation is sufficiently small. UAVs also need short-distance secure links to receive instructions or transmit data before dispersing to fulfill their remote controlled or autonomous missions. Extremely narrow beams (pencil-beam directionality) reduce the probability of eavesdropping. In this context, the large channel bandwidth of THz allows for specific protection measures against various attacks like jamming. THz links could be also utilized between UAVs and airplanes, and for HAPS acting as a relay node in the sky linking ground station and airplane.

Advantages and drawbacks

THz-band offers many benefits as described in previous subsection and represents a promising solution to current spectrum crunch. However, THz channels in outdoor environment experience significant loss due to molecular absorption and weather conditions. Interestingly, concentration of the water vapor molecules decreases at higher altitudes (e.g., HAPs) enabling the communication over the THz-band to be more feasible as compared to ground network.

6.3.4 Sidelink (Device-to-Device or D2D)

Technology overview

3GPP release 12 started its normative efforts in development of a new feature, "sidelink" to enable direct transmission between two devices bypassing the base station infrastructure. It is continued in the subsequent 3GPP releases as "proximity services (ProSe)". Emerging applications of sidelink proximity services include public safety, vehicle-to-vehicle (V2V) communications, content offloading and distribution etc. Empowered by sensing-based semi-persistent scheduling (SB-SPS) and use of dedicated licensed physical channels for sidelink transmission, it is envisioned as a strong candidate to perform V2V or U2U communication.

Standardization progress

3GPP's enhancements for vehicle-to-everything (V2X) communication (a.k.a. eV2X) using sidelink [225] focus on four areas: (*i*) vehicle platooning, (*ii*) advanced driving, (*iii*) extended sensors, and (*iv*) remote driving. eV2X supports mutual information exchange within the vehicle platoon; this concept greatly contemplates aerial swarm control and communication. Advanced driving leverages the freedom of inter-vehicle signaling to coordinate cooperative, safe vehicle movements. The extended sensors allow transfer of data between roadside units or camera video improving the perception of the driving environment. Remote driving allows control of the vehicle remotely especially matching dangerous mission scenarios when people cannot drive by themselves. IEEE

also has a similar standardization initiative in the name of "Dedicated Short Range Communications" (DSRC) using 802.11p assisting inter-device communication [226].

Integration with UAVs

Sidelink is envisioned to operate in A2A network segment wherein the devices in proximity can establish peer-to-peer transmission links for control and data exchange. Periodic information such as location updates, flight states can efficiently be shared within the UAV swarm for optimal mission-aware decision making and collision avoidance [227]. Hence, U2U communication offer high integration synergies with cellular sidelink feature.

Advantages and drawbacks

Application of sidelink to support A2A communication is significantly different from existing solutions for V2X communications. The primary challenge is due to the signal propagation environment, as well as the mobility. UAVs fly in 3D space with varying altitudes and the propagation medium suffers from additional attenuation and distortion effects. Secondly, UAVs are battery-constrained unlike terrestrial vehicles. Proper energy-aware path planning is essential for aerial missions encompassing UAVs.

6.3.5 Free Space Optical (FSO)

FSO and Visible Light Communication (VLC) are the two main candidates of optical wireless communications (OWC). FSO mainly refers to the use of outdoor/space laser links at the infrared band, while VLC relies on the use of light emitting diodes (LEDs) at the visible band mostly in indoor environments. VLC will be discussed in Section 6.3.6.

Technology overview

FSO communications have been proposed as a promising technique to overcome the radio frequency (RF) drawbacks by providing high-speed transmissions in unregulated bands. License free spectrum, immunity to electromagnetic interference and inherent security are some notable advantages of FSO compared to conventional RF-based systems. FSO can efficiently establish high data rate point-to-point communication links, which can offer high bandwidth and ease the deployment efforts.

Standardization progress

Standardization efforts on OWC are still ongoing. At the international level, there are several large-scale projects on OWC technologies, such as (*i*) USA – LESA, UC-LIGHT, NASA-LCRD and COWA, (*ii*) Japan – VLCA and NICT space communication SOCRATES mission, and (*iii*) China - R&D for key VLC technologies. The on-going VLC standardization efforts at IEEE and ITU (*e.g.* IEEE P802.15.13 and P802.11bb, and ITU-T G.vlc) further involve a number of international companies such as Intel, Huawei, LG, Cisco, Broadcom, and Nokia.

Integration with UAVs

The adoption of FSO for high data rate G2A and A2A links for airborne vehicles has recently attracted a great deal of attention *e.g.,* "Airborne Internet", relays. Besides A2A, FSO is seen to be useful for extending communication to space/ground networks [228]. In addition to the

need for efficient pointing, acquisition and tracking solutions, a better understanding of optical propagation is required for G2A links.

Advantages and drawbacks

FSO-based UAV communication is adversely impacted by weather interference and high UAV mobility. Harsh weather conditions lead to the signal loss and reduction of effective data rate. Besides atmospheric turbulence-induced fading, U2U links employing FSO are negatively affected by pointing error due to the position deviations of tall buildings. Distance longer than few kilometers affects FSO link reliability when incident beam is not always orthogonal in FSO-based UAV systems. To overcome such limitations, technical solutions attempt to mitigate the geometric and misalignment losses, considering the non-orthogonality of the laser beam and the random fluctuations of the position and orientation of the UAV. Finally, hybrid solutions based on the use of both RF and FSO are largely adopted for UAVs [229].

6.3.6 Visible Light Communication (VLC)

Technology overview

VLC has gained great interest in the last years, mainly due to the development of LEDs, as well as to its "green" feature. VLC mainly consists in the two-fold paradigm of both illumination and data communication, simultaneously by the same physical carrier. The fundamental components are: the transmitter (*e.g.* LED, camera), receiver (*e.g.* photodetector, camera) and the VLC channel. Besides LED, different light sources can be considered for transmitter. LED is an incoherent source, namely photons are emitted spontaneously with different uncorrelated phases. Photodetector as receivers in a VLC system, absorb the photons impinging on its frontend surface and generate an electrical signal. Channel modeling in VLC plays a crucial role for realizing effective, robust yet low complex systems. The easiest and most cost-effective modulation is based on Intensity Modulation/Direct Detection (IM/DD), which is not concerned by frequency and phase of the signal.

Standardization progress

Like FSO, the standardization progress related to VLC is still ongoing. The first standard for optical communication is IrDA, elaborated first time in 1993 for short range communication, but undergone several enhancements since then. In 2009, IEEE proposed the first standard for VLC *i.e.,* 802.15.7. The next versions of this standard include infra-red, ultraviolet, and optical camera communications (OCC). In 2018, a new working group for VLC, namely the IEEE 802.11bb, started activities for integrating the Li-Fi (Light-Fidelity) in order to make this technology interoperable with the Wi-Fi standard IEEE 802.11. This standard mainly focuses on MAC layer. Also, the IEEE 802.15.3 working group is considering OWC for wavelengths comprised between $10\mu m$ and $190nm$ with a bit rate of multi-Gbps. ITU is working on a standard for indoor optic communication, *i.e.*, the ITU-G99991.

Integration with UAVs

As demonstrated by the intense standardization activities, there have been significant advances on efficient physical layer design. One of the first contributions towards positioning the use of VLC for UAV is DroneVLC [230], where the VLC has been proposed as effective and robust

Table 6.1: Technology highlights assisting UAV networking in 6G vision.

Candidate Technology	Network Segment	Standardization Trends	Applications	Synergy between 6G and UAVs
Massive MIMO	Ground, G2A	Rel-13 & 14: beam-based NR with 16-32 antenna elements, Rel-15: 64+ antenna elements	Robust Surveillance & Centralized Info. dissemination	Enabler of Cellular-connected UAV swarm in 6G
mmWave	Ground, G2A, A2A	-	Flying Base stations, Relays	High throughput links for UAV-assisted cellular communication
Terahertz	Ground, G2A, A2A	IEEE 802.15.3d: 100G Wireless	Information Showers, Security-sensitive communications, Data center networking	HAPs and Space-to-Aerial data links, Short distance secure U2U links
Sidelink	Ground, A2A	Rel-12: D2D, Rel-13: UE-to-Network Relay, Rel-14: V2X, Rel-15: eV2X, IEEE 802.11p [226]	ProSe, V2X, Relay UE, C-U2X	Key enabler of U2U links in 6G
Free Space Optical	Ground, G2A, A2A, A2G	IEEE P802.15.13, P802.11bb, ITU-T G.vlc	Direct U2U communications, links from UAV to space or terrestrial networks	High data rate links between a ground station and UAVs, long distance end-to-end connections
Visible Light	Ground, A2A	JEITA CP-1221 (VLC system), and JEITA CP-1222, (VL ID system), ITU G.9991 IEEE 802.15.7	Indoor Localization, Indoor Communication, V2X	High synergy for U2U links in 6G

communication technology among UAVs. However, many challenges still remain to be addressed for enabling VLC-based UAV networking, such as the need of LoS and occlusion robustness.

Advantages and Drawbacks

VLC exploits a portion of spectrum not used by other technologies. VLC is considered most effective in the absence of obstacles. The most important challenge while employing VLC for UAV communication is represented by a deep analysis of the specific characteristics of the channel and a precise channel modeling. Currently, VLC has been mostly applied for indoor applications. The presence of environmental source of interference (*e.g.,* sunlight), if not properly addressed, could prevent effective working of such a kind of technology. Moreover, it has been demonstrated that VLC is not completely immune to RF interference [231] and it needs to be carefully implemented in real environments (via realistic measurements) in order to exploit all its potential.

All the technologies previously described are characterized with different features such as communication range, network topology, latency, data rates, mobility, etc. Each feature distinguishes different technologies according to their suitability for UAV communications and based on the specific type of mission/application they are devoted. Table 6.1 summarizes the candidate wireless technologies, by distinguishing where they can be applied with respect to the integrated space-air-ground communication network, and which applications they are reserved to. Also, in Table 6.1 we have collected the advances in the standardization progress, as well as the benefits carried out for UAV networking in 6G scenarios.

6.4 Socio-economic Concerns

UAVs can pose serious risks in terms of socio-economic operational capabilities. Therefore, utmost care must be taken by the policy makers and legislation in order to integrate UAVs into national and international aviation systems. To this end, in this section, we outline the perspectives of regulatory activities, market and social challenges, which the UAV service providers and cellular operators must take into consideration before successfully roll-out use cases pertaining to UAV cellular applications.

6.4.1 Regulatory Concerns

Ubiquitous accessibility and rapid emergence of UAV technology mandate development of regulatory frameworks for harmonious operation of UAVs in the national and international airspace. Although, each country has a specific set of internal rules for UAV operation, few global bodies tend to harmonize their operation across international airspace. The regulatory framework mainly target around three key aspects [232]:

- To regulate and control the use of unmanned aircraft in the airspace to prevent danger to manned aircraft;
- To ensure proper operational limitations to the flight;
- To manage and control the administrative privileges such as pilot licenses, flight authorizations and data handling techniques.

In European Union (EU), European Commission and European Aviation Safety Agency (EASA) are primarily involved for regulating UAVs. EASA in December, 2020 categorized UAV into (a) low risk (open), (b) medium risk (specific) and (c) high risk (certified) that are defined based on type of goods carried on them, size, weight. Another EU regulation 2018/1139 Section VII on "unmanned aircraft" discusses the importance of "public security or protection of privacy and personal data" [233]. Article 132 of Regulation 2018/1139 includes a privacy protection provision that relates to the implementation of the General Data Protection Regulation (GDPR) Regulation (EU) 2016/679 and Regulation (EC) No 45/2001 (repealed by Regulation (EU) 2018/1725).

The legal framework for drones is a multifaceted and intricate area of EU law. The new 2018 Regulation established a centralized structure, with primary rulemaking authority shared between the European Commission and the EASA. Reg.(EC) 2008/216 delegated extensive authority over drone activities to individual Member States and their respective national agencies, but the need for certainty, standardization, and explanation of laws has advised moving away from this dual approach. Nonetheless, a series of implementing and delegated acts shall be issued by the European Commission to supplement the requirements of the rule.

In addition, EASA is obligated to recommend to the European Commission technical norms and standards for civil drones of all sizes. Recital 78 states, "when adopting the delegated acts amending the Annexes II to IX to this Regulation, the Commission should take due account of the international standards and recommended practices, in particular of the international standards set out in all of the Annexes to the Chicago Convention". It is difficult to get a clear image of the EU legal framework and its goal to offer legal certainty in the field, due to the intricate web of formal competencies and substantive rules.

6.4.2 Market Concerns

Recent years have seen spectacular expansion for the UAV industry. UAVs exist in many shapes and sizes and serve many functions, including but not limited to internet delivery, aerial photography, surveillance, and reconnaissance. The UAV ecosystem leveraging the emerging technologies such as IoT, AI, AR/VR are not much explored by the manufacturers and their usages are also researched by a handful of organizations. Real-time surveillance is one of the major use case that has been widely explored by the UAV industry for relaying live information to target audience. The ecosystem is still in its infancy to showcase diverse capabilities of UAVs. Additionally, the skills necessary for UAV industry to roll out interesting use case demand sufficient domain training to the equipment providers and technical users. It is key to eradicate the bottleneck in setting up the ecosystem. Extracting the right set of specifications and requirements from the users is needed to maximize the benefit of the use case and to generate large scale development of UAV applications.

Because to the promising prospects in the global market, digital giants like Google, Airbus, DHL, Amazon, Uber, Nokia and Boeing, have been pouring significant resources into research and development of UAV technology in recent years. However, it has seen a meteoric rise in popularity for use in a wide variety of commercial, scientific, recreational, and government contexts. In disaster relief, forest monitoring, and vegetation monitoring, they are employed to collect massive amounts of data. These days, most people use their consumer drones for filming, surveying, and aerial mapping.

The PwC 2018 research estimates that by 2030, the global construction industry's volume would have grown by 85% to USD 15.5 trillion. Key nations including the United States, China, and India will account for around 57% of the entire industry expansion. Design and planning are crucial in this sector before large-scale infrastructure and building projects can begin. Data gathering from surveys and map creation for complicated surfaces is in high demand. Drones can save corporations millions of dollars by giving more precise information in less time compared to traditional methods of conducting surveys and collecting data in this area. Drone software has the potential to revolutionize many industries, and the UAV business is no exception. Around USD 45 Billion is expected to be generated by the construction sector over the projection period [234].

6.4.3 Social Concerns

The UAV operation must be properly regulated to protect the privacy of business organizations as well as individuals. Advancement of drone technology with aerial surveillance and photography with high definition images and streaming can easily violate the privacy, even when it is unintentional. The existing regulations to protect privacy may not be sufficient due to rapid evolution of UAV technology and its increasing capability, thereby further legislation is needed to be formulated to protect privacy.

Most of the UAV use cases deal with gathering a lot of vital data depending upon the application and processing them to extract useful information for taking decisions. During a mission, the onboard sensors collect personal or business data can be transmitted to a remote location or made live from the present location. The data collection capabilities may infringe data protection rules and abuse personal information without the knowledge of data subject. Additionally, if someone obtains the control of the UAV, the sensors or data processing circuitry could be tempered for data misuse. Hence, strict guidelines must be governed to protect the personal and business data.

In the due course of flight or mission control, any sort of discontinuity in proper command

and control poses serious safety risks. This may lead to collisions and causes harm to civilians and other UAVs in the vicinity. Collisions with manned aircraft can pose serious risks in terms of catastrophic consequence and loss of assets. In case of high density urban regions, collisions of UAVs with the ground terrain pose threats to human lives and assets. Hence, the challenges with respect to public safety must be taken into account and researched thoroughly.

6.5 3GPP Standardization for UAVs

Third Generation Partnership Project (3GPP) is a standardization body that governs the specifications for the technical platforms used by the cellular networks. The global partnership 3GPP develops standards to which almost all commercial cellular network providers and operators adhere to. In order to cater to the present and future needs of UAV communication, 3GPP aims to layout a unified platform for design and development of wireless innovations by gaining wider consensus from various contributors from industry and academia. The evolutions in the standards are published in the name of "3GPP release". From the perspective of UAV operations over cellular networks, we are interested in 3GPP Release-15, Release-16, Release-17 and Release-18. In Release-15, the study mainly concerns with the radio level aspects for supporting UAVs. In Release-16 and 17, the study is in the perspective of System and Application layer aspects.

6.5.1 Release-15

3GPP led a study item (SI) in Release-15 to investigate various prospects of utilizing an LTE network for UAV communication. The key outcomes of this study are summarized in the technical report TR 36.777, which was approved in January, 2018. This study focuses on two broad goals: First, how the aerial users (cellular-connected UAVs) impact overall LTE performance in the presence of terrestrial (ground) users. Second, to investigate on whether an LTE network is able to provide good support low altitude UAVs? The comprehensive list of items studied in this release are: channel modelling between aerial UEs and ground BSs, uplink and downlink interference problems due to LoS channel propagation characteristics, identification of aerial UE for legitimate cellular usage and subscription information, mobility performance, and flight path signalling. The result of the SI shows that existing LTE networks are able to support UAV communication and there is no notable impact in coexistence of small number of aerial and ground users (low density or rural regions). However, increase in the number of aerial and ground users have adverse impact on uplink/downlink performance due to interference. To some extent, existing LTE standards are found useful to mitigate the interference situation. After the completion of aforementioned study, a work item (WI) is pursued and got approved for enhancement of LTE standards. They are as follows:

- Introduction of new radio events and enhanced height dependent reporting for aerial UEs;
- Support of signalling in subscription based aerial user identification;
- Improvement of mobility and interference detection, uplink power control, airborne status and flight path plan.

6.5.2 Release-16

This release plan started in September, 2016 and the approval for stage-3 development was conducted on December, 2019. This release work is mainly on System and Application layer

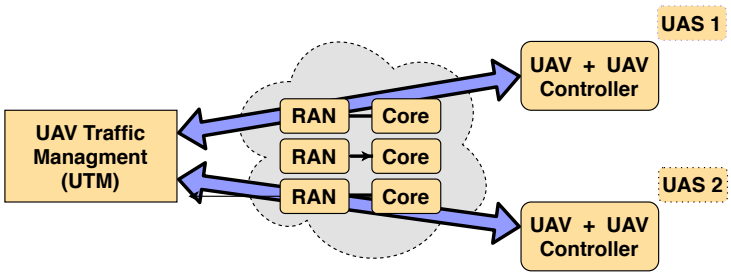

Figure 6.3: High level architecture of 3GPP Release 16 work on remote identification of UAS

aspects. A study item on "Remote Identification of Unmanned Aerial Systems" is pursued on this release and it led to the approved report 22.829. This study aims at the identification of UAV over the command and control data via a 3GPP network exchanged between UAS and centralized UAV Traffic Management (UTM) component. A UAS comprises of UAV and UAV controller. Fig. 6.3 depicts above model. 3GPP standards must make provisions for UAS to send the application data traffic to UTM along with various radio network information, identification and tracking details for UAS. After this study, a WI was agreed by 3GPP to advance the work on service requirement for identification of UAV.

3GPP TS 22.125 defines the standards for providing UAV services over 3GPP networks, whereas 3GPP TR 22.829 describes many UAV-enabled applications and use cases to be supported by 5G networks. Release-16 aims to define standards to address the global needs of UAV operators, law enforcement, regulatory authorities, and original equipment manufacturers through its analysis and subsequent normative work. The research relies on the idea of identifying UAVs using control data that may be communicated over the 3GPP network between a UAV or UAV controller and a centralized network-based UTM function.

6.5.3 Release-17

In this release, 3GPP proposes a number of study items. The idea is to come up with diverse scenarios and metrics to cater to wide variety of UAV applications and use cases. The study items are as follows:

- 5G Enhancement for UAVs- It includes several Key Performance Indicators (KPIs) relevant to UAV services. The KPIs are provided for command and control, and payload communication.
- Study on application layer support for Unmanned Aerial System (UAS)- This includes the UAS service requirements that may have impact on the UAS application layer. These requirements are in terms of general requirements, UE capability identification, location, security etc.
- Study on supporting UAS Connectivity, Identification, and Tracking- This study item deals with a mechanism that enables the UAS tracking and identification within 3GPP systems and UTM.

In 2019, the 3GPP released TR 22.829, which details the many UAV-enabled applications and use cases that 5G networks must support, as well as the required communications and networking performance enhancements. Throughout 2020, the work items related to UAS communications in Rel-17 concentrated on two important aspects: the network infrastructure and procedures to

support the connection, identification, and tracking of UAVs (TR 23.754), and the application architecture to support efficient UAS operations (TR 23.755).

To facilitate a wide variety of UAS applications and needs, 3GPP released specification details for a set of UAS communication services in release-17. Regulatory standards and air traffic management demands are addressed in release-17 with capabilities including remote UAV identification and support for UTM. In June of 2022, development on 3GPP release-17 is frozen. The development of the release-17 architecture by the 3GPP has included support for UAV applications. Two possible interfaces between the 3GPP system and UAV-related apps have been described in release-17 by 3GPP. The first interface, 3GPP's Network Exposure Function (NEF) interface, provides direct access to 3GPP network functions that facilitate UAV applications and is specified in TS 23.256. Services affiliated with the 3GPP standard, such as UAV Traffic Management (UTM) and UTM Service Providers (USS), can make use of this interface. The second interface, defined in TS 23.255, provides a higher-level, more generalized interface to 3GPP network capabilities. The 3GPP Service Enabler Architecture Layer for Verticals (SEAL) framework's general capabilities are also included in this interface. These details may be found in TS 23.434.

6.5.4 Release-18 and beyond

With the 5G specifications supplied by 3GPP, systems performance was enhanced, and new scenarios were made possible to better serve a wide range of industry verticals. There will be several improvements to the network architecture, physical layer, new services, security, and automation in the forthcoming release-18, which is known as "5G Advanced" and is a major step towards 6G. The first version of the 5G-Advanced standard, known as 3GPP release-18, has been released. UAVs have a wide range of potential uses, and 3GPP Release-18 will bring 5G NR compatibility for devices carried by UAVs. Work item RP-213600: NR support for UAV (uncrewed aerial vehicles) has been accepted for release-18 by the 3GPP RAN group. It is expected that 5G-Advanced will cover numerous releases, at least release-18 and maybe release-19 and beyond. The second part of 2021 saw the beginning of RAN scoping for release-18, the first target release for 5G-Advanced, with completion of the core specification expected by the end of 2023.

6.6 Conclusions

Mutual synergies of UAVs integrated with 6G systems may offer a cost-effective ecosystem and unlock several emerging use cases. High date rates, very low latency, global coverage, and programmability are expected in next generation networks. However, as several innovative convergence technologies for drone networks in 6G continue to sprout up, more promising discussions are needed on how these candidate technologies unify in futuristic 6G vision. We believe this work will serve as a basis for exploring unique innovations and moving towards establishing a road map for UAVs in 6G futuristic network. UAVs not only impose technical challenges, but also require solutions pertaining to privacy, security, licenses, public safety, administrative procedures governing them. Operation of UAVs over cellular spectrum requires strict regulations to operate in national and international airspace without causing trouble to other manned or unmanned aerial vehicles. There are rules applied to control UAV operation that varies with countries. However, a unified set of rules governing UAV operation in cellular spectrum is still far away. The commercial production of UAVs must consider the true requirements and specifications to maximize the benefit of a use case. Care must be taken to safeguard the data collected

by the sensors of UAV and ensuring that it does not infringe the privacy of unwanted individuals and organizations. It must be guarded against hackers and malicious intruders, whose intent is to control the UAVs for unauthorized activity, e.g., during aerial surveillance and photography. Standardization bodies such as 3GPP have put together study items and working groups in order to harmonize the development efforts from industry, academia and independent research bodies. We discussed the progress on standardization activities by 3GPP, national and international regulations and concerns pertaining to socio-economic barriers which must be accounted before successful adoption this new technology.

Chapter 7

Conclusions and Future outlooks

7.1 Conclusions

- The detailed taxonomy of various application domains with emerging use cases as well as the technical synergistic challenges of UAV integration with cellular network are discussed first.

- We present an architectural unification and prototyping framework of UAV-BS encompassing open-source hardware and software modules related to UAV autopilot and open-source 3GPP-compliant, 5G stack. Then, a series of open sky field experiments are conducted in real-time (i) to assess the prototype for fail-safe and flexible UAV maneuver, and (ii) to evaluate the UAV-BS communication performance. The experimental results demonstrate that careful positioning of UAV-BS substantially enhances the communication performance for ground UEs. We believe that, this work will inspire more investigation into the prototype of UAV-assisted cellular communication.

- In order to support three heterogeneous class of 5G slice service types, namely eMBB, uRLLC and mMTC, the UAV-BS is empowered with network slicing capabilities. The coexistence of eMBB, uRLLC and mMTC services multiplexed over radio resources of common UAV-BS leads to incredibly challenging downlink scheduling problem due to underlying trade-off of end-user requirements in terms of coverage, traffic demand, data rates, latency, reliability along with the UAV-specific constraints. We proposed a modular and customizable two-phase resource slicing optimization framework is proposed for UAV-BS known as *EASIER* that is decomposed into: (1) resource optimizer (RO) and (2) scheduling validator (SV). The reciprocation of RO and SV guided by two-phase optimization model can generate efficient scheduling decisions.

- We provided a comprehensive study on the cellular-assisted UAV communication paradigm (cellular-connected UAVs) where UAV is integrated to existing 5G and beyond cellular systems as a new aerial UE.

- The range of UAV radios are finite and hence, they tend to fly beyond the BS coverage in a typical mission. Considering the limited coverage, we studied a cooperative, multi-hop sidelink-assisted design of C-U2X communication model that optimizes the scheduling decisions of data transmission employing sidelink sub-channels. The model is validated using both centralized and distributed algorithms. The formulated problem is solved in centralized manner by mathematical optimization framework. A distributed auction-class

of algorithms, D-CBBA is proposed to generate efficient sub-channel scheduling decision for maximizing data transmission from PoIs to central BS. Our performance assessment demonstrates that the distributed algorithm potentially enhances the cellular infrastructure coverage via multi-hop communications over the 5G sidelink.

- We provided an overview of the technological and standards synergies that exist between several 6G enabling technologies and UAVs.Next-generation networks will have stricter latency constraints (in ms granularity) and Gbps data throughput, as well as ubiquitous connection. SATCOM technologies provide worldwide communication for this purpose, albeit at a high cost and with prohibitive delays. Mutual synergies between UAVs and 6G systems may provide a cost-effective ecosystem and enable various developing use cases. Yet, since various unique convergence technologies for UAV networks in 6G continue to emerge, more hopeful conversations on how these candidate technologies might be integrated into the futuristic 6G vision are required. Many technological obstacles remain for the deployment of futuristic 6G networks, which include a space-air-ground integrated communication network and assistive technology.

- The progress on UAV standardization activities by 3GPP, national and international regulations and concerns pertaining to socio-economic barriers are also discussed which must be accounted before successful adoption this new technology.

- We believe that the presented chapters will be a very useful and motivating resource for researchers working on UAV-cellular communication in order to unlock a holistic view and to exploit its full potential. We hope that our effort will serve as a foundation for investigating novel ideas and developing a road map for UAVs in 5G and futuristic 6G network.

7.2 Future outlooks

Despite of several studies, there is still a considerable number of open problems that needs to be investigated. This section aims to bring out such future opportunities for researchers and shed light on interesting open research topics. We split the open research areas into two subsections. Section 7.2.1 presents an overview of open research directions that could be followed up based on this thesis work. Section 7.2.2 presents a broad scope of future directions with respect to UAV-cellular integration domain.

7.2.1 Future extensions of the thesis

Gigabit backhaul network in the sky

When a number of UAV-BSs are placed in the sky to provide on-demand communication services, they exchange and route user data to the core network while also distributing incoming traffic from faraway servers. The bandwidth requirements for novel 5G and beyond applications are very high and are referred to as gigabit backhaul network in the sky. While some previous studies [235] illustrate the usage of 60 GHz mmWave mesh backhaul working at 1 Gbps for such needs, little progress has been achieved in this study area due to the fragility and wireless nature of UAV networks, frequent UAV topological reconfiguration, and user traffic routing.

We believe that our current prototype on UAV-BS described in Chapter 2, could be improved in terms of the backhaul support. The current prototype rely on an existing 5G backhaul, but

it would be worth investigating the possibility and challenges to integrate a 60 GHz mmWave radio backhaul to cater communication for a massive number of ground users.

Comprehensive evaluation of slicing-aware UAV-BS

Based on the findings obtained in Chapter 3, future works can be extended in different directions: (i) designing a more effective algorithm determining the best positioning of UAV-BS in an online manner by learning methods including also a trajectory planning for the UAV movements, (ii) enriching the proposed framework to also include the ability to handle multiple UAV-BSs, and (iii) evaluating the optimization framework performance in a real-world, practical testbed. We believe our current work will be a motivating and useful contribution in the field of application of network slicing principles and methodologies to airborne UAVs, thereby unlocking the service-oriented vision of UAV-enabled 5G and emerging 6G cellular network.

Cellular Network using UAV-BSs and UAV-UEs

In this thesis, we have described four synergies of UAV and cellular integration. From a different, perspective, if we wish to realize a network deployment where a group of UAV-BSs are deployed on the air, not only to provide communication services to ground UEs, but also to extend communication services to UAV-UEs. Such a network deployment is challenging and would need further study with respect to UAV-BS optimal positioning, up-facing antenna designs, interference criteria, coexistence of ground UEs and UAV-UEs, and many more.

Environmental effects on UAV

The transmission medium and channel conditions are less prone to errors in ideal circumstances, without the presence of wind or severe temperature conditions (extremely cold or very hot). These environmental influences, which should be taken into account based on regional circumstances, were not taken into account in this study. In addition, although it is not highlighted in our findings, drone vibrations have a negative impact on signal propagation. Studying the impact of wind, vibration of drone, and temperature when the UAV is realized as UAV-BS or UAV-UE in the deployed network would be an intriguing challenge.

7.2.2 Open topics in UAV-Cellular research

End-to-end testing platforms

Simulations and measurement campaigns are not sufficient to fully characterize the performance and working principles of UAV cellular communication. The solution approaches to the integration challenges must be complemented by extensive field trials and real-world testbed-based evaluation. However, there are not enough working prototypes to study and evaluate the behaviour of UAV-BS or aerial UE from practical standpoint.

It is worth mentioning that, "Aerial Experimentation and Research Platform for Advanced Wireless", or AERPAW provides open-source experimental ecosystem to investigate convergence of 5G and autonomous UAVs [236]. The goals of such platform is to foster wireless innovation and solutions to problems that lie in the intersection of UAVs and 5G network. In order to bridge the gap between theoretical proposal and practical evaluation, it will be necessary to pursue the growth of accessible and experimental platforms abundant in open-source software-defined radios and 3GPP-compliant cellular stack.

Energy constraints

Onboard energy is a bottleneck in UAVs. Latest advances to rechargeable battery cells and utilization of solar cells are some of the techniques to prolong the flight time of UAV. The UAVs require constant power source to operate since they utilize a substantial amount of battery power in keeping them aloft in air. Hovering, signal processing functions, software execution, and any path-planning optimization, all consume battery power. The majority of existing works on UAV cellular domain do not account for this energy limitation in their research. There is a lot of scope to examine the performance of UAV-BSs and UAV-UEs given the limiting energy limitations, particularly in the areas of VNF deployment on UAVs for automated operation, trajectory optimization, learning-based approaches, and mission lifetime computation in a use case.

AI and ML-based methods

AI and machine learning-based technologies have been viewed as powerful solutions for solving many real-world wireless networking difficulties, transforming 5G and beyond networks. With the introduction of UAV cellular connectivity, new possibilities for autonomous UAV operation in terms of security, performance, and dynamic complicated deployment situations have emerged. There are several research topics to consider while exploring and assessing AI/ML-enabled solutions to handle obstacles such as UAV-ground interference management, power control, multi-UAV collaboration, and so on. Q-learning approaches aid UAVs in addressing security issues by adaptively controlling UAV transmission based on the malicious type of attack.

Furthermore, it is difficult to get complete RF data sets with distinct classification in order to employ data-driven methods on the study of research problems. Researchers from Northeastern and Rice have joined forces on a project called "RFDataFactory" to fill this need [237]. The goal of RFDataFactory is to facilitate access to, creation of, sharing of, and storage of wireless datasets, as well as to increase basic knowledge and design tools for research relating to ML in 5G and beyond networks. RFDataFactory is a central hub for the wireless community's datasets, serving as a hub for RF-centric datasets, software APIs, and tutorials for data collection and processing from experimental testbeds and simulations.

3D Mobility and Handovers

Ground UEs are typically movable in 2D space, while base station antennas are ideally suited for ground users. UAVs are often serviced by the side lobes of present base stations, and their aerial patterns differ, leading in distinct handover characteristics distinct from ground UEs. The frequent handover pattern is heavily influenced by obstruction, mobility, and altitude fluctuations. There is a need for enhanced handover procedures that are compatible with the features of high mobility UAVs. Therefore, cell selection strategies based on closest received signal received power (RSRP) may no longer be an acceptable strategy for cellular-connected UAVs.

Computational Offloading

Due to moderate computational capabilities and limited onboard energy of UAVs, mobile-edge computing (MEC) can be helpful for offloading computationally heavy tasks from UAV to edge nodes to improve flying endurance and life time. Some examples of such intense tasks are real-time face recognition in a crowd surveillance use case. For such use case, leveraging MEC capabilities along with UAV, the recognition task can be offloaded to complete the job in a timely

manner. Additionally, to save the information from eavesdropper, proper security mechanisms needs to be integrated to the MEC-UAV platform for optimum performance. These research areas are largely unexplored so far and numerous scopes exists for design and development of UAV-MEC frameworks.

Résumé étendu en Français

En tant que sujet en expansion de la robotique aérienne, les véhicules aériens sans pilote (UAV) ont fait l'objet d'une attention particulière de la part de la communauté de recherche sur les réseaux sans fil. Dès que les législations nationales permettront aux drones de voler de manière autonome, nous verrons des essaims de drones envahir le ciel de nos villes intelligentes pour accomplir diverses missions : livraison de colis, surveillance des infrastructures, vidéographie événementielle, surveillance, suivi, etc. Les réseaux cellulaires de cinquième génération (5G) et au-delà peuvent améliorer les communications des drones de diverses manières et profiter ainsi à l'écosystème des drones. Il existe une grande variété d'applications sans fil et de cas d'utilisation qui peuvent bénéficier des capacités de ces dispositifs intelligents, y compris les caractéristiques inhérentes du drone de mobilité agile dans l'espace tridimensionnel, le fonctionnement autonome et le placement intelligent. L'objectif général de cette thèse est de fournir une analyse complète des synergies qui peuvent être réalisées en combinant les réseaux cellulaires 5G et au-delà avec la technologie des drones.

Cette thèse présente quatre types de modèles d'intégration d'écosystèmes de drones et cellulaires, comme le montre la Fig. 1. Le paradigme du cellulaire assisté par drone fait référence à des scénarios de communication dans lesquels les drones sont utilisés comme stations de base volantes (ou aériennes) ou comme relais pour augmenter la connectivité cellulaire terrestre actuelle ou pour atténuer les situations de catastrophe. Le paradigme du drone assisté par téléphone cellulaire prévoit l'intégration des drones dans le réseau cellulaire actuel en tant que nouvel utilisateur aérien (UE volant) pour servir une grande variété d'applications et de cas d'utilisation. Le paradigme du drone à drone met l'accent sur la force collective d'une flotte de drones en tant qu'essaim et sur la communication entre les drones à l'intérieur de l'essaim. Le paradigme hybride non terrestre englobe les réseaux satellitaires et aériens, examinant ainsi l'ensemble du spectre des liaisons de communication du sol à l'air et à l'espace sous la forme d'un réseau de communication intégré espace-air-sol.

La première partie de cette thèse se concentre sur les stations de base aériennes, qui ont fait l'objet d'une grande attention de la part des universitaires afin de fournir des services de communication flexibles et à la demande aux utilisateurs au sol. À cette occasion, nous construisons une plateforme prototype de démonstration de faisabilité qui délimite les composants de conception requis pour mettre en œuvre de telles plateformes dans le monde réel, et nous expliquons ensuite la nécessité d'un placement optimal des stations de base aériennes pour augmenter les services de communication. Le prototype est réalisé avec une pile 4G/5G open source, srsRAN et le micrologiciel de gestion de vol Pixhawk. Il est équipé d'un logiciel intermédiaire basé sur l'API MAVROS avec des interfaces soignées pour gérer les tâches et les interactions avec les blocs de traitement de vol ou RF. Il est utilisé pour valider les avantages en termes de performance en ce qui concerne le positionnement flexible du UAV-BS afin d'atteindre les objectifs de qualité de service spécifiques à l'UE. Nous avons effectué des essais en vol dans le monde réel qui démontrent les gains pour différents choix de positionnement des UAV-BS. Le schéma du banc

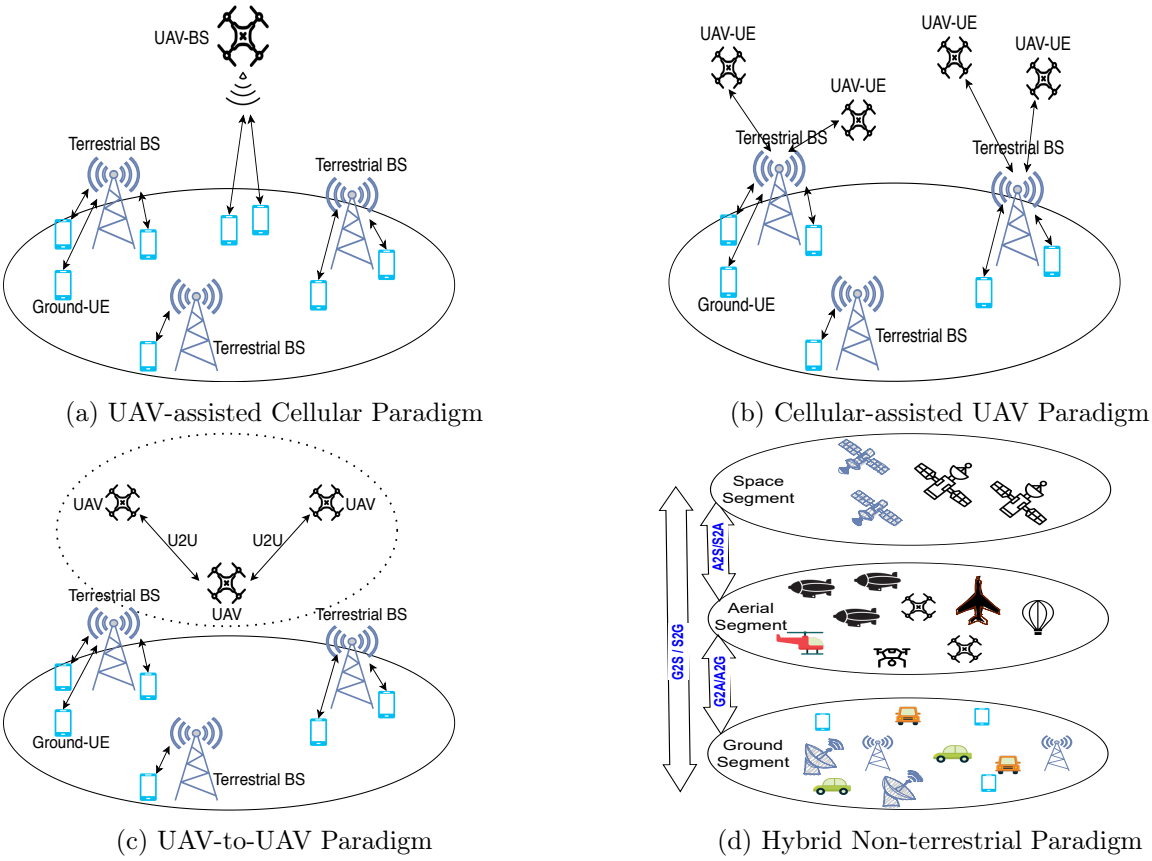

(a) UAV-assisted Cellular Paradigm

(b) Cellular-assisted UAV Paradigm

(c) UAV-to-UAV Paradigm

(d) Hybrid Non-terrestrial Paradigm

Figure 1: Integration Synergies of UAVs and Cellular System

d'essai développé est illustré à la Fig. 2. D'un point de vue général, *FlightStack* et *CommStack* sont deux entités fondamentales en interaction dans le cadre UAV-BS. *FlightStack* désigne le microprogramme du pilote automatique et les programmes associés qui gèrent étroitement le matériel du drone pour le maintenir en l'air, tout en étant contrôlé en retour par l'opérateur au sol. *CommStack* désigne la pile de protocoles du réseau d'accès radio (RAN) "5G et au-delà" qui permet d'utiliser les fonctions de la station de base sur le drone. Le prototype développé exploite l'unification des composants de robotique et de réseau pour améliorer les performances du système par rapport aux conceptions découplées UAV-BS présentes dans la littérature existante. Nous envisageons un logiciel intermédiaire qui, contrairement aux prototypes précédents, intègre le *FlightStack* et le *CommStack*, tout en les gardant indépendants et modulaires.

Pour prendre en charge une classe hétérogène de services 5G provenant de diverses industries verticales (appelées locataires des opérateurs de réseaux 5G), nous proposons un cadre de station de base aérienne sensible au découpage dans lequel les utilisateurs au sol ayant des exigences de trafic différenciées en termes de débit de données, de latence et de déploiement massif sont pris en charge par le biais d'un approvisionnement intelligent en ressources. Un mélange probabiliste de différents types d'UE et de demandes de trafic de données est pris en compte pour évaluer les gains de performance. Nous proposons un cadre d'optimisation du découpage en deux phases, léger et séparé, connu sous le nom de cadre d'optimisation du découpage en tranches (*EASIER*). Il se compose (i) d'un module d'optimisation des ressources (RO) et (ii) d'un module de validation de l'ordonnancement (SV), qui contribue à l'élaboration d'une politique dynamique de découpage des ressources pour une plateforme UAV-BS soumise à des contraintes

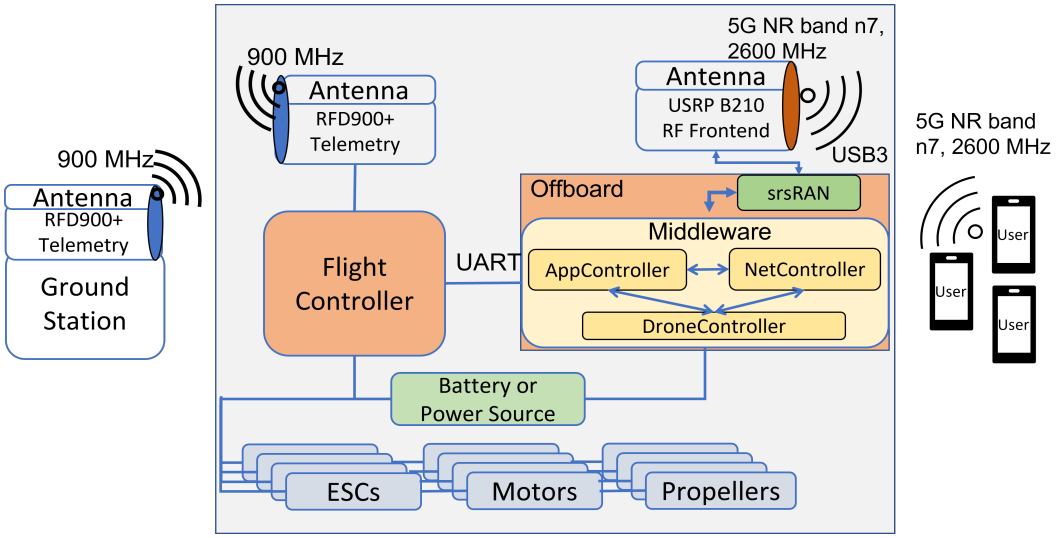

Figure 2: Design and Schematics of UAV-BS prototype

de calcul. Nous montrons qu'il garantit non seulement la qualité de service convenue à tous les utilisateurs requis/obligatoires, mais qu'il maximise également l'acceptation des utilisateurs supplémentaires/optionnels chaque fois qu'il est possible de le faire dans les limites de la capacité du système. Le cadre d'optimisation proposé garantit que la décision d'attribution des ressources est prise par l'OR et que sa validation est effectuée par le SV. Si la décision d'affectation proposée par l'OR respecte la qualité de service requise par tous les utilisateurs concernés, le SV n'effectue aucune validation supplémentaire. Dans le cas contraire, si au moins une des mesures de qualité de service n'est pas satisfaite conformément à l'accord de niveau de service convenu avec le locataire de la tranche, une nouvelle contrainte est ajoutée au niveau de l'OR. De cette manière, le module RO utilise les réponses périodiques en retour du module SV pour réduire l'espace de solution et converger vers une décision d'affectation efficace qui respecte les exigences de qualité de service des utilisateurs de la tranche.

La deuxième partie de cette thèse décrit les utilisateurs aériens (également appelés UAV connectés à la téléphonie cellulaire ou UAV-UE) qui sont pris en charge par l'infrastructure cellulaire actuelle. Les communications aériennes et la mise en réseau des drones connectés à un réseau cellulaire posent plusieurs défis qu'il convient d'étudier en profondeur. Par exemple, une communication fiable et à faible latence pour un contrôle efficace du drone est de la plus haute importance. Les infrastructures cellulaires existantes sont principalement conçues et développées pour offrir des services de communication améliorés aux utilisateurs terrestres. En outre, les terrains géographiques où la couverture des stations de base est limitée peuvent ne pas fournir les services de connectivité nécessaires aux drones connectés au réseau cellulaire, ce qui exige des solutions prometteuses pour l'adoption réussie de cette technologie. Nous examinons donc des difficultés telles que la couverture 3D, l'interférence de la ligne de visée dominante, les transferts et l'optimisation de la trajectoire en fonction de la communication. Nous nous concentrons sur les architectures de réseau prometteuses et les améliorations de la couche physique dans les systèmes 5G et au-delà, en tenant compte des défis de conception matérielle et logicielle des drones connectés au réseau cellulaire. Les principales technologies innovantes de la 5G sont élaborées pour permettre l'intégration transparente et la prise en charge de la communication des drones sur le spectre cellulaire. Afin de caractériser les avantages en termes de performances de conception et d'étudier les problèmes de déploiement réalistes, nous avons également mis en

évidence les efforts déployés pour développer des prototypes fonctionnels ainsi que des essais et des simulations sur le terrain.

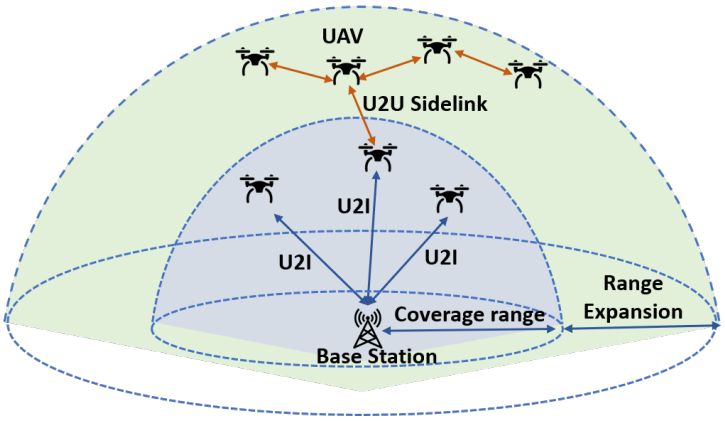

Figure 3: UAV-to-UAV links using Sidelink

L'utilisation d'un essaim de drones est considérablement plus rentable qu'un seul drone effectuant une mission, si l'on considère des objectifs de mission réalistes. Un essaim de drones ouvre de nouvelles perspectives pour de nouveaux services et applications, car les drones peuvent coordonner leurs opérations de manière indépendante et travailler ensemble pour accomplir une tâche donnée. En raison de la dynamique spatio-temporelle de la topologie de l'essaim, le développement d'un réseau fiable avec une communication transparente entre les drones est essentiel pour que toute opération soit couronnée de succès. Dans le cadre de cette thèse, nous proposons des modèles de réseaux centralisés et décentralisés pour la communication de drone à drone (U2U) au sein de l'essaim et nous menons une étude complète de la communication U2U assistée par liaison latérale avec une évaluation des performances. La Fig 3 présente la liaison latérale comme un outil potentiel de communication U2U dans un essaim de drones. Les liaisons U2I exploitent l'interface radio cellulaire (Uu) pour connecter les drones à la station de base pour les services à charge utile élevée en liaison montante et les services CNPC essentiels en liaison descendante. Les liaisons U2U sont utilisées pour diffuser des informations périodiques relatives à la charge utile et à la sécurité via l'interface radio de liaison latérale (PC5) avec la communication D2D ProSe. Ces liaisons permettent une communication robuste et fiable pour plusieurs drones.

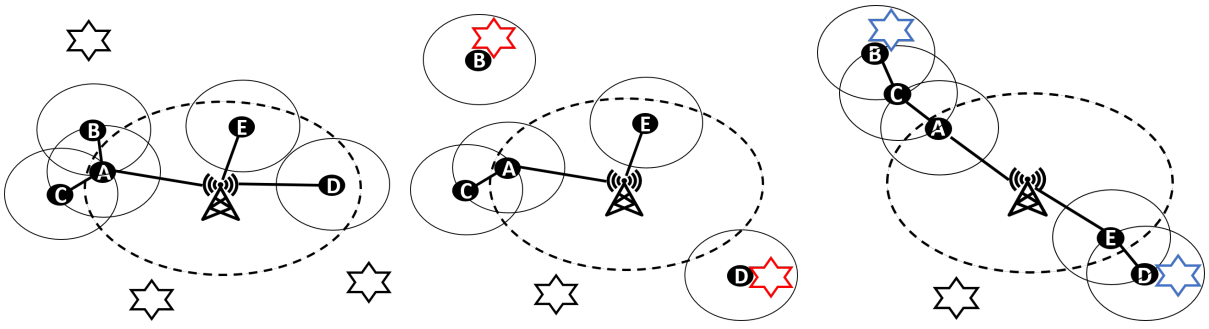

(a) Initial scenario (b) Non-cooperative planning (c) Spatio-temporal cooperation

Figure 4: Dynamic aerial network formation and coverage constraints

Une mission générique de surveillance vidéo est décrite à la Fig. 4, dans laquelle un essaim de drones connectés à un réseau cellulaire doit surveiller une région cible et renvoyer les données

de détection à la station de base. À cette fin, nous supposons que la région entière est divisée en petites zones ou points d'intérêt (PoI), marqués par des étoiles sur la figure. Les PoI sont supposés être statiques et leur position est connue des UAV avant l'exécution de la mission. Les drones doivent survoler les PoI et transmettre les flux vidéo en temps réel vers la station de base, en utilisant une combinaison de liaisons U2I et U2U. Pour atteindre les objectifs de la mission, les drones doivent voler autour des points d'intérêt cibles, éventuellement au-delà de la portée de communication supportée par la station de base, ce qui entraîne des déconnexions potentielles et réduit le débit global du système de surveillance. Ce cas est illustré à la Fig. 4b et correspond à un déploiement aléatoire et non coopératif des UAV où les contraintes de connectivité de l'essaim ne sont pas prises en compte. À l'inverse, la Fig. 4c illustre un déploiement entièrement coopératif où certains drones servent de relais (*i.e.* relais UE) pour étendre la couverture cellulaire, garantissant ainsi un déploiement de l'essaim entièrement connecté.

Le modèle de communication coopérative multi-sauts ci-dessus, basé sur le C-U2X (Cellular UAV-to-Everything) est présenté pour une programmation efficace du flux de données des drones au sein de l'essaim. La conception du modèle vise à optimiser la communication C-U2X par le biais d'une programmation des flux de données tenant compte des interférences. Le modèle est présenté mathématiquement comme un problème d'optimisation des flux multicanaux (MCFOP) qui calcule l'ordonnancement optimal des flux de données pour un essaim de drones connectés de manière centralisée. Nous prouvons que le problème lui-même est NP-hard, et pour cette raison nous introduisons un modèle d'optimisation où la fonction objectif consiste en une partie linéaire et une partie quadratique. Le modèle proposé peut optimiser simultanément l'acheminement des informations et l'allocation des différents sous-canaux. Nous étendons le modèle ci-dessus au scénario distribué sans autorité centrale (dans notre cas, la station de base) et proposons deux algorithmes distribués pour l'attribution des canaux et la programmation des transmissions. Plus précisément, nous décrivons une extension de l'algorithme CBBA (Consensus-Based Bundle Algorithm), basé sur les enchères, pour produire une affectation sans conflit des possibilités de transmission aux UAV.

En outre, nous avons évalué un modèle de communication multi-sauts assisté par des liens latéraux afin d'établir une connectivité avec les drones hors couverture pendant la mission. La couverture de l'infrastructure cellulaire étant limitée, au cours d'une mission, un essaim de drones a tendance à voler au-delà de la couverture cellulaire, ce qui entraîne une dégradation du signal. Les drones sont alors incapables de transmettre des informations essentielles à la station de base centrale. Toutefois, les liaisons multi-sauts reliant un drone à un autre drone étendent la connectivité et la couverture de l'infrastructure du réseau. Dans le modèle multi-sauts, certains drones agissent comme des nœuds de relais pour transmettre des messages au drone suivant. Trois déploiements différents de réseaux multi-sauts assistés par le couloir ont été étudiés et les avantages en termes de performances ont été présentés dans cette thèse, en tenant compte des principaux paramètres de programmation de l'algorithme de programmation distribuée basé sur la détection.

Dans la dernière partie de cette thèse, une discussion approfondie est fournie sur la façon dont nous prévoyons que les progrès technologiques actuels dans les drones et la 5G se traduiront par de futurs systèmes 6G et quels sont les facilitateurs technologiques de cette vision ambitieuse de la 6G. L'intégration de réseaux hétérogènes, tels que "5G avec des satellites" ou "5G avec des drones", fait déjà partie du processus de normalisation de la 5G par le 3GPP. En raison de l'énorme potentiel des drones, on s'attend à ce qu'ils deviennent bientôt un outil technologique essentiel de l'espace aérien. Au-delà des réseaux terrestres, le concept de la 6G inclut les réseaux non terrestres tels que les réseaux satellitaires et aériens, et étudie donc un large éventail de canaux de communication disparates en vue d'atteindre l'objectif d'une infrastructure unifiée

entre l'espace et l'air, d'une part, et le sol, d'autre part. Les technologies candidates telles que les ondes millimétriques ou les fréquences inférieures à 6 GHz sont largement étudiées et leurs performances sont déjà évaluées pour les systèmes de communication 5G. Bien que ces technologies marquent des avancées essentielles vers une plus grande efficacité spectrale, le réseau sans fil 6G nécessite une exploration plus poussée des réseaux d'accès et des liaisons de communication pour répondre à sa vision multiforme. Plus précisément, nous avons envisagé le MIMO massif, les ondes millimétriques, le THz, les liaisons latérales, l'optique spatiale libre (FSO) et les communications à lumière visible (VLC) comme les principales technologies pour le scénario 6G.

Outre les difficultés technologiques, les questions relatives à la vie privée, à la sécurité, à l'octroi de licences, à la sécurité publique et aux procédures administratives entourant les UAV doivent être abordées. Pour que les UAV puissent opérer en toute sécurité dans l'espace aérien national et international, ils doivent adhérer à des lois strictes qui les empêchent d'interférer avec d'autres formes d'aéronefs avec ou sans pilote. Pour garantir la synchronisation des activités de développement des entreprises, des universités et des organismes de recherche indépendants, les organismes de normalisation tels que le 3GPP ont mis en place des sujets d'étude et des groupes de travail. Cette thèse met en lumière plusieurs technologies habilitantes 6G innovantes et présente la recherche et l'évaluation approfondies des candidats aux technologies de communication, les préoccupations socio-économiques et les activités de normalisation entreprises pour harmoniser les opérations des drones.

Bibliography

[1] Kimon P Valavanis and George J Vachtsevanos. *Handbook of unmanned aerial vehicles*. Springer, 2015.

[2] Randal W Beard and Timothy W McLain. *Small unmanned aircraft: Theory and practice*. Princeton university press, 2012.

[3] Mahdi Asadpour, Bertold Van den Bergh, Domenico Giustiniano, Karin Anna Hummel, Sofie Pollin, and Bernhard Plattner. Micro aerial vehicle networks: an experimental analysis of challenges and opportunities. *IEEE Communications Magazine*, 52(7):141–149, 2014.

[4] Lumawant Godage. Global Unmanned Aerial Vehicle Market (UAV) Industry Analysis and Forecast (2018-2026). *Montana Ledger*, 2019.

[5] Samira Hayat, Evşen Yanmaz, and Raheeb Muzaffar. Survey on Unmanned Aerial Vehicle Networks for Civil Applications: A Communications Viewpoint. *IEEE Communications Surveys & Tutorials*, 18(4):2624–2661, 2016.

[6] Reza Shakeri, Mohammed Ali Al-Garadi, Ahmed Badawy, Amr Mohamed, Tamer Khattab, Abdulla Khalid Al-Ali, Khaled A Harras, and Mohsen Guizani. Design Challenges of Multi-UAV Systems in Cyber-Physical Applications: A Comprehensive Survey and Future Directions. *IEEE Communications Surveys & Tutorials*, 21(4):3340–3385, 2019.

[7] Haijun Wang, Haitao Zhao, Jiao Zhang, Dongtang Ma, Jiaxun Li, and Jibo Wei. Survey on Unmanned Aerial Vehicle Networks: A Cyber Physical System Perspective. *IEEE Communications Surveys & Tutorials*, 2019.

[8] Mohammad Mozaffari, Walid Saad, Mehdi Bennis, Young-Han Nam, and Mérouane Debbah. A Tutorial on UAVs for Wireless Networks: Applications, Challenges, and Open Problems. *IEEE communications surveys & tutorials*, 21(3):2334–2360, 2019.

[9] Haque Nawaz, Husnain Mansoor Ali, and Asif Ali Laghari. UAV Communication Networks Issues: A Review. *Archives of Computational Methods in Engineering*, pages 1–21, 2020.

[10] Yong Zeng, Rui Zhang, and Teng Joon Lim. Wireless communications with unmanned aerial vehicles: opportunities and challenges. *IEEE Communications Magazine*, 54(5): 36–42, 2016.

[11] Maede Zolanvari, Raj Jain, and Tara Salman. Potential Data Link Candidates for Civilian Unmanned Aircraft Systems: A Survey. *IEEE Communications Surveys & Tutorials*, 22 (1):292–319, 2019.

[12] Nozhan Hosseini, Hosseinali Jamal, Jamal Haque, Thomas Magesacher, and David W Matolak. UAV Command and Control, Navigation and Surveillance: A Review of Potential 5G and Satellite Systems. *IEEE Aerospace Conference*, pages 1–10, 2019.

[13] Azade Fotouhi, Haoran Qiang, Ming Ding, Mahbub Hassan, Lorenzo Galati Giordano, Adrian Garcia-Rodriguez, and Jinhong Yuan. Survey on UAV Cellular Communications: Practical Aspects, Standardization Advancements, Regulation, and Security Challenges. *IEEE Communications Surveys & Tutorials*, 21(4):3417–3442, 2019.

[14] Zaib Ullah, Fadi Al-Turjman, and Leonardo Mostarda. Cognition in UAV-Aided 5G and Beyond Communications: A Survey. *IEEE Transactions on Cognitive Communications and Networking*, 2020.

[15] Robert J Kerczewski, Jeffrey D Wilson, and William D Bishop. Frequency spectrum for integration of unmanned aircraft. *2013 IEEE/AIAA 32nd Digital Avionics Systems Conference (DASC)*, pages 6D5–1, 2013.

[16] 36.777. Technical specification group radio access network:study on enhanced LTE support for aerial vehicles. *3GPP TR*, V15.0.0, Dec, 2017.

[17] Patrick Marsch, Icaro Da Silva, Omer Bulakci, Milos Tesanovic, Salah Eddine El Ayoubi, Thomas Rosowski, Alexandros Kaloxylos, and Mauro Boldi. 5G Radio Access Network Architecture: Design Guidelines and Key Considerations. *IEEE Communications Magazine*, 54(11):24–32, 2016.

[18] Patrick Marsch, Icaro Da Silva, Ömer Bulakci, Milos Tesanovic, Salah Eddine El Ayoubi, and Mikko Säily. Emerging network architecture and functional design considerations for 5G radio access. *Transactions on Emerging Telecommunications Technologies*, 27(9):1168–1177, 2016.

[19] Siva D Muruganathan, Xingqin Lin, Helka-Liina Maattanen, Zhenhua Zou, Wuri A Hapsari, and Shinpei Yasukawa. An Overview of 3GPP Release-15 Study on Enhanced LTE Support for Connected Drones. *arXiv preprint arXiv:1805.00826*, 2018.

[20] Bin Li, Zesong Fei, and Yan Zhang. UAV Communications for 5G and Beyond: Recent Advances and Future Trends. *IEEE Internet of Things Journal*, 6(2):2241–2263, 2018.

[21] Irem Bor-Yaliniz, Mohamed Salem, Gamini Senerath, and Halim Yanikomeroglu. Is 5G Ready for Drones: A Look into Contemporary and Prospective Wireless Networks from a Standardization Perspective. *IEEE Wireless Communications*, 26(1):18–27, 2019.

[22] Syed Ahsan Raza Naqvi, Syed Ali Hassan, Haris Pervaiz, and Qiang Ni. Drone-Aided Communication as a Key Enabler for 5G and Resilient Public Safety Networks. *IEEE Communications Magazine*, 56(1):36–42, 2018.

[23] Yongs Zeng, Qingqing Wu, and Rui Zhang. Accessing From the Sky: A Tutorial on UAV Communications for 5G and Beyond. *Proceedings of the IEEE*, 107(12):2327–2375, 2019.

[24] Evgenii Vinogradov, Hazem Sallouha, Sibren De Bast, Mohammad Mahdi Azari, and Sofie Pollin. Tutorial on UAV: A Blue Sky View on Wireless Communication. *arXiv preprint arXiv:1901.02306*, 2019.

[25] Ayon Chakraborty, Eugene Chai, Karthikeyan Sundaresan, Amir Khojastepour, and Sampath Rangarajan. SkyRAN: a self-organizing LTE RAN in the sky. *Proceedings of the 14th International Conference on emerging Networking EXperiments and Technologies*, pages 280–292, 2018.

[26] Karthikeyan Sundaresan, Eugene Chai, Ayon Chakraborty, and Sampath Rangarajan. SkyLiTE: End-to-End Design of Low-Altitude UAV Networks for Providing LTE Connectivity. *arXiv preprint arXiv:1802.06042*, 2018.

[27] Fadi Al-Turjman, Mohammad Abujubbeh, Arman Malekloo, and Leonardo Mostarda. UAVs assessment in software-defined IoT networks: An overview. *Computer Communications*, 150:519–536, 2020.

[28] Yong Zeng, Jiangbin Lyu, and Rui Zhang. Cellular-Connected UAV: Potential, Challenges, and Promising Technologies. *IEEE Wireless Communications*, 26(1):120–127, 2018.

[29] M Mahdi Azari, Giovanni Geraci, Adrian Garcia-Rodriguez, and Sofie Pollin. Cellular UAV-to-UAV Communications. *IEEE 30th Annual International Symposium on Personal, Indoor and Mobile Radio Communications (PIMRC)*, pages 1–7, 2019.

[30] Shuhang Zhang, Hongliang Zhang, Boya Di, and Lingyang Song. Cellular UAV-to-X Communications: Design and optimization for multi-UAV networks. *IEEE Transactions on Wireless Communications*, 18(2):1346–1359, 2019.

[31] Debashisha Mishra et al. Drone Networking in the 6G Era: A Technology Overview. *IEEE Communications Standards Magazine*, 5(4):88–95, 2021.

[32] Albert Banchs et al. A 5G mobile network architecture to support vertical industries. *IEEE Communications Magazine*, 57(12):38–44, 2019.

[33] Oscar Alvear, Nicola Roberto Zema, Enrico Natalizio, and Carlos T Calafate. Using UAV-Based Systems to Monitor Air Pollution in Areas with Poor Accessibility. *Journal of Advanced Transportation*, 2017, 2017.

[34] Oscar Alvear, Carlos Calafate, Nicola Zema, and et al. A Discretized Approach to Air Pollution Monitoring Using UAV-based Sensing. *Mobile Network Applications*, 23:1693–1702, 2018.

[35] Hazim Shakhatreh, Ahmad H Sawalmeh, Ala Al-Fuqaha, Zuochao Dou, Eyad Almaita, Issa Khalil, Noor Shamsiah Othman, Abdallah Khreishah, and Mohsen Guizani. Unmanned Aerial Vehicles (UAVs): A Survey on Civil Applications and Key Research Challenges. *IEEE Access*, 7:48572–48634, 2019.

[36] Milan Erdelj, Osamah Saif, Enrico Natalizio, and Isabelle Fantoni. UAVs that fly forever: Uninterrupted structural inspection through automatic UAV replacement. *Ad Hoc Networks*, 94:101612, 2019.

[37] Angelo Trotta, Fabio D Andreagiovanni, Marco Di Felice, Enrico Natalizio, and Kaushik Roy Chowdhury. When UAVs Ride A Bus: Towards Energy-efficient City-scale Video Surveillance. *IEEE Conference on Computer Communications (INFOCOM)*, pages 1043–1051, 2018.

[38] Pasquale Grippa, Doris A Behrens, Friederike Wall, and Christian Bettstetter. Drone delivery systems: job assignment and dimensioning. *Autonomous Robots*, 43(2):261–274, 2019.

[39] Xingqin Lin, Vijaya Yajnanarayana, Siva D Muruganathan, Shiwei Gao, Henrik Asplund, Helka-Liina Maattanen, Mattias Bergstrom, Sebastian Euler, and Y-P Eric Wang. The Sky Is Not the Limit: LTE for Unmanned Aerial Vehicles. *IEEE Communications Magazine*, 56(4):204–210, 2018.

[40] Jacob Chakareski. Aerial UAV-IoT sensing for ubiquitous immersive communication and virtual human teleportation. *IEEE Conference on Computer Communications Workshops (INFOCOM WKSHPS)*, pages 718–723, 2017.

[41] Milan Erdelj, Michał Król, and Enrico Natalizio. Wireless Sensor Networks and Multi-UAV systems for natural disaster management. *Computer Networks*, 124:72–86, 2017.

[42] Milan Erdelj, Enrico Natalizio, Kaushik R Chowdhury, and Ian F Akyildiz. Help from the Sky: Leveraging UAVs for Disaster Management. *IEEE Pervasive Computing*, 16(1): 24–32, 2017.

[43] Milan Erdelj, Borey Uk, David Konam, and Enrico Natalizio. From the Eye of the Storm: An IoT Ecosystem Made of Sensors, Smartphones and UAVs. *Sensors*, 18(11):3814, 2018.

[44] Naser Hossein Motlagh, Miloud Bagaa, and Tarik Taleb. UAV-Based IoT Platform: A Crowd Surveillance Use Case. *IEEE Communications Magazine*, 55(2):128–134, 2017.

[45] Piero Boccardo, Filiberto Chiabrando, Furio Dutto, Fabio Tonolo, and Andrea Lingua. UAV Deployment Exercise for Mapping Purposes: Evaluation of Emergency Response Applications. *Sensors*, 15(7):15717–15737, 2015.

[46] Daojing He, Sammy Chan, and Mohsen Guizani. Drone-Assisted Public Safety Networks: The Security Aspect. *IEEE Communications Magazine*, 55(8):218–223, 2017.

[47] Marouane Salhaoui, Antonio Guerrero-González, Mounir Arioua, Francisco J Ortiz, Ahmed El Oualkadi, and Carlos Luis Torregrosa. Smart Industrial IoT Monitoring and Control System Based on UAV and Cloud Computing Applied to a Concrete Plant. *Sensors*, 19 (15):3316, 2019.

[48] Thomas Lagkas, Vasileios Argyriou, Stamatia Bibi, and Panagiotis Sarigiannidis. UAV IoT framework views and challenges: Towards protecting drones as "Things". *Sensors*, 18(11): 4015, 2018.

[49] Pham Q Viet and Daniel Romero. Aerial base station placement: A tutorial introduction. *IEEE Communications Magazine*, 60(5):44–49, 2022.

[50] Sanchez et al. Millimeter-wave base stations in the sky: An experimental study of UAV-to-ground communications. *IEEE Transactions on Mobile Computing*, 2020.

[51] Wang et al. Modeling and analysis of aerial base station-assisted cellular networks in finite areas under LoS and NLoS propagation. *IEEE Trans. on Wireless Communications*, 17 (10):6985–7000, 2018.

[52] Ahmad Sawalmeh et al. Providing wireless coverage in massively crowded events using UAVs. In *IEEE 13th Malaysia International Conference on Communications (MICC)*, pages 158–163, 2017.

[53] Tianyang Bai, Rahul Vaze, and Robert W. Heath. Analysis of blockage effects on urban cellular networks. *IEEE Transactions on Wireless Communications*, 13(9):5070–5083, 2014. doi: 10.1109/TWC.2014.2331971.

[54] E. Vinogradov, H. Sallouha, S. De Bast, M.M. Azari, and S. Pollin. Tutorial on UAVs: A Blue Sky View on Wireless Communication. *Journal of Mobile Multimedia*, 14(4):395–468, 2018. ISSN 1550-4654. doi: https://doi.org/10.13052/jmm1550-4646.1443.

[55] B. Clerckx and C. Oestges. *MIMO Wireless Networks*. 2nd ed. Elsevier Academic Press, 2013.

[56] 3rd Generation Partnership Project (3GPP). 36.777: Study on Enhanced LTE Support for Aerial Vehicles, December 2017.

[57] ITU-R. Propagation data and prediction methods required for the design of terrestrial broadband radio access systems operating in a frequency range from 3 to 60 GHz, February 2012. URL `https://www.itu.int/rec/R-REC-P.1410-5-201202-I/en`.

[58] A. Al-Hourani, S. Kandeepan, and A. Jamalipour. Modeling air-to-ground path loss for low altitude platforms in urban environments. In *2014 IEEE Global Communications Conference*, pages 2898–2904, December 2014. doi: 10.1109/GLOCOM.2014.7037248.

[59] A.F. Molisch. *Wireless Communications*. Wiley - IEEE. Wiley, 2011.

[60] A. Al-Hourani, S. Kandeepan, and S. Lardner. Optimal LAP altitude for maximum coverage. *IEEE Wireless Communications Letters*, 3(6):569–572, December 2014. ISSN 2162-2337. doi: 10.1109/LWC.2014.2342736.

[61] M.M. Azari, F. Rosas, K.-W. Chen, and S. Pollin. Joint sum-rate and power gain analysis of an aerial base station. In *IEEE Globecom Workshops (GC Wkshps)*, pages 1–6, December 2016.

[62] M. Mozaffari, W. Saad, M. Bennis, and M. Debbah. Efficient deployment of multiple unmanned aerial vehicles for optimal wireless coverage. *IEEE Communications Letters*, 20 (8):1647–1650, 2016.

[63] W. Khawaja, I. Guvenc, and D. Matolak. UWB Channel Sounding and Modeling for UAV Air-to-Ground Propagation Channels. In *2016 IEEE Global Communications Conference (GLOBECOM)*, pages 1–7, December 2016. doi: 10.1109/GLOCOM.2016.7842372.

[64] E. Yanmaz, R. Kuschnig, and C. Bettstetter. Channel measurements over 802.11a-based UAV-to-ground links. In *2011 IEEE GLOBECOM Workshops (GC Wkshps)*, pages 1280–1284, December 2011. doi: 10.1109/GLOCOMW.2011.6162389.

[65] E. Yanmaz, R. Kuschnig, and C. Bettstetter. Achieving air-ground communications in 802.11 networks with three-dimensional aerial mobility. In *2013 Proceedings IEEE INFOCOM*, pages 120–124, April 2013. doi: 10.1109/INFCOM.2013.6566747.

[66] W. G. Newhall, R. Mostafa, C. Dietrich, C. R. Anderson, K. Dietze, G. Joshi, and J. H. Reed. Wideband air-to-ground radio channel measurements using an antenna array at 2 GHz for low-altitude operations. In *IEEE Military Communications Conference, 2003. MILCOM 2003.*, volume 2, pages 1422–1427 Vol.2, October 2003. doi: 10.1109/MILCOM.2003.1290436.

[67] H. D. Tu and S. Shimamoto. A Proposal of Wide-Band Air-to-Ground Communication at Airports Employing 5-GHz Band. In *2009 IEEE Wireless Communications and Networking Conference*, pages 1–6, April 2009. doi: 10.1109/WCNC.2009.4917538.

[68] D. W. Matolak and R. Sun. Air-ground channel characterization for unmanned aircraft systems: The near-urban environment. In *MILCOM 2015 - 2015 IEEE Military Communications Conference*, pages 1656–1660, October 2015. doi: 10.1109/MILCOM.2015.7357682.

[69] D. W. Matolak and R. Sun. Air-Ground Channel Characterization for Unmanned Aircraft Systems—Part III: The Suburban and Near-Urban Environments. *IEEE Transactions on Vehicular Technology*, 66(8):6607–6618, August 2017. ISSN 0018-9545. doi: 10.1109/TVT.2017.2659651.

[70] G. R. Maccartney, T. S. Rappaport, M. K. Samimi, and S. Sun. Millimeter-wave omnidirectional path loss data for small cell 5G channel modeling. *IEEE Access*, 3:1573–1580, 2015. ISSN 2169-3536. doi: 10.1109/ACCESS.2015.2465848.

[71] Mohammad Mahdi Azari, Fernando Rosas, Alessandro Chiumento, and Sofie Pollin. Coexistence of Terrestrial and Aerial Users in Cellular Networks. *IEEE Globecom Workshops (GC Wkshps)*, pages 1–6, 2017.

[72] M. M. Azari, F. Rosas, K. Chen, and S. Pollin. Optimal UAV Positioning for Terrestrial-Aerial Communication in Presence of Fading. In *2016 IEEE Global Communications Conference (GLOBECOM)*, pages 1–7, December 2016. doi: 10.1109/GLOCOM.2016.7842099.

[73] Tatsuaki Kimura and Masaki Ogura. Distributed collaborative 3D-deployment of UAV base stations for on-demand coverage. In *IEEE conference on computer communications (INFOCOM)*, pages 1748–1757, 2020.

[74] Margarita Gapeyenko, Vitaly Petrov, Dmitri Moltchanov, Sergey Andreev, Nageen Himayat, and Yevgeni Koucheryavy. Flexible and reliable UAV-assisted backhaul operation in 5G mmWave cellular networks. *IEEE Journal on Selected Areas in Communications*, 36 (11):2486–2496, 2018.

[75] Angelo Trotta, Marco Di Felice, Kaushik R Chowdhury, and Luciano Bononi. Fly and recharge: Achieving persistent coverage using small unmanned aerial vehicles (SUAVs). In *2017 IEEE International Conference on Communications (ICC)*, pages 1–7. IEEE, 2017.

[76] Mohammad Mozaffari, Ali Taleb Zadeh Kasgari, Walid Saad, Mehdi Bennis, and Mérouane Debbah. Beyond 5G with UAVs: Foundations of a 3D wireless cellular network. *IEEE Transactions on Wireless Communications*, 18(1):357–372, 2018.

[77] Bor-Yaliniz et al. Efficient 3-D placement of an aerial base station in next generation cellular networks. In *IEEE international conference on communications (ICC)*, pages 1–5, 2016.

[78] Jiangbin Lyu et al. Placement optimization of UAV-mounted mobile base stations. *IEEE Communications Letters*, 21(3):604–607, 2016.

[79] Gangula Rajeev et al. Flying Rebots: First Results on an Autonomous UAV-Based LTE Relay Using OpenAirinterface. In *19th International Workshop on Signal Processing Advances in Wireless Communications (SPAWC)*, pages 1–5. IEEE, 2018.

[80] Francesco D'Alterio et al. Quality aware aerial-to-ground 5G cells through open-source software. In *2019 IEEE Global Communications Conference (GLOBECOM)*, pages 1–6. IEEE, 2019.

[81] OpenAirInterface:5G software alliance for democratising wireless innovation. `https://openairinterface.org/`. Accessed: 2022-06-05.

[82] Ashutosh Dhekne et al. Extending cell tower coverage through drones. In *Proceedings of the 18th International Workshop on Mobile Computing Systems and Applications*, pages 7–12, 2017.

[83] Ludovico Ferranti et al. SkyCell: A prototyping platform for 5G aerial base stations. In *IEEE 21st International Symposium on" A World of Wireless, Mobile and Multimedia Networks"(WoWMoM)*, pages 329–334, 2020.

[84] John Buczek et al. What is A Wireless UAV? a design blueprint for 6G flying wireless nodes. In *Proceedings of the 15th ACM Workshop on Wireless Network Testbeds, Experimental evaluation & CHaracterization*, pages 24–30, 2022.

[85] srsRAN:Your own mobile network. `https://www.srslte.com/`. Accessed: 2022-06-05.

[86] MAVROS:MAVLink to ROS gateway with proxy for Ground Control Station. `https://github.com/mavlink/mavros`. Accessed: 2022-06-05.

[87] CppCheck:A tool for static C/C++ code analysis. `https://cppcheck.sourceforge.io/`. Accessed: 2022-06-05.

[88] ZeroMQ: An open-source universal messaging library. `https://zeromq.org/`. Accessed: 2022-06-05.

[89] Jorge Navarro-Ortiz et al. A survey on 5G usage scenarios and traffic models. *IEEE Communications Surveys & Tutorials*, 22(2):905–929, 2020.

[90] Salah Eddine Elayoubi et al. 5G RAN slicing for verticals: Enablers and challenges. *IEEE Communications Magazine*, 57(1):28–34, 2019.

[91] Open RAN Alliance. O-RAN: towards an open and smart RAN. *White paper*, pages 1–19, 2018.

[92] Ramon Ferrus et al. On 5G radio access network slicing: Radio interface protocol features and configuration. *IEEE Communications Magazine*, 56:184–192, 2018.

[93] Ruoyu Su et al. Resource allocation for network slicing in 5G telecommunication networks: A survey of principles and models. *IEEE Network*, 33:172–179, 2019.

[94] Alexandros Kaloxylos. A survey and an analysis of network slicing in 5G networks. *IEEE Communications Standards Magazine*, 2(1):60–65, 2018.

[95] Ibrahim Afolabi et al. Network slicing and softwarization: A survey on principles, enabling technologies, and solutions. *IEEE Communications Surveys & Tutorials*, 20(3):2429–2453, 2018.

[96] Mohammed Chahbar et al. A comprehensive survey on the e2e 5g network slicing model. *IEEE Trans. on Network and Service Management*, 18(1):49–62, 2020.

[97] Peter Rost et al. Network slicing to enable scalability and flexibility in 5G mobile networks. *IEEE Communications magazine*, 55(5):72–79, 2017.

[98] Peng Yang et al. Proactive UAV Network Slicing for URLLC and Mobile Broadband Service Multiplexing. *IEEE JSAC*, 2021.

[99] Shashi Raj Pandey et al. Latency-sensitive Service Delivery with UAV-Assisted 5G Networks. *IEEE Wireless Communications Letters*, 2021.

[100] Lingfeng Shen et al. Energy-Awareness Dynamic Trajectory Planning for UAV-Enabled Data Collection in mMTC Networks. In *IEEE VTC2020-Fall*, pages 1–6, 2020. doi: 10.1109/VTC2020-Fall49728.2020.9348455.

[101] Salma Brihi et al. UAV for IoT Communications: Beam Selection Using Matching Game and Network Slicing. In *2020 WINCOM*, pages 1–7. IEEE.

[102] Adlen Ksentini et al. Toward enforcing network slicing on RAN: Flexibility and resources abstraction. *2017 IEEE Communications Magazine*, 55(6):102–108.

[103] Sihem Bakri et al. Dynamic slicing of RAN resources for heterogeneous coexisting 5G services. In *IEEE GLOBECOM*, pages 1–6, 2019.

[104] Anupam Kumar Bairagi et al. Coexistence mechanism between eMBB and uRLLC in 5G wireless networks. *2020 IEEE Trans. on Communications*, 69:1736–1749.

[105] Jing Li and Xing Zhang. Deep reinforcement learning-based joint scheduling of eMBB and URLLC in 5G networks. *IEEE Wireless Communications Letters*, 9(9):1543–1546, 2020.

[106] Madyan Alsenwi et al. Intelligent resource slicing for eMBB and URLLC coexistence in 5G and beyond: A deep reinforcement learning based approach. *IEEE Trans. on Wireless Communications*, 2021.

[107] Peng Yang et al. Repeatedly energy-efficient and fair service coverage: UAV slicing. In *IEEE GLOBECOM*, pages 1–6, 2020.

[108] Igor Donevski et al. Standalone deployment of a dynamic drone cell for wireless connectivity of two services. In *IEEE WCNC*, pages 1–7, 2021.

[109] Salvatore Costanzo et al. Dynamic network slicing for 5G IoT and eMBB services: A new design with prototype and implementation results. In *IEEE CIoT*, pages 1–7, 2018.

[110] Jun-Woo Cho et al. Service-Aware Resource Allocation Design of UAV RAN Slicing. In *2020 ICTC*, pages 801–805. IEEE, 2020.

[111] Giuseppe Faraci et al. Reinforcement-learning for management of a 5G network slice extension with UAVs. In *IEEE INFOCOM WKSHPS*, pages 732–737, 2019.

[112] Mohammed Almekhlafi et al. Joint resource allocation and phase shift optimization for RIS-aided eMBB/URLLC traffic multiplexing. *IEEE Transactions on Communications*, 70(2):1304–1319, 2021.

[113] Saifur Rahman Sabuj et al. Delay Optimization in Mobile Edge Computing: Cognitive UAV-Assisted eMBB and mMTC Services. *IEEE Transactions on Cognitive Communications and Networking*, 2022.

[114] Jian Song. *A Stochastic Geometry Approach to the Analysis and Optimization of Cellular Networks*. PhD thesis, Université Paris-Saclay (ComUE), 2019.

[115] Marco Zambianco and Giacomo Verticale. Interference minimization in 5G physical-layer network slicing. *IEEE Trans. on Communications*, 68:4554–4564, 2020.

[116] Salvatore D'Oro et al. The slice is served: Enforcing radio access network slicing in virtualized 5G systems. In *IEEE INFOCOM*, pages 442–450, 2019.

[117] Salvatore D'Oro et al. Coordinated 5G network slicing: How constructive interference can boost network throughput. *IEEE/ACM Trans. on Networking*, 2021.

[118] Yan Kyaw Tun et al. A Business Model for Resource Sharing in Cell-Free UAVs-Assisted Wireless Networks. *arXiv preprint arXiv:2107.00845*, 2021.

[119] Boris Galkin et al. Coverage analysis for low-altitude UAV networks in urban environments. In *2017 IEEE Global Communications Conference*, pages 1–6.

[120] Elham Kalantari et al. Backhaul-aware robust 3D drone placement in 5G+ wireless networks. In *2017 IEEE ICC workshops*, pages 109–114.

[121] Arjun Anand et al. Joint scheduling of URLLC and eMBB traffic in 5G wireless networks. *IEEE/ACM Trans. on Networking*, 28(2):477–490, 2020.

[122] Trung-Kien Le et al. An overview of physical layer design for Ultra-Reliable Low-Latency Communications in 3GPP Releases 15, 16, and 17. *IEEE access*, pages 433–444, 2020.

[123] Amin Azari et al. Risk-aware resource allocation for URLLC: Challenges and strategies with machine learning. *IEEE Communications Magazine*, 57(3):42–48, 2019.

[124] Yury Polyanskiy et al. Channel coding rate in the finite blocklength regime. *IEEE Transactions on Information Theory*, 56(5):2307–2359, 2010.

[125] Yulin Hu, Anke Schmeink, and James Gross. Blocklength-limited performance of relaying under quasi-static rayleigh channels. *IEEE Transactions on Wireless Communications*, 15 (7):4548–4558, 2016. doi: 10.1109/TWC.2016.2542245.

[126] John N Hooker. Logic-based Benders decomposition for large-scale optimization. In *Large Scale Optimization in Supply Chains and Smart Manufacturing*, pages 1–26. Springer, 2019.

[127] Gianni Codato and Matteo Fischetti. Combinatorial Benders' cuts for mixed-integer linear programming. *Operations Research*, 54(4):756–766, 2006.

[128] Martin Riedler et al. Solving a selective dial-a-ride problem with logic-based Benders decomposition. *Computers & Operations Research*, 96:30–54, 2018.

[129] John N Hooker et al. On Integrating Constraint Propagation and Linear Programming for Combinatorial Optimization. In *AAAI/IAAI*, pages 136–141, 1999.

[130] Egon Balas and Robert Jeroslow. Canonical cuts on the unit hypercube. *SIAM Journal on Applied Mathematics*, 23(1):61–69, 1972.

[131] Rabe Arshad et al. Integrating UAVs into Existing Wireless Networks: A Stochastic Geometry Approach. In *IEEE Globecom Workshops (GC Wkshps)*, pages 1–6, 2018. doi: 10.1109/GLOCOMW.2018.8644504.

[132] Hanif Ullah, Nithya Gopalakrishnan Nair, Adrian Moore, Chris Nugent, Paul Muschamp, and Maria Cuevas. 5G Communication: An Overview of Vehicle-to-Everything, Drones, and Healthcare Use-Cases. *IEEE Access*, 7:37251–37268, 2019.

[133] Mohammad Mozaffari, Ali Taleb Zadeh Kasgari, Walid Saad, Mehdi Bennis, and Mérouane Debbah. 3D Cellular Network Architecture with Drones for beyond 5G. *IEEE Global Communications Conference (GLOBECOM)*, pages 1–6, 2018.

[134] Xiaoli Xu and Yong Zeng. Cellular-Connected UAV: Performance Analysis with 3D Antenna Modelling. *IEEE International Conference on Communications Workshops (ICC Workshops)*, pages 1–6, 2019.

[135] Rui Lyu, Jiangbin; Zhang. Network-Connected UAV: 3-D System Modeling and Coverage Performance Analysis. *IEEE Internet of Things Journal*, 6, 8 2019.

[136] Aziz Altaf Khuwaja, Yunfei Chen, Nan Zhao, Mohamed-Slim Alouini, and Paul Dobbins. A Survey of Channel Modeling for UAV Communications. *IEEE Communications Surveys & Tutorials*, 20(4):2804–2821, 2018.

[137] Weidong Mei, Qingqing Wu, and Rui Zhang. Cellular-Connected UAV: Uplink Association, Power Control and Interference Coordination. *IEEE Transactions on Wireless Communications*, 18(11):5380–5393, 2019.

[138] Lai Zhou, Zhi Yang, Shidong Zhou, and Wei Zhang. Coverage Probability Analysis of UAV Cellular Networks in Urban Environments. *IEEE International Conference on Communications Workshops (ICC Workshops)*, pages 1–6, 2018.

[139] 3GPP TR 38.901. Study on channel model for frequencies from 0.5 to 100 GHz. V14.0.0.

[140] Jedrzej Stanczak, Istvan Z Kovacs, Dawid Koziol, Jeroen Wigard, Rafhael Amorim, and Huan Nguyen. Mobility Challenges for Unmanned Aerial Vehicles Connected to Cellular LTE Networks. *IEEE 87th Vehicular Technology Conference (VTC Spring)*, pages 1–5, 2018.

[141] Rabe Arshad, Hesham ElSawy, Sameh Sorour, Tareq Y Al-Naffouri, and Mohamed-Slim Alouini. Handover Management in 5G and Beyond: A Topology Aware Skipping Approach. *IEEE Access*, 4:9073–9081, 2016.

[142] Chiya Zhang, Weizheng Zhang, Wei Wang, Lu Yang, and Wei Zhang. Research Challenges and Opportunities of UAV Millimeter-Wave Communications. *IEEE Wireless Communications*, 26(1):58–62, 2019.

[143] Aymen Fakhreddine, Christian Bettstetter, Samira Hayat, Raheeb Muzaffar, and Driton Emini. Handover Challenges for Cellular-Connected Drones. *Proceedings of the 5th Workshop on Micro Aerial Vehicle Networks, Systems, and Applications*, pages 9–14, 2019.

[144] Ursula Challita, Walid Saad, and Christian Bettstetter. Deep Reinforcement Learning for Interference-Aware Path Planning of Cellular-Connected UAVs. *IEEE International Conference on Communications (ICC)*, pages 1–7, 2018.

[145] Shuowen Zhang, Yong Zeng, and Rui Zhang. Cellular-Enabled UAV Communication: A Connectivity-Constrained Trajectory Optimization Perspective. *IEEE Transactions on Communications*, 67(3):2580–2604, 2018.

[146] Nilupuli Senadhira, Salman Durrani, Xiangyun Zhou, Nan Yang, and Ming Ding. Uplink NOMA for Cellular-Connected UAV: Impact of UAV Trajectories and Altitude. *arXiv preprint arXiv:1910.13595*, 2019.

[147] Eyuphan Bulut and Ismail Guevenc. Trajectory Optimization for Cellular-Connected UAVs with Disconnectivity Constraint. *IEEE International Conference on Communications Workshops (ICC Workshops)*, pages 1–6, 2018.

[148] Chaitanya Rani, Hamidreza Modares, Raghavendra Sriram, Dariusz Mikulski, and Frank L Lewis. Security of unmanned aerial vehicle systems against cyber-physical attacks. *The Journal of Defense Modeling and Simulation*, 13(3):331–342, 2016.

[149] Gaurav Choudhary, Vishal Sharma, Ilsun You, Kangbin Yim, Ray Chen, and Jin-Hee Cho. Intrusion Detection Systems for Networked Unmanned Aerial Vehicles: A Survey. *14th International Wireless Communications & Mobile Computing Conference (IWCMC)*, pages 560–565, 2018.

[150] Ursula Challita, Aidin Ferdowsi, Mingzhe Chen, and Walid Saad. Machine Learning for Wireless Connectivity and Security of Cellular-Connected UAVs. *IEEE Wireless Communications*, 26(1):28–35, 2019.

[151] Borja Nogales, Victor Sanchez-Aguero, Ivan Vidal, Francisco Valera, and Jaime Garcia-Reinoso. A NFV system to support configurable and automated multi-UAV service deployments. *Proceedings of the 4th ACM Workshop on Micro Aerial Vehicle Networks, Systems, and Applications*, pages 39–44, 2018.

[152] Borja Nogales, Victor Sanchez-Aguero, Ivan Vidal, and Francisco Valera. Adaptable and Automated Small UAV Deployments via Virtualization. *Sensors*, 18(12):4116, 2018.

[153] János Czentye, János Dóka, Árpád Nagy, László Toka, Balázs Sonkoly, and Róbert Szabó. Controlling Drones from 5G Networks. *Proceedings of the ACM SIGCOMM Conference on Posters and Demos*, pages 120–122, 2018.

[154] Fuhui Zhou, Rose Qingyang Hu, Zan Li, and Yuhao Wang. Mobile Edge Computing in Unmanned Aerial Vehicle Networks. *IEEE Wireless Communications*, 2020.

[155] Xiaowen Cao, Jie Xu, and Rui Zhang. Mobile edge computing for cellular-connected UAV: Computation offloading and trajectory optimization. *IEEE 19th International Workshop on Signal Processing Advances in Wireless Communications (SPAWC)*, pages 1–5, 2018.

[156] Christian Grasso and Giovanni Schembra. A fleet of MEC UAVs to extend a 5G Network Slice for Video Monitoring with Low-Latency Constraints. *Journal of Sensor and Actuator Networks*, 8(1):3, 2019.

[157] Naser Hossein Motlagh, Tarik Taleb, and Osama Arouk. Low-Altitude Unmanned Aerial Vehicles-Based Internet of Things Services: Comprehensive Survey and Future Perspectives. *IEEE Internet of Things Journal*, 3(6):899–922, 2016.

[158] Waleed Ejaz, Muhammad Awais Azam, Salman Saadat, Farkhund Iqbal, and Abdul Hanan. Unmanned aerial vehicles enabled IoT Platform for Disaster Management. *Energies*, 12 (14):2706, 2019.

[159] Pablo Royo, Juan López, Cristina Barrado, and Enric Pastor. Service Abstraction Layer for UAV Flexible Application Development. *46th AIAA Aerospace Sciences Meeting and Exhibit*, page 484, 2008.

[160] Anis Koubâa, Basit Qureshi, Mohamed-Foued Sriti, Azza Allouch, Yasir Javed, Maram Alajlan, Omar Cheikhrouhou, Mohamed Khalgui, and Eduardo Tovar. Dronemap Planner: A service-oriented cloud-based management system for the Internet-of-Drones. *Ad Hoc Networks*, 86:46–62, 2019.

[161] Juan A Besada, Ana M Bernardos, Luca Bergesio, Diego Vaquero, Iván Campaña, and José R Casar. Drones-as-a-service: A management architecture to provide mission planning, resource brokerage and operation support for fleets of drones. *IEEE International Conference on Pervasive Computing and Communications Workshops (PerCom Workshops)*, pages 931–936, 2019.

[162] GSNFV ETSI. 002: Network Functions Virtualisation (NFV); Architectural Framework. *Group Specification*, 2014.

[163] Rupendra Nath Mitra and Dharma P Agrawal. 5G mobile technology: A survey. *ICT Express*, 1(3):132–137, 2015.

[164] Adrian Garcia-Rodriguez, Giovanni Geraci, David López-Pérez, Lorenzo Galati Giordano, Ming Ding, and Emil Bjornson. The Essential Guide to Realizing 5G-Connected UAVs with Massive MIMO. *IEEE Communications Magazine*, 2019.

[165] Giovanni Geraci, Adrian Garcia-Rodriguez, Lorenzo Galati Giordano, David López-Pérez, and Emil Björnson. Understanding UAV cellular communications: from existing networks to massive MIMO. *IEEE Access*, 6:67853–67865, 2018.

[166] William Xia, Michele Polese, Marco Mezzavilla, Giuseppe Loianno, Sundeep Rangan, and Michele Zorzi. Millimeter Wave Remote UAV Control and Communications for Public Safety Scenarios. *16th Annual IEEE International Conference on Sensing, Communication, and Networking (SECON)*, pages 1–7, 2019.

[167] Wahab Khawaja, Ozgur Ozdemir, and Ismail Guvenc. UAV Air-to-Ground Channel Characterization for mmWave Systems. *IEEE 86th Vehicular Technology Conference (VTC-Fall)*, pages 1–5, 2017.

[168] Lorenzo Bertizzolo, Tuyen X Tran, Brian Amento, Bharath Balasubramanian, Rittwik Jana, Hal Purdy, Yu Zhou, and Tommaso Melodia. Live and let Live: Flying UAVs

Without affecting Terrestrial UEs. *Proceedings of the 21st International Workshop on Mobile Computing Systems and Applications*, pages 21–26, 2020.

[169] Muhammad Farhan Sohail, Chee Yen Leow, and Seunghwan Won. Non-Orthogonal Multiple Access for Unmanned Aerial Vehicle Assisted Communication. *IEEE Access*, 6:22716–22727, 2018.

[170] Weidong Mei and Rui Zhang. Uplink Cooperative NOMA for Cellular-Connected UAV. *IEEE Journal of Selected Topics in Signal Processing*, 13(3):644–656, 2019.

[171] Ali Rahmati, Yavuz Yapıcı, Nadisanka Rupasinghe, Ismail Guvenc, Huaiyu Dai, and Arupjyoti Bhuyany. Energy efficiency of RSMA and NOMA in cellular-connected mmwave UAV networks. *arXiv preprint arXiv:1902.04721*, 2019.

[172] Peter J Burke. A Safe, Open Source, 4G Connected Self-Flying Plane With 1 Hour Flight Time and All Up Weight (AUW)< 300 g: Towards a New Class of Internet Enabled UAVs. *IEEE Access*, 7:67833–67855, 2019.

[173] Lassi Sundqvist et al. Cellular controlled drone experiment: Evaluation of network requirements. 2015.

[174] George N Solidakis, Fanourios M Tsokas, Michael C Batistatos, Nikos C Sagias, George V Tsoulos, Dimitra A Zarbouti, and Georgia E Athanasiadou. An Arduino-based subsystem for controlling UAVs through GSM. *IEEE 6th International Conference on Modern Circuits and Systems Technologies (MOCAST)*, pages 1–4, 2017.

[175] Deniss Brodņevs. Development of a Flexible Software Solution for Controlling Unmanned Air Vehicles via the Internet. *Transport and Aerospace Engineering*, 6(1):37–43, 2018.

[176] Xingqin Lin, Richard Wiren, Sebastian Euler, Arvi Sadam, Helka-Liina Maattanen, Siva Muruganathan, Shiwei Gao, Y-P Eric Wang, Juhani Kauppi, Zhenhua Zou, et al. Mobile Network-Connected Drones: Field Trials, Simulations, and Design Insights. *IEEE Vehicular Technology Magazine*, 14(3):115–125, 2019.

[177] Raheeb Muzaffar, Christian Raffelsberger, Aymen Fakhreddine, José López Luque, Driton Emini, and Christian Bettstetter. First Experiments with a 5G-Connected Drone. *arXiv preprint arXiv:2004.03298*, 2020.

[178] LTE Qualcomm. Unmanned Aircraft Systems—Trial Report, 2017.

[179] Rafhael Amorim, Preben Mogensen, Troels Sorensen, István Z Kovács, and Jeroen Wigard. Pathloss measurements and modeling for UAVs connected to cellular networks. *IEEE 85th Vehicular Technology Conference (VTC Spring)*, pages 1–6, 2017.

[180] Samira Hayat, Christian Bettstetter, Aymen Fakhreddine, Raheeb Muzaffar, and Driton Emini. An experimental evaluation of LTE-A throughput for drones. *Proceedings of the 5th Workshop on Micro Aerial Vehicle Networks, Systems, and Applications*, pages 3–8, 2019.

[181] Rafhael Amorim, Jeroen Wigard, Huan Nguyen, Istvan Z Kovacs, and Preben Mogensen. Machine-learning identification of airborne UAV-UEs based on LTE radio measurements. *IEEE Globecom Workshops (GC Wkshps)*, pages 1–6, 2017.

[182] Rafhael Amorim, Huan Nguyen, Jeroen Wigard, István Z Kovács, Troels B Sorensen, and Preben Mogensen. LTE radio measurements above urban rooftops for aerial communications. *IEEE Wireless Communications and Networking Conference (WCNC)*, pages 1–6, 2018.

[183] Hugo Marques, Paulo Marques, Jorge Ribeiro, Tiago Alves, and Luis Pereira. Experimental Evaluation of Cellular Networks for UAV Operation and Services. *IEEE 24th International Workshop on Computer Aided Modeling and Design of Communication Links and Networks (CAMAD)*, pages 1–6, 2019.

[184] Evşen Yanmaz et al. Communication and Coordination for Drone Networks. *Ad hoc networks*, pages 79–91, 2017.

[185] Aicha Idriss Hentati and Lamia Chaari Fourati. Comprehensive Survey of UAVs Communication Networks. *Computer Standards & Interfaces*, page 103451, 2020.

[186] Wu Chen et al. Toward Robust and Intelligent Drone Swarm: Challenges and Future Directions. *IEEE Network*, 2020.

[187] Prabhu Chandhar, Danyo Danev, and Erik G. Larsson. Massive MIMO for Communications With Drone Swarms. *IEEE Transactions on Wireless Communications*, 17(3): 1604–1629, 2018. doi: 10.1109/TWC.2017.2782690.

[188] Arash Asadi, Qing Wang, and Vincenzo Mancuso. A Survey on Device-to-Device Communication in Cellular Networks. *IEEE Communications Surveys & Tutorials*, 16(4):1801–1819, 2014. doi: 10.1109/COMST.2014.2319555.

[189] Furqan Jameel, Zara Hamid, Farhana Jabeen, Sherali Zeadally, and Muhammad Awais Javed. A Survey of Device-to-Device Communications: Research Issues and Challenges. *IEEE Communications Surveys & Tutorials*, 20(3):2133–2168, 2018. doi: 10.1109/COMST.2018.2828120.

[190] M. Gonzalez-Martín, M. Sepulcre, R. Molina-Masegosa, and J. Gozalvez. Analytical models of the performance of c-v2x mode 4 vehicular communications. *IEEE Transactions on Vehicular Technology*, 68(2):1155–1166, 2019. doi: 10.1109/TVT.2018.2888704.

[191] Nestor Bonjorn et al. Enhanced 5G V2X Services using Sidelink Device-to-Device Communications. *2018 17th annual mediterranean ad hoc networking workshop (Med-Hoc-Net)*, pages 1–7, 2018.

[192] Rafael Molina-Masegosa and Javier Gozalvez. LTE-V for sidelink 5G V2X vehicular communications: A new 5G technology for short-range vehicle-to-everything communications. *IEEE Vehicular Technology Magazine*, 12(4):30–39, 2017.

[193] Shao-Yu Lien et al. 3GPP NR Sidelink Transmissions Toward 5G V2X. *IEEE Access*, 8: 35368–35382, 2020.

[194] Karthikeyan Ganesan et al. NR Sidelink Design Overview for Advanced V2X Service. *IEEE Internet of Things Magazine*, 3(1):26–30, 2020.

[195] Debashisha Mishra, Anna Vegni, Valeria Loscri, and Enrico Natalizio. Drone Networking in 6G Era-A Technology Overview. *IEEE Communications Standards Magazine*, 2022.

[196] S. Xiaoqin, M. Juanjuan, L. Lei, and Z. Tianchen. Maximum-throughput sidelink resource allocation for nr-v2x networks with the energy-efficient csi transmission. *IEEE Access*, 8: 73164–73172, 2020.

[197] A. Mansouri, V. Martinez, and J. Härri. A first investigation of congestion control for lte-v2x mode 4. In *2019 15th Annual Conference on Wireless On-demand Network Systems and Services (WONS)*, pages 56–63, 2019.

[198] Vara Prasad Karamchedu. A Path from Device-to-Device to UAV-to-UAV Communications. In *2020 IEEE 92nd Vehicular Technology Conference (VTC2020-Fall)*, pages 1–5, 2020. doi: 10.1109/VTC2020-Fall49728.2020.9348841.

[199] Debashisha Mishra, Angelo Trotta, Marco Di Felice, and Enrico Natalizio. Performance Analysis of Multi-hop Communication based on 5G Sidelink for Cooperative UAV Swarms. In *2021 IEEE International Mediterranean Conference on Communications and Networking (MeditCom)*, pages 395–400, 2021. doi: 10.1109/MeditCom49071.2021.9647449.

[200] M Mahdi Azari et al. UAV-to-UAV Communications in Cellular Networks. *IEEE Transactions on Wireless Communications*, 2020.

[201] Q. N. Tran et al. Downlink Resource Allocation Maximized Video Delivery Capacity over Multi-hop Multi-path in Dense D2D 5G Networks. In *2020 4th International Conference on Recent Advances in Signal Processing, Telecommunications Computing (SigTelCom)*, pages 72–76, 2020. doi: 10.1109/SigTelCom49868.2020.9199027.

[202] Zhifeng He et al. Link scheduling and channel assignment with a graph spectral clustering approach. In *MILCOM 2016 - 2016 IEEE Military Communications Conference*, pages 73–78, 2016. doi: 10.1109/MILCOM.2016.7795304.

[203] M. Li, S. Salinas, P. Li, X. Huang, Y. Fang, and S. Glisic. Optimal Scheduling for Multi-Radio Multi-Channel Multi-Hop Cognitive Cellular Networks. *IEEE Transactions on Mobile Computing*, 14(1):139–154, 2015. doi: 10.1109/TMC.2014.2314107.

[204] L. Song, M. Tao, and Y. Xu. Exploiting hop diversity with frequency sharing in multi-hop ofdm networks. *IEEE Communications Letters*, 13(12):908–910, 2009. doi: 10.1109/LCOMM.2009.12.091902.

[205] M Mahdi Azari, Fernando Rosas, and Sofie Pollin. Cellular Connectivity for UAVs: Network Modeling, Performance Analysis, and Design Guidelines. *IEEE Transactions on Wireless Communications*, 18(7):3366–3381, 2019.

[206] Hesham ElSawy, Ahmed Sultan-Salem, Mohamed-Slim Alouini, and Moe Z Win. Modeling and analysis of cellular networks using stochastic geometry: A tutorial. *IEEE Communications Surveys & Tutorials*, 19(1):167–203, 2016.

[207] Angelo Trotta, Marco Di Felice, Luca Bedogni, Luciano Bononi, and Fabio Panzieri. Connectivity recovery in post-disaster scenarios through cognitive radio swarms. *Computer Networks*, 91:68 – 89, 2015. ISSN 1389-1286.

[208] Michael R Garey and David S Johnson. Computers and intractability. *A Guide to the*, 1979.

[209] H. Choi et al. Consensus-based decentralized auctions for robust task allocation. *IEEE Transactions on Robotics*, 25(4):912–926, 2009.

[210] IBM, 2013. IBM ILOG CPLEX 12.8 User Manual. IBM Corp. URL `http://public.dhe.ibm.com/software/products/Decision_Optimization/docs/pdf/usrcplex.pdf`.

[211] Saif Sabeeh et al. Estimation and Reservation for Autonomous Resource Selection in C-V2X Mode 4. In *30th International Symposium on PIMRC*, pages 1–6, 2019.

[212] Nestor Bonjorn et al. Cooperative resource allocation and scheduling for 5G eV2X services. *IEEE Access*, 7:58212–58220, 2019.

[213] Ahlem Masmoudi et al. Efficient scheduling and resource allocation for D2D-based LTE-V2X communications. In *15th IEEE IWCMC*, pages 496–501, 2019.

[214] Xinxin He et al. Design and Analysis of a Short-Term Sensing-Based Resource Selection Scheme for C-V2X Networks. *IEEE Internet of Things Journal*, 7(11):11209–11222, 2020.

[215] Leonardo Babun et al. Multi-hop and D2D communications for extending coverage in public safety scenarios. In *IEEE 40th LCN Workshops*, pages 912–919. IEEE, 2015.

[216] Leila Melki et al. Radio resource management scheme and outage analysis for network-assisted multi-hop D2D communications. *Digital Communications and Networks*, 2(4): 225–232, 2016.

[217] C. E. Perkins and E. M. Royer. Ad-hoc on-demand distance vector routing. In *Proceedings WMCSA'99. Second IEEE Workshop on Mobile Computing Systems and Applications*, pages 90–100, 1999. doi: 10.1109/MCSA.1999.749281.

[218] B. McCarthy and A. O'Driscoll. OpenCV2X Mode 4: A Simulation Extension for Cellular Vehicular Communication Networks. In *IEEE 24th International Workshop on CAMAD*, pages 1–6, 2019. doi: 10.1109/CAMAD.2019.8858436.

[219] Ian F. Akyildiz, Ahan Kak, and Shuai Nie. 6G and Beyond: The Future of Wireless Communications Systems. *IEEE Access*, 8:133995–134030, 2020. doi: 10.1109/ACCESS.2020.3010896.

[220] G. Wikström, J. Peisa, P. Rugeland, N. Johansson, S. Parkvall, M. Girnyk, G. Mildh, and I. L. Da Silva. Challenges and Technologies for 6G. In *2020 2nd 6G Wireless Summit (6G SUMMIT)*, pages 1–5, 2020. doi: 10.1109/6GSUMMIT49458.2020.9083880.

[221] Harish Viswanathan and Preben E. Mogensen. Communications in the 6G Era. *IEEE Access*, 8:57063–57074, 2020. doi: 10.1109/ACCESS.2020.2981745.

[222] Debashisha Mishra et al. A high-end IoT devices framework to foster beyond-connectivity capabilities in 5G/B5G architecture. *IEEE Communications Magazine*, 59(1):55–61, 2021.

[223] Giovanni Geraci, Adrian Garcia-Rodriguez, M. Mahdi Azari, Angel Lozano, Marco Mezzavilla, Symeon Chatzinotas, Yun Chen, Sundeep Rangan, and Marco Di Renzo. What Will the Future of UAV Cellular Communications Be? A Flight From 5G to 6G. *IEEE Communications Surveys & Tutorials*, 24(3):1304–1335, 2022. doi: 10.1109/COMST.2022.3171135.

[224] Hadeel Elayan, Osama Amin, Basem Shihada, Raed M. Shubair, and Mohamed-Slim Alouini. Terahertz Band: The Last Piece of RF Spectrum Puzzle for Communication Systems. *IEEE Open Journal of the Communications Society*, 1:1–32, 2020. doi: 10.1109/OJCOMS.2019.2953633.

[225] Shao-Yu Lien, Der-Jiunn Deng, Chun-Cheng Lin, Hua-Lung Tsai, Tao Chen, Chao Guo, and Shin-Ming Cheng. 3GPP NR Sidelink Transmissions Toward 5G V2X. *IEEE Access*, 8:35368–35382, 2020. doi: 10.1109/ACCESS.2020.2973706.

[226] Jennifer Gielis and Amanda Prorok. Improving 802.11p for Delivery of Safety-Critical Navigation Information in Robot-to-Robot Communication Networks. *IEEE Communications Magazine*, 59(1):16–21, 2021. doi: 10.1109/MCOM.001.2000545.

[227] A. Balasubramanian, Nagi Mahalingam, Ravi Pragada, and Philip Pietraski. Group Feedback Protocols for UAV Swarming Applications. In *2018 IEEE Globecom Workshops (GC Wkshps)*, pages 1–7, 2018. doi: 10.1109/GLOCOMW.2018.8644393.

[228] Huaicong Kong, Min Lin, Wei-Ping Zhu, Hamidreza Amindavar, and Mohamed-Slim Alouini. Multiuser Scheduling for Asymmetric FSO/RF Links in Satellite-UAV-Terrestrial Networks. *IEEE Wireless Communications Letters*, 9(8):1235–1239, 2020. doi: 10.1109/LWC.2020.2986750.

[229] Ju-Hyung Lee, Ki-Hong Park, Mohamed-Slim Alouini, and Young-Chai Ko. On the Throughput of Mixed FSO/RF UAV-Enabled Mobile Relaying Systems with a Buffer Constraint. In *IEEE International Conference on Communications (ICC)*, pages 1–6, 2019. doi: 10.1109/ICC.2019.8761378.

[230] Ashwin Ashok. Position: DroneVLC: Visible Light Communication for Aerial Vehicular Networking. In *Proceedings of the 4th ACM Workshop on Visible Light Communication Systems*, VLCS '17, page 29–30, New York, NY, USA, 2017. ACM. ISBN 9781450351423. doi: 10.1145/3129881.3129894. URL `https://doi.org/10.1145/3129881.3129894`.

[231] Antonio Costanzo, Valeria Loscrí, Virginie Deniau, and Jean Rioult. On the Interference Immunity of Visible Light Communication (VLC). In *GLOBECOM 2020 - 2020 IEEE Global Communications Conference*, pages 1–6, 2020. doi: 10.1109/GLOBECOM42002.2020.9348209.

[232] Claudia Stöcker, Rohan Bennett, Francesco Nex, Markus Gerke, and Jaap Zevenbergen. Review of the current state of UAV regulations. *Remote sensing*, 9(5):459, 2017.

[233] Eleonora Bassi. European drones regulation: Today's legal challenges. In *2019 international conference on unmanned aircraft systems (ICUAS)*, pages 443–450. IEEE, 2019.

[234] UAV Market Size. `https://www.fortunebusinessinsights.com/industry-reports/unmanned-aerial-vehicle-uav-market-101603`. Accessed: 2023-03-01.

[235] Ramanujan K. Sheshadri, Eugene Chai, Karthikeyan Sundaresan, and Sampath Rangarajan. SkyHAUL: A Self-Organizing Gigabit Network In The Sky. In *Proceedings of the Twenty-Second International Symposium on Theory, Algorithmic Foundations, and Protocol Design for Mobile Networks and Mobile Computing*, MobiHoc 2021, page 101–110.

[236] Vuk Marojevic, Ismail Guvenc, Rudra Dutta, Mihail L Sichitiu, and Brian A Floyd. Advanced wireless for unmanned aerial systems: 5G standardization, research challenges, and AERPAW architecture. *IEEE Vehicular Technology Magazine*, 15(2):22–30, 2020.

[237] RFDataFactory. `https://www.rfdatafactory.com/home-page`. Accessed: 2023-03-20.